JNC TJ7400 2004-013

核種の溶解度評価に関する地下水の地球化学パラメータの感度解析

(核燃料サイクル開発機構 契約業務報告書)

2004年3月

三菱商事株式会社

〒319-1184 茨城県那珂郡東海村村松 4 番地 49

核燃料サイクル開発機構

技術展開部 技術協力課

電話：029-282-1122

ファックス：029-282-7980

電子メール：jserv@jnc.go.jp

Technical Cooperation Section,

Technology Management Division,

Japan Nuclear Cycle Development Institute

4-49 Muramatsu,Naka-gun,Ibaraki 319-1184, JAPAN

JNC TJ7400 2004-013
2004年3月

核種の溶解度評価に関する地下水の地球化学パラメータの感度解析

要旨

R. Metcalfe *, D. Savage **, A.H. Bath ***, C. Walker **

本報告書は，平成15年度に実施された東濃地域の地下水を対象とした放射性核種の溶解度評価に関する業務成果をまとめたものである。本業務の目的は，天然バリア（岩盤・岩石，地下水）中での核種移行現象のうち，特に地下水の地球化学特性に強く支配されると考えられる放射性核種の溶解度評価の観点から，地下水の地球化学特性の調査における取得データの要求品質を明確にすることである。溶解度評価の観点に限らず，あらゆる核種移行現象の観点から，地下水の地球化学特性に関する要求品質があらかじめ明確になっていれば，より合理的な採水調査が可能となるものと考えられる。本業務では，東濃地域における既往の地下水データを使用して，調査時や分析時に発生し得る不確実性，地下水の地球化学特性の3次元的な不均一性，長期的な時間スケールにおける地下水の地球化学特性が有する不確実性について整理して，これらの不確実性や不均一性が放射性核種の溶解度に与え得る影響について評価を行い，各成分の要求品質（精度やそのばらつき幅の範囲など）についての考察を行った。

本業務において解析の対象とする放射性核種は，第二次取りまとめ報告書（JNC, 2000）において“考慮すべき重要な核種”とされている以下の18元素とし，溶解度の計算には以下の解析コード・データベースを使用した。

- 解析対象の核種；Se, Zr, Nb, Tc, Pd, Sn, Cs, Sm, Pb, Ra, Ac, Th, Pa, U, Np, Pu, Am, Cm
- 解析コード；PHREEQC v 2.8
- 溶解度を制限する鉱物相の計算；GWB (the code Geochemist's Workbench)
- 熱力学データベース；JNC-TDB, database 011213g0.tdb (GWB version) / 011213c0.tdb (PHREEQC version).

調査時や分析時に発生し得る不確実性の影響の評価については，以下の結論を得た。

- 全体評価として，分析上の不確実性に起因する溶解度のばらつきは，核種の溶解度に対して著しい影響とはならない。
- Se, Tc, Uは，分析上の不確実性に起因する溶解度のばらつきを1オーダ以上有する。
- Nbは，Cs（非可溶性の元素）を除いて，最も溶解性が高い核種である（Mb濃度約10^{-5} mol/kgであり，1 ppmと等価）。
- Pdは，極めて難溶解性を示す（Pb濃度1.6×10^{-24} mol/kg未満であり，溶媒1 kg当たりで原子1個の溶解程度と等価）。
- 地下水中のPO_4の濃度は，Sm, Pb, Ac, Cmの溶解度のばらつきにある程度の影響を与える可能性がある。
- 既往の掘削水データ（DH-6, 7, 8）を用いた検討では，掘削水の残留率が1％程度に低い場合でも，いくつかの核種の溶解度に影響を与える可能性がある。この場合，相対的に大きな影響を受ける核

種は，U（$10^{1.5}$の範囲のばらつき）とTc（10^{4}の範囲のばらつき）である。
・多くの地下水データには，陽イオンと陰イオンとの当量比に大きなずれが認められる。この理由として，HCO_3，全無機炭素（TIC），アルカリ度，pHの分析値・測定値が，正確でない可能性がある。対象核種のうちUの溶解度の計算上では，これらの成分が溶解度のばらつきに大きな影響を与え得るが，その他の核種では影響は小さい。

地下水の地球化学特性の3次元的な不均一性の影響の評価については，以下の結論を得た。
・東濃地域に分布する代表的な地下水である，Na-Cl型とNa-Ca-HCO_3型の地下水に対する核種の溶解度には，明瞭な違いが認められない。このことから，東濃地域における既往のデータに関しては，3次元的な不均一性の影響については，特別な考慮は必要ないと考えられる。
・ただし，既往データのほとんどは，天水起源の水が還元された状態で採水された地下水である。酸素を溶存する地下水が分布するような地下浅部からの地下水データが取得された場合，そのデータを用いた溶解度の計算では，大きな差異が発生する可能性がある。
・サイトスケールでの地球化学特性の不均一性は溶解度に対する影響を与えないと評価されるが，個々の断層・破砕帯，割れ目帯などでは，溶解度に著しい差異が発生する可能性がある。東濃地域の断層・破砕帯，割れ目帯などは，高透水性のゾーンとなり得ることが知られており，これらは酸化的な地下水の流入経路となる可能性がある。

長期的な時間スケールにおける，地下水の地球化学特性が有する不確実性の影響の評価については，東濃地域のみに限らない一般的な評価として以下の結論を得た。
・数十万～百万年程度の時間スケールを考慮した場合，地下水の状態は大きく変化し得るが，この変化を規制する主な要因は気候変化である。この気候変化の原因は，降水量の変化，気温変化，植生変化，海水準変動などの事象である。これらの事象はいずれも，酸素を溶存する地下水の浸透の割合に，直接的もしくは間接的に影響を与えることになるため，酸化還元状態に敏感に反応する鉱物に溶解度が制限される核種の場合は，その溶解度に影響を受ける可能性がある。
・隆起・沈降の事象（日本の場合，これらは主に構造運動に起因）も，溶解度に影響を与える可能性がある。この場合，割れ目が拡大したり密閉したりすることによって，酸素を溶存する地下水の浸透が変化する可能性がある。

本報告書は，三菱商事株式会社が核燃料サイクル開発機構との契約により実施した業務成果を取りまとめたものである。
機構担当課室：東濃地科学センター　瑞浪超深地層研究所　超深地層研究グループ
* Quintessa Japan　** Quintessa UK　*** Intellisci Ltd

JNC TJ7400 2004-013

March, 2004

Sensitivity analysis to the geochemical parameters of the groundwater about solubilities of nuclides

Abstract

R. Metcalfe *, D. Savage **, A.H. Bath ***, C. Walker **

This report describes calculations of element solubilities for the groundwaters of the Tono area. An important aim is to demand quality of the groundwater data in geochemical investigation from a viewpoint of solubility evaluation of the radioactive nuclide. For more rational investigation, it is necessary to clarify quality about the geochemical characteristic of groundwater. In this work, it arranged about the uncertainty and the heterogeneity concerning analytical uncertainties, concerning 3D variations, and concerning geochemical uncertainty over long-term time scales, and the influence about solubility was considered.

This work would focus on following 18 elements which positioned as "The safety-relevant radionuclides" in JNC's Report (JNC, 2000) :

Se, Zr, Nb, Tc, Pd, Sn, Cs, Sm, Pb, Ra, Ac, Th, Pa, U, Np, Pu, Am, Cm

The approach was initially to review the published literature concerning the chemistry of these elements, to establish the main chemical controls on their solubilities. Hence, the code Geochemist's Workbench (GWB) was used to identify likely solubility-controlling minerals under the chemical conditions of the Tono groundwaters. In parallel with this work, a review of information about the quality of water chemical data in the Tono area was also undertaken. This review highlighted key areas of uncertainty. Subsequent calculations were made using both GWB and the code PHREEQC v 2.8, to evaluate the significance of these uncertainties. The geochemical calculations used JNC's thermodynamic database 011213g0.tdb (GWB version)/ 011213c0.tdb (PHREEQC version).

The following conclusions can be drawn concerning analytical uncertainties:

- Analytical uncertainties do not lead to significant uncertainties in the estimated solubility.
- For Se, Tc and U, analytical uncertainties could potentially lead to uncertainties in concentrations that are > 1 order of magnitude.
- Nb is the most soluble of the considered elements in this water (in the order of 10^{-5} molal, equivalent to approximately 1 ppm), excluding Cs, which is not solubility-controlled.
- Pd is effectively insoluble in the water considered (all concentrations are < 1.6×10^{-24} molal, equivalent to 1 atom per kilogram).
- Uncertainties in PO_4 concentrations could lead to large uncertainties in the estimated solubilities of Sm, Pb, Ac, Am and Cm.
- Drilling fluid contamination, even as little as 1 % could significantly affect the solubilities of some of the

elements. The greatest effects would be seen for U (1.5 orders of magnitude) and Tc (4 orders of magnitude).

- Many of the reported groundwater (based on the drilling fluid composition reported for boreholes DH-6, 7, 8) analyses have large charge imbalances and inconsistencies between the reported HCO_3, Total inorganic carbon (TIC) alkalinities and pH. These inconsistencies could exert a significant effect on the calculated solubilities of elements that may form CO_3-complexes, notably U. However, in other cases, the effect on calculated solubilities is small.

The following conclusions can be drawn concerning 3D variations in element solubilities :

- There were no discernible systematic differences in solubilities in groundwaters from different parts of the Tono area. It was noteworthy that broadly similar solubilities were calculated for the Na-Cl dominated groundwater and also for the Na-Ca-HCO_3 dominated groundwater.
- However, all the sampled groundwaters are reducing relative to recharging meteoric water. If shallow waters containing dissolved oxygen were to be sampled, then there could be substantial contrasts with respect to the sampled groundwaters.
- While chemical variations in the deep groundwaters at the site scale show no systematic variations in element solubilities, at individual fractures, there could be significant variations in calculated solubilities. Fracture zones and fault zones in the Tono area are known to have variable hydraulic conductivities and a range of evidence suggests that some of them may conduct relatively oxidizing groundwater.

The following conclusions can be drawn concerning geochemical uncertainty over long-term time scales:

- During such long time intervals (several hundreds of thousands of years to around 1 Ma) groundwater conditions can change considerably. Climate change is a major factor controlling these changes. Variations in climate may cause:

  Changes in precipitation, Changes in temperature, Changes in vegetation, Changes in sea level

  These factors may all influence, directly or indirectly, the rate of invasion of oxygenated groundwater. Any redox variations that are caused in the deep sub-surface as a result could potentially influence the solubilities of redox-sensitive minerals.
- Uplift or subsidence, which in Japan are likely to be driven principally by tectonic processes may also exert an influence. Dilation or sealing of fractures as a consequence of such tectonic variations could conceivably influence the distribution of oxygenated water.

This report is related with the work performed by Mitsubishi Corporation under construct with Japan Nuclear Cycle Development Institute.

JNC Liaison : Underground Reseach Group, Mizunami Underground Research Laboratory, Tono Geoscience Center

* Quintessa Japan ** Quintessa UK *** Intellisci Ltd

Contents

1	**Introduction**	1
2	**Approach**	2
3	**Establishing parameters**	3
	3.1 Selenium	3
	3.2 Zirconium	4
	3.3 Niobium	6
	3.4 Technetium	6
	3.5 Palladium	7
	3.6 Tin	7
	3.7 Caesium	8
	3.8 Samarium	9
	3.9 Radium	10
	3.10 Thorium	11
	3.11 Protactinium	12
	3.12 Uranium	12
	3.13 Neptunium	14
	3.14 Plutonium	14
	3.15 Americium	15
	3.16 Curium	15
	3.17 Lead	16
4	**Solubility calculations using past data**	18
	4.1 Computer modelling codes	18
	4.2 Past geochemical data	18
	4.2.1 Geochemical data	18
	4.2.2 Review of geochemical data quality	19
	4.2.3 Application of Scoring System to Tono Samples	30
	4.3 Solubility calculations	34
	4.3.1 Solubility diagrams	34
	4.3.2 Sensitivity calculations	70
5	**Initial analysis of 3D heterogeneity in geochemical characteristics**	103
	5.1 3D heterogeneity in chemical conditions	103
	5.2 3D variations in element solubilities	110
6	**Geochemical uncertainty over PA time scales**	127
7	**Evaluation of calculation results**	127
	References	129

Figures

Figure 4.2-1	Locations of the boreholes that yielded the data considered in the project.	20
Figure 4.3-1	Variation of selenium solubility with pH for a range of representative Tono groundwaters.	35
Figure 4.3-2	Eh-pH diagrams for selenium in a range of representative Tono groundwaters.	36
Figure 4.3-3	Variation of zirconium solubility with pH for a range of representative Tono groundwaters.	37
Figure 4.3-4	Eh-pH diagrams for zirconium in a range of representative Tono groundwaters.	38
Figure 4.3-5	Variation of niobium solubility with pH for a range of representative Tono groundwaters.	39
Figure 4.3-6	Eh-pH diagrams for niobium in a range of representative Tono groundwaters.	40
Figure 4.3-7	Variation of technetium solubility with pH for a range of representative Tono groundwaters.	41
Figure 4.3-8	Eh-pH diagrams for technetium in a range of representative Tono groundwaters.	42
Figure 4.3-9	Variation of palladium solubility with pH for a range of representative Tono groundwaters.	43
Figure 4.3-10	Eh-pH diagrams for palladium in a range of representative Tono groundwaters.	44
Figure 4.3-11	Variation of tin solubility with pH for a range of representative Tono groundwaters.	45
Figure 4.3-12	Eh-pH diagrams for tin in a range of representative Tono groundwaters.	46
Figure 4.3-13	Variation of samarium solubility with pH for a range of representative Tono groundwaters.	47
Figure 4.3-14	Eh-pH diagrams for samarium in a range of representative Tono groundwaters.	48
Figure 4.3-15	Variation of lead solubility with pH for a range of representative Tono groundwaters.	49
Figure 4.3-16	Eh-pH diagrams for lead in a range of representative Tono groundwaters.	50
Figure 4.3-17	Variation of radium solubility with pH for a range of representative Tono groundwaters.	51
Figure 4.3-18	Eh-pH diagrams for radium in a range of representative Tono groundwaters.	52
Figure 4.3-19	Variation of actinium solubility with pH for a range of representative Tono groundwaters.	53
Figure 4.3-20	Eh-pH diagrams for actinium in a range of representative	

Tono groundwaters. 54
Figure 4.3-21 Variation of thorium solubility with pH for a range of representative Tono groundwaters. 55
Figure 4.3-22 Eh-pH diagrams for thorium in a range of representative Tono groundwaters. 56
Figure 4.3-23 Variation of protoactinium solubility with pH for a range of representative Tono groundwaters. 57
Figure 4.3-24 Eh-pH diagrams for protoactinium in a range of representative Tono groundwaters. 58
Figure 4.3-25 Variation of uranium solubility with pH for a range of representative Tono groundwaters. 59
Figure 4.3-26 Eh-pH diagrams for uranium in a range of representative Tono groundwaters. 60
Figure 4.3-27 Variation of neptunium solubility with pH for a range of representative Tono groundwaters. 61
Figure 4.3-28 Eh-pH diagrams for neptunium in a range of representative Tono groundwaters. 62
Figure 4.3-29 Variation of plutonium solubility with pH for a range of representative Tono groundwaters. 63
Figure 4.3-30 Eh-pH diagrams for plutonium in a range of representative Tono groundwaters. 64
Figure 4.3-31 Variation of americium solubility with pH for a range of representative Tono groundwaters. 65
Figure 4.3-32 Eh-pH diagrams for americium in a range of representative Tono groundwaters. 66
Figure 4.3-33 Variation of curium solubility with pH for a range of representative Tono groundwaters. 67
Figure 4.3-34 Eh-pH diagrams for curium in a range of representative Tono groundwaters. 68
Figure 4.3-35 Total selenium concentration versus pH defined by the solubility of elemental Se in a Tono groundwater composition (DH-7/563.75) varied randomly according to analytical uncertainties. 72
Figure 4.3-36 Total selenium concentration versus pH defined by the solubility of $FeSe_2$ in a Tono groundwater composition (DH-7/563.75) varied randomly according to analytical uncertainties. 72
Figure 4.3-37 Total zirconium concentration versus pH defined by the solubility of amorphous zirconium dioxide in a Tono groundwater composition (DH-7/563.75) varied randomly according to analytical uncertainties. 73
Figure 4.3-38 Total niobium concentration versus pH defined by the solubility of Nb2O5 in a Tono groundwater composition (DH-7/563.75) varied randomly according to analytical uncertainties. 73
Figure 4.3-39 Total techentium concentration versus pH defined by the solubility

of crystalline Tc in a Tono groundwater composition (DH-7/563.75) varied randomly according to analytical uncertainties. 74
Figure 4.3-40 Total techentium concentration versus pH defined by the solubility of crystalline TcO_2(cr) in a Tono groundwater composition (DH-7/563.75) varied randomly according to analytical uncertainties. 74
Figure 4.3-41 Total palladium concentration versus pH defined by the solubility of crystalline palladium in a Tono groundwater composition (DH-7/563.75) varied randomly according to analytical uncertainties. 75
Figure 4.3-42 Total tin concentration versus pH defined by the solubility of tin dioxide (cassiterite) in a Tono groundwater composition (DH-7/563.75) varied randomly according to analytical uncertainties. 75
Figure 4.3-43 Total samarium concentration versus pH defined by the solubility of $SmOHCO_3$ in a Tono groundwater composition (DH-7/563.75) varied randomly according to analytical uncertainties. 76
Figure 4.3-44 Total samarium concentration versus pH defined by the solubility of $SmPO_4$ in a Tono groundwater composition (DH-7/563.75) varied randomly according to analytical uncertainties. 76
Figure 4.3-45 Total lead concentration versus pH defined by the solubility of $PbCO_3$ (cerussite) in a Tono groundwater composition (DH-7/563.75) varied randomly according to analytical uncertainties. 77
Figure 4.3-46 Total lead concentration versus pH defined by the solubility of $Pb_5(PO_4)_3Cl$ in a Tono groundwater composition (DH-7/563.75) varied randomly according to analytical uncertainties. 77
Figure 4.3-47 Total radium concentration versus pH defined by the solubility of radium in a Tono groundwater composition (DH-7/563.75) varied randomly according to analytical uncertainties. 78
Figure 4.3-48 Total actinium concentration versus pH defined by the solubility of $AcOHCO_3$ in a Tono groundwater composition (DH-7/563.75) varied randomly according to analytical uncertainties. 78
Figure 4.3-49 Total actinium concentration versus pH defined by the solubility of $AcPO_4$ in a Tono groundwater composition (DH-7/563.75) varied randomly according to analytical uncertainties. Variations in solubility depend only moderately upon pH variations. 79
Figure 4.3-50 Total thorium concentration versus pH defined by the solubility of amorphous thorium dioxide in a Tono groundwater composition (DH-7/563.75) varied randomly according to

analytical uncertainties. 79
Figure 4.3-51 Total protoactinium concentration versus pH defined by the solubility of Pa_2O_5 in a Tono groundwater composition (DH-7/563.75) varied randomly according to analytical uncertainties. 80
Figure 4.3-52 Total uranium concentration versus pH defined by the solubility of amorphous uranium dioxide in a Tono groundwater composition (DH-7/563.75) varied randomly according to analytical uncertainties. 80
Figure 4.3-53 Total neptunium concentration versus pH defined by the solubility of amorphous neptunium dioxide in a Tono groundwater composition (DH-7/563.75) varied randomly according to analytical uncertainties. 81
Figure 4.3-54 Total plutonium concentration versus pH defined by the solubility of plutonium dioxide in a Tono groundwater composition (DH-7/563.75) varied randomly according to analytical uncertainties. 81
Figure 4.3-55 Total plutonium concentration versus pH defined by the solubility of $NaPu(CO_3)_2$ in a Tono groundwater composition (DH-7/563.75) varied randomly according to analytical uncertainties. 82
Figure 4.3-56 Total plutonium concentration versus pH defined by the solubility of $PuOHCO_3$ in a Tono groundwater composition varied randomly (DH-7/563.75) according to analytical uncertainties. 82
Figure 4.3-57 Total plutonium concentration versus pH defined by the solubility of $PuPO_4$ in a Tono groundwater composition varied randomly (DH-7/563.75) according to analytical uncertainties. 83
Figure 4.3-58 Total americium concentration versus pH defined by the solubility of $AmOHCO_3$ in a Tono groundwater composition varied randomly (DH-7/563.75) according to analytical uncertainties. 83
Figure 4.3-59 Total americium concentration versus pH defined by the solubility of $AmPO_4$ in a Tono groundwater composition (DH-7/563.75) varied randomly according to analytical uncertainties. 84
Figure 4.3-60 Total curium concentration versus pH defined by the solubility of $CmOHCO_3$ in a Tono groundwater composition (DH-7/563.75) varied randomly according to analytical uncertainties. 84
Figure 4.3-61 Total curium concentration versus pH defined by the solubility of $CmPO_4$ in a Tono groundwater composition (DH-7/563.75) varied randomly according to analytical

uncertainties. 85
Figure 4.3-62 Results of factor analyses for the subset of samples in Table 4.2-1 for which solubility-controlled concentrations could be calculated for Sn Sm Pd Pa Th Pb Ac Tc U Pu Np Cm Am Ra Nb Zr Se. 85
Figure 4.3-63 Simulation of the effects of drilling fluid contamination on the calculated solubilities of U and Tc. 93
Figure 4.3-64 Simulation of the effects of drilling fluid contamination on the calculated solubility of Se ($FeSe_2$ was the solubility-controlling phase). 93
Figure 4.3-65 Simulation of the effects of drilling fluid contamination on the calculated solubility of Zr. 94
Figure 4.3-66 Simulation of the effects of drilling fluid contamination on the calculated solubility of Nb. 94
Figure 4.3-67 Simulation of the effects of drilling fluid contamination on the calculated solubility of Sm.. 95
Figure 4.3-68 Simulation of the effects of drilling fluid contamination on the calculated solubility of Pb. 95
Figure 4.3-69 Simulation of the effects of drilling fluid contamination on the calculated solubility of Ra. 96
Figure 4.3-70 Simulation of the effects of drilling fluid contamination on the calculated solubility of Ac. 96
Figure 4.3-71 Simulation of the effects of drilling fluid contamination on the calculated solubility of Th. 97
Figure 4.3-72 Simulation of the effects of drilling fluid contamination on the calculated solubility of Pa. 97
Figure 4.3-73 Simulation of the effects of drilling fluid contamination on the calculated solubility of Np. 98
Figure 4.3-74 Simulation of the effects of drilling fluid contamination on the calculated solubility of Pu. 98
Figure 4.3-75 Simulation of the effects of drilling fluid contamination on the calculated solubility of Am. 99
Figure 4.3-76 Simulation of the effects of drilling fluid contamination on the calculated solubility of Cm. 99
Figure 4.3-77 Comparison between element concentrations calculated when the water from DH-7, 563.75 m depth is charge-balanced with HCO_3^- and concentrations calculated when the same water is equilibrated with atmospheric CO_2. 101
Figure 4.3-78 Comparison between element concentrations calculated when various constraints are imposed on redox and the concentration of dissolved carbon in the water from 563.75 m depth in DH-7. 102
Figure 5.1-1 Variations in groundwater chemistry in the Tono area (after JNC, 2000). 104
Figure 5.1-2 Variations in groundwater chemistry in the area around the

Mizunami Underground Research Laboratory site (after JNC, 2003).105
Figure 5.1-3 Illustration of the variations in redox conditions observed in groundwaters from the Tono area. 106
Figure 5.1-4 Schematic illustration of Ozone(O3) simulations of redox front migration. 107
Figure 5.1-5 Calculated propagation of a redox front at which oxygen is completely depleted through the Toki Granite. 109
Figure 5.2-1 Permeability field around the Mizunami Underground Research Laboratory site consistent with the maximum interpreted frequency of IMFs. 111
Figure 5.2-2 Permeability field around the Mizunami Underground Research Laboratory site consistent with the minumum interpreted frequency of IMFs. 112
Figure 5.2-3 Summary of calculated element solubilities in the groundwaters from Table 4.2-1. 114
Figure 5.2-4 Summary of calculated solubilities shown in Figure 5.2-3 with an expanded concentration scale and with Pd removed. 115
Figure 5.2-5 Summary of calculated element solubilities in the groundwaters from Table 4.2-1. 116
Figure 5.2-6 Summary of calculated solubilities shown in Figure 5.2-5 with an expanded concentration scale and with Pd removed. 117
Figure 5.2-7 Solubilities of elements as a function of Eh for all the reported groundwaters in Table 4.2-1 for which solubilities of the listed elements could be calculated. 119
Figure 5.2-8 Relationships between element concentrations, Eh and pH for a water composition based on that from DH-7, depth of 563.75 m. 122
Figure 5.2-9 Relationship between Pu concentration and Eh for a water composition based on that from DH-7, depth of 563.75 m. 126

Tables

Table 4.2-1 Summary of the geochemical data from Tono used in the calculations. 21
Table 4.3-1 Potential solubility-controlling mineral phases in the Tono groundwater system. 69
Table 4.3-2 Estimated analytical uncertainties used in sensitivity calculations 71
Table 4.3-3 Correlations between calculated solubilities and input parameter values. 87

1 Introduction

The work considers the extent to which uncertainties in site information (principally geochemical data and the relationships between geochemical and hydrogeological heterogeneities) are relevant to Performance Assessment/Safety Assessment (hereafter just 'PA').

Over timescales that are relevant to PA the 3D-heterogeneity in the geochemical characteristics of groundwater could potentially influence the solubility and migration of radionuclides. It is important to evaluate this possible control, taking into account uncertainties in the groundwater chemistry.

The purpose of the work described here was to develop a method for making such evaluations, using past analytical data and site investigation results from the on-going generic geoscientific investigations in the Tono area. It is also aimed to indicate clearly what data quality must be attained to enable the geochemical characteristics of groundwater to be evaluated adequately, so as to assess the 3D-heterogeneity of the groundwater chemistry.

2 Approach

It is important to indicate the significance of geochemical and geological uncertainties in a way that is readily understandable by both geoscientists involved in site characterisation and workers involved in PA. A convenient way to do this is to calculate the effects of these uncertainties on the solubilities of PA-relevant elements.

Following discussions with JNC, it was decided that the work would focus on 18 the elements which positioned as "The safety-relevant radionuclides" in JNC's Report (JNC, 2000), listed below:

Se, Zr, Nb, Tc, Pd, Sn, Cs, Sm, Pb, Ra, Ac, Th, Pa, U, Np, Pu, Am, Cm

It is emphasised that consideration of these elements is purely illustrative. It is recognized that in fact many of them are unlikely to be solubility-controlled in the geosphere around any future repository.

Following an evaluation of the solubilities of these elements and an appraisal of the chemical parameters that control these solubilities, the likely 3D variability in the concentrations of these elements is discussed. The discussion takes into account uncertainties in the hydrogeological heterogeneity of the geosphere. Alternative possible relationships between these heterogeneities and variations in groundwater chemistry are also considered.

3 Establishing parameters

To enable meaningful solubility calculations to be made, published literature on the solubility and aqueous speciation of the above elements was reviewed.

3.1 Selenium

The solubility-limiting solid phase for this element is critically dependent on the redox state of the system. Under reducing conditions, the solubility of selenium is limited by the precipitation of selenides, mainly of Fe, Cu and Pb, keeping Se at low concentration levels. The predominant aqueous species under reducing conditions is likely to be HSe^-.

Due to similarities of selenide in charge and ionic radius with sulphide, substitution and co-precipitation of these anions can occur (Sellin and Bruno, 1992). The availability of sulphide is thus an important factor in controlling Se solubility. Under oxidising conditions, solubilities increase dramatically. However, even under oxidising conditions, the reported Se levels in UK groundwaters (Edmunds et al., 1989) are in the range (1.2×10^{-8} to 3×10^{-10} M).

The other effect on selenium solubilities is the concentration of Fe in the groundwaters, in such case, the solubility of the solid phase increases when decreasing the iron concentration. A realistic solubility limit is expected to be below 6×10^{-7} M calculated for $FeSe_2$ (Berner, 1994).

Selenium has a crustal abundance of 0.05 ppm and is thus a comparatively rare element. Selenium has an order of magnitude higher concentration in shales (0.6 ppm) than in igneous rocks such as granite or basalt (Krauskopf, 1967). An estimate of the ratio of sulphur to selenium in igneous rocks is 6000 to 1. In seleniferous soils, selenium contents may be as high as 80 ppm.

Concentrations of selenium in coal and fuel oil range from 1.47 to 8.1 and 2.4 to 7.5 ppm, respectively. The combustion of fossil fuels mobilises ~4.5×10^8 g of selenium annually, whereas the annual flux from river discharges to the oceans is 7.2×10^9 g (Siu and Berman, 1989). Because of the similarity of ionic radius between sulphur (S^{2-} = 1.84 Å) and selenium (Se^{2-} = 1.91 Å), selenium will substitute readily for sulphur in solid sulphides and occurs in varying proportions in pyrite, chalcopyrite, pyrrhotite, galena, sphalerite, cinnababar, stibnite, molybdenite, arsenopyirte and others. Native Se occurs in nature only rarely. Selenium is a major component of 40 minerals and a minor constituent of 37 others (Elkin, 1982). Some selenium-bearing minerals are: ferroselite $FeSe_2$); clausthalite (PbSe); stilleite (ZnSe); cadmoselite (CdSe); berzelianite (Cu_2Se); and eucairite (AgCuSe). Galena (PbS) and clausthalite (the most abundant Se-mineral) form an isomorphous series. Se also occurs as selenites (cf.

sulphites, which do not occur in nature). Selenates are very rare minerals, many selenates are isostructural with their corresponding sulphates (e.g. $PbSO_4$ is isostructural with $PbSeO_4$, kerstenite). Silicates of Se are not known. Typical Se contents in minerals are (Wedepohl, 1978): galena - 0-20 %; molybdenite - 0-1000 ppm; pyrite - 0-3 %; pyrrhotite - 1-60 ppm; pentlandite - 27-67 ppm; sphalerite - 1-120 ppm; millerite - 5-10 ppm; marcasite - 3-80 ppm.

Ferroselite occurs in roll-front type uranium deposits in sandstones and occurs at the interface between oxidised sandstone (containing goethite, limonite, and hematite) and reduced pyritic uranium ore (Howard, 1977). This implies that selenium and ferrous iron in aqueous solution produced by the oxidation of seleniferous pyrite have combined to form ferroselite. Therefore, ferroselite is stable under conditions more oxidising than those required for pyrite.

The normal Se contents of the rock samples from Pocos de Caldas ranges between 0 and 10 ppm but at the redox front it can surpass 120 ppm (MacKenzie et al., 1991).

In aqueous systems, selenium may occur as one of three oxidation states (-II, IV, VI). Only two oxidation states of selenium are thought to be important in seawater: +4 and +6. Se contents in sea water ranges between 0.2 and 2.4×10^{-9} M, and the average residence time is 30000 years (Whitfield and Turner, 1987).

The total selenium content of rivers worldwide is in the range $0.2^{-9} \times 10^{-9}$ M (Cutter, 1989). Selenium concentrations in the Truckee, Walker, and Carson River systems which drain the eastern slope of the low Se content Sierra Nevada, California and Nevada, are low, ranging from less than 0.3×10^{-9} M to about 16×10^{-9} M (Doyle et al., 1995). The Se concentration in dilute oxygenated groundwater at pH 7 range between 1.2×10^{-9} and 1.2×10^{-8} M (Edmunds et al., 1989). The amount of Se in Cigar Lake groundwater never reaches the limit of detection 0.38 µM (Cramer et al., 1994).

3.2 Zirconium

ZrO_2 is likely to be the solubility limiting solid phase in most groundwaters. This solid phase, presents different degrees of stability depending on crystallinity, a common thread in many four-valent metal oxides. Zirconium contents in natural waters is in general much lower than the calculated solubilities, this is mainly because Zr normally resides in very weathering-resistant silicates, and it dissolution is kinetically controlled at the source. This fact is normally used in geochemistry to define the background unaltered level in bedrock. The dominant aqueous species is likely to be $Zr(OH)_4(aq)$. Zr solubilities are independent of redox, but may be pH-dependent according to the range of pH considered.

Zirconium is a refractory lithophile element and occurs predominantly in the 4+ valence state with an ionic radius of 0.78 Å. The average abundance of zirconium in soils,

earth crust, sediments and igneous rocks is 300, 190, 200 and 170 ppm, respectively (Bockris, 1977).

The most abundant Zr minerals are zircon ($ZrSiO_4$) and baddeleyite (ZrO_2). Zr forms a range of oxides, silicates, halides, oxyhalides and chalcogenides. Zr will substitute for a range of elements of similar ionic radius, such as: Mg2+ (0.80 Å); Fe^{2+} (0.86 Å), Y^{3+} (0.98 Å); Ti^{4+} (0.69 Å), Nb^{3+} (0.72 Å); and Ta^{5+} (0.72 Å). Ilmenite, rutile, and perovskite can contain up to 0.1 % Zr. Varying, but significant amounts of Zr can be found in clinopyroxene, amphibole, mica and garnet. Concentrations of ~100 ppm in these minerals are frequently encountered. These substitutions may be of the type: $Zr^{4+} = Na^{+} + Fe^{3+}$. There are ~10 oxides, 2 carbonates and sulphates and ~20 silicates listed in Wedepohl (1978).

The samples of the massive U-ore from Cigar Lake site have a Zr content who reach 2740 ppm (Smellie et al., 1994). The normal Zr contents of the rock samples from Poços de Caldas ranges between 100 and 2500 ppm (MacKenzie et al., 1991).

In seawater, Zr is predicted to occur as $Zr(OH)_5^-$ and is rapidly removed from seawater on the surfaces of sinking particles (McKelvey and Orians, 1993). These authors measured a dissolved Zr content of seawater varying from 12-95 x 10^{-12} M in surface waters to 300 x 10^{-12} M in deep water. This suggests that there is both a detrital and a sea-floor source of Zr in the oceans. Ferromanganese nodules in the equatorial by iron/manganese oxyhydroxides (Calvert and Piper, 1984). Phosphatic fish debris can act as a major sink for Zr and REE dissolved in seawater, suggesting strong complexation of Zr by phosphate ligands (Oudin and Cocherie, 1988).

Salvi and Williams-Jones (1990) inferred from fluid inclusion compositions that hydrothermal solutions (~100 ° C) transporting Zr in an altered peralkaline granite were of low-salinity and fluorine-rich.

Only in a few groundwater samples from Poços de Caldas, Zr contents surpass 1.1 µM (Nordstrom et al., 1991).

In a survey of alkaline thermal waters in granites in southern Europe, Alaux-Negrel et al. (1993) concluded that zirconium (along with other tri- and tetravalent elements) was associated with a particulate fraction (<450 µm) in the groundwaters. This indicates that Zr was sorbed on the particulate fraction in the groundwaters and not in true solution. In a survey of over 400 groundwater compositions in a variety of rocks in the U.K., Edmunds et al. (1989) detected Zr in only one sample of groundwater (34 x 10^{-9} M). Elsewhere, Zr was below detection limits (2.1-7.7 x 10^{-9} M). Zr in oilfield waters of the U.S.A. is in the range 0.11-0.22 x 10^{-9} M (Rittenhouse et al., 1969).

3.3 Niobium

Solubility is likely to be limited by the Nb_2O_3 phase, and solubilities increase with pH. The speciation in granitic groundwaters is likely to be dominated by NbO_3^- and $Nb(OH)_5(aq)$, depending on the pH of the groundwater considered. Its solubility is independent of redox and ligands other than OH^-.

Niobium is a refractory lithophilic element (like zirconium) and has an identical abundance of 20 ppm in the crust, granite, basalt and shale (Krauskopf, 1967). The greatest abundance of Nb is in syenites and alkalic rocks (~100 ppm). The lowest abundance is in peridotites (1.5 ppm).

Niobium minerals are almost exclusively oxides. Niobite, (F, Mn)(Nb, $Ta)_2O_6$ shows continuous solid solution with tantalite, thus forming the columbite suite of minerals. The chief hosts for Nb in most rocks are ferromagnesian minerals such as pyroxene, amphibole, biotite, muscovite, sphene, ilmenite and magnetite. Nb contents in these minerals may be up to a few 1000 ppm. Approximately 50 oxides/hydroxides, 1 borate and 10 silicates of Nb are listed in Wedepohl (1978) as occurring in nature. ~30 minerals are listed as containing up to 5 % Nb. Considerable amount of Nb may be found in natural cassiterites (SnO_2) of magmatic and hydrothermal origin, suggesting possible coherence of geochemical behaviour with tin under hydrothermal conditions (Möller et al., 1988).

The samples of the massive U-ore from the Cigar Lake site have a Nb content which reach 50 ppm (Smellie et al., 1994). The normal Nb contents of the rock samples from Poços de Caldas ranges between 30 and 320 ppm (MacKenzie et al., 1991).

Nb(V) is the dominant redox state under natural water conditions (Baes and Mesmer, 1976). Its abundance in seawater is 10^{-10} M.

3.4 Technetium

Under reducing conditions, the solubility limiting solid phase is likely to be hydrous technetium dioxide, although solubility will vary according to the assumed degree of crystallinity of the solid phase. The calculated solubilities are not affected by the different water compositions considered. The aqueous speciation is dominated by $TcO(OH)_2$ in the $TcOCO_3(aq)$ and $Tc(OH)_3CO_3^-$. Solubilities will thus vary with pH, redox and carbonate contents of groundwaters.

The maximum 99Tc contents of one sample from Cigar Lake ore is 0.85×10^{-6} ppm (Fabryka-Martin et al., 1994).

At the Cigar Lake site, the bounding concentrations for nuclear reaction products in groundwaters had been calculated. The maximum calculated 99Tc concentrations in those waters is 10^{-9} M (Fabryka-Martin et al., 1994).

3.5 Palladium

Palladium oxide is the most likely solubility-limiting solid phase. Several insoluble palladium compounds, i.e., sulphides, elemental palladium, can be considered under reducing conditions as solubility limiting solid phases. However, these phases give unrealistically low solubility values. The dominant aqueous complex is likely to be $Pd(OH)_2(aq)$. Pd solubility is thus governed by redox and pH.

Palladium is a platinum metal and its behaviour is strongly linked with other elements of this kind (platinum, ruthenium, osmium, rhodium, iridium), and is thus strongly siderophilic. These metals have a crustal abundance of < 0.05 ppm (Krauskopf, 1967). There are 6 naturally-occurring isotopes of Pd: ^{102}Pd (0.96 %), ^{104}Pd (10.97 %), ^{105}Pd (22.2 %), ^{106}Pd (27.3 %), ^{108}Pd (26.7 %), ^{110}Pd (11.8 %).

Pd may occur in olivine (50 ppb), bronzite (10 ppb), diopside (20 ppb) and serpentine (80 ppb). Zircon may contain 5000 ppb Pd. The average Pd content of rock-forming minerals is < 10 ppb. Accessory minerals such as gadolinite and columbite may be enriched in Pd. Major ore deposits are associated with dunitic ultrabasic rocks and gabbros containing Cu-sulphides. Ni-sulphides are much higher in Pd than non Ni-sulphides. Platinum metals are also found in dunites as discrete native metal occurrences. Platinum metals are strongly enriched in so-called 'black (bituminous) shales', along with elements such as arsenic, silver, zinc, cadmium, lead, uranium, vanadium, molybdenum, antimony and bismuth. Although these rocks are organic-rich, the presence of high concentrations of rare metals are more likely due to deposition from oxidising chloride-rich fluids at a redox front.

The normal Pd contents of the rock samples from Pocos de Caldas ranges between 0.4 and 3 ppm but at the redox front, 26 ppm can be reached (MacKenzie et al., 1991).

The Pd concentration in seawater ranges between 0.18 and 0.66 x 10^{-12} M, and the residence time in the ocean is 50000 years (Whitfield and Turner, 1987).

3.6 Tin

Under reducing conditions SnO_2 is the solubility limiting solid phase, although in theory, tin sulphides could also be stable. The dominant aqueous species are likely to be $Sn(OH)_4(aq)$ and $Sn(OH)_5^-$. Solubilities vary with pH and redox and the availability of sulphide.

The average abundance of tin in soils, earth crust, sediments and igneous rocks is 10, 40, 16, and 32 ppm respectively (Bockris, 1977).

The principal economic source of tin is the oxide, cassiterite (SnO_2) which is associated with granitic magmatism. Sn will also form solid solutions with various ferromagnesian silicates such as pyroxenes, micas and amphiboles. This relates to the substitution of

Sn (ionic radius 0.71 Å) for Ti (ionic radius 0.68 Å) and Fe^{3+} (ionic radius 0.64 Å). Sn in biotite and muscovite may be as high as 1250 ppm. Tin will also occur in sulphides such as stannite, Cu_2FeSnS_4, canfieldite, Ag_2SnSS_6 and teallite, $PbSnS_2$. Tin minerals are comparatively few.

The normal Sn contents of the rock samples from Poços de Caldas ranges between 5 and 20 ppm (MacKenzie et al., 1991).

The oxidation state of tin in seawater is IV, and the content ranges between 5 and 20 x 10^{-12} M (Whitfield and Turner, 1987).

Byrd and Andreae (1986) measured an arithmetic mean for dissolved tin in the world's rivers of 20.5 x 10^{-12} M and estimated a dissolved flux of tin to the oceans of 0.76 x 10^6 mol yr and 300-600 x 10^6 mol yr for the particulate fraction.

Edmunds et al. (1989) measured tin concentrations in groundwaters in various aquifers of the U.K. Values in the range 2.5-8.4 x 10^{-9} M were found in groundwaters in the Millstone Grit and Carboniferous Limestone of Derbyshire, the Old Red Sandstone of Moray, the Trias of Shropshire, the Wealden and Lower Greensand. In only one sample was tin above 8.4 x 10^{-9} M. 19 Bulgarian saline deep groundwaters have Sn concentrations in the range 0-5.6 µM (Pentcheva, 1965). The abundance of tin in hot springs (16-92 °C) in Japan was in the range 0.84-8.4 x 10^{-9} M (Ikeda, 1955).

3.7 Caesium

Caesium is generally assumed to be unlimited by solubility in radioactive waste safety assessments. However, there is a strong likelihood that concentrations in groundwaters will be limited by pollucite-analcime solid solutions. Cs solubility will thus vary with pH and the activities of species such as Al and Si.

The average abundance of caesium in soils, earth crust, sediments and igneous rocks is 5, 1, 10, and 10 ppm, respectively (Bockris, 1977). Pollucite (Cs and Na aluminosilicate) is the Cs bearing mineral with the highest content of Cs, and is found in pegmatitic rocks.

Studies on bentonites from Cabo de Gata (Spain), a result of the alteration of volcanic rocks, show that the Cs is the least mobile element of all the trace elements studied (Caballero et al., 1986).

Cs concentration for rocks from Äspö site is 3.3 ppm whereas the average contents of the groundwaters is 1.9 10^{-8} M (Miller et al., 1994).

The normal Cs contents of the rock samples from Poços de Caldas is about 0.5 ppm but at the redox front it can exceed 5 ppm (MacKenzie et al., 1991). The samples of

the massive U-ore from Cigar Lake site have a Cs content who can reach 1.3 ppm (Smellie et al., 1994).

Cs is a cation with a low polarising power that is so weakly complexed in both freshwater and seawater that its speciation is dominated by the free cation (Turner et al., 1981). The Cs concentration in seawater ranges between 2.3 10^{-9} M (Whitfield and Turner, 1987) and 3.7 10^{-9} M (Lloyd and Heathcote, 1985) and the principal form in which cesium occurs is Cs^{+}. The residence time of Cs in the ocean is 6 x 10^{5} years (Whitfield and Turner, 1987).

3.8 Samarium

The most likely solubility-limiting solid phase is $Sm_2(CO_3)_3$. Aqueous speciation is likely to be dominated by samarium carbonate species. Sm solubility is thus sensitive to pH and carbonate concentrations of groundwaters.

The calculated solubilities are not affected by the different water compositions assumed. Only a slight increase in solubility is calculated by increasing pH.

Sixteen isotopes of samarium exist. Natural samarium is a mixture of seven isotopes, three of which are unstable with long half-lives (Weast, 1975).

Samarium has a crustal abundance of 7.3 ppm, being concentrated in granitic rocks (9.4 ppm) (Krauskopf, 1967).

Grauch (1989) made a comprensive review of the samarium contents in metamorphic rocks. McLennan (1989) studied the contents and processes related with the LREE occurrence in sedimentary rocks.

Samarium is found along with other members of the REE in many minerals, including monazite (to the extent of 2.8 %) and bastnaesite (Weast, 1975). ~200 minerals are known which contain up to 0.01 % lanthanides. The highest concentrations are in bastnaesite (64 wt %), monazite (60 wt %) and cerite (59 wt %). 3 fluorides, 10 oxides, 10 carbonates, 1 borate, 1 sulphate, 8 phosphates and 20 silicate minerals containing REE are listed in Wedepohl (1978). REE contents of basalts and gabbros are concentrated in clinopyroxene rather than plagioclase. Biotites from granites contain more REE than feldspars and quartz.

The natural Sm contents of the reactor zone of Oklo ranges between 1 .7 and 24 ppm (Gauthier-Lafaye, 1995). The samples of the massive U-ore from Cigar Lake site have a Sm content which reach 48.2 ppm (Smellie et al., 1994). The normal Sm contents of the rock samples from Poços de Caldas ranges between 3 and 10 ppm (MacKenzie et al., 1991).

Sm contents in sea water ranges between 2.7 and 6. 8 x 10^{-12} M, and the average residence time is 200 years (Whitfield and Turner, 1987). In the North Atlantic ocean the Sm content increase slightly with depth and its around 4.5 x 10^{-12} M (Elderfield and Greaves, 1989). Elderfield et al. (1990) reported REE analyses of rivers and seawaters. Sm values in river waters are in the range 46-810 x 10^{-12} M.

Sm concentrations in the range 9-239 x 10^{-12} M are reported by Michard et al. (1987) in CO_2-rich groundwaters in granites from Vals-les Bains, France. Their enrichment of heavy REE in these waters is ascribed to carbonate complexing. REE abundances in alkaline groundwaters in granites in southern Europe were associated with colloids (Alaux-Negrel et al., 1993). Smedley (1991) measured samarium concentrations in shallow groundwaters in the Carnmenellis granite and surrounding metasedimentary rocks in the range 0.3-66 x 10^{-9} M. Gosselin et al. (1992) investigated concentrations of REE in chloride-rich groundwater in the Palo Duro Basin, Texas. These authors noted Sm concentrations in the range 0.035-48 x 10^{-9} M. They concluded that chloride complexes dominated the REE speciation with only minor contributions from carbonate and sulphate species. Fresh groundwaters from wells in the schists of the Virginia Piedmont area of the U.S.A. have 60 ppb REE (Wedepohl, 1978).

3.9 Radium

The aqueous speciation is most likely dominated by the Ra^{2+} free cation, however, in waters with higher sulphate content, $RaSO_4$(aq) becomes the dominant aqueous species. The most probable solubility limiting solid phase is $RaSO_4$ or more realistically, a solid solution of $RaSO_4$ with other sulphates (e.g barite). The equilibrium concentrations vary with pH and sulphate content.

Radium is isovalent (+2), with an ionic radius of 1.43 Å. 226Ra is the dominant isotope and exceeds 99 % of total Ra.

Trace radium concentrations in groundwaters will tend to co-precipitate with barium to form barite solid solutions (Doerner and Hoskins, 1925), and is the basis for the removal of radium from mine waters and uranium mill tailings solutions (Sebesta et al., 1981, Paige et al., 1993). The calculated partition coefficient for Ra in alkaline-earth sulphates is greatest in celestite, $SrSO_4$ (280), decreasing through anglesite, $PbSO_4$ (11) to barite (1.8) (Langmuir and Riese, 1985). Ra-Ba sulphates and carbonates should behave as ideal solid solutions.

Radium concentrations are often high in saline waters (Kraemer and Reid, 1984; Dickson, 1985; Laul et al., 1985a, b), geothermal waters (Mazor, 1962; Wollenberg, 1975), but relatively low in low-temperature, low salinity groundwaters (Michel and Moore, 1980; Krishnaswami et al., 1982).

Radium isotope activities in thermal waters of Yellowstone National Park have been investigated by Sturchio et al. (1993). They found that radium concentrations in the

waters were inversely correlated with temperature and that controls on these concentrations were either the solubility of a Ra-barite solid solution in some instances, or ion exchange of Ra with zeolites.

Radium concentrations in natural water rarely exceed 10^{-12} M (Langmuir and Melchior, 1985). Ra contents in seawater ranges between 1.6×10^{-16} and 7×10^{-16} M (Whitfield and Turner, 1987).

The groundwaters from Cigar Lake have a content of Ra between 0.012 and 0.5×10^{-12} M (Cramer et al., 1994).

3.10 Thorium

Likely solubility-limiting phases are ThO_2 and $Th(OH)_4$ of varying degrees of crystallinity. Aqueous speciation is likely to be dominated by the complex $Th(OH)_4(aq)$, but stabilisation of the $Th(CO3)_5^{6-}$ species may increase Th solubility. Th solubility is thus dependent upon pH and carbonate content. However, Th concentrations in natural waters are more likely to be limited by mineral dissolution kinetics and sorption than by true mineral-fluid solubility equilibria (Langmuir and Herman, 1980).

The actinides thorium and uranium are ubiquitous in nature with concentrations in soils, sediments and rocks as high as several tens of parts per million (Choppin and Stout, 1989). Thorium is a lithophilic element and has a crustal abundance of 9.6 ppm (Krauskopf, 1967). The average granite, basalt and shale contain 17, 2.2 and 11 ppm, respectively. The ionic radius of Th^{4+} is 1.02 Å. Similarities in ionic size and bond character link thorium, cerium, uranium and zirconium. ^{232}Th is the dominant isotope of thorium (~100 % of natural abundance) and has a half-life of 1.4×10^{10} years.

Thorium is found in natural systems as the tetravalent cation only. It occurs as a major mineral only in rare phases such as thorianite (ThO_2) and thorite ($ThSiO_4$). The former mineral is isomorphous with uraninite, the latter with zircon. Consequently, a large part of naturally-occurring Th is in zircon. The chief source of Th is in monazite (Ce, La, Y, Th)PO_4 which usually contains 3-9 % and up to 20 % ThO_2. There are many examples of isostructural compounds of Th, Ce, U and Zr: ThS, US, CeS and ZrS; ThO_2, CeO_2, ZrO_2, $ThSiO_4$, $USiO_4$, $ZrSiO_4$; $ThGeO_4$, $UGeO_4$, $CeGeO_4$, $ZrGeO_4$; $BaThO_3$, $BaUO_3$, $BaCeO_3$, $BaZrO_3$. However, there are only a few Th silicates known as compared with the large number of Zr-silicates. A large number of Th sulphides, selenides and tellurides is known. Th is a major cation in only a few minerals, none of which is common. Feldspars, biotites and amphiboles may contain only 0.5-50 ppm Th. Most Th host minerals are refractory to weathering so that Th is considered a pcorly soluble and immobile element. Th is usually fractionated from U during weathering because of the solubility of U(VI). Th is strongly adsorbed by clays and oxyhydroxides so that relatively high concentrations of Th occur in bentonites, marine pelagic clays, manganese nodules and bauxites.

Th in fresh surface waters ranges from 0.043 to 4.3 x 10^{-9} M.

Copenhaver et al. (1993) investigated retardation of ^{232}Th decay chain radionuclides in aquifers in Long Island and Connecticut. They measured retardation coefficients of the order 104-105 for Th. The samples of the massive U-ore from Cigar Lake site have a Th content which reach 141 ppm (Smellie et al., 1994).

In natural waters, Th concentrations are lower and it is often uncertain how the measured concentrations are distributed between species in true solution and those sorbed on suspended material. Uranium is rather abundant in surface seawater, 12 10-9 M, while thorium is present only at 2.5 x 10^{-12} M (Choppin and Stout, 1989). In oceanic water the contents of Th ranges between 5 and 148 x 10^{-14} (Whitfield and Turner, 1987). The residence time is 50 years. The groundwaters from Cigar Lake have contents of Th below 1.5 x 10^{-9} M (Cramer et al., 1994).

Th in alkaline groundwaters in granites in southern Europe was found to be associated with particulate material and not contained in true solution (Alaux-Negrel et al., 1993). Th concentrations of 0.06-0.14 x 10^{-9} M were measured in groundwaters in altered phonolites at Poços de Caldas (Bruno et al., 1992). Th was significantly associated with colloids in groundwaters in contact with uranium ore bodies at Nabarlek and Koongarra in the Alligator Rivers region, Northern Territory, Australia (Short and Lowson, 1988).

3.11 Protactinium

The solubility limiting solid phase could be various oxides and hydroxides.

The aqueous speciation is dominated by hydroxyl complexes. In reality, co-precipitation of Pa with U is most likely (Berner, 1994). Pa solubility will be governed by pH and the nature of U-bearing solids.

The concentration of Pa in marine sediments is 10^{-5} ppm and in the continental earth crust 10^{-6} ppm (Fukai and Yokoyama, 1982). Protactinium occurs in pitchblende to the extent of about 0.1 ppm. Ores from the African Congo have about 3 ppm. Protactinium has thirteen isotopes, the most common of which is ^{231}Pa with a half-life of 32500 years (Weast, 1975). Protactinium is one of the rarest natural occurring elements.

In sea water the concentration of Pa ranges between 10^{-14} M (Lloyd and Heathcote, 1985) and 10-17 M (Fukai and Yokoyama, 1982).

3.12 Uranium

Uranium solubilities are sensitive to redox, pH and carbonate contents of groundwaters. The most likely solubility limiting solid phase is UO_2.

Uranium is a lithophilic element whose geochemistry is intimately linked with that of thorium. Uranium has a crustal abundance of 2.7 ppm, concentrated in granite (4.8 ppm) and shale (3.2 ppm) (Krauskopf, 1967). Naturally-occurring uranium consist of three isotopes: ^{238}U; ^{235}U; and ^{234}U. ^{238}U and ^{235}U are parent isotopes for 2 separate radioactive decay series. No natural fractionation of ^{238}U and ^{235}U has been observed and all materials have a $^{238}U/^{235}U$ ratio of 137.5. Although valence states between +3 and +6 could exist in nature, only the +4 and +6 valence states are of geochemical relevance.

Uranium occurs in a variety of minerals but is concentrated in only a few. The most abundant uranium mineral is uraninite with a formula from UO_2 to U_3O_8. Well-crystallised UO_2 is described as uraninite and the microcrystalline form, pitchblende. Typical uranium contents of rock-forming minerals are as follows: feldspar - 0.1-10 ppm; biotite - 1-60 ppm; muscovite - 2-8 ppm; hornblende - 0.2-60 ppm,; pyroxene - 0.1-50 ppm; olivine ~0.05 ppm; allanite - 30-1000 ppm; apatite - 10-100 ppm. In Wedepohl (1978) the following uranium minerals are listed: 15 oxides, 12 carbonates, 6 sulphates, 30 phosphate-arsenates, 10 vanadates, 15 silicates, 4 niobates and 5 molybdates.

Under oxidising conditions, pitchblende and uraninite are converted to brightly-coloured minerals such as carnotite, $K_2(UO_2)_2(VO_4)2.3H_2O$, tyuyamunite, $Ca(UO_2)_2(VO_4)2.nH_2O$, autunite, $Ca(UO_2)_2(PO_4)2.nH_2O$, and rutherfordine, $UO_2.CO_3$. These minerals are soluble so that uranium may be transported by oxidising groundwater to be re-deposited under more reducing conditions.

The samples of the massive U-ore from Cigar Lake site have a U content which reach 220 ppm (Smellie et al., 1994).

Seawater contains 13.5×10^{-9} M of uranium, mainly in the VI oxidation state. The ocean residence time is 3×10^5 years (Whitfield and Turner, 1987).

Edmunds et al., (1989) noted that most analyses of uranium in groundwaters in aquifers in the UK were below 10^{-7} M, although several anomalous values up to 10^{-5} M were observed. Uranium concentrations in alkaline thermal waters in granites in southern Europe were limited by uraninite solubility (Alaux-Negrel et al., 1993). Bruno et al. (1992) concluded that waters in the alkaline rocks at Poços de Caldas were in equilibrium with pitchblende co-precipitated with Fe(III) oxy-hydroxides, with concentrations in the range: 1.7×10^{-7} - 1.7×10^{-8} M. A similar behaviour across the redox transition was observed in waters in contact with deep seabed sediments of the North Atlantic Abyssal Plain (Santschi et al., 1988), with concentrations ranging from 0.4 to 8×10^{-9} M. In CO_2-rich waters from Valles-Bains (France), uranium concentrations are in the range $1\text{-}3.5 \times 10^{-9}$ M (Michard et al., 1987).

Edmunds et al. (1987), measured uranium concentrations in deep groundwaters of the Carnmenellis granite in the range: 8×10^{-11} - 1.8×10^{-7} M. Uranium concentrations in

Stripa are in the range: 4×10^{-8} to 3.7×10^{-7} M. In the Cigar Lake uranium deposit, uranium concentrations in the reduced zone are in the range 6×10^{-9} to 10^{-7} M, indicating that the waters are in equilibrium with a slightly oxidised uraninite, represented by the stoichiometry $U_3O_7(s)$ (Bruno and Casas, 1994). In the oxidised part of Cigar Lake, the uranium concentrations range between 10^{-9} and 2×10^{-6} M. This would suggest a control by the association of U(VI) to Fe(III) oxyhydroxides, present in this zone. Uranium concentrations associated with the uranium deposit at Crawford (Nebraska), have been reported by Spalding et al. (1984), in the range 20 to 300×10^{-9} M.

At higher temperatures and under reducing conditions the concentrations of uranium appear to be controlled by the uraninite-coffinite transition. Kraemer and Kharaka (1986) measured uranium concentrations in saline waters in geo-pressured aquifers (T: 109-166 °C), in the US Gulf Coast, in the range $0.1\text{-}2 \times 10^{-10}$ M.

The groundwaters from Cigar Lake have under 0.24 μM of U (Cramer et al., 1994).

3.13 Neptunium

At the Cigar Lake site, the bounding concentrations for nuclear reaction products in groundwaters had been calculated. The maximum xNp concentration in those waters is 10^{-10} M (Fabryka-Martin et al., 1994).

3.14 Plutonium

The predominant aqueous species are likely to be $Pu(OH)_4(aq)$ and $Pu(OH)^{2+}$, and Pu^{3+}. Solubility-limiting solids could be oxides or hydroxides. Pu solubility is dependent upon redox, pH, and the abundance of carbonate and sulphate species in groundwater.

Plutonium exists in trace quantities in naturally-occurring uranium ores. It is formed in much the same manner as neptunium, by irradiation of natural uranium with the neutrons which are present (Weast, 1975). The average ^{239}Pu contents of three samples from Cigar Lake ore is 1.2×10^{-6} ppm (Fabryka-Martin et al., 1994). Fifteen isotopes of plutonium are known. By far the most important is the isotope ^{239}Pu, with a half-life of 24360 years, produced in extensive quantities in nuclear reactors from natural uranium (Weast, 1975).

Of the synthetic transuranium elements, plutonium and, to a lesser extent, americium are detectable in ecosystems (Choppin and Stout, 1989). Plutonium is found in relatively higher concentrations in the soil and water near nuclear test sites and reprocessing facilities, primarily associated with sub-surface soils, sediments or suspended particulates in water columns. When vegetation, animals, litter, and soils

are compared, more than 99 % of the plutonium is found in the sediments. Pu is transported mainly in groundwater in the form of soluble species.

Very little plutonium is found in natural aquatic systems (2.89×10^{-17} M), making it difficult to obtain reliable values for the concentration (Choppin and Stout, 1989). Moreover, the amount of plutonium associated with suspended particulates may be more than an order of magnitude greater than that in true solution. The Pu concentrations in seawater, rivers and fresh water ranges between 2.6×10^{-18} M in the Mediterranean Sea and 1.6×10^{-14} M in the Irish Sea, near to Windscale (Choppin and Stout, 1989).

In marine natural waters, the limiting solubility of actinides is usually associated with either carbonate or hydroxide compounds. The insolubility of $Pu(OH)_4$ determines the amount of plutonium in solution, even if Pu(V) or Pu(VI) are the more stable states (Choppin and Stout, 1989).

At the Cigar Lake site, the bounding concentrations for nuclear reaction products in groundwaters had been calculated. The maximum ^{239}Pu concentrations in those waters is 10^{-9} M (Fabryka-Martin et al., 1 994).

3.15 Americium

$AmOHCO_3$ is the likely solubility-limiting phase. Am solubility depends upon redox, pH and carbonate contents of groundwaters.

Among the three isotopes of americium, ^{243}Am is the most stable with a half-life of 8800 years, compared to 470 years for ^{241}Am (Weast, 1975).

Trans-plutonium actinides (Am, Cm) have important III valences analogous to the lanthanides, at least through Bk. The only important Am (IV) aqueous species may be $Am(OH)_5^-$ (Brookins, 1989). The same author gives stability constants for carbonate complexes of trivalent Am and Cm. The stability fields for the Am species with and without carbonate (Brookins, 1988) shows that the most important valence is +3.

Observations of the distribution of ^{241}Am in marine environments indicate that Am has a high affinity for solid surfaces (Shanbhag and Morse, 1982).

3.16 Curium

The solubility limiting solid phase is likely to be $CmOHCO_3(s)$. The aqueous speciation is dominated by the complex $Cm(OH)^{2+}$. Solubility will vary with pH and carbonate content of groundwater.

Thirteen isotopes of curium are known. The most stable, ^{247}Cm, with a half-life of 16 millions years, is so short compared to the earth's age at any primordial curium must

have disappeared. Natural curium has never been detected, not even in natural deposits of uranium (Weast, 1975). The trivalent oxidation state is by far the most stable for the curium element (Baes and Mesmer, 1976).

The stability constants for carbonate complexes of trivalent Cm are given by Brookins (1989).

3.17 Lead

The solubility of lead is governed by redox, pH, and the abundances of carbonate, and sulphate/sulphide in groundwater. Lead is predominantly a chalcophile element and has a crustal abundance of 12.5 ppm (Krauskopf, 1967). Granite and shale have abundances of 20 ppm and basalt 5 ppm. Lead has an abundance in seawater of 0.00003 ppm. Pb behaviour is intimately linked with that of U and Th. Pb^{2+} is more common than Pb^{4+}. Pb^{2+} (1.20 Å) is similar in ionic size to K^+ (1.33 Å); Sr^{2+} (1.12-1.27 Å); and Ba^{2+} (1.34-1.43 Å).

Lead is comprised of four stable isotopes: ^{204}Pb, ^{206}Pb, ^{207}Pb and ^{208}Pb. ^{204}Pb is not of radioactive origin, whereas the others are derived from radioactive decay of 238U, ^{235}U and ^{232}Th. There are 4 radioactive isotopes: ^{210}Pb and ^{214}Pb in the ^{238}U decay chain; ^{211}Pb in the ^{235}U chain and ^{212}Pb in the ^{232}Th chain. All except ^{210}Pb have half-lives less than 12 hours.

The main lead mineral is galena, PbS. Because of its size Pb^{2+} will be incorporated into silicates as large monovalent or divalent metals. It replaces K^+ in minerals (e.g. in feldspar). Mica usually contains less Pb than feldspar. Biotite typically contains 20 ppm Pb and muscovite contains 25 ppm. In K-feldspar, Pb may be greater than 50 ppm. Pb may also occur in plagioclase and amphibole. 240 minerals are listed in Wedepohl (1978). Greater than 33 % of these are sulphides and sulphosalts. Sulphates and phosphates are almost as numerous. Lead halides are relatively rare. Metallic Pb is occasionally found in nature (e.g. Oklo).

Lead is soluble as a chloride complex ($PbCl_2^0$) at pH < 7 and moderately oxidising redox conditions, although fields of stability of $PbCO_3.PbCl_2$ (phosgenite) and $PbCO_3$ (cerussite) extend down to pH 7. Under reducing conditions, Pb is insoluble as galena.

Chloride complexation of lead is important in deep groundwater environments. Complexation of lead with chloride has been investigated in the temperature range 25-300 °C by Seward (1984). At 25 °C, 5 species occur: Pb^{2+}, $PbCl^+$, $PbCl_2^0$, $PbCl_3^-$, $PbCl_4^{2-}$. Free Pb^{2+} predominates at Cl^- < 0.05 m. Acetate complexation of lead has been investigated by Yang et al. (1989). Strong $Pb(Ac)^+$, $Pb(Ac)_2$ and possibly $Pb(Ac)_3^-$ complexes were observed.

The solubility of galena (PbS) has been measured in 1-5 m NaCl solutions by Barrett and Anderson (1988) at temperatures up to 95 °C. The solubility of galena increases with temperature and increasing NaCl concentration. Galena is considerably less soluble than sphalerite (ZnS) under these conditions.

The kinetics of dissolution of lead-barium sulphate solid solutions has been investigated by Paige et al. (1993). The solubility of lead sulphate in brines has been modelled by Paige et al. (1992).

Erel et al. (1991) report Pb concentrations in streamwaters of the Sierra Nevada, U.S.A.

They observed that lead is taken up by particles (mostly iron oxides). Erel and Morgan (1992) concluded that lead both coprecipitates and is adsorbed on Fe-rich particles during early phases of the rock weathering cycle.

Bruno et al. (1992) measured Pb concentrations in groundwaters in alkaline rocks at Poços de Caldas in Brazil in the range 1-5 x 10^{-9} mol dm^{-3}. Edmunds et al. (1989) measured positive values for Pb in U.K. groundwaters only in aquifers in the Millstone Grit and Carboniferous Limestone of Derbyshire and these were all below 1µg/l.

Pb contents of oilfield brines may be as high as 1-17 ppm due to complexing with chloride ions (Kharaka et al., 1980; Carpenter et al., 1974). Relatively high concentrations of Pb have been observed in Salton Sea brines (up to 111 µg/g) which was attributed to chloride complexation (Zukin et al., 1987).

Sorption of lead onto chabazite, vermiculite, montmorillonite, hectorite and kaolinite was investigated by Liang and Sherriff (1993). These minerals contained 27, 16, 9, 9 and 0.4 wt % Pb respectively after equilibration with 0.01 M $Pb(NO_3)_2$ solutions. Ion exchange reached equilibrium after 24 hours for chabazite and vermiculite, but less than 5 minutes for montmorillonite and hectorite. Calcite impurities in the clay minerals effectively removed Pb from solution by the precipitation of cerussite, $PbCO_3$.

4 Solubility calculations using past data

4.1 Computer modelling codes

Solubility diagrams were constructed using the code Geochemist's Workbench (GWB; Bethke, 1996). The thermodynamic database 011213g0.tdb (Yoshida and Yui, 2003) was used.

Solubility calculations, which evaluated a range of alternative geochemical conditions, were made using the code PHREEQC v 2.8 (Parkhurst and Appelo, 1999). In this case, the PHREEQC version of the above thermodynamic database, 011213c0.tdb, was employed.

It is noted that the thermodynamic data in JNC's databases 011213g0.tdb and 011213c0.tdb were taken at face value when drawing conclusions from calculations. This is reasonable in view of the main requirement being to understand the significance of uncertainties associated with site investigations (sampling, analytical uncertainties etc). However, it should be borne in mind that significant uncertainties remain as to the quality of much of the data and that this would have implications for the absolute magnitudes of calculated solubilities. For example, these databases contain the same equilibrium constants describing the solubility of $AmOHCO_3$ and $CmOHCO_3$. An implication is that the perhaps one is used as an analogue of the other.

Additional uncertainties arise because the thermodynamic data in these databases are quoted only for 25°C. While most of the in-situ groundwaters have temperatures that are little different from this temperature, the significance of these small differences is cannot be estimated precisely.

4.2 Past geochemical data

4.2.1 Geochemical data

The geochemical modelling used groundwater analyses from several of the boreholes at Tono (Table 4.2-1). Of these boreholes, DH-2, DH15, MSB-2, MSB-4 and MIZ-1 are located in or near the site of the Mizunami underground research laboratory. The other boreholes, DH-4, DH-5, DH-6, DH-7 and DH-8 are located around near the Tono Geoscience Center, towards the west of the area that has been investigated by JNC (Figure 4.2-1). Additionally, other data obtained from the boreholes, including geological information and rock core information, together with supporting information concerning data quality, were supplied by JNC.

4.2.2 Review of geochemical data quality

The geochemical data were supplied with information about their quality, which was summarised as a Quality Score (QS). The QS is based on eight factors that involve both hydrochemical measurements and descriptions of sampling conditions, and is somewhat similar to the Swedish/Finnish QS system though it has been altered and simplified to make it practicable with the amount of data and other information that are available for the Tono data set.

The eight quality factors that are taken into account are:

- Degree of contamination by drilling water, as indicated by fluorescent dye;
- Cation-anion charge balance;
- Delay time between sampling and analysis of unstable determinands: alkalinity, reduced sulphur and ferrous iron;
- Sampling container, i.e. whether in a downhole gas-tight vessel or pumped into an open bottle at the surface;
- Evidence from pH, EC and Eh stability from time series monitoring;
- Length of discrete sampling interval between packers, i.e. the longer the interval, the greater chance there is of mixing of chemically-discrete groundwater flows within the interval;
- Sampling logistics, i.e. whether in a downhole 'in situ' sampler or pumped to the surface (possibly by air-lifting);
- Location where measurement or analyses of physico-chemical parameters, i.e. downhole, surface monitoring (with flow cell where appropriate), or laboratory.

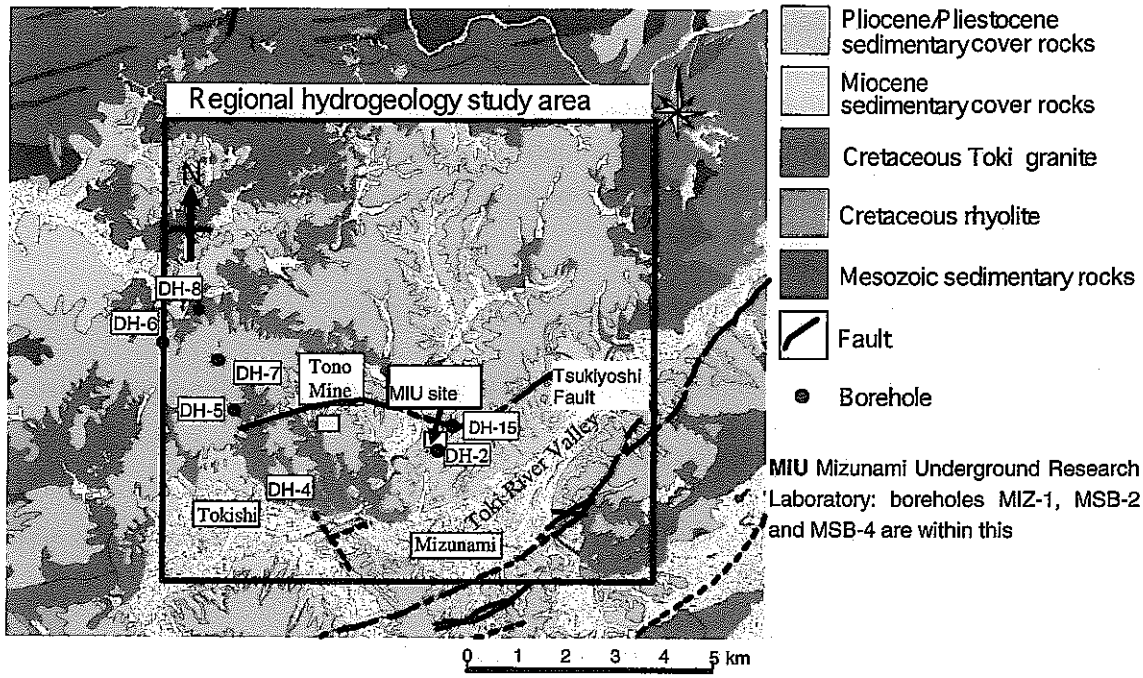

Figure 4.2-1 Locations of the boreholes that yielded the data considered in the project.

Table 4.2-1 Summary of the geochemical data from Tono used in the calculations. The data in a red column is located in or near the site of MIU. And, the data in a yellow column is located around near the Tono Geoscience Center.

No.	location	Min. Depth	Max. Depth	Elevation		Sampling or Analyzing	Temp.	pH	Eh	cond.	Na^+	K^+	Ca^{2+}	Mg^{2+}	Sr^{2+}
		mbgl	mbgl	masl	masl	Date	degC		mv	mS/m	ppm	ppm	ppm	ppm	ppm
AKEYO F.															
1	DH-15	63.0	72.5			2003.10.10		6.8		38	58.3	1.6	3.2	0.4	<0.3
2	DH-15	84.5	97.5			2003.10.4		9.1		39	65.4	1.1	2.4	0.2	<0.3
TOKI LIGNITE BEARING F. (LOWER)															
3	MSB-2	79.0	130.5	119.5	68.0	2002.7.7	21.8	9.1	-116	-	107	0.23	15.00	0.18	<0.3
4	MSB-3	132.0	154.0	66.5	44.5	2002.6.29	21.3	8.8	-75	-	130	1.90	27.00	0.11	<0.3
TOKI GRANITE															
5	DH-2	207.5	209.5	-13.9	-15.9	2002.9.23	24.2		-60	48	78.0	1.09	15.1	0.20	
6	DH-2	226.5	237.0	-34.9	-43.4	2002.10.9	22.4	8.7	-36	53	99.5	0.97	17.6	0.17	
7	DH-2	302.7	304.7	-109.1	-111.1	2002.9.25	22.5		0	65	96.6	0.96	19.2	0.12	
8	DH-2	305.6	307.6	-111.9	-113.9	2002.9.10	23.5		-61	63	88.6	0.56	16.5	0.10	
9	DH-2	309.7	311.7	-116.1	-118.1	2002.9.17	23.2		-19	65	91.0	0.64	22.1	0.12	
10	DH-2	313.0	315.0	-119.4	-121.4	2002.9.20	24.7		-90	66	97.0	0.62	21.7	0.11	
11	DH-2	320.9	328.4	-127.3	-134.8	2002.10.6	23.2	8.6	-103	66	103	0.65	19.9	0.12	
12	DH-2	347.8	349.8	-154.2	-156.2	2002.9.27	23.7	8.7	-32	77	117	0.64	25.5	0.10	
13	DH-2	365.5	367.5	-171.9	-173.9	2002.10.1	24.6	8.8	-121	78	114	0.60	25.3	0.10	
14	DH-2	439.5	448.0	-245.9	-254.4	2002.10.12	23.2	8.8	-80	88	141	0.86	36.3	0.12	
15	DH-2	451.2	459.7	-257.6	-266.1	2002.10.15	25.0	8.7	-122	100	157	1.00	42.1	0.19	
16	DH-4	185.5	188.5	81.1	78.1	1995.4.18	13.0	6.8	49	17.2	13.3	6.13	17.6	1.88	0.11
17	DH-5	323.8	330.8	-13.4	-20.4	1997.8.6 21	19.3	7.8	-16	15.9	10.3	3.00	19.0	0.82	0.15
18	DH-6	733.0	740.0	-413.7	-420.7	1997.12.19 22	25.5	8.9	-303	14.8	21.4	0.59	3.20	0.05	n.d.
19	DH-7	438.0	444.5	-97.8	-104.3	1999.5		8.9	-	9.78	7.7	1.56	11.9	0.70	

Table 4.2-1 continued.

index	location	Min. Depth mbgl	Max. Depth mbgl	Elevation masl	masl	Sampling or Analyzing Date	Temp. degC	pH	Eh mv	cond. mS/m	Na^{+} ppm	K^{+} ppm	Ca^{2+} ppm	Mg^{2+} ppm	Sr^{2+} ppm
TOKI GRANITE continued															
20	DH-7	479.0	485.5	-138.8	-145.3	1999.6		10.3	-	13.3	13.3	2.49	13.7	0.24	
21	DH-7	479.0	485.5	-138.8	-145.3	2000.7		9.9	-	13.4	18.6	2.36	9.25	0.03	
22	DH-7	560.5	567.0	-220.3	-226.8	1998.4.20 22	26.2	10.1	-400	17.9	25.4	2.30	5.4	0.31	0.08
23	DH-7	560.5	567.0	-220.3	-226.8	1999.7		10.4	-	19.2	20.4	3.65	13.0	0.01	
24	DH-7	560.5	567.0	-220.3	-226.8	2000.8		10.1	-	13.1	19.0	2.42	10.6	0.01	
25	DH-7	598.0	604.5	-257.8	-264.3	1999.8		10.8	-	25.0	27.2	3.40	20.3	0.01	
26	DH-7	598.0	604.5	-257.8	-264.3	2000.9		10.8	-	20.2	28.8	2.84	18.2	<0.01	
27	DH-7	660.0	666.5	-319.8	-326.3	1999.9		10.1	-	15.3	18.6	1.63	13.5	0.29	
28	DH-7	660.0	666.5	-319.8	-326.3	2000.10		9.6	-	17.5	30.8	0.96	10.2	0.01	
29	DH-7	735.5	742.0	-395.3	-401.8	1999.10		11.1	-	32.3	40.7	5.72	20.0	0.02	
30	DH-7	735.5	742.0	-395.3	-401.8	2000.11		11.2	-	30.7	45.6	4.58	18.8	0.02	
31	DH-7	833.5	840.0	-493.3	-499.8	1998.4.2 9	29.3	9.6	-373	29.8	31.3	9.10	3.2	0.58	0.06
32	DH-7	833.5	840.0	-493.3	-499.8	1999.11		10.7	-	23.7	40.6	1.92	8.2	0.04	
33	DH-7	880.0	886.5	-539.8	-546.3	1998.3.11 19	30.9	9.4	-355	29.7	48.0	22.0	5.4	0.71	0.06
34	DH-7	880.0	886.5	-539.8	-546.3	1999.12		10.5	-	23.5	46.0	4.2	9.7	0.14	
35	DH-7	880.0	886.5	-539.8	-546.3	2000.12		10.7	-	24.9	49.0	3.7	10.0	0.07	
36	DH-8	641.5	648.0	-371.7	-378.2	1998.3.16 27	27.3	9.0	-353	19.5	23.2	5.10	2.8	0.04	0.18
37	DH-8	693.5	700.0	-423.7	-430.2	1998.4.2 5	28.2	8.5	-274	18.7	22.1	0.48	6.9	0.09	0.25
38	DH-8	745.5	752.0	-475.7	-482.2	1998.4.13 16	29.3	8.4	-298	20.7	28.0	4.50	1.0	0.09	0.23
39	DH-8	869.0	875.5	-599.2	-605.7	1998.4.29 5.3	31.8	8.8	-305	32.7	39.1	11.0	4.3	0.65	0.18
40	DH-8	975.0	981.5	-705.2	-711.7	1998.5.14 18	33.7	8.8	-364	26.2	25.8	0.93	6.8	0.65	0.16
41	MSB-2	171.5	178.5	27.0	23.0	2002.7.22	26.5	8.6	-140	-	110	1.10	27	0.23	<0.3
42	MSB-4	95.5	99.0	119.0	115.5	2002.8.13	23.0	8.6	-86	-	74	0.23	14	<0.1	<0.3
43	MIZ-1	113.1	116.3			2003.4.20	19.6	9.2	-71	352	59	0.3	5.9	<0.1	<0.3
44	MIZ-1	215.0	226.7			2003.7.9	22.3	8.9	-280	480	66	0.9	11	<0.1	<0.3

Table 4.2-1 continued.

index	location	Min. Depth mbgl	Max. Depth mbgl	Elevation masl	Elevation masl	Sampling or Analyzing Date	TC ppm	IC ppm	TOC ppm	CO_3^{2-} 1) ppm	HCO_3^- 1) ppm	alk. meq/l	SO_4^{2-} ppm	HS^- ppm	S^{2-} ppm
AKEYO F.															
1	DH-15	63.0	72.5			2003.10.10	26.2	25.8	2.4			2.53	11.9		<0.0004
2	DH-15	84.5	97.5			2003.10.4	29.2	26.5	3.7			2.60	11.6		1.28
TOKI LIGNITE BEARING F. (LOWER)															
3	MSB-2	79.0	130.5	119.5	68.0	2002.7.7	7.6	6.0	1.6			0.68	0.81		0.062
4	MSB-2	132.0	154.0	66.5	44.5	2002.6.29	4.8	4.0	0.73			0.45	<0.4		0.042
TOKI GRANITE															
5	DH-2	207.5	209.5	-13.9	-15.9	2002.9.23	12.3	12.3	<2	<3	66.9		6.27		
6	DH-2	228.5	237.0	-34.9	-43.4	2002.10.9	10.8	10.8	<2	<3	56.7		3.66		
7	DH-2	302.7	304.7	-109.1	-111.1	2002.9.25	3.85	3.9	<2	4.52	33.2		3.88		
8	DH-2	305.6	307.6	-112.0	-113.9	2002.9.10	7.06	7.1	<2	6.59	30.9		3.91		
9	DH-2	309.7	311.7	-116.1	-118.1	2002.9.17	7.14	7.1	<2	5.07	33.0		3.90		
10	DH-2	313.0	315.0	-119.4	-121.4	2002.9.20	7.32	7.3	<2	3.83	35.3		3.74		
11	DH-2	320.9	326.4	-127.3	-134.8	2002.10.6	7.18	7.2	<2	<3	45.6		3.70		
12	DH-2	347.8	349.8	-154.2	-156.2	2002.9.27	5.51	5.5	<2	<3	34.9		3.96		
13	DH-2	365.5	367.5	-171.9	-173.9	2002.10.1	5.13	5.1	<2	5.14	23.6		3.74		
14	DH-2	439.5	448.0	-245.9	-254.4	2002.10.12	4.71	4.7	<2	4.9	21.9		3.22		
15	DH-2	451.3	459.7	-257.6	-266.1	2002.10.15	4.43	4.4	<2	2.9	24.5		2.86		
16	DH-4	185.5	188.5	81.1	78.1	1995.4.18				<1	88.5		0.09		<0.05
17	DH-5	323.8	330.8	-13.4	-20.4	1997.8.6 21	16.2	14.5	1.7				7.8		n.d.
18	DH-6	733.0	740.0	-413.7	-420.7	1997.12.19 22	14.1	12.4	1.7			0.7	5.47		n.d.
19	DH-7	438.0	444.5	-97.8	-104.3	1999.5						0.73	5.6		
20	DH-7	479.0	485.5	-138.8	-145.3	1999.6						0.89	6.8		
21	DH-7	479.0	485.5	-138.8	-145.3	2000.7						0.83	5.73		

Table 4.2-1 continued.

index	location	Min. Depth mbgl	Max. Depth mbgl	Elevation masl	masl	Sampling or Analyzing Date	TC ppm	IC ppm	TOC ppm	CO_3^{2-} 1) ppm	HCO_3^- 1) ppm	alk. meq/l	SO_4^{2-} ppm	HS^- ppm	S^{2-} ppm
TOKI GRANITE continued															
22	DH-7	560.5	567.0	-220.3	-226.8	1998.4.20 22	20.8	18.4	2.4			1.51	4.64		n.d.
23	DH-7	560.5	567.0	-220.3	-226.8	1999.7						1.25	6.5		
24	DH-7	560.5	567.0	-220.3	-226.8	2000.8						0.83	6.33		
25	DH-7	598.0	604.5	-257.8	-264.3	1999.8						1.49	4.5		
26	DH-7	598.0	604.5	-257.8	-264.3	2000.9						1.26	4.19		
27	DH-7	660.0	666.5	-319.8	-326.3	1999.9						0.97	5.0		
28	DH-7	660.0	666.5	-319.8	-326.3	2000.10						1.01	4.57		
29	DH-7	735.5	742.0	-395.3	-401.8	1999.10						2.08	6.0		
30	DH-7	735.5	742.0	-395.3	-401.8	2000.11						1.96	2.78		
31	DH-7	833.5	840.0	-493.3	-499.8	1998.4.2 9	21.6	20.3	1.3			1.65	5.55		n.d.
32	DH-7	833.5	840.0	-493.3	-499.8	1999.11						1.48	4.2		
33	DH-7	880.0	886.5	-539.8	-546.3	1998.3.11 19	24.8	22	2.8			1.79	5.35		n.d.
34	DH-7	880.0	886.5	-539.8	-546.3	1999.12						1.63	2.8		
35	DH-7	880.0	886.5	-539.8	-546.3	2000.12						1.55	1.96		
36	DH-8	641.5	648.0	-371.7	-378.2	1998.3.16 27	15.0	14.2	0.81			1.11	n.d.		n.d.
37	DH-8	693.5	700.0	-423.7	-430.2	1998.4.2 5	18.1	17.2	0.93			1.36	4.18		n.d.
38	DH-8	745.5	752.0	-475.7	-482.2	1998.4.13 16	17.3	16.3	1.0			1.32	3.73		n.d.
39	DH-8	869.0	875.5	-599.2	-605.7	1998.4.29 5.3	15.7	15.1	0.6			1.32	3.09		n.d.
40	DH-8	975.0	981.5	-705.2	-711.7	1998.5.14 18	15.9	15.0	0.9			1.26	1.70		n.d.
41	MSB-2	171.5	178.5	27.0	23.0	2002.7.22	6.0	5.4	0.6			0.56	1.6		0.048
42	MSB-4	95.5	99.0	119.0	115.5	2002.8.13	10.0	8.9	1.1			0.77	40.4		0.5
43	MIZ-1	113.1	116.3			2003.4.30	10.1	9.6	<1			1.27	6.8		0.060
44	MIZ-1	215.0	225.7			2003.7.9	9.4	6.6	2.8			0.66	8.4		4.49

Table 4.2-1 continued. In column of Quality SCORE, the samples/data with QS >3 are shown by red character. And the samples/data with 3> QS >2 are coloured by blue column

index	location	Min. Depth mbgl	Max. Depth mbgl	Elevation masl	masl	F^- ppm	Cl^- ppm	NO_2^- ppm	NO_3^- ppm	Br^- ppm	I^- ppm	NH_4^+ ppm	PO_4^{3-} ppm	Si ppm	Al ppm	Σ Fe ppm	Fe^{2+} ppm	Fe^{3+} ppm	Σ Mn ppm	Quality SCORE
AKEYO F.																				
1	DH-15	68.0	72.5			0.8	0.8	<0.2	<0.3	<0.1	<0.7	<0.2		34.6	0.023	0.061			0.0044	4.065
2	DH-15	84.5	97.5			1.4	1.2	<0.2	<0.3	<0.1	<0.7	<0.2		21.9	0.21	0.25			0.0056	3.774
TOKI LIGNITE BEARING F. (LOWER)																				
3	MSB-2	79.0	130.5	119.5	68.0	11	155	<0.2	<0.3	0.29	<0.5	<0.1		4.9	0.012	0.019	<0.05		0.0042	4.005
4	MSB-2	132.0	154.0	66.5	44.5	8.3	223	<0.2	<0.3	0.42	<0.5	<0.1		5.7	0.014	0.017	<0.05		0.03	3.737
TOKI GRANITE																				
5	DH-2	207.5	209.5	-13.9	-15.9	0.65	93.9		<0.05	0.18				6.94		0.02			0.02	2.201
6	DH-2	225.5	237.0	-34.9	-43.4	5.79	106		<0.05	0.21				6.85		<0.01			<0.01	1.580
7	DH-2	302.7	304.7	-109.1	-111.1	9.85	145		<0.05	0.29				6.51		<0.01			<0.01	2.600
8	DH-2	305.6	307.6	-111.9	-113.9	9.18	138		<0.05	0.27				6.04		0.03			<0.01	2.006
9	DH-2	309.7	311.7	-116.1	-118.1	9.46	145		<0.05	0.28				6.66		0.01			<0.01	2.249
10	DH-2	313.0	315.0	-119.4	-121.4	9.07	150		<0.05	0.29				6.59		0.02			<0.01	2.600
11	DH-2	320.9	328.4	-127.3	-134.8	8.76	156		<0.05	0.28				6.24		<0.01			<0.01	2.257
12	DH-2	347.6	349.6	-154.2	-156.2	8.05	191		<0.05	0.34				6.77		0.03			<0.01	2.600
13	DH-2	365.5	367.5	-171.9	-173.9	7.78	211		<0.05	0.36				6.42		<0.01			<0.01	1.950
14	DH-2	439.5	449.0	-245.9	-254.4	6.52	228		<0.05	0.42				6.50		<0.01			<0.01	1.838
15	DH-2	451.2	459.7	-257.6	-266.1	6.12	267		<0.05	0.47				6.38		<0.01			<0.01	1.946
16	DH-4	185.5	188.5	81.1	78.1	4.99	2.74	<0.02	0.02	0.08			<0.02	5.57	<0.1	9.34	9.34	<0.05	0.77	3.557
17	DH-5	323.8	330.8	-13.4	-20.4	2.5	1.4	<0.01	<0.01	n.d.		<0.01	0.1	19.60	<0.01	0.41	0.24		0.32	4.230
18	DH-6	733.0	740.0	-413.7	-420.7	4.1	3.36	n.d.	n.d.	n.d.		0.31	n.d.	8.6	0.04	0.18	0.2		0.008	4.225
19	DH-7	438.0	444.5	-97.8	-104.3	0.75	4.31		<0.1					4.5		<0.01				2.691
20	DH-7	479.0	485.5	-138.8	-145.3	2.38	4.47		<0.1					9.7		<0.01				2.530
21	DH-7	479.0	485.5	-138.8	-145.3	3.81	3.87		<0.1					13.0		<0.05				2.387
22	DH-7	560.5	567.0	-220.3	-226.8	2.11	4.37	0.01	0.01	n.d.		22.9	0.086	1.9	0.19	8.9	8.5		0.16	3.730
23	DH-7	560.5	567.0	-220.3	-226.8	5.34	4.20		<0.1					24.3		<0.01				2.133

Table 4.2-1 continued.

Index	location	Min. Depth	Max. Depth	Elevation		F^-	Cl^-	NO_2^-	NO_3^-	Br^-	I^-	NH_4^+	PO_4^{3-}	Si	Al	Σ Fe	Fe^{2+}	Fe^{3+}	Σ Mn	Quality SCORE
		mbgl	mbgl	masl	masl	ppm	ppm	ppm	ppm	ppm	ppm	ppm	ppm	ppm	ppm	ppm	ppm	ppm	ppm	
TOKI GRANITE continued																				
24	DH-7	560.5	567.0	-220.3	-226.8	4.79	3.53		<0.1					20.1		<0.1				**2.213**
25	DH-7	598.0	604.5	-257.8	-264.3	6.37	5.87		<0.1					22.3		0.04				**2.129**
26	DH-7	598.0	604.5	-257.8	-264.3	7.11	5.67		<0.1					20.8		<0.05				**1.925**
27	DH-7	660.0	666.5	-319.8	-326.3	4.42	4.20		<0.1					12.6		0.01				**2.174**
28	DH-7	660.0	666.5	-319.8	-326.3	7.79	2.84		0.20					13.2		<0.1				**1.944**
29	DH-7	735.5	742.0	-395.3	-401.8	6.34	6.41		0.40					27.7		0.03				**2.291**
30	DH-7	735.5	742.0	-395.3	-401.8	8.67	6.10		<0.1					27.6		<0.1				**1.980**
31	DH-7	833.5	840.0	-493.3	-499.8	9.95	3.09	0.1	0.05	n.d.		2.98	0.039	8.5	1.2	7.2	6.9		0.10	3.577
32	DH-7	833.5	840.0	-493.3	-499.8	9.24	4.31		<0.1					17.1		0.02				**2.691**
33	DH-7	880.0	886.5	-539.8	-546.3	8.62	5.08	0.09	0.03	n.d.		4.56	0.328	14.7	4.3	7.5	8.8		0.31	3.585
34	DH-7	880.0	886.5	-539.8	-546.3	10.2	6.48		<0.1					29.8		0.87				**2.201**
35	DH-7	880.0	886.5	-539.8	-546.3	10.2	5.80		<0.1					22.4		0.6				**1.919**
36	DH-8	641.5	648.0	-371.7	-378.2	3.16	3.77	0.01	n.d.	n.d.		0.21	0.01	13.6	0.68	0.03	0.03		0.005	3.950
37	DH-8	693.5	700.0	-423.7	-430.2	3.58	3.84	0.09	0.01	n.d.		1.43	n.d.	17.0	0.05	0.19	0.17		0.015	3.571
38	DH-8	745.5	752.0	-475.7	-482.2	4.35	3.9	0.01	n.d.	n.d.		1.1	n.d.	16.7	0.32	0.18	0.21		0.008	3.338
39	DH-8	869.0	875.5	-599.2	-605.7	11.21	19.2	n.d.	0.01	n.d.		1.08	n.d.	12.8	0.98	0.07	0.08		0.004	3.370
40	DH-8	975.0	981.5	-705.2	-711.7	6.75	6.42	n.d.	n.d.	n.d.		0.31	0.008	14.5	0.08	0.19	0.2		0.011	3.571
41	MSB-2	171.5	175.5	27.0	23.0	8.0	159	<0.2	<0.3	0.35	<0.5	<0.1		5.3	0.004	0.058	<0.05		0.02	3.356
42	MSB-4	96.5	99.0	119.0	115.2	12	96	<0.2	<0.3	0.16	<0.5	<0.1		6.1	0.069	0.042	<0.05		0.0062	4.216
43	MIZ-1	113.1	116.3			3.7	38	<0.2	<0.3	<0.1	<0.7	<0.2		6.6	0.056	0.021	<0.05		0.0018	3.353
44	MIZ-1	215.0	225.7			11.9	86	<0.2	<0.3	0.2	<0.7	<0.2		4.5	0.860	0.066	<0.05		0.004	**2.895**

The rationale for including each of these factors in the QS system and the method for scoring them and weighting them is discussed in the following paragraphs.

(a) Degree of contamination by drilling water, as indicated by fluorescent dye.

The score is 1/C (where C = contamination in %), but when C<1% score = 1. If no tracer has been used, then score = 0.

An inverse relationship between contamination and score is reasonable, because the reliability of a water sample diminishes very rapidly as contamination increases. If a tracer has not been used, then other less quantitative ways of detecting drilling water contamination should be tried, either with 'natural' tracers for example TOC or ^{3}H (tritium) or by inference from general compositional patterns. Using a zero score is understandably precautionary for cases where tracer has not been used. However the impact of sample contamination and the possibility for tracing and quantification are of such direct significance that it is arguable whether they should be just one of many factors in a scoring system where their indication of sample reliability can be 'overruled' by scores from other less direct factors. It is suggested that in cases where contamination by drilling water can be quantified with tracer data, then the analytical data should be corrected for contamination in a separate stage of data processing. After that correction has been made, then the adjusted composition should be scored.

(b) Cation-anion charge balance.

The score is 2/B, where B is the cation-anion charge balance as % (or rather ABS[%]), i.e. when B = 2%, score is 1. When balance is <2%, B = 2% so that maximum score is 1. Some allowance is made for greater possibilities for reasonable analytical error in both more concentrated (Σ cations >10 meq/L) and more dilute (Σ cations <3 meq/L) groundwater samples, by giving the maximum score for balances up to 5% and 3.3% respectively.

The decrease of the score for this factor for samples where the charge balance exceeds these thresholds seems to be reasonable, in that a 10-20% charge imbalance is an indication of significant analytical error, and accordingly the score in such cases would be 0.2-0.1. However in samples for which the analyses give poor charge balances, the priority should be on identifying the cause of error, which may or may not diminish the value of that data set for interpretation.

(c) Delay time between sampling and analysis of unstable determinands: alkalinity, reduced sulphur and ferrous iron.

The score is 1 if the delay time is 6 hours or less, and 0.25 if it is >6 hours.

This score only has significance for interpretation of alkalinity, reduced sulphur and reduced iron (or total iron). It seems to be a very subjective assessment of potential errors, and may be optimistic or pessimistic depending on many other factors. It

would be helpful to see evidence in support of the 6 hour threshold, though 'same day analysis' is sometimes used as a guideline for analyses of unstable parameters. Analysis within, say, 2 hours would inevitably give more reliable data if the rate of degradation of relevant parameters is not known.

The stability of in situ alkalinity in a water sample depends on the relative values of in situ PCO_2 and the atmosphere. However a greater threat to the reliability of alkalinity (and thus of data for carbonate species and of modelled carbonate mineral equilibria) is contamination either in the borehole or after sampling.

The stability of reduced sulphur and of dissolved iron in water samples is very dependent on whether the in situ condition is reducing or oxidising, and thus on the impact of a potential change of conditions when sampled and exposed to oxidisation. Reduced sulphur and ferrous iron that are at relatively elevated concentrations in reducing conditions very rapidly become oxidised, even when precautions are taken to preserve redox conditions (e.g. sealed container). In such cases, the 6 hour threshold is probably far too optimistic.

(d) Sampling container, i.e. whether in a downhole gas-tight vessel or pumped into an open bottle at the surface.

The score is 1 for an air-tight or downhole sampling vessel, and is 2 for a polythene bottle. However it is reported that these scores are not used in the overall QS. These scores appear to take a too simplistic view of the relative merits of sample containers. For example, samples may be preserved in air-tight vessels but are equally liable to many artefacts and technical problems when they are transferred for analysis.

(e) Evidence from pH, EC and Eh stability from time series monitoring.

The scoring system for this factor is not entirely clear. If SpH, SEC, and SEh are the magnitudes of drift for pH, EC and Eh respectively, then the scores are 0.0002/SpH, 0.002/SEC, and 0.02/SEh respectively. It seems that the maximum score is limited to 0.2 for each of pH, EC and Eh to reflect an inevitable effect of contamination by drilling fluid on reliability. It also seems to assume sensitivities of 0.002 pH units, 0.02 EC units, and 0.2 Eh units.

The reasoning behind these measurement sensitivities and scoring formulae is not clear. The three parameters have very different reasons for drifting as they are monitored over time. EC changes only is mixing with a chemically-different water is progressively affecting the sample, so it is likely to occur only in a monitored outflow from pumping. pH drifts for various reasons including mixing/contamination, CO_2 outgassing or ingassing, and carbonate precipitation. Eh for groundwaters that are reducing in situ is the most unstable of these three parameters and commonly drifts due to oxygenation (drift to lower values as reducing water flushes oxygen out of the sampling line, or drift to higher values if oxygen leaks into an anaerobic sampling line

or if oxidising water mixes in. Eh for oxygenated groundwaters should be more stable at high Eh values, but anyway Eh measurements in these conditions are of no value for quantitative chemical modelling other than to confirm oxidising conditions. Intermediate Eh measurements (around 0 V) are certainly liable to drift and may be the most problematical to interpret, so assessing the reliability of such measurements may be important.

(f) Length of discrete sampling interval between packers, i.e. the longer the interval, the greater chance there is of mixing of chemically-discrete groundwater flows within the interval.

The score is 1 if the length of packered interval is 0.7 m or less, and above that length (L, m) the score is 0.7/L.

Whilst there is some logic in expressing greater reliability in terms of being representative of a single flow zone for a sample from a short sampled interval, other factors may also come into play in these conditions. For example, there may be a greater probability of water being drawn around the packers (either due to packer leakage or to bypass flow through the formation) into a short interval.

Mixing that would result from inflow from more than one independent flow zones in a packered interval would be better treated as a mixing problem rather than a sample quality problem that is ranked alongside contamination and other perturbations from external sources.

(g) Sampling logistics, i.e. whether in a downhole 'in situ' sampler or pumped to the surface (possibly by air-lifting).

The score is 1 if downhole sampling has been deployed and, in principal, 0.5 if the sample has been taken at the surface. However it seems that in the latter case there is a possibility that air lifting was used, in which case the perturbation due to that is reflected by a 0 score.

Again, there is some logic in these scores, however it should be recognised that air-lifting of water samples strongly affects redox-sensitive parameters due to oxygenation. In such cases, measurements of these parameters may be effectively meaningless. However other parameters may be relatively unaffected. Therefore applying these scores has to be carried out with caution, so as not to reject adequate data.

(h) Location where measurement or analyses of physico-chemical parameters, i.e. downhole, surface monitoring (with flow cell where appropriate), or laboratory.

The score is 1 for parameters that are measured in situ (e.g. pH, EC, Eh, T with a downhole hydrochemical tool), 0.5 for data measured at the surface in flow cells or similar in-line devices (e.g. Eh, pH, DO, EC), and 0.33 for data measured in the laboratory.

It is assumed that these scores apply only to measurements of unstable parameters, i.e. pH, Eh, DO, alkalinity; otherwise it would be illogical to give low scores to lab measurements of normal solutes in well-preserved samples.

As already discussed above, it is a rather arbitrary judgement to score downhole measurements always higher than flow-through cell measurements on pumped water at the surface. Equally to give any score for lab measurements of Eh would be misleading, since these will inevitably be oxygenated (except for sealed downhole containers?) and thus totally unreliable.

4.2.3 Application of Scoring System to Tono Samples

The outcome of applying the QS system to the Tono hydrochemical data set should be an objective and credible ranking of groundwater analyses according to their reliability. More specifically, it is assumed here that the following assessments might be expected from the QS and ranking system:

- Identify the most reliable samples and analyses overall, for general interpretation of hydrochemical and isotopic data in terms of water sources, evolution and mixing, geochemical equilibria;
- Highlight specific sampling or analytical issues, ensuring that highly-ranked samples do not have single deleterious factors or erroneous data that 'slip through' the QS system;
- Give appropriate relative weights and ranks to problematic data so that causes of unreliability are flagged and also that information is not lost;
- Provide valid guidance on the quality of data for isotope, gases and trace elements, in addition to indicating reliability of general compositional data.

These three expectations from the QS system are considered in the following paragraphs.

(a) Are the samples/data with QS >3 the most reliable data overall?

As discussed above, contamination by drilling fluid is probably the greatest threat to sample reliability overall. It is therefore of concern that the QS system has scored a sample from DH-11 (132-135 m) at 3.75 although it has 48% contamination.

The low score due to contamination is offset by high scores due to short delay time, pH/EC/Eh monitoring and stability, and on the fact that these were monitored with a downhole tool. Stability of downhole monitoring and other positive aspects of sampling/analytical performance do not offset the basic impact of contamination on representativeness of a water sample. This high score therefore exposes a flaw in the QS system.

Other samples with less severe degrees of contamination also have the resulting low scores offset by the same factors and also by relatively good charge balance (e.g. KNA-6) and/or by low delay time (e.g. DH-13, 10.5 m). DH-4, -5, -6 have high scores due to short delay time, even though contamination has not been traced. Whilst these factors may be significant contributors to sample quality, they do not make up for poor quality due to contamination. The spread of scores that are possible due to variations in delay times, monitoring stability, charge balance, and sampling/monitoring logistics are illustrated by the range from <2 to >3 for DH-7 samples, regardless of the degrees of contamination which are unknown. Further examples are given by samples from DH-8, -9, -12, -13 that mostly have scores >3 although two of these samples have 7.9 and 21% contamination.

Another key aspect of data quality is the reliability of Eh measurements. Sample DH-12 (157.5-164 m) has a score >3 and low contamination, but the Eh stability is relatively poor (though this assessment may be too negative because the criteria for Eh stability seem to be very stringent). In many cases the high scores include contributions from the scores awarded to samples that have had pH/EC/Eh monitored, and the high scores are thus justified in this respect.

It is concluded that most of the samples with scores >3 are indeed among the most reliable, although it is clear that a few samples with contamination problems have 'slipped through' into this highly scored category. Further, it is suggested that too much weight is given in the QS system to factors such as delay time, sampling/monitoring logistics that may be important but are not independent factors – in other words if contamination is present, these factors do not offset the impact on reliability. Also, it is suggested that degree of contamination should be treated independently as a self-standing indication of reliability.

(b) Are specific issues highlighted and correctly weighted?

Probably the most important specific issue with relevance to geochemical interpretation is the stability and representativeness of Eh measurements. Firstly, it should be clear that stability of Eh is only meaningful if monitoring is done either downhole or in a flow-through device at the surface. For one sample, DH-15, it seems that stability is scored even though monitoring seems to have been done in the laboratory – in such a case, the stability score would be meaningless. Another Eh value, -11 mV for DH-13, seems to be a laboratory measurement and if so would also be unreliable.

Many of the reported Eh values are strongly negative, i.e. reducing, e.g. –323 mV for DH-11, -360 mV for KNA-6, and these seem to be reliable data because contamination almost invariably causes drift towards oxidising, positive, Eh. A range of Eh values are reported for DH-12, MIU-4 and MSB-2, from –118 to –42 mV, although these samples have >3 scores. Monitoring indicated relatively poor stability for these measurements, so they may be unreliable, i.e. more reducing in situ values that are affected adversely by oxygen ingress during pumping/sampling. Reliable Eh values in

this range that are intermediate between oxidising and reducing would be significant for geochemical interpretation, so how the QS system handles these data is important. In the same context, Eh values reported for DH-12 are similarly in the range –54 to –20 mV but have lower QS. However their consistency over several sampling intervals in the borehole suggests reliability. On the other hand, the direction of drift in monitoring is mostly towards more negative values which could indicate slow removal of oxygen contamination.

Stability of pH measurements is of similar significance to that of Eh, except that it depends on in situ carbonate speciation and equilibria and the partial pressure of CO_2, PCO_2 (see discussion above). Many of these groundwaters from Tono area are notable for their low alkalinities and high pH values (ca. 8 to 9.5 range). Such solutions might be unstable after sampling due to ingassing of atmospheric CO_2. Samples MIU-4 and MSB-2 are dilute groundwaters and have low alkalinities and pH >9, but they have fairly good stability during pH monitoring and also high QS. Samples DH-8, -9 and –10 are similar.

The conclusion from these considerations of pH and Eh reliabilities, and whether these are adequately reflected in the QS system, is that they are of such importance to geochemical interpretation and modelling that they need to be assessed directly as well as via the QS. Whether they are representative of in situ chemistry depends on a wide and varying range of influences and chemical relationships.

(c) Are appropriate weights and ranks given to problematic data so that causes of unreliability are flagged and so that information is not lost ? What do low QS mean ?

Inspection of the Tono data set shows that low QS originate primarily from the absence of tracer data with which to quantify drilling fluid contamination. Secondary factors according to the weights given to the scores are lack of pH/EC/Eh monitoring, monitoring and sampling carried out on water pumped to surface rather than downhole, and charge balance. In most of these situations, low scores do not positively indicate unreliable samples and analyses – they often indicate a minor possibility of deviation from in situ composition relative to the deviation caused by contamination or Eh and/or pH perturbation. Therefore low QS are a warning to data users to critically inspect the sampling conditions and data more thoroughly.

(d) How useful are QS as indicators of data quality for isotopes, dissolved gases and trace elements?

Isotopes, dissolved gases and trace elements each have particular sensitivities to sampling logistics, sample handling and analyses. Thus QS are not adequate on their own as indicators of data reliability. Individual factors have specific effects on data reliability. For example, sample container must be an air-tight sealed vessel for dissolved gases, i.e. score = 1 only, otherwise data are meaningless. Carbon isotopes ($\delta^{13}C$ and ^{14}C) need relatively large volume samples from a flowing source

plus special preservation after sampling for data to have greatest reliability. High pH groundwaters, which are prevalent at Tono, may easily take up CO_2 from the atmosphere and thus contaminate the in situ compositions.

Tritium (^3H) is a particularly sensitive and potentially important data quality issue. In deep groundwaters it may be a reliable indicator of contamination by drilling water or near-surface water (as was the case for data from the Sellafield site in England; Nirex, 1997). In more shallow groundwaters where nucleogenic ^3H may occur naturally, its detection provides an indication of how deep young (<50 y) groundwaters have penetrated. In historically mined areas (e.g. in Canada and England), ^3H analyses of tunnel/mine inflows have been a primary source of evidence for rapid flow rates and interconnections from the surface under the influence of induced drawdowns of groundwater pressures. Therefore decisions to sample, analyse and interpret ^3H in undisturbed or underground laboratory situations have to be matched by very careful quality control of data. QS on their own would not be adequate for this, and specific indicators of ^3H interferences/contamination must be examined alongside the overall QS system. The representativeness of ^3H may be strongly affected by even 5% contamination in some groundwaters, e.g. those where 'young' drilling water contaminates old groundwater. The relationship between % contamination and ^3H content is unclear in the Tono samples, where for example DH-13 (408-442 m) has 21% contamination according to the fluorescent tracer and also has 1.1 TU of ^3H; this suggests that drilling water has a rather low ^3H content.

There is a more general discrepancy in that several water samples (e.g. DH-5, -6, -7, -8) have low ^{14}C contents indicating old (e.g. >5000 y) groundwaters, which nevertheless have measurable ^3H contents. The latter evidence indicates young water contents, i.e. contamination/mixing, but tracer indications of drilling water contamination do not seem to be high enough to account for the ^3H. It may be that contamination by in-mixing of shallow, untraced, groundwater within the borehole is being indicated. Thus, integrated interpretation of isotopic and hydrochemical data in this way may give useful evidence of sample quality that would supplement or replace what the QS might suggest.

The trace element of most immediate interest is uranium (U). QS alone is unlikely to be a direct indication of reliability of U data, since the factors being considered in QS are not those directly affecting the quality of U sampling. Although U data in the Tono data set are predominantly very low values (<1 ppb), consistent with reducing conditions, there are several anomalies that are unexplained by the QS rankings. For example, TH-1 and –2 have QS >2, but have high U of 28 and 8 ppb. In DH-6, -7 and –8 samples, U varies up to 4.4 ppb in samples that also have confirmed highly negative Eh values, i.e. there is not a correlation of U variation with redox variation. This suggests that there may be artefacts in U sampling, for example due to variable amounts of colloidal material passing through filters. As in the previous paragraph, this shows that careful inspection, comparison and interpretation of trace element and other hydrochemical data provides additional insights on data quality.

Another consistency test that gives positive support to the QS system is the correspondence of detectable dissolved CH_4 in samples from DH-6, -7 and –8 with reducing Eh.

4.3 Solubility calculations

4.3.1 Solubility diagrams

Bearing in mind the results of the review of chemical speciation of the 18 elements outlined in Section 3 and the review of data quality described in Section 4.2, solubility diagrams were constructed using GWB. The purpose of these diagrams was to better understand the chemical speciation of the 18 elements in the Tono groundwaters and to identify appropriate solubility-controlling mineral phases. The aim was then to focus the solubility calculations using PHREEQC on these minerals.

The solubility diagrams were constructed for 4 different water compositions:

- Water 171 fromDH-2, between 228.5 and 237.0 m depth;
- Water 180 from DH-2 between 451.2 and 459.7 m depth;
- Water 5 from DH-4 between 185.5 and 188.5 m depth;
- Water 108 from DH-7 between 560.5 and 567.0 m depth

These water compositions were chosen because they span a wide range of the compositional variability seen in the Tono groundwaters.

The solubility diagrams are summarised in Figure 4.3-1 to Figure 4.3-34.

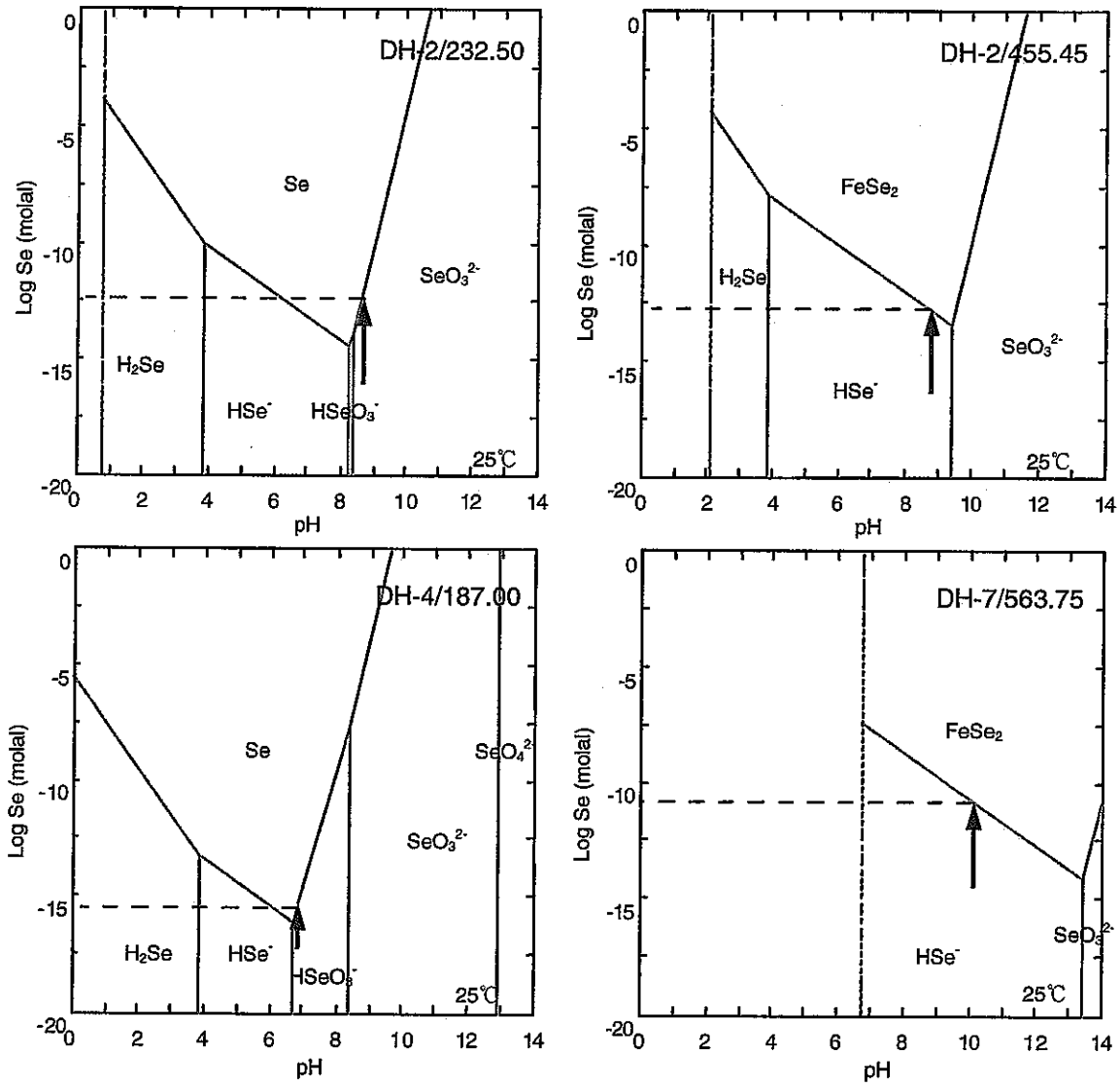

Figure 4.3-1 Variation of selenium solubility with pH for a range of representative Tono groundwaters: DH-2/232.5 (intermediate pH, oxidising); DH-2/455.45 (intermediate pH, reducing); DH-4/187.0 (intermediate pH, oxidising); and DH-7/563.75 (high pH, reducing). The precise pH of each groundwater is arrowed and its accompanying Se solubility indicated by a dashed line. Am solubility ranges from approximately 10^{-15} to10^{-12} M in shallow, oxidising groundwaters to 10^{-13} to 10^{-11} M in reducing groundwaters. Slight variations in pH (± 1 pH units) could shift Am solubility by 1-2 orders of magnitude in some cases. Solubility control is by equilibration with Se in shallow oxidising groundwaters and $FeSe_2$ in the deeper reducing groundwaters.

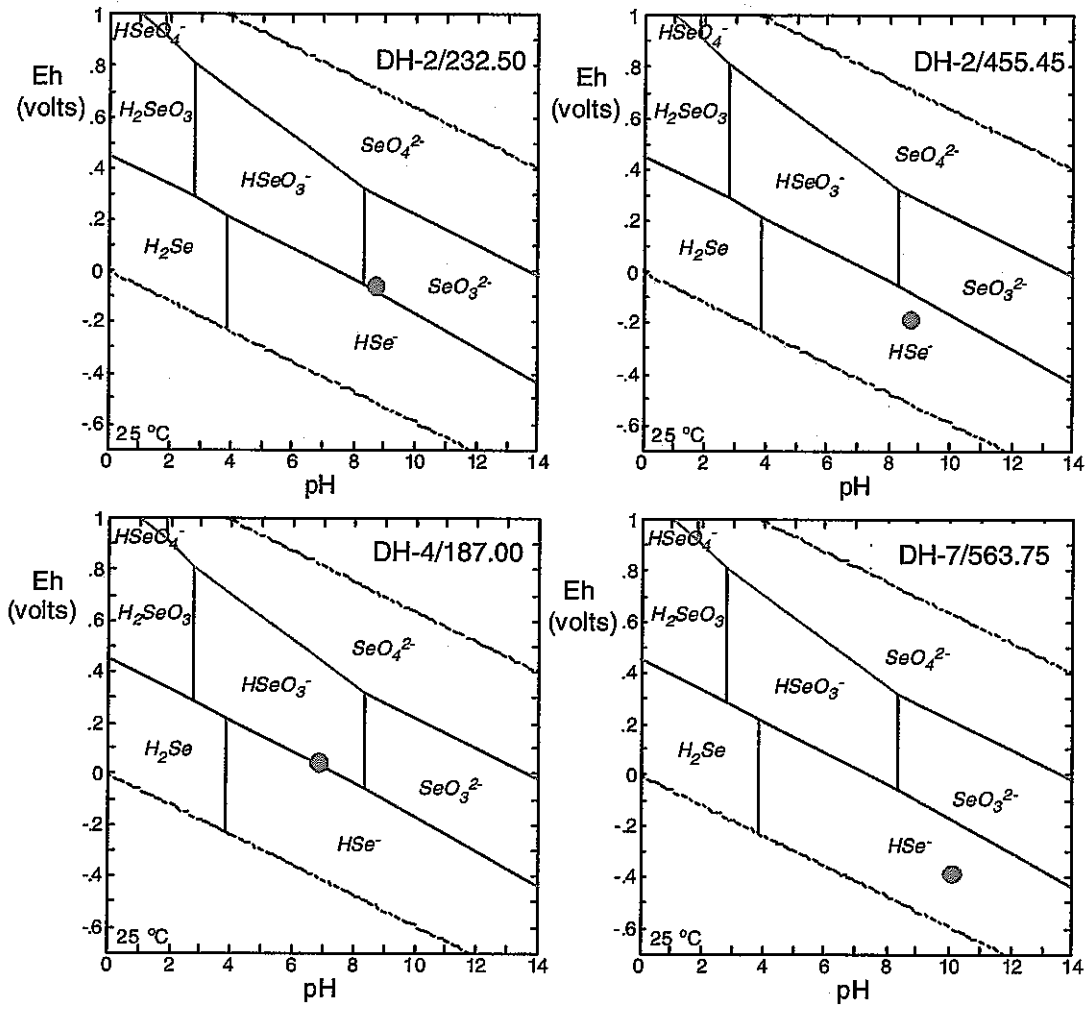

Figure 4.3-2 Eh-pH diagrams for selenium in a range of representative Tono groundwaters: DH-2/232.5 (intermediate pH, oxidising); DH-2/455.45 (intermediate pH, reducing); DH-4/187.0 (intermediate pH, oxidising); and DH-7/563.75 (high pH, reducing). The precise Eh-pH values of each groundwater is indicated by a red dot in each Figure. Se speciation is dominated by HSe^-, SeO_3^{2-}, or $HSeO_3^-$ depending upon the precise Eh-pH of each groundwater.

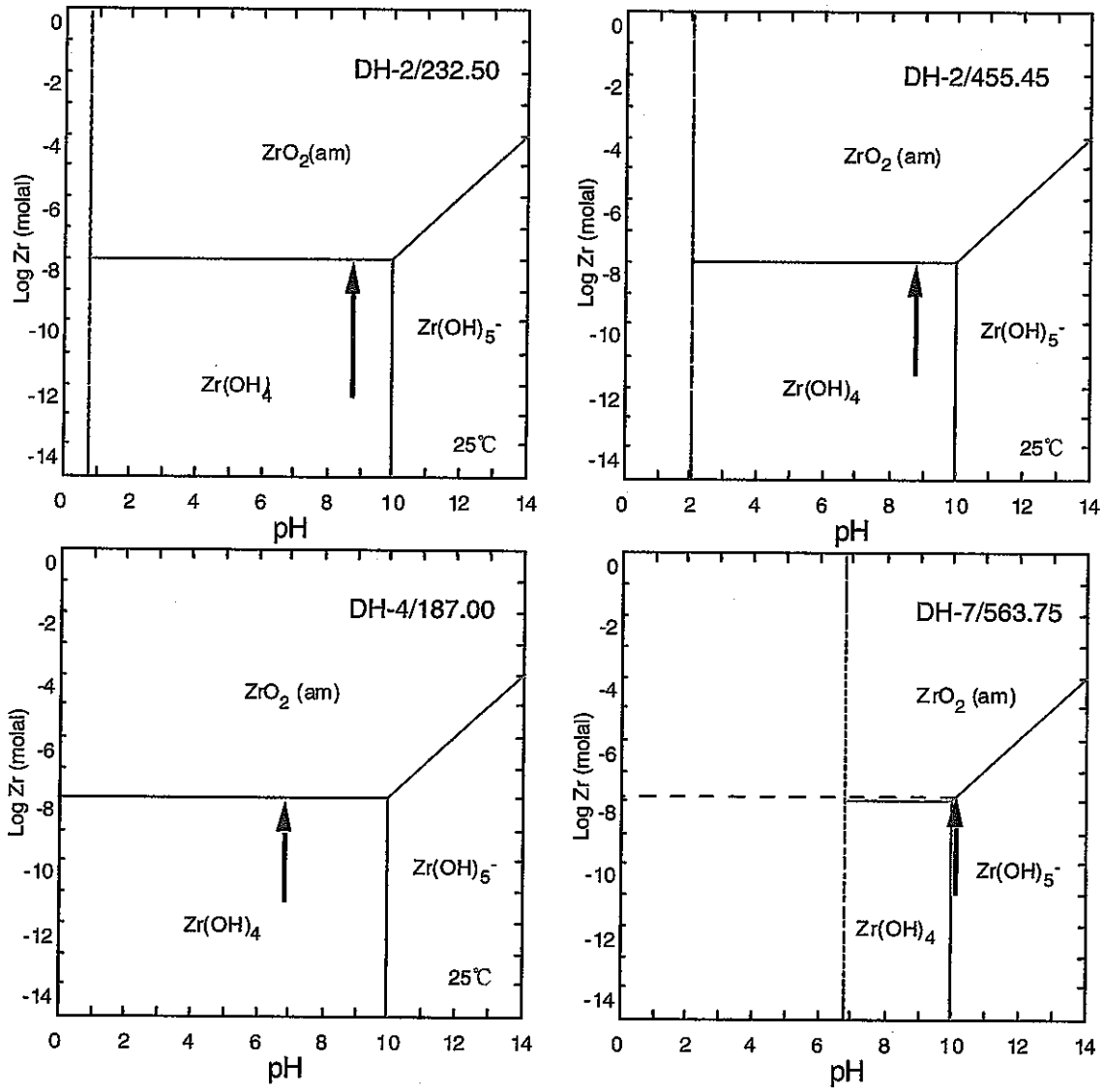

Figure 4.3-3 Variation of zirconium solubility with pH for a range of representative Tono groundwaters: DH-2/232.5 (intermediate pH, oxidising); DH-2/455.45 (intermediate pH, reducing); DH-4/187.0 (intermediate pH, oxidising); and DH-7/563.75 (high pH, reducing). The precise pH of each groundwater is arrowed and its accompanying Zr solubility indicated by a dashed line. Am solubility is approximately 10^{-8} M in all groundwaters. Solubility is independent of pH at pH < 10 and independent of Eh under all conditions. Solubility control is by equilibration of with amorphous zirconium dioxide in all cases.

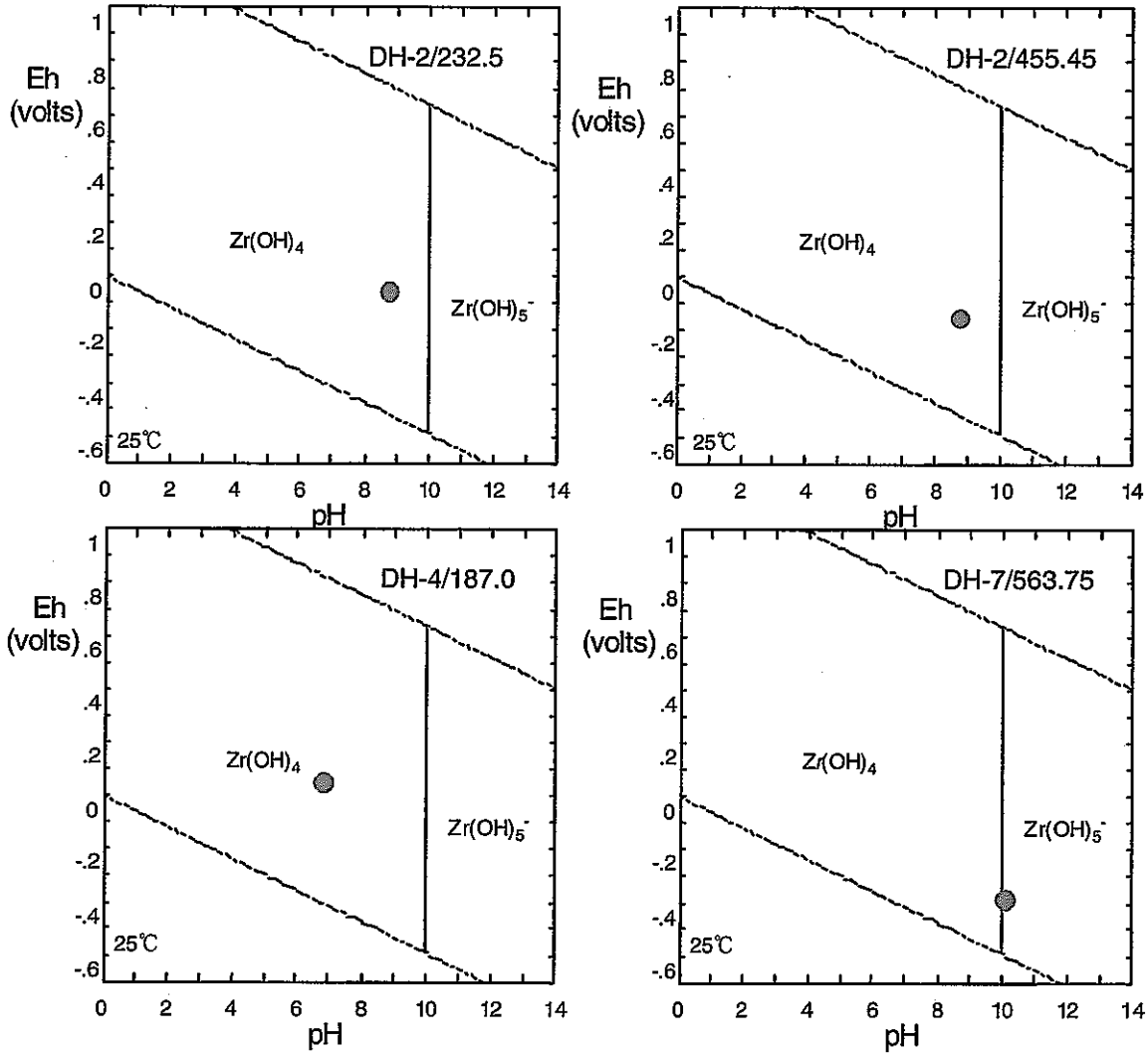

Figure 4.3-4 Eh-pH diagrams for zirconium in a range of representative Tono groundwaters: DH-2/232.5 (intermediate pH, oxidising); DH-2/455.45 (intermediate pH, reducing); DH-4/187.0 (intermediate pH, oxidising); and DH-7/563.75 (high pH, reducing). The precise Eh-pH values of each groundwater is indicated by a red dot. Zr speciation is dominated by $Zr(OH)_4$ or $Zr(OH)_5^-$. Aqueous speciation is independent of Eh.

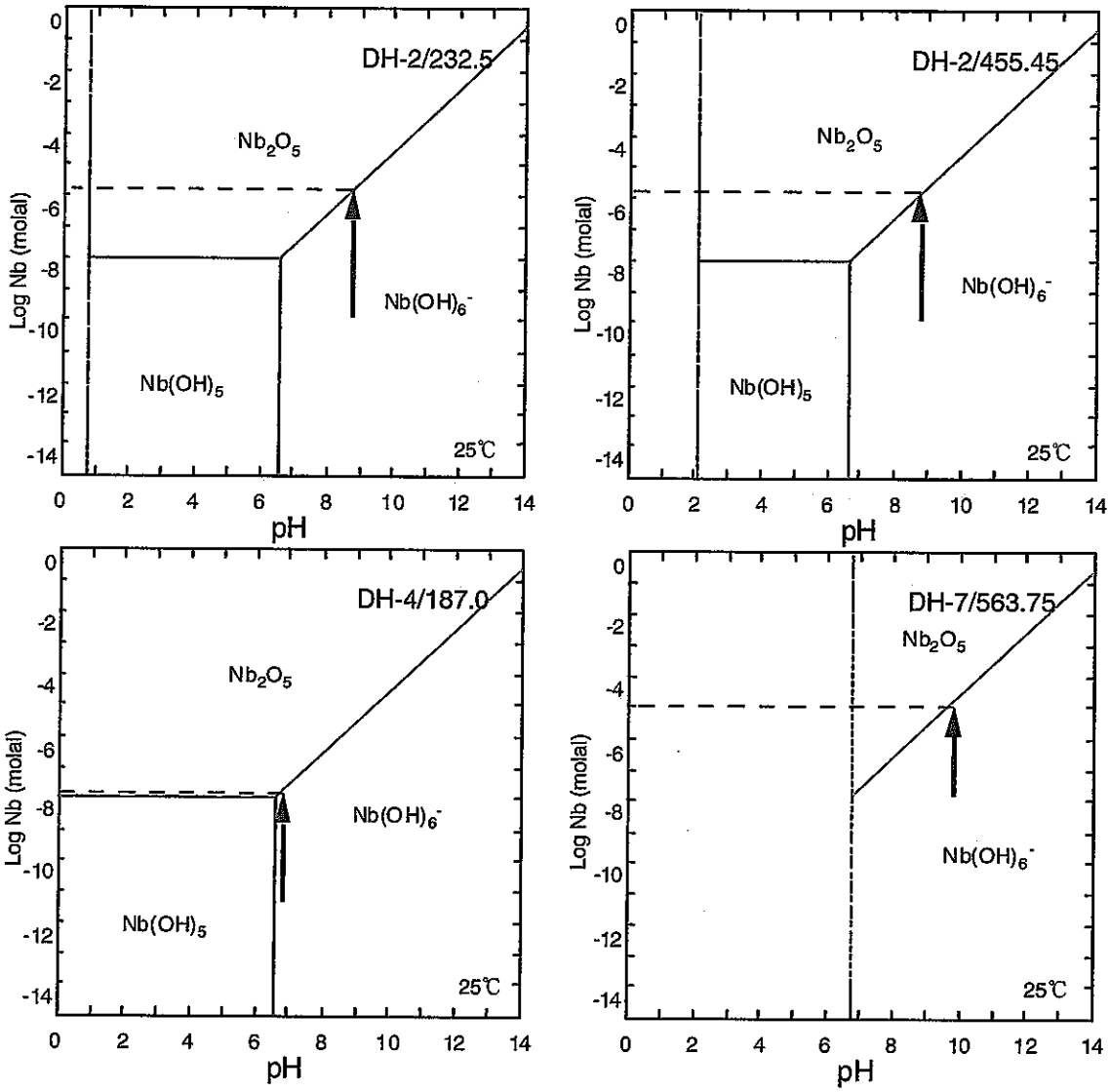

Figure 4.3-5 Variation of niobium solubility with pH for a range of representative Tono groundwaters: DH-2/232.5 (intermediate pH, oxidising); DH-2/455.45 (intermediate pH, reducing); DH-4/187.0 (intermediate pH, oxidising); and DH-7/563.75 (high pH, reducing). The precise pH of each groundwater is arrowed and its accompanying Nb solubility indicated by a dashed line. Nb solubility ranges from approximately 10^{-8} to10^{-6} M in shallow, oxidising groundwaters and 10^{-6} to 10^{-5} M in reducing groundwaters. Slight variations in pH (± 1 pH units) could shift Nb solubility by 1-2 orders of magnitude in all cases. Solubility control is by equilibration of with Nb_2O_5 in all cases.

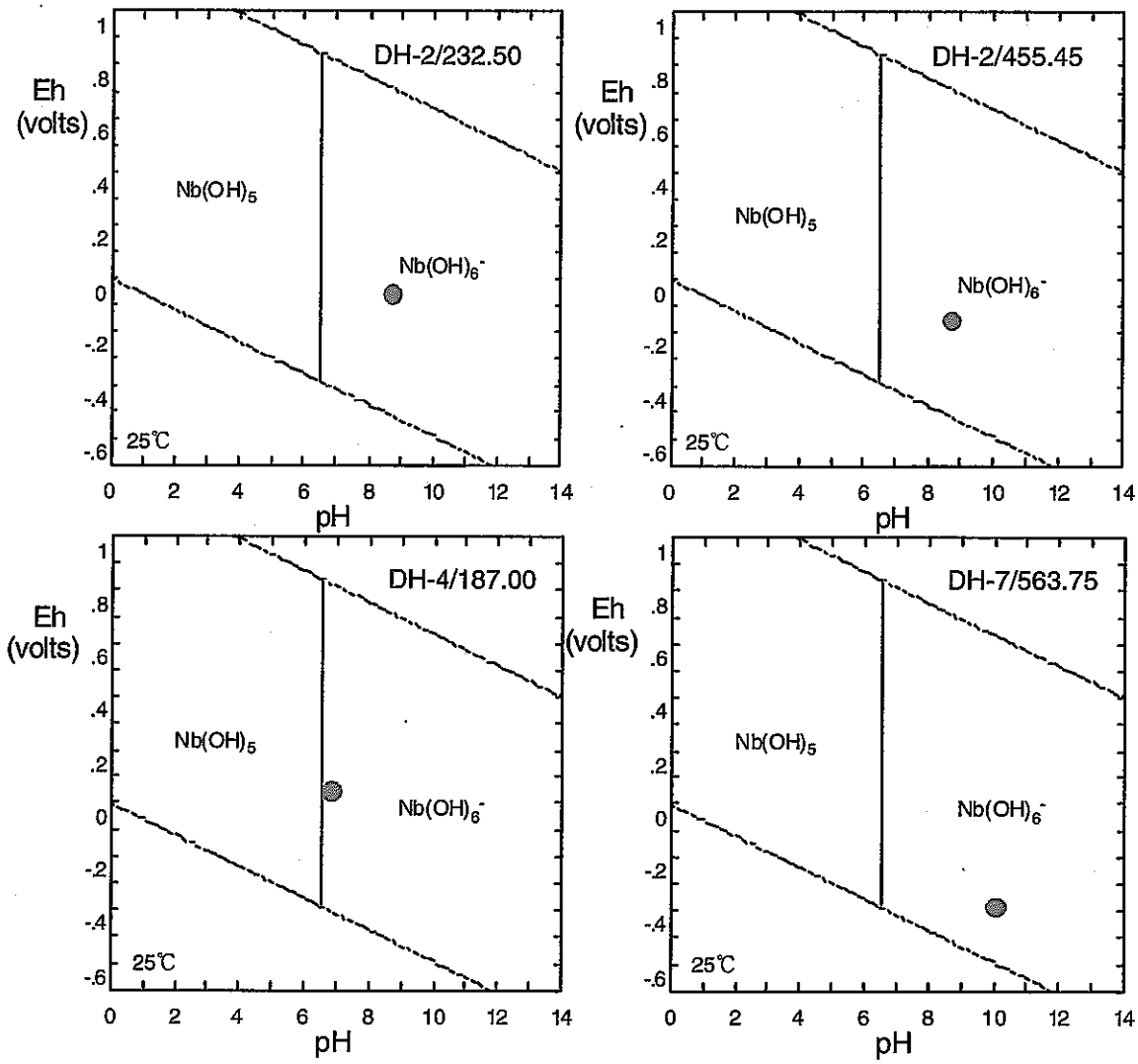

Figure 4.3-6 Eh-pH diagrams for niobium in a range of representative Tono groundwaters: DH-2/232.5 (intermediate pH, oxidising); DH-2/455.45 (intermediate pH, reducing); DH-4/187.0 (intermediate pH, oxidising); and DH-7/563.75 (high pH, reducing). The precise Eh-pH values of each groundwater is indicated by a red dot in each Figure. Nb speciation is dominated by $Nb(OH)_6^-$ in all cases. Nb speciation is independent of Eh.

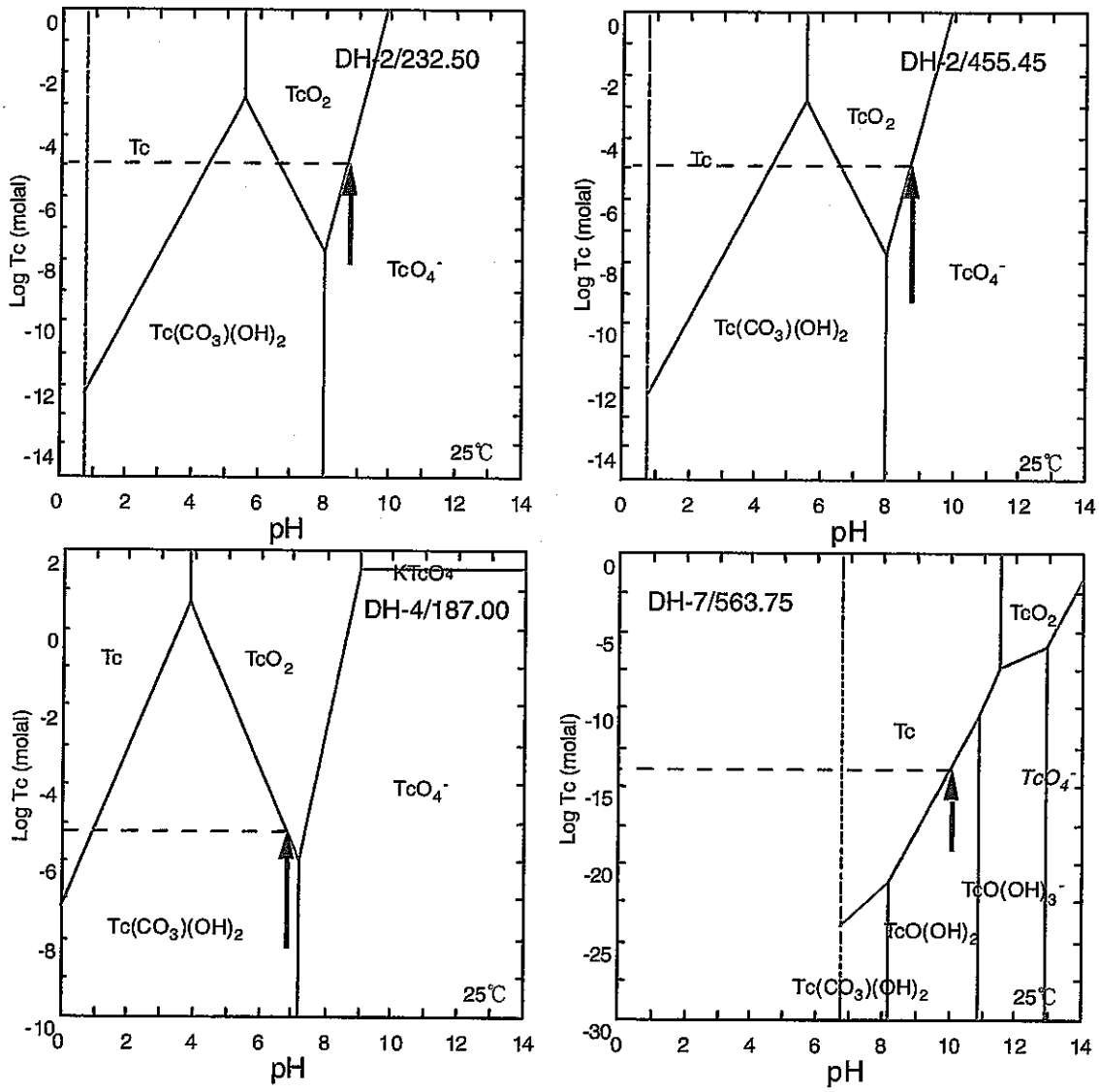

Figure 4.3-7 Variation of technetium solubility with pH for a range of representative Tono groundwaters: DH-2/232.5 (intermediate pH, oxidising); DH-2/455.45 (intermediate pH, reducing); DH-4/187.0 (intermediate pH, oxidising); and DH-7/563.75 (high pH, reducing). The precise pH of each groundwater is arrowed and its accompanying Tc solubility indicated by a dashed line. Tc solubility is approximately 10^{-5} M in relatively oxidising groundwaters to 10^{-14} M in reducing groundwater. Slight variations in pH (± 1 pH units) could shift Tc solubility by 1-2 orders of magnitude. Solubility control is by equilibration with TcO_2 or Tc.

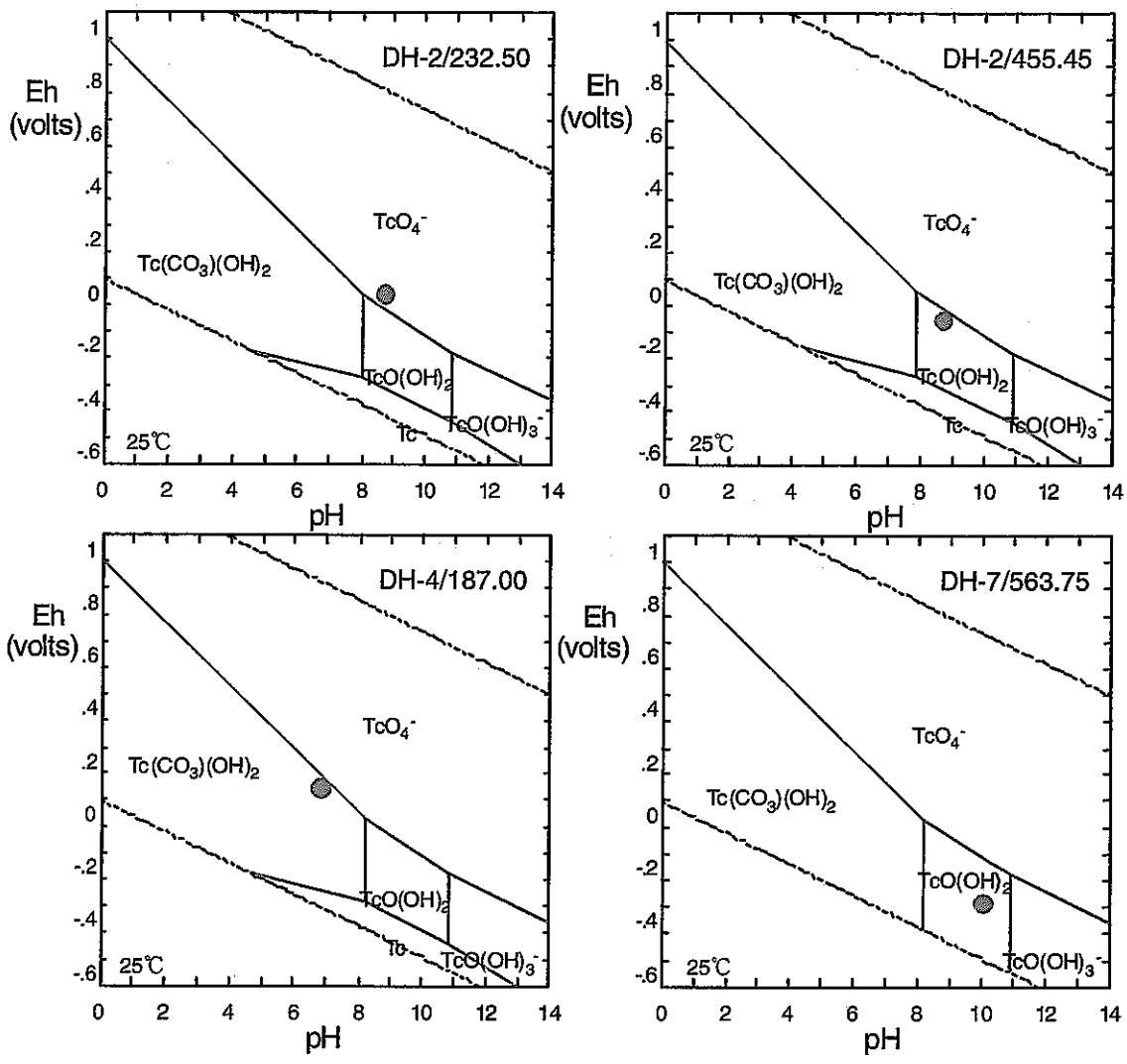

Figure 4.3-8 Eh-pH diagrams for technetium in a range of representative Tono groundwaters: DH-2/232.5 (intermediate pH, oxidising); DH-2/455.45 (intermediate pH, reducing); DH-4/187.0 (intermediate pH, oxidising); and DH-7/563.75 (high pH, reducing). The precise Eh-pH values of each groundwater is indicated by a red dot. Tc speciation is dominated by TcO_4^-, $Tc(CO_3)(OH)_2$, or $TcO(OH)_2$. Tc speciation is sensitive to both Eh and pH.

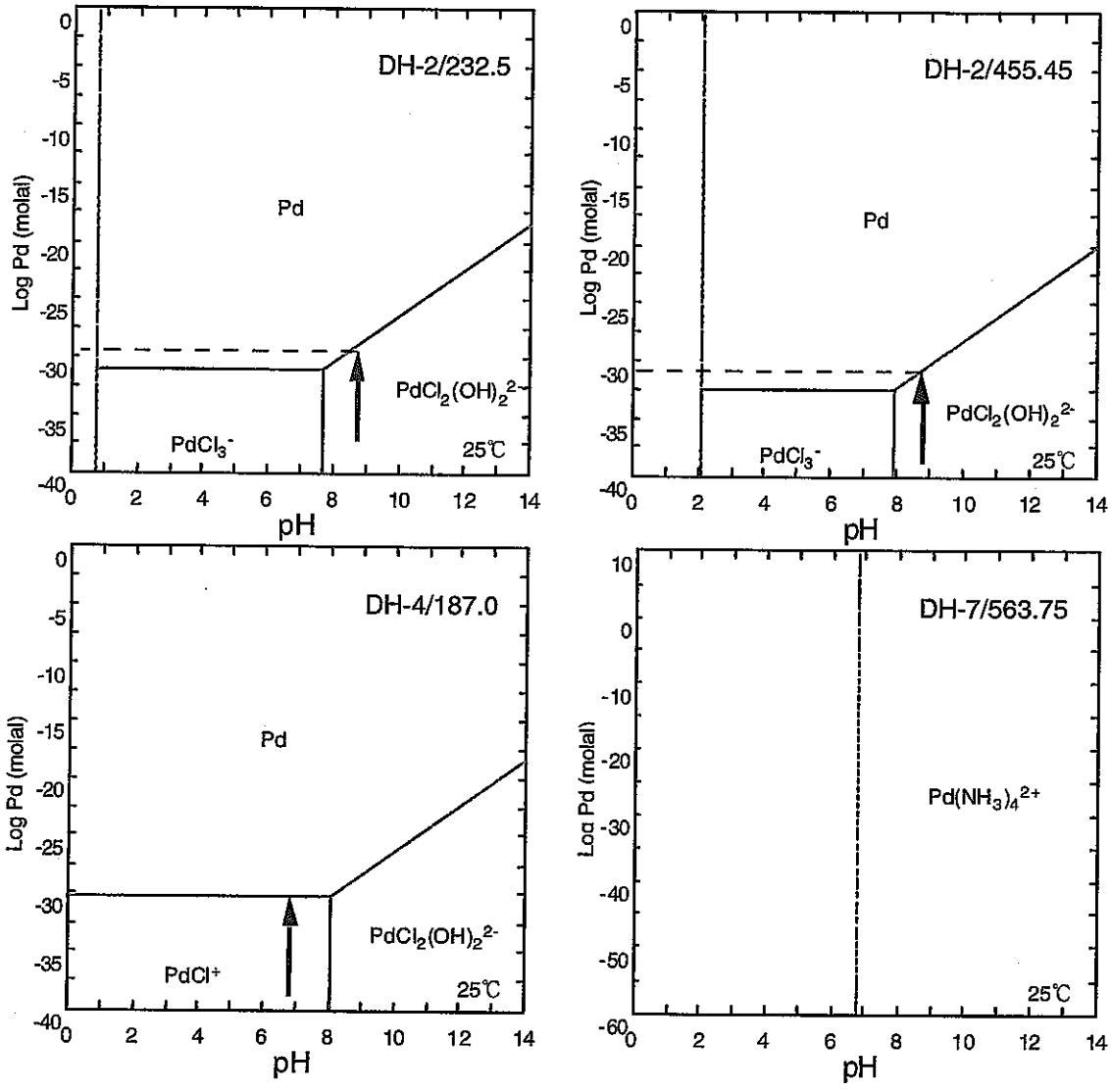

Figure 4.3-9 Variation of palladium solubility with pH for a range of representative Tono groundwaters: DH-2/232.5 (intermediate pH, oxidising); DH-2/455.45 (intermediate pH, reducing); DH-4/187.0 (intermediate pH, oxidising); and DH-7/563.75 (high pH, reducing). The precise pH of each groundwater is arrowed and its accompanying Pd solubility indicated by a dashed line. Pd solubility is approximately 10^{-30} M in three out of four groundwaters. The presence of appreciable ammonium concentrations in DH-7/563.75 results in lack of solubility control for Pd. Slight variations in pH (± 1 pH units) could shift Pd solubility by 1-2 orders of magnitude in some cases. Solubility control is by equilibration of with Pd in three cases.

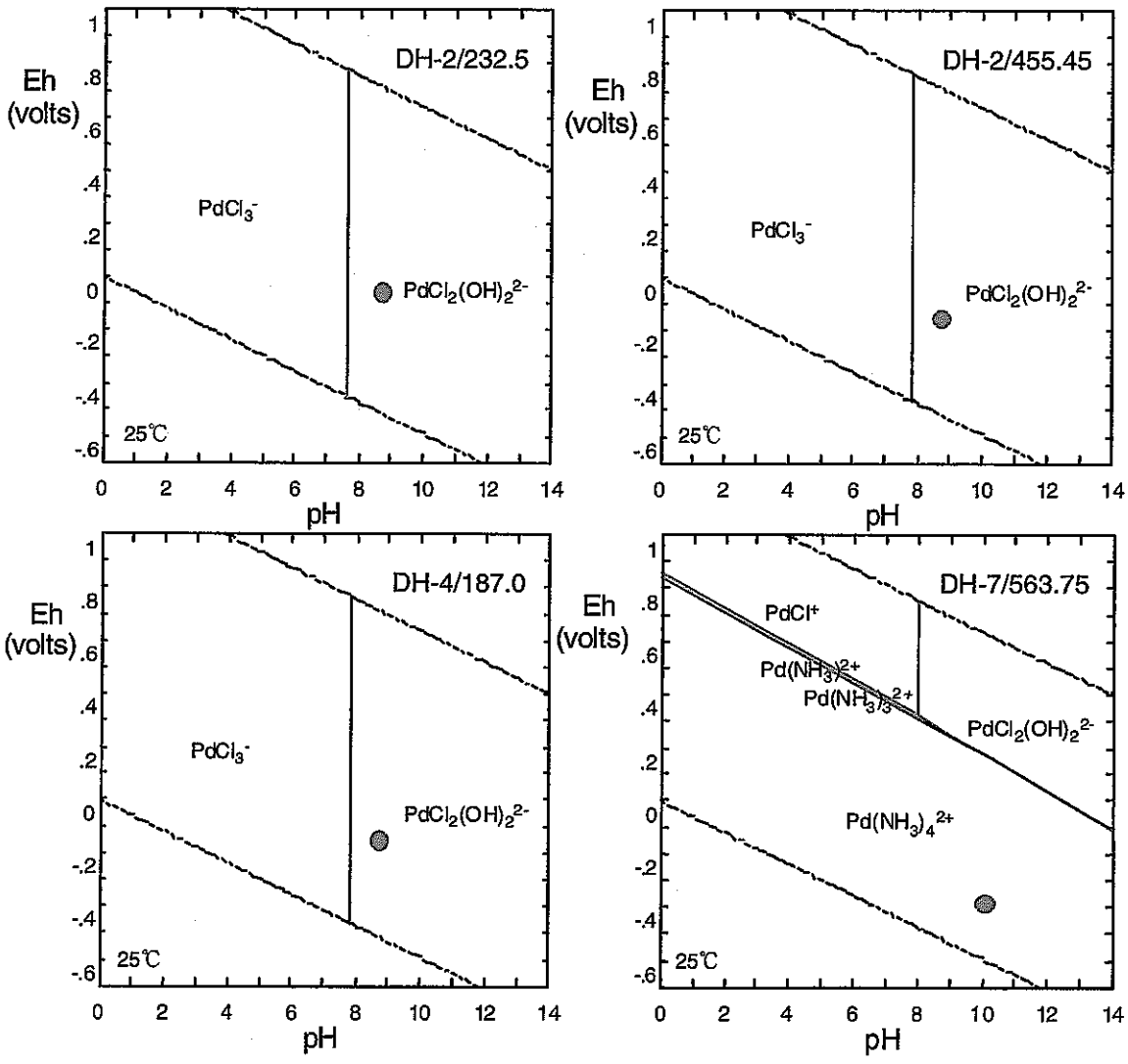

Figure 4.3-10 Eh-pH diagrams for palladium in a range of representative Tono groundwaters: DH-2/232.5 (intermediate pH, oxidising); DH-2/455.45 (intermediate pH, reducing); DH-4/187.0 (intermediate pH, oxidising); and DH-7/563.75 (high pH, reducing). The precise Eh-pH values of each groundwater is indicated by a red dot. Pd speciation is dominated by $PdCl_2(OH)_2^{2-}$ in three out of four groundwaters and by $Pd(NH_3)_4^{2+}$ in the remaining groundwater. The presence of appreciable ammonium concentrations apparently has a significant impact upon Pd speciation (and solubility).

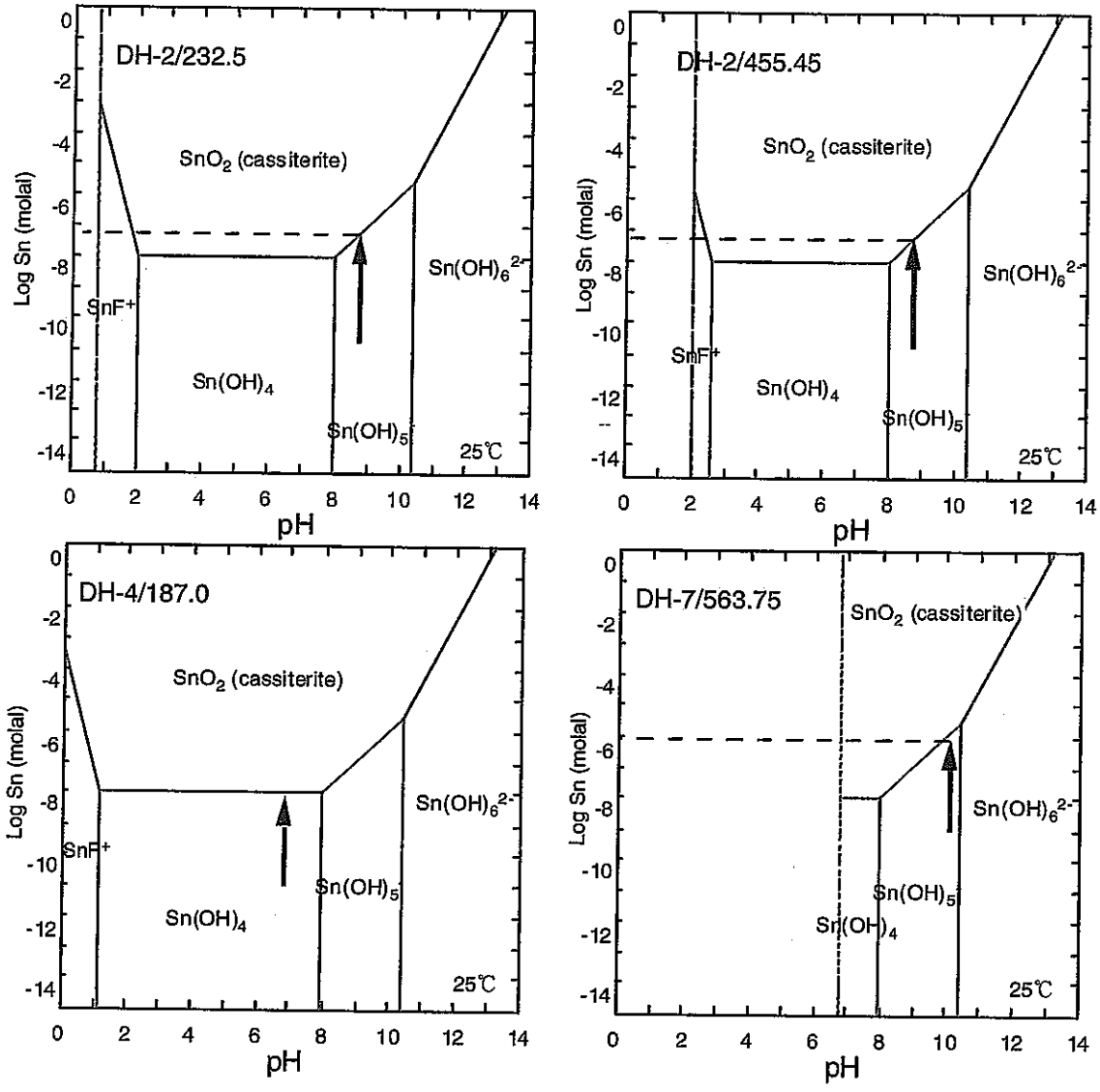

Figure 4.3-11 Variation of tin solubility with pH for a range of representative Tono groundwaters: DH-2/232.5 (intermediate pH, oxidising); DH-2/455.45 (intermediate pH, reducing); DH-4/187.0 (intermediate pH, oxidising); and DH-7/563.75 (high pH, reducing). The precise pH of each groundwater is arrowed and its accompanying Sn solubility indicated by a dashed line. Sn solubility ranges from approximately 10^{-8} to10^{-6} M. Slight variations in pH (± 1 pH units) could shift Sn solubility by 1-2 orders of magnitude in some cases. Solubility control is by equilibration of with SnO_2 (cassiterite) in all cases.

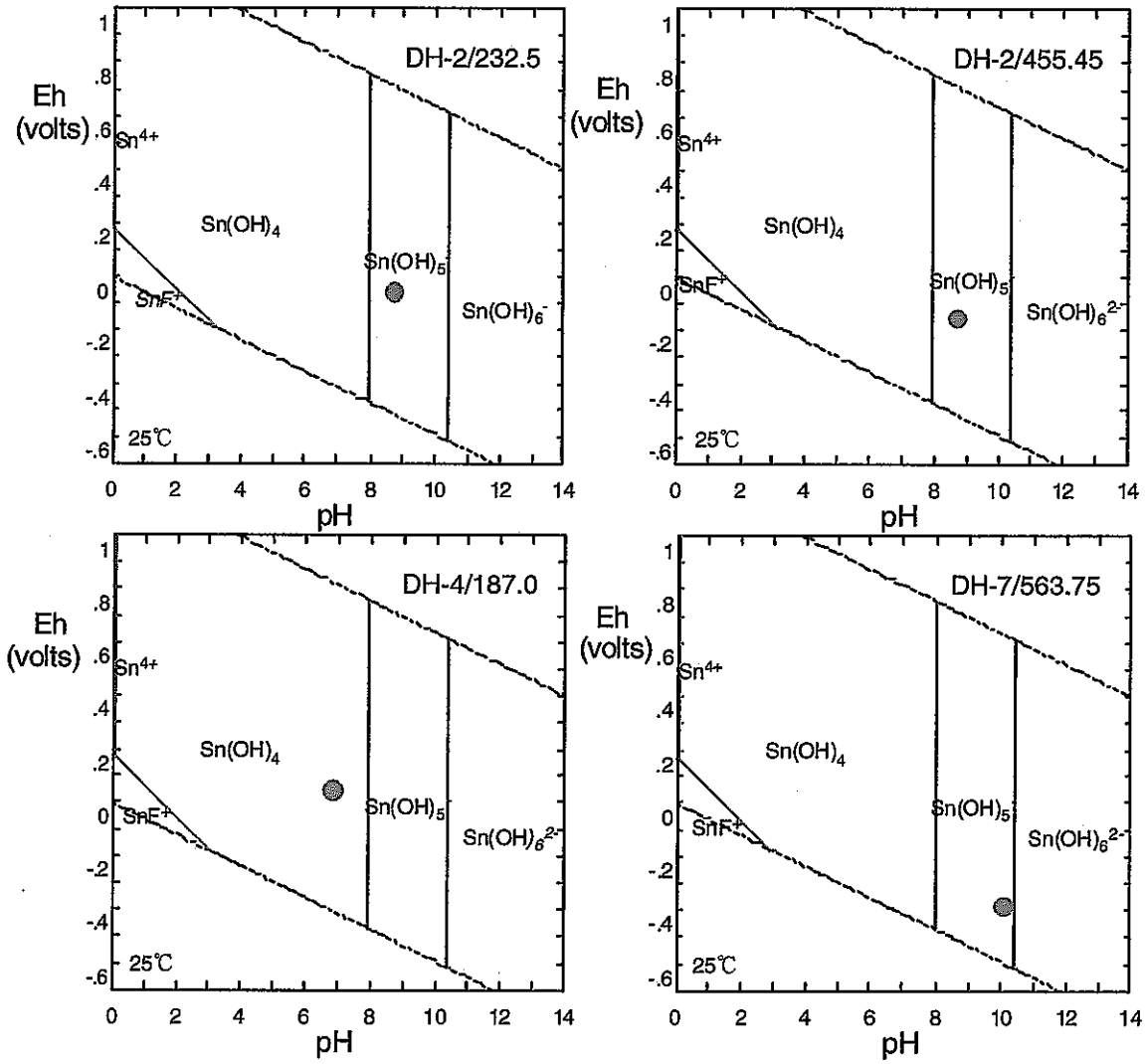

Figure 4.3-12 Eh-pH diagrams for tin in a range of representative Tono groundwaters: DH-2/232.5 (intermediate pH, oxidising); DH-2/455.45 (intermediate pH, reducing); DH-4/187.0 (intermediate pH, oxidising); and DH-7/563.75 (high pH, reducing). The precise Eh-pH values of each groundwater is indicated by a red dot. Sn speciation is dominated by $Sn(OH)_5^-$ or $Sn(OH)_6^{2-}$. Tin speciation is independent of Eh.

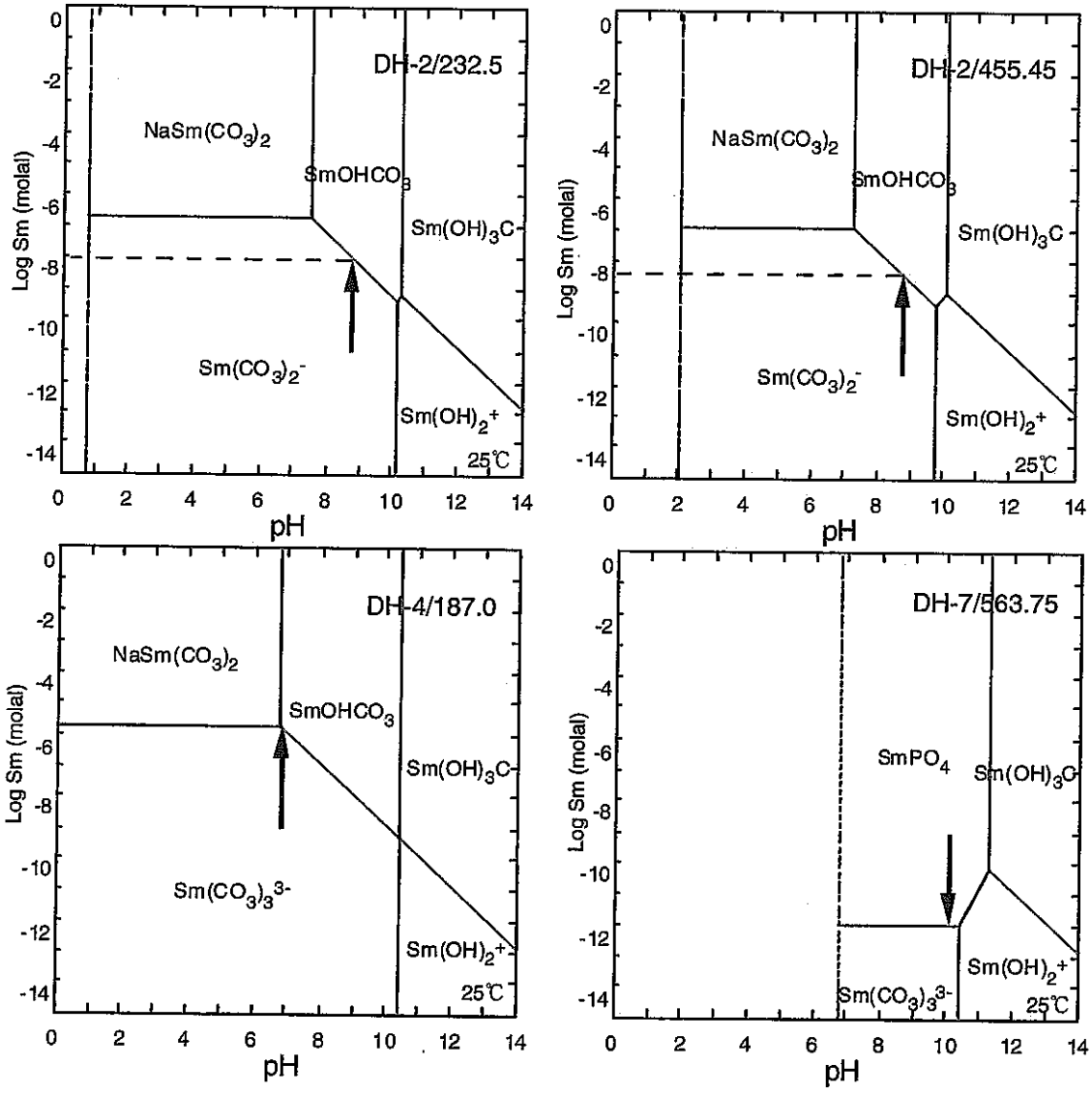

Figure 4.3-13 Variation of samarium solubility with pH for a range of representative Tono groundwaters: DH-2/232.5 (intermediate pH, oxidising); DH-2/455.45 (intermediate pH, reducing); DH-4/187.0 (intermediate pH, oxidising); and DH-7/563.75 (high pH, reducing). The precise pH of each groundwater is arrowed and its accompanying Sm solubility indicated by a dashed line. Am solubility ranges from approximately 10^{-12} to 10^{-6} M depending upon pH. Slight variations in pH (± 1 pH units) could shift Sm solubility by 1-2 orders of magnitude in some cases. Solubility control is by equilibration of with $SmOHCO_3$ in three cases and $SmPO_4$ in the other. Trace amounts of phosphate in groundwater DH-7/563.75 have a significant impact upon samarium solubility.

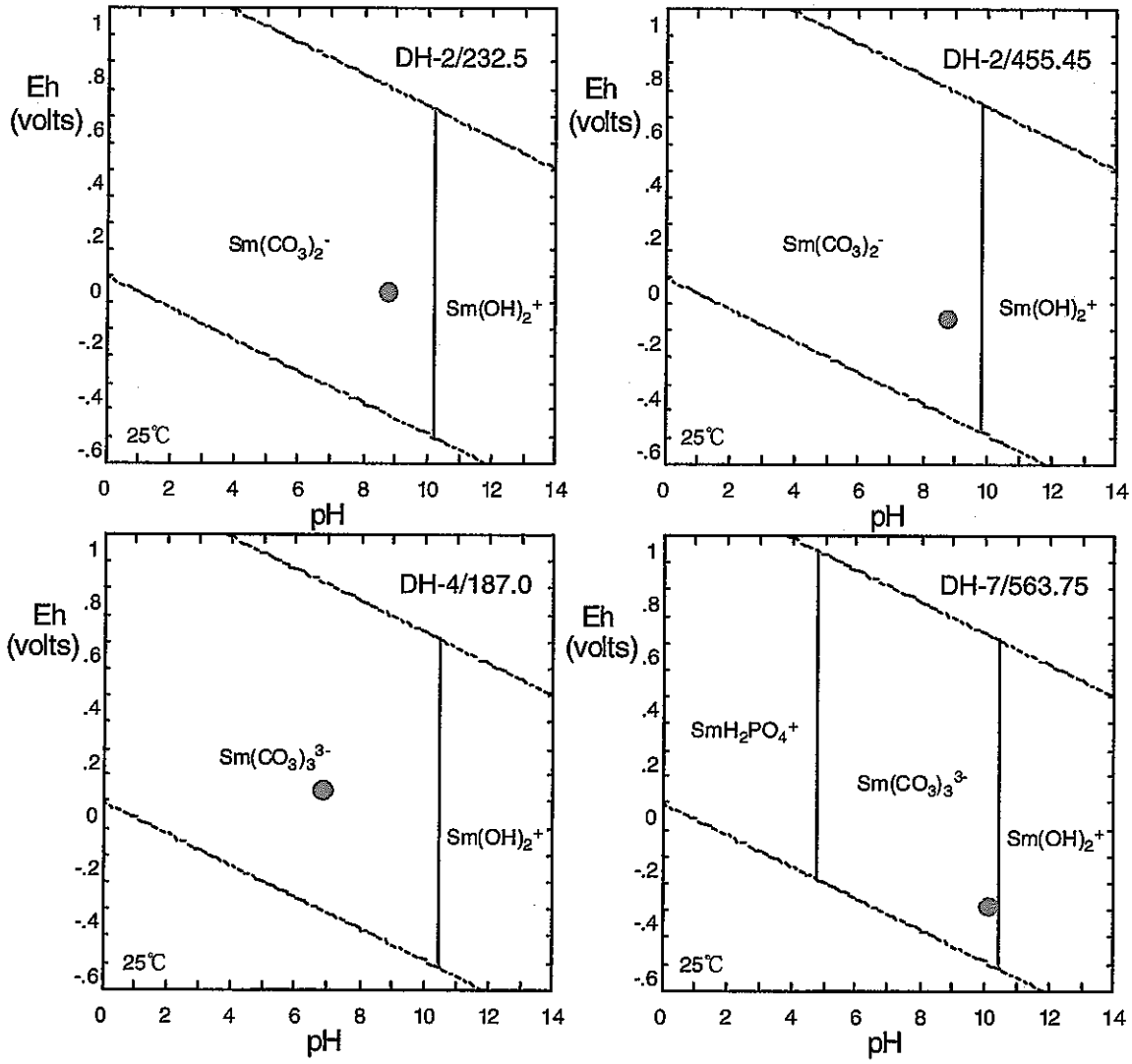

Figure 4.3-14 Eh-pH diagrams for samarium in a range of representative Tono groundwaters: DH-2/232.5 (intermediate pH, oxidising); DH-2/455.45 (intermediate pH, reducing); DH-4/187.0 (intermediate pH, oxidising); and DH-7/563.75 (high pH, reducing). The precise Eh-pH values of each groundwater is indicated by a red dot. Sm speciation is dominated by $Sm(CO_3)_3^{3-}$ in all cases. Trace amounts of phosphate in groundwater DH-7/563.75 have a significant impact upon americium speciation at pH < 5.

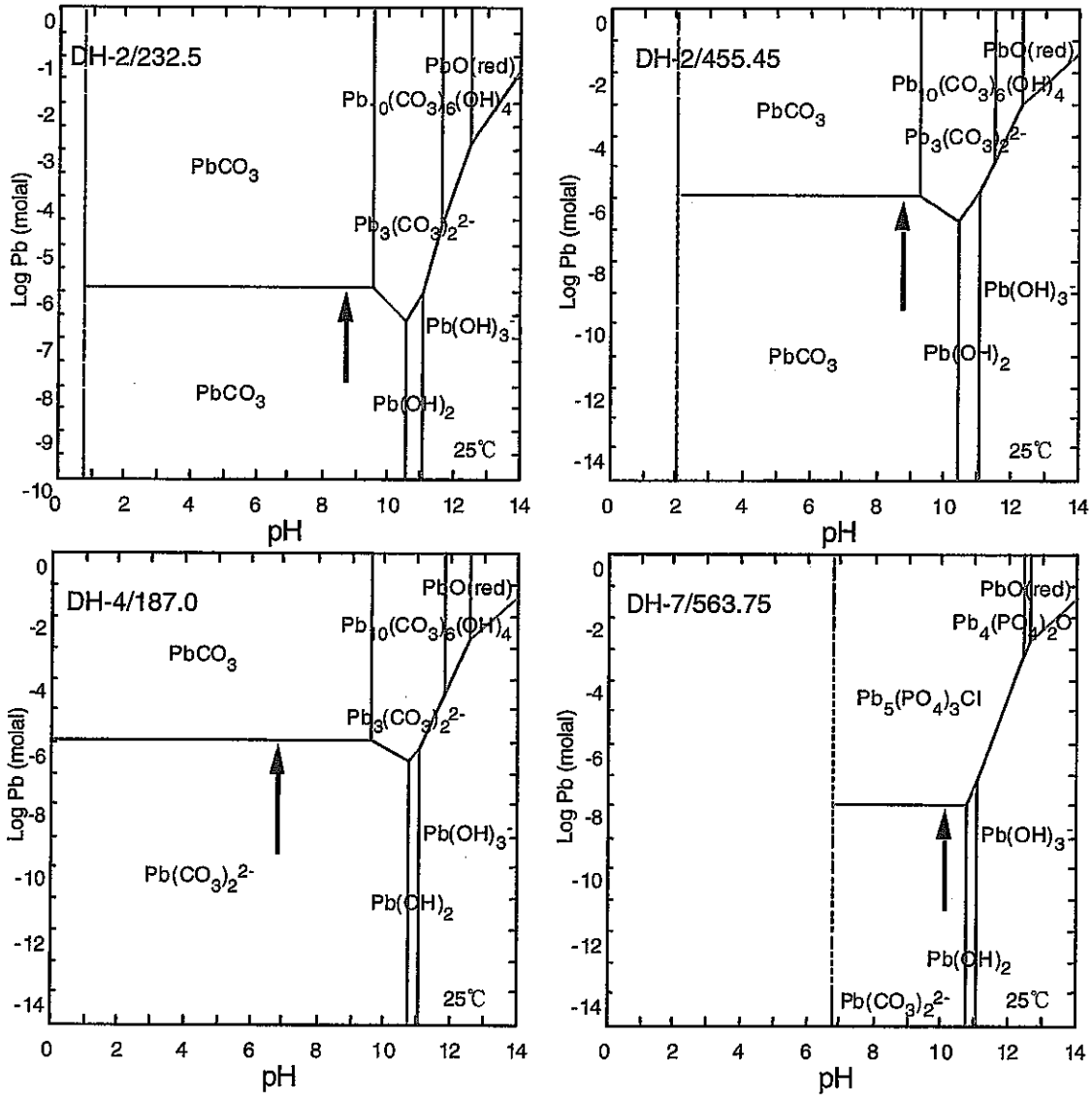

Figure 4.3-15 Variation of lead solubility with pH for a range of representative Tono groundwaters: DH-2/232.5 (intermediate pH, oxidising); DH-2/455.45 (intermediate pH, reducing); DH-4/187.0 (intermediate pH, oxidising); and DH-7/563.75 (high pH, reducing). The precise pH of each groundwater is arrowed and its accompanying Pb solubility indicated by a dashed line. Pb solubility ranges from approximately 10^{-8} to 10^{-6} M. Solubility control is by equilibration of with $PbCO_3$ in three cases and $Pb_5(PO_4)_3Cl$ in the other.

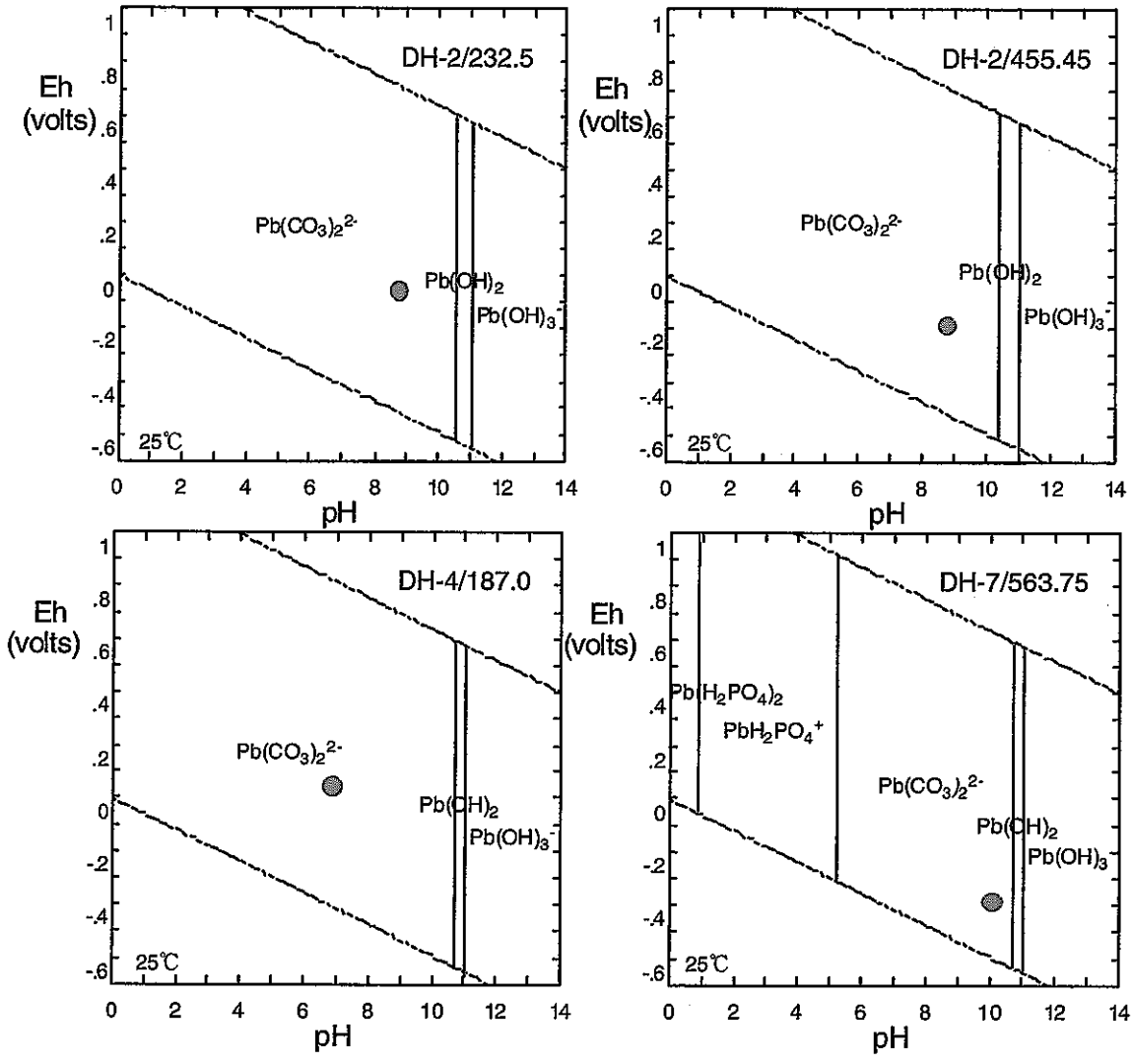

Figure 4.3-16 Eh-pH diagrams for lead in a range of representative Tono groundwaters: DH-2/232.5 (intermediate pH, oxidising); DH-2/455.45 (intermediate pH, reducing); DH-4/187.0 (intermediate pH, oxidising); and DH-7/563.75 (high pH, reducing). The precise Eh-pH values of each groundwater is indicated by a red dot. Pb speciation is dominated by $Pb(CO_3)_2^{2-}$ in all cases. Trace amounts of phosphate in groundwater DH-7/563.75 have a significant impact upon lead speciation at pH < 5.

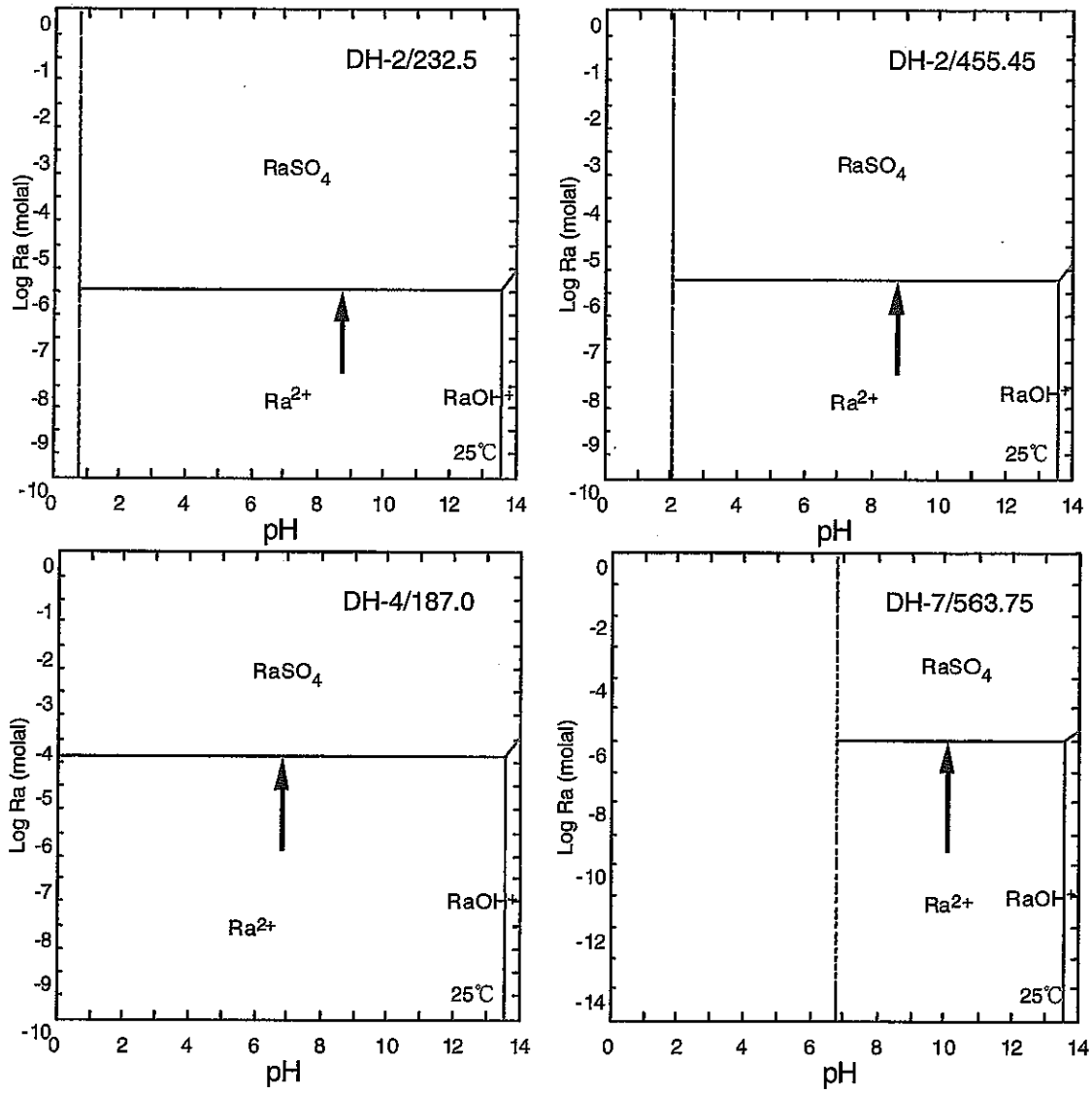

Figure 4.3-17 Variation of radium solubility with pH for a range of representative Tono groundwaters: DH-2/232.5 (intermediate pH, oxidising); DH-2/455.45 (intermediate pH, reducing); DH-4/187.0 (intermediate pH, oxidising); and DH-7/563.75 (high pH, reducing). The precise pH of each groundwater is arrowed and its accompanying Ra solubility indicated by a dashed line. Ra solubility ranges from approximately 10^{-6} to 10^{-4} M depending upon the amount of sulphate in each groundwater. Ra solubility is independent of pH (at pH < 13.5) and Eh. Solubility control is by equilibration with $RaSO_4$ in all cases. In reality, $RaSO_4$ will form as a solid-solution with other alkaline-earth metals, particularly Ba and Sr).

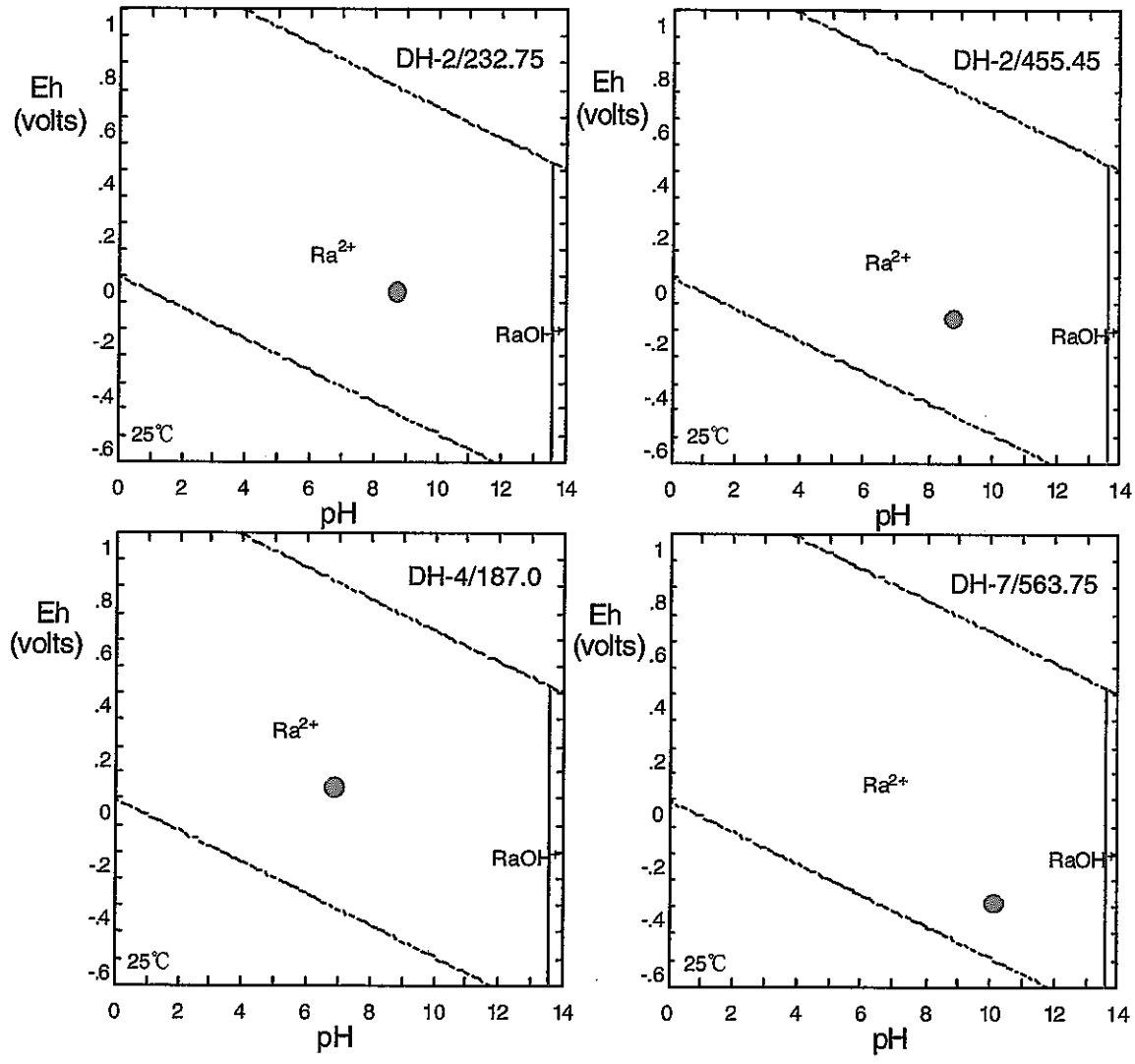

Figure 4.3-18 Eh-pH diagrams for radium in a range of representative Tono groundwaters: DH-2/232.5 (intermediate pH, oxidising); DH-2/455.45 (intermediate pH, reducing); DH-4/187.0 (intermediate pH, oxidising); and DH-7/563.75 (high pH, reducing). The precise Eh-pH values of each groundwater is indicated by a red dot. Ra speciation is dominated by Ra^{2+}.

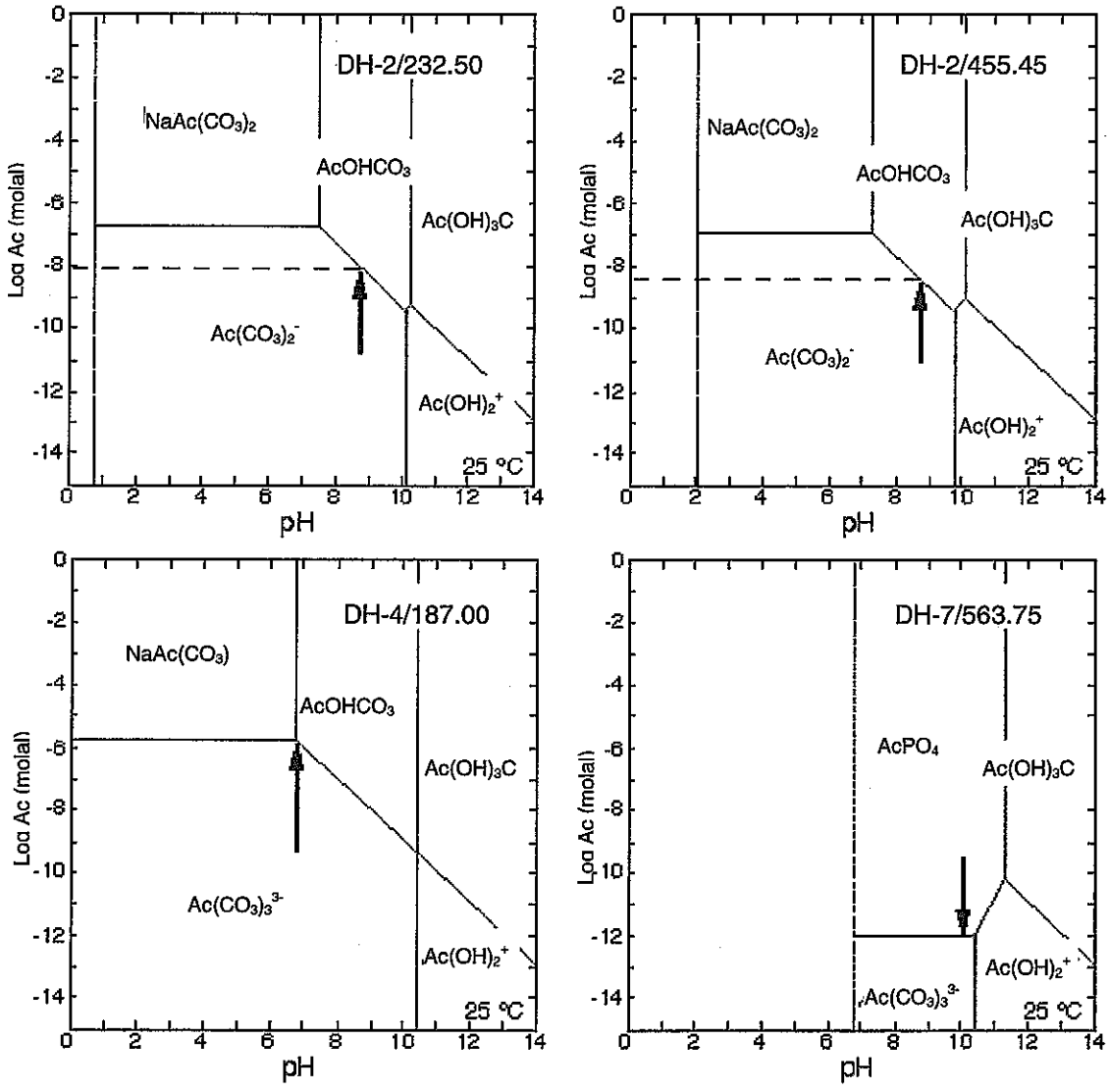

Figure 4.3-19 Variation of actinium solubility with pH for a range of representative Tono groundwaters: DH-2/232.5 (intermediate pH, oxidising); DH-2/455.45 (intermediate pH, reducing); DH-4/187.0 (intermediate pH, oxidising); and DH-7/563.75 (high pH, reducing). The precise pH of each groundwater is arrowed and its accompanying Ac solubility indicated by a dashed line. Ac solubility ranges from approximately 10^{-12} to 10^{-6} M. Slight variations in pH (± 1 pH units) could shift Ac solubility by 1-2 orders of magnitude in some cases. Solubility control is by equilibration of with $AcOHCO_3$ in three cases and $AcPO_4$ in the other.

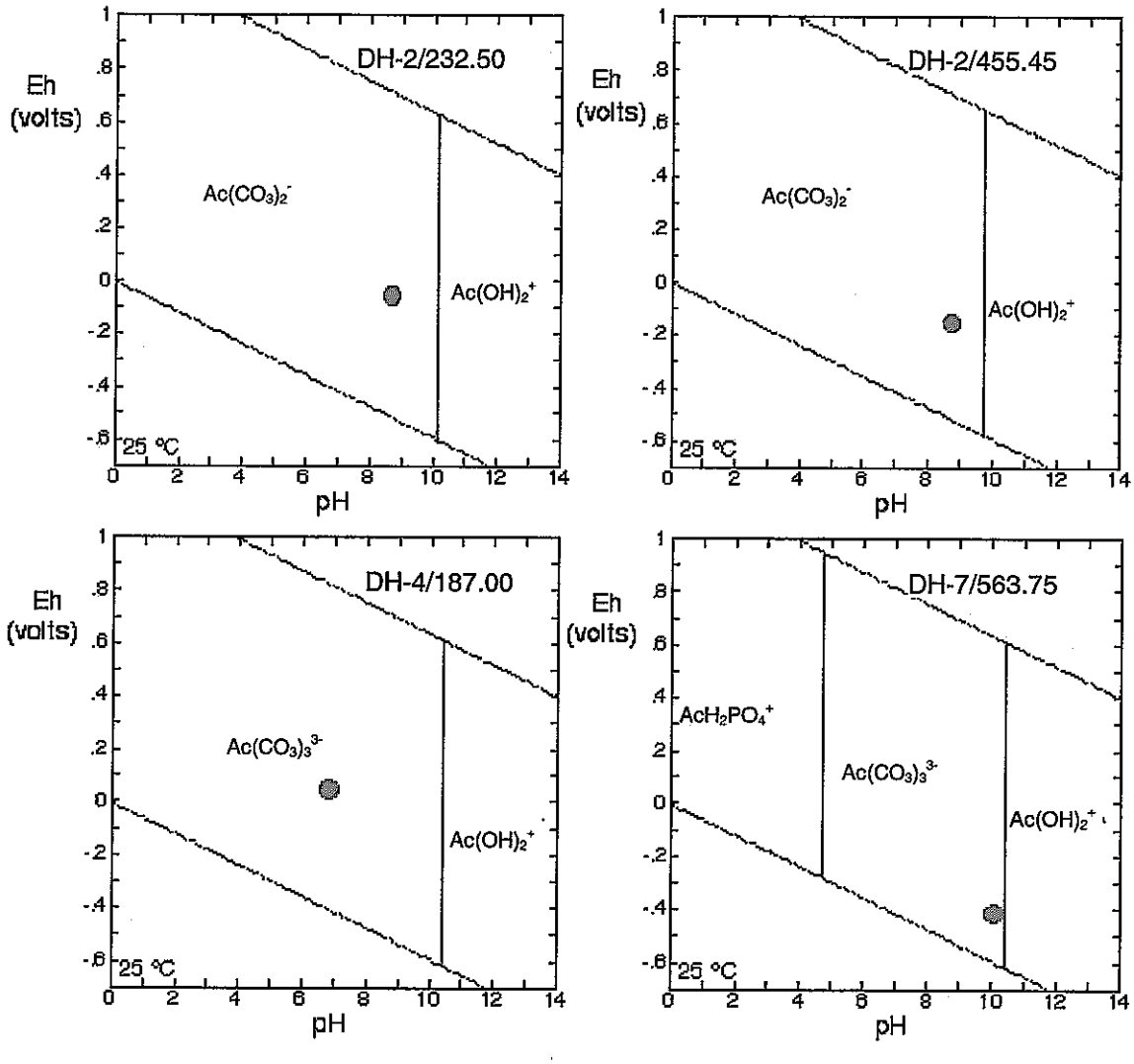

Figure 4.3-20 Eh-pH diagrams for actinium in a range of representative Tono groundwaters: DH-2/232.5 (intermediate pH, oxidising); DH-2/455.45 (intermediate pH, reducing); DH-4/187.0 (intermediate pH, oxidising); and DH-7/563.75 (high pH, reducing). The precise Eh-pH values of each groundwater is indicated by a red dot. Ac speciation is dominated by $Ac(CO_3)_3^{3-}$. Trace amounts of phosphate in groundwater DH-7/563.75 have a significant impact upon actinium speciation at pH < 5.

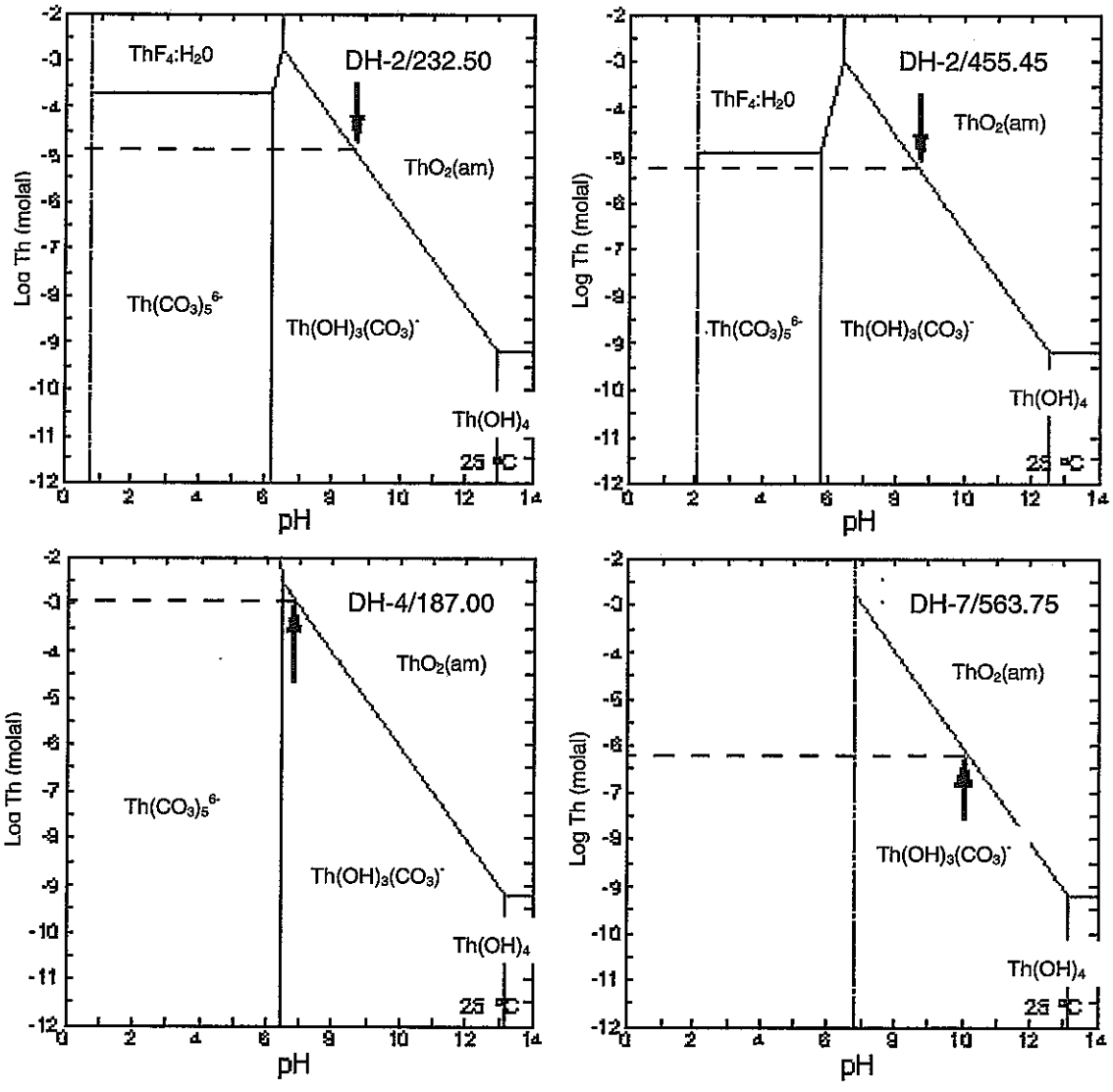

Figure 4.3-21 Variation of thorium solubility with pH for a range of representative Tono groundwaters: DH-2/232.5 (intermediate pH, oxidising); DH-2/455.45 (intermediate pH, reducing); DH-4/187.0 (intermediate pH, oxidising); and DH-7/563.75 (high pH, reducing). The precise pH of each groundwater is arrowed and its accompanying Th solubility indicated by a dashed line. Th solubility ranges from approximately 10^{-6} to10^{-3} M. Slight variations in pH (± 1 pH units) could shift Th solubility by 1-2 orders of magnitude in all cases. Solubility control is by equilibration with amorphous ThO_2 in all cases.

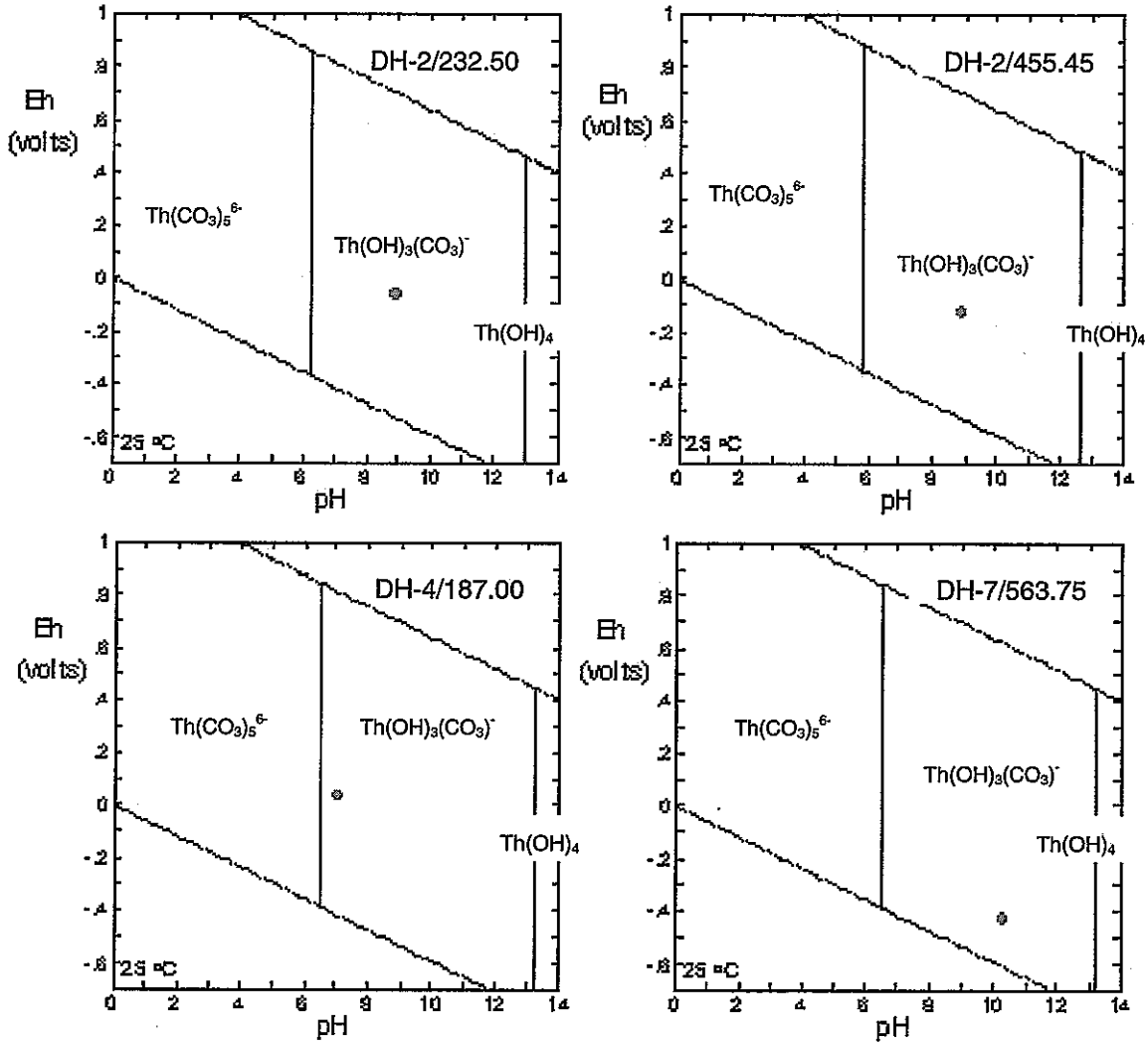

Figure 4.3-22 Eh-pH diagrams for thorium in a range of representative Tono groundwaters: DH-2/232.5 (intermediate pH, oxidising); DH-2/455.45 (intermediate pH, reducing); DH-4/187.0 (intermediate pH, oxidising); and DH-7/563.75 (high pH, reducing). The precise Eh-pH values of each groundwater is indicated by a red dot. Th speciation is dominated by $Th(OH)_3(CO_3)^-$ in each case. Th speciation is insensitive to redox.

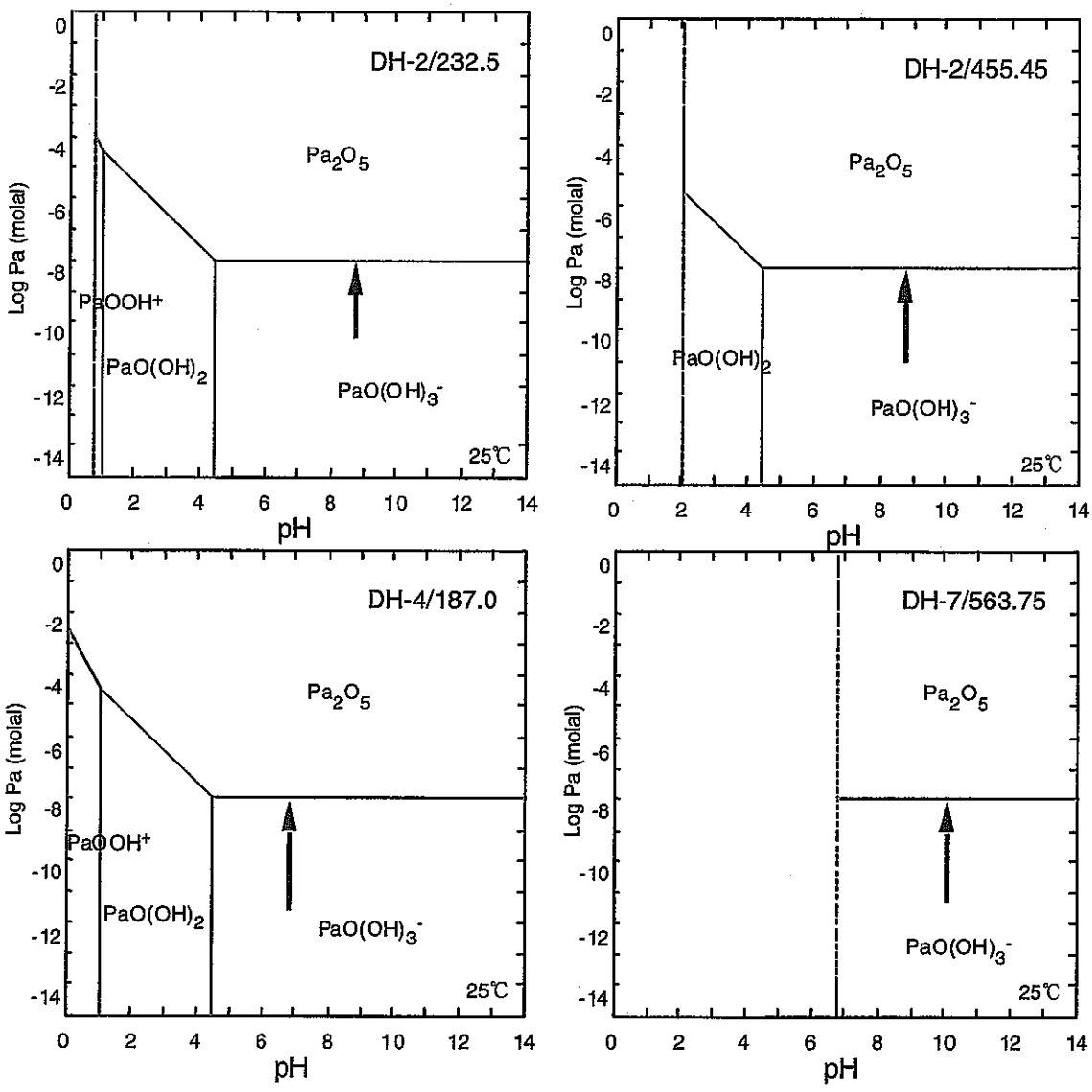

Figure 4.3-23 Variation of protoactinium solubility with pH for a range of representative Tono groundwaters: DH-2/232.5 (intermediate pH, oxidising); DH-2/455.45 (intermediate pH, reducing); DH-4/187.0 (intermediate pH, oxidising); and DH-7/563.75 (high pH, reducing). The precise pH of each groundwater is arrowed and its accompanying Pa solubility indicated by a dashed line. Pa solubility is approximately 10^{-8} M in all groundwaters. Pa solubility is independent of Eh and pH at pH > 4.5. Solubility control is by equilibration of with Pa_2O_5 in all cases.

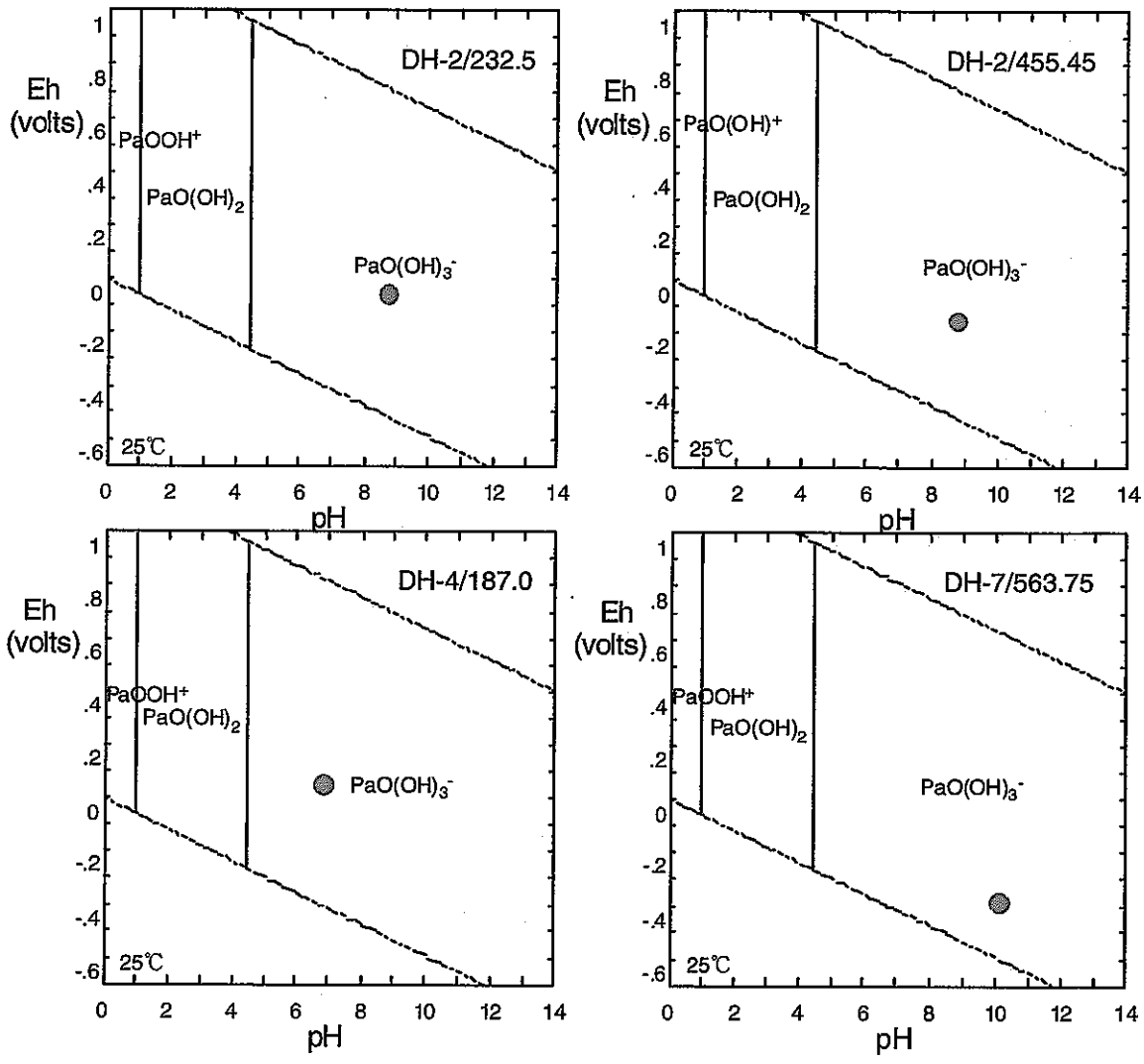

Figure 4.3-24 Eh-pH diagrams for protoactinium in a range of representative Tono groundwaters: DH-2/232.5 (intermediate pH, oxidising); DH-2/455.45 (intermediate pH, reducing); DH-4/187.0 (intermediate pH, oxidising); and DH-7/563.75 (high pH, reducing). The precise Eh-pH values of each groundwater is indicated by a red dot. Pa speciation is dominated by $PaO(OH)_3^-$ in all cases. Pa speciation is independent of Eh.

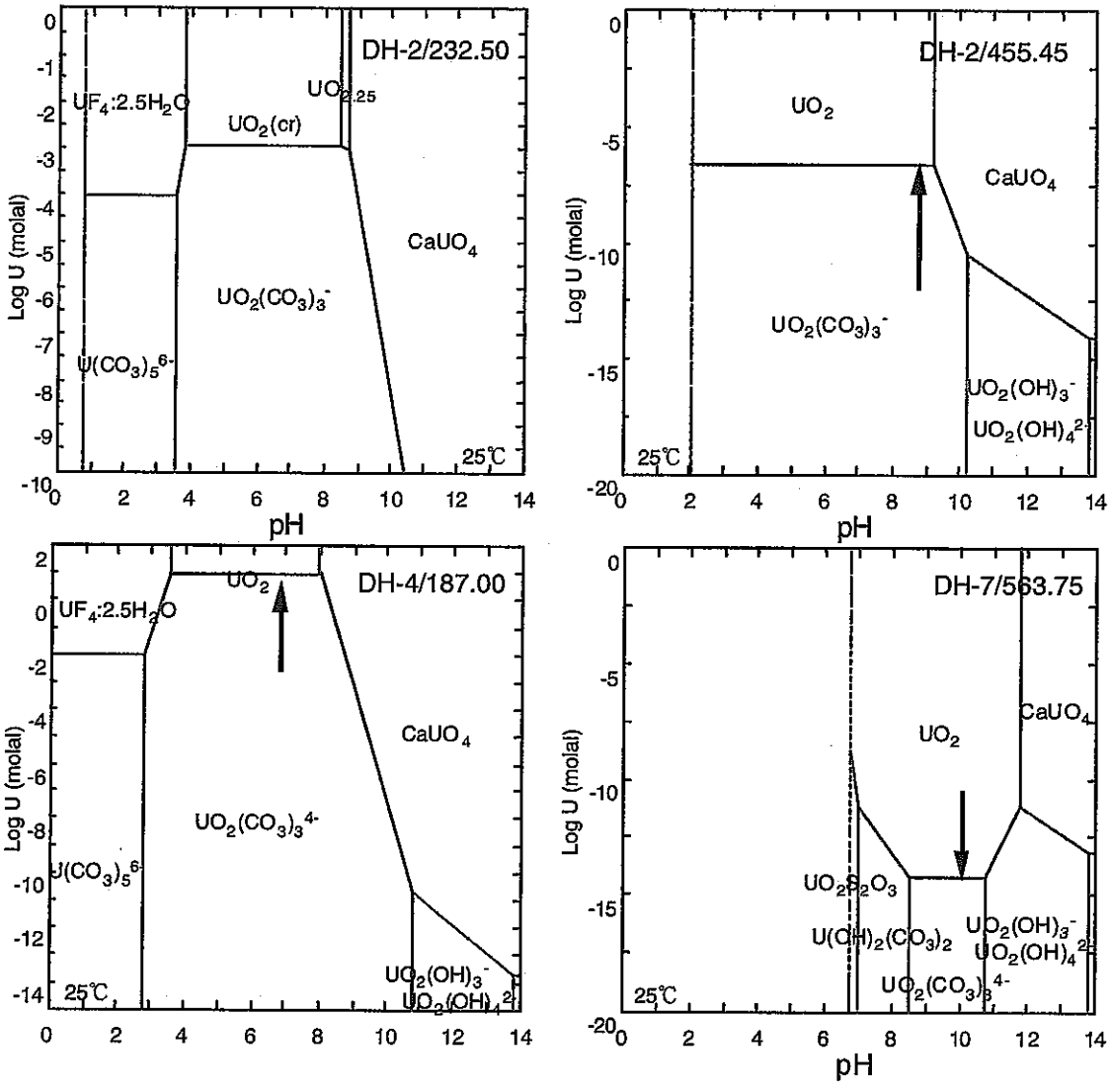

Figure 4.3-25 Variation of uranium solubility with pH for a range of representative Tono groundwaters: DH-2/232.5 (intermediate pH, oxidising); DH-2/455.45 (intermediate pH, reducing); DH-4/187.0 (intermediate pH, oxidising); and DH-7/563.75 (high pH, reducing). The precise pH of each groundwater is arrowed and its accompanying U solubility indicated by a dashed line. U solubility ranges from approximately 10^{-4} to10^{-2} M in shallow, oxidising groundwaters to 10^{-14} to 10^{-7} M in reducing groundwaters. Variations in pH (± 2 pH units) could shift U solubility by 1-2 orders of magnitude in some cases. Solubility control is by equilibration of with UO_2 in all cases. U solubility depends upon Eh, pH, and carbonate concentration.

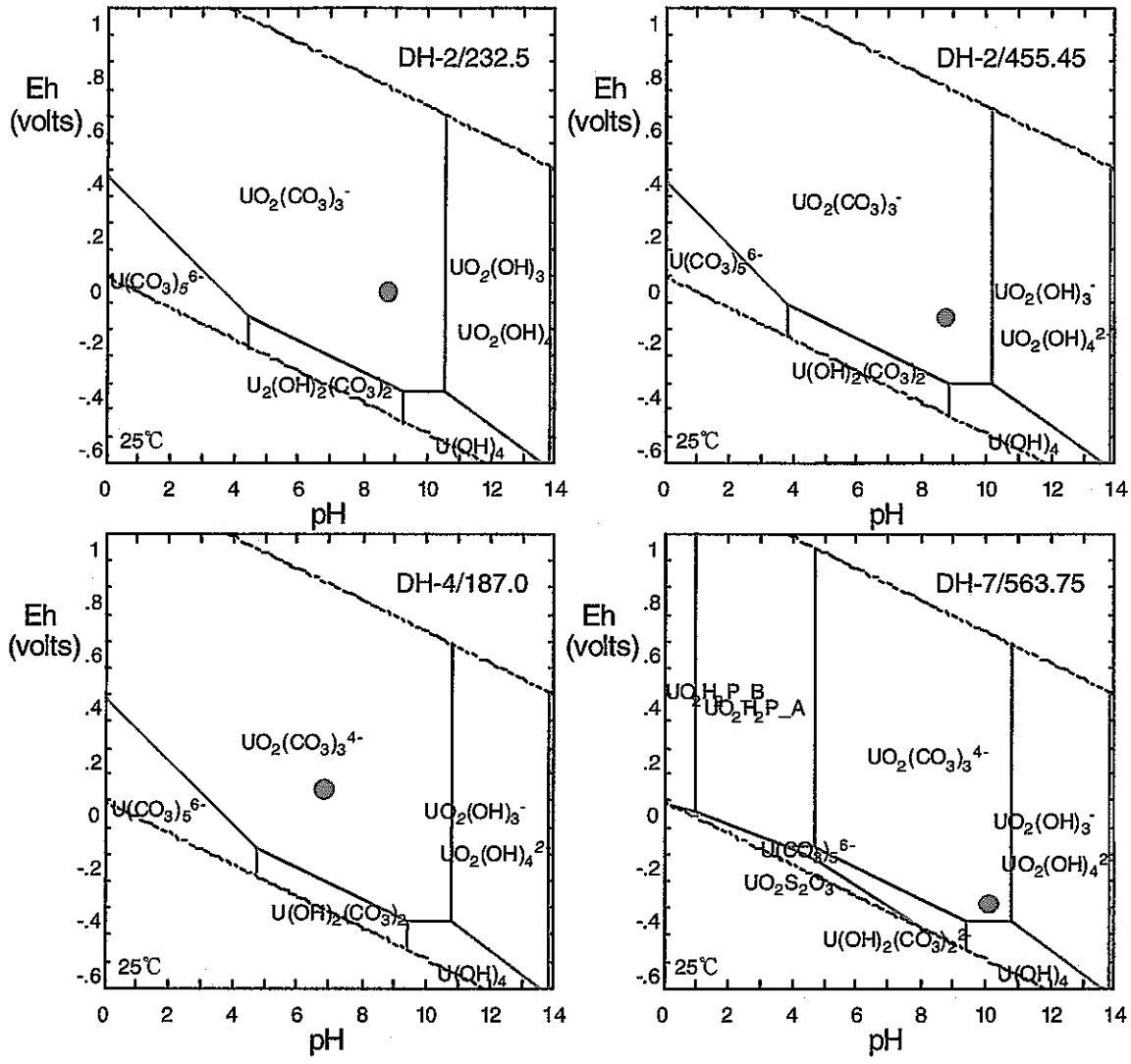

Figure 4.3-26 Eh-pH diagrams for uranium in a range of representative Tono groundwaters: DH-2/232.5 (intermediate pH, oxidising); DH-2/455.45 (intermediate pH, reducing); DH-4/187.0 (intermediate pH, oxidising); and DH-7/563.75 (high pH, reducing). The precise Eh-pH values of each groundwater is indicated by a red dot. U speciation is dominated by $UO_2(CO_3)_3^{4-}$ in all cases. Trace amounts of phosphate in groundwater DH-7/563.75 have a significant impact upon uranium speciation at pH < 5.

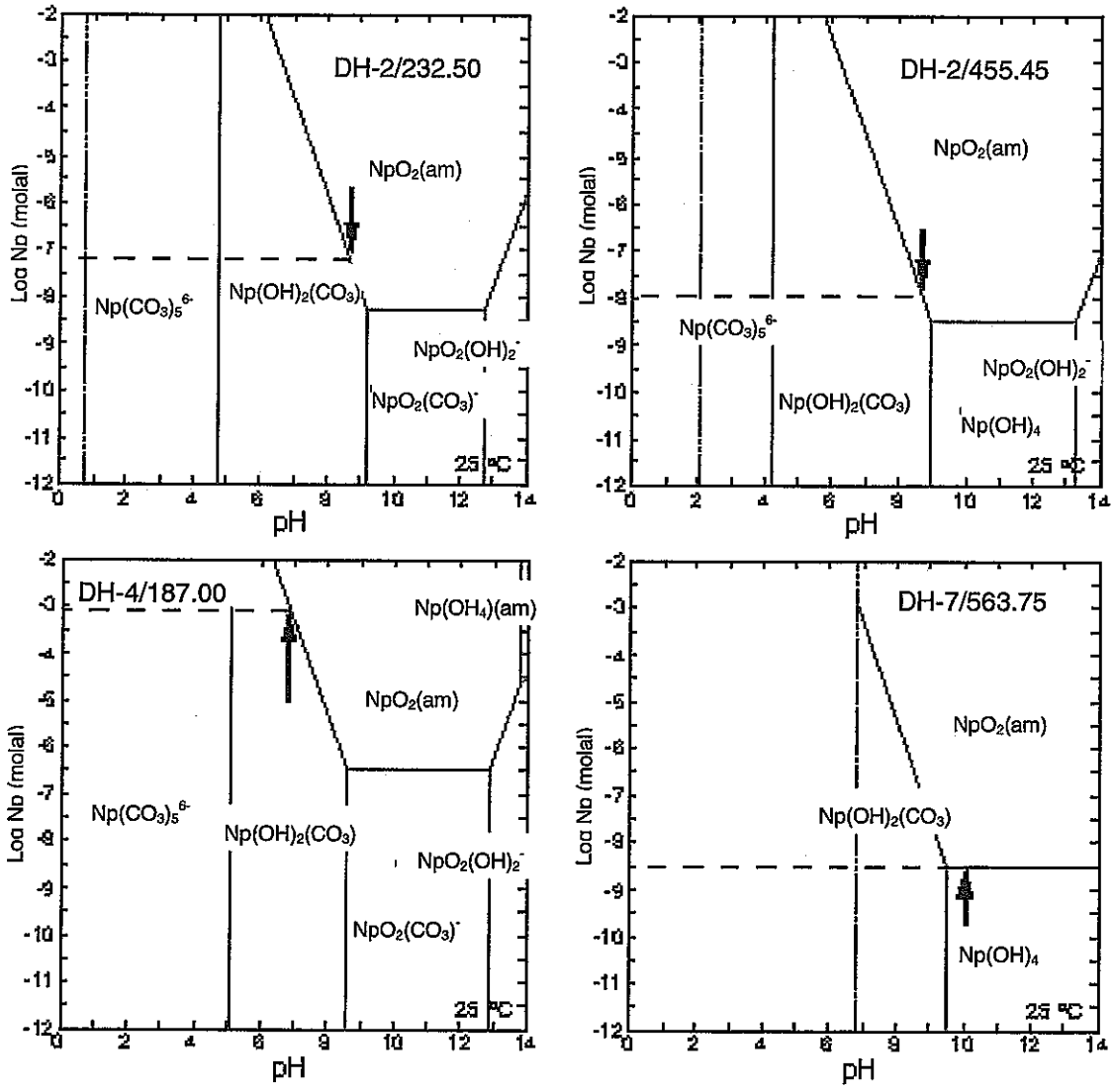

Figure 4.3-27 Variation of neptunium solubility with pH for a range of representative Tono groundwaters: DH-2/232.5 (intermediate pH, oxidising); DH-2/455.45 (intermediate pH, reducing); DH-4/187.0 (intermediate pH, oxidising); and DH-7/563.75 (high pH, reducing). The precise pH of each groundwater is arrowed and its accompanying Np solubility indicated by a dashed line. Np solubility ranges from approximately 10^{-7} to 10^{-3} M in shallow, oxidising groundwaters to 10^{-9} to 10^{-8} M in reducing groundwaters. Slight variations in pH (± 1 pH units) could shift Np solubility by 1-2 orders of magnitude in all cases. Solubility control is by equilibration with amorphous NpO_2 in all cases.

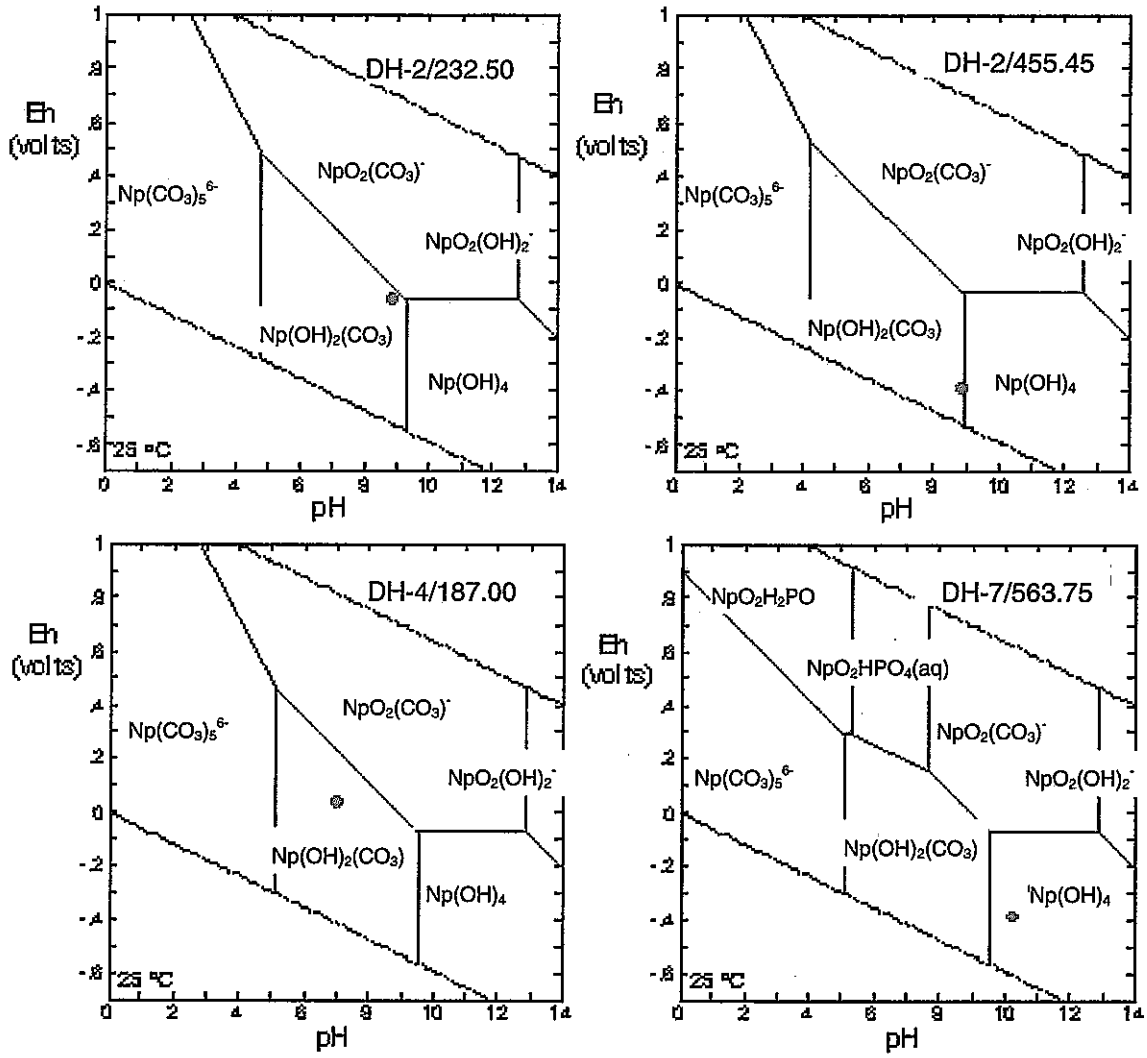

Figure 4.3-28 Eh-pH diagrams for neptunium in a range of representative Tono groundwaters: DH-2/232.5 (intermediate pH, oxidising); DH-2/455.45 (intermediate pH, reducing); DH-4/187.0 (intermediate pH, oxidising); and DH-7/563.75 (high pH, reducing). The precise Eh-pH value of each groundwater is indicated by a red dot in each Figure. Np speciation is dominated by $Np(OH)_2(CO_3)$ or $Np(OH)_4$. Redox is important for Np speciation.

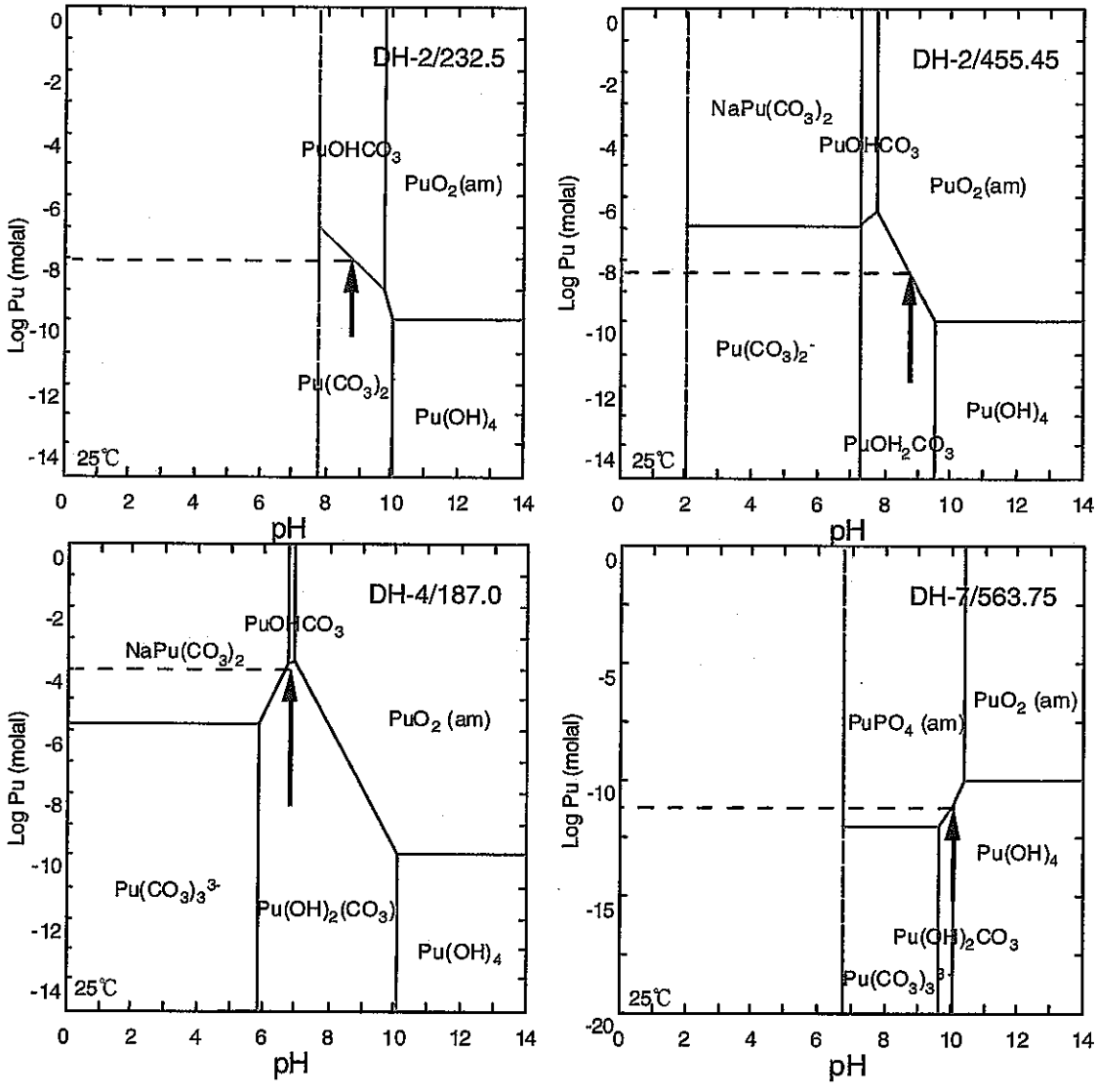

Figure 4.3-29 Variation of plutonium solubility with pH for a range of representative Tono groundwaters: DH-2/232.5 (intermediate pH, oxidising); DH-2/455.45 (intermediate pH, reducing); DH-4/187.0 (intermediate pH, oxidising); and DH-7/563.75 (high pH, reducing). The precise pH of each groundwater is arrowed and its accompanying Pu solubility indicated by a dashed line. Pu solubility ranges from approximately 10^{-8} to 10^{-6} M in shallow, oxidising groundwaters to 10^{-11} to 10^{-8} M in reducing groundwaters. Slight variations in pH (± 1 pH units) could shift Pu solubility by 1-2 orders of magnitude. Solubility control is by equilibration with either $NaPu(CO_3)_2$, $PuOHCO_3$, PuO_2 (am), or $PuPO_4$ (am).

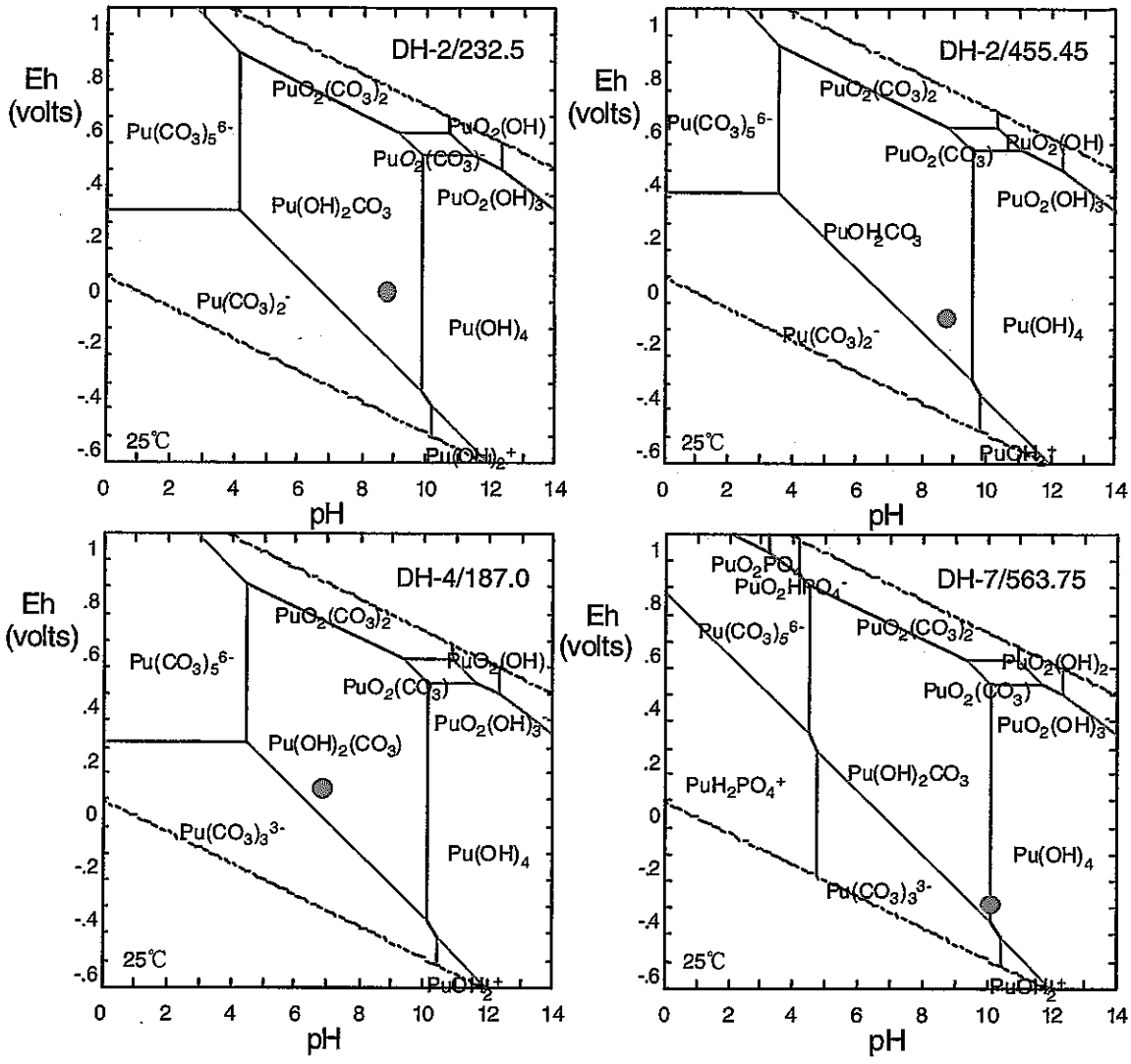

Figure 4.3-30 Eh-pH diagrams for plutonium in a range of representative Tono groundwaters: DH-2/232.5 (intermediate pH, oxidising); DH-2/455.45 (intermediate pH, reducing); DH-4/187.0 (intermediate pH, oxidising); and DH-7/563.75 (high pH, reducing). The precise Eh-pH values of each groundwater is indicated by a red dot. Pu speciation is dominated by $Pu(OH)_2(CO_3)$ in all cases Plutonium speciation is sensitive to pH, Eh and carbonate concentration.

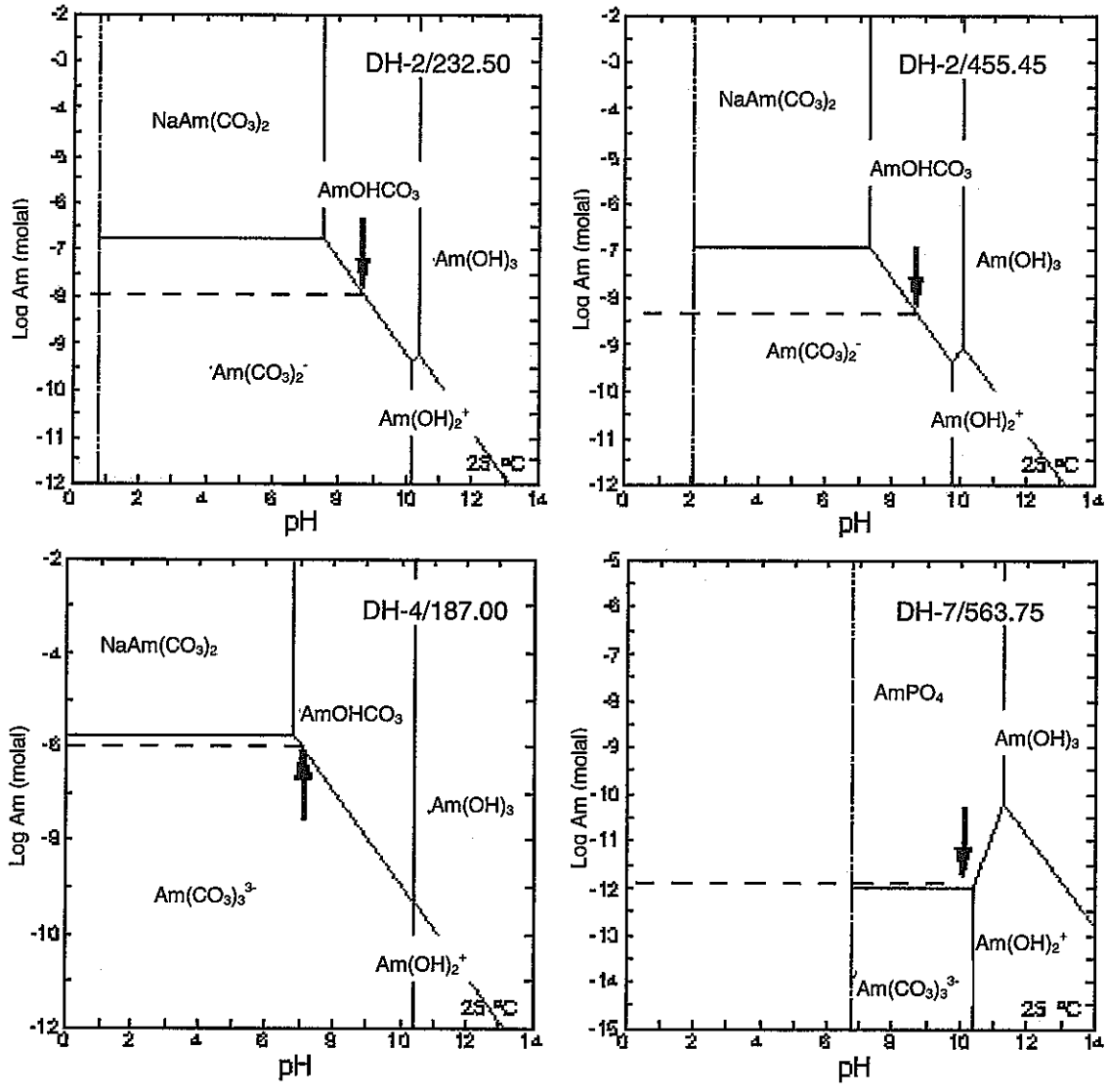

Figure 4.3-31 Variation of americium solubility with pH for a range of representative Tono groundwaters: DH-2/232.5 (intermediate pH, oxidising); DH-2/455.45 (intermediate pH, reducing); DH-4/187.0 (intermediate pH, oxidising); and DH-7/563.75 (high pH, reducing). The precise pH of each groundwater is arrowed and its accompanying Am solubility indicated by a dashed line. Am solubility ranges from approximately 10^{-8} to 10^{-6} M in shallow, oxidising groundwaters to 10^{-12} to 10^{-9} M in reducing groundwaters. Slight variations in pH (± 1 pH units) could shift Am solubility by 1-2 orders of magnitude in some cases. Solubility control is by equilibration of with $AmOHCO_3$ in three cases and $AmPO_4$ in the other.

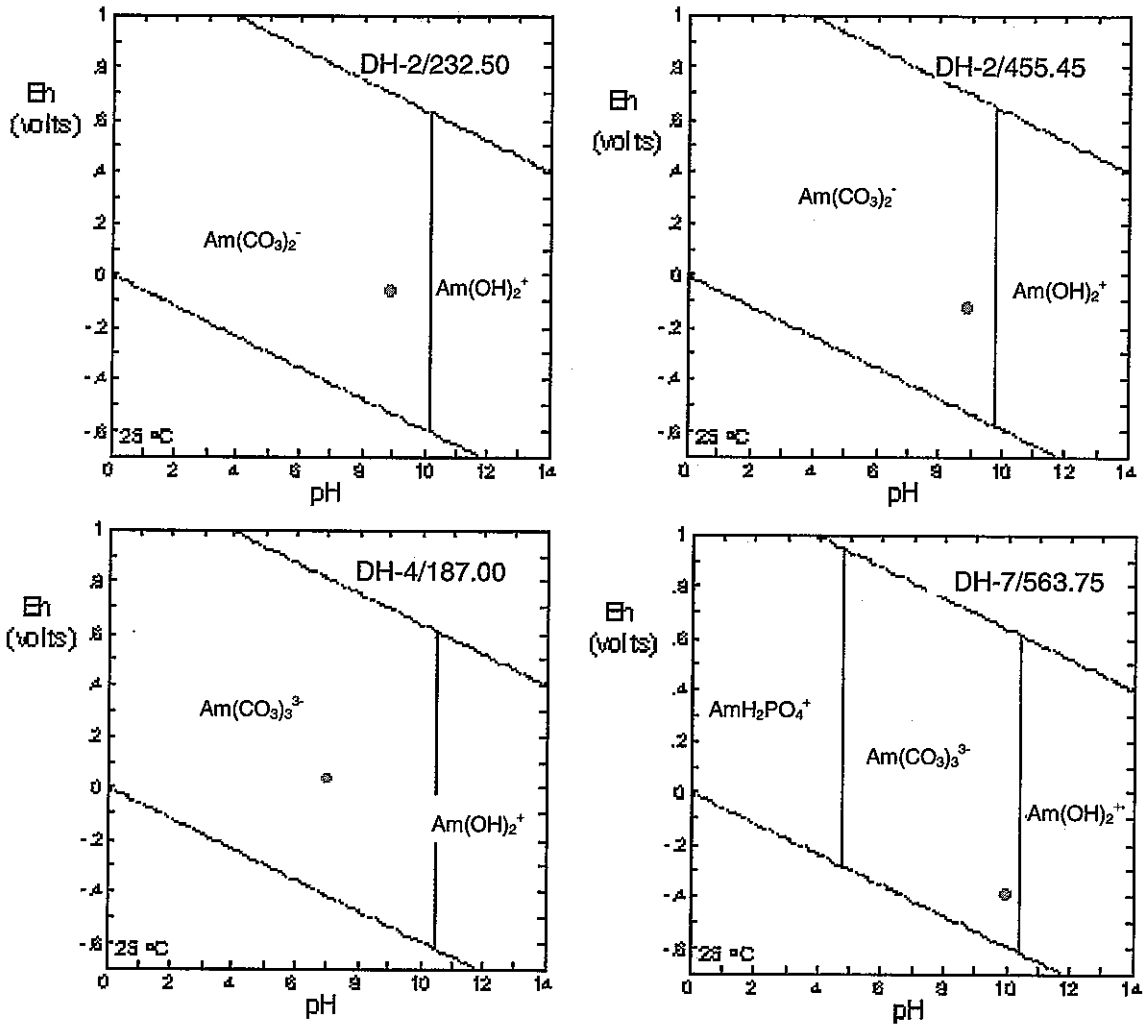

Figure 4.3-32 Eh-pH diagrams for americium in a range of representative Tono groundwaters: DH-2/232.5 (intermediate pH, oxidising); DH-2/455.45 (intermediate pH, reducing); DH-4/187.0 (intermediate pH, oxidising); and DH-7/563.75 (high pH, reducing). The precise Eh-pH values of each groundwater is indicated by a red dot. Am speciation is dominated by $Am(CO_3)_2^-$ or $Am(CO_3)_3^{3-}$. Trace amounts of phosphate in groundwater DH-7/563.75 have a significant impact upon americium speciation at pH < 5.

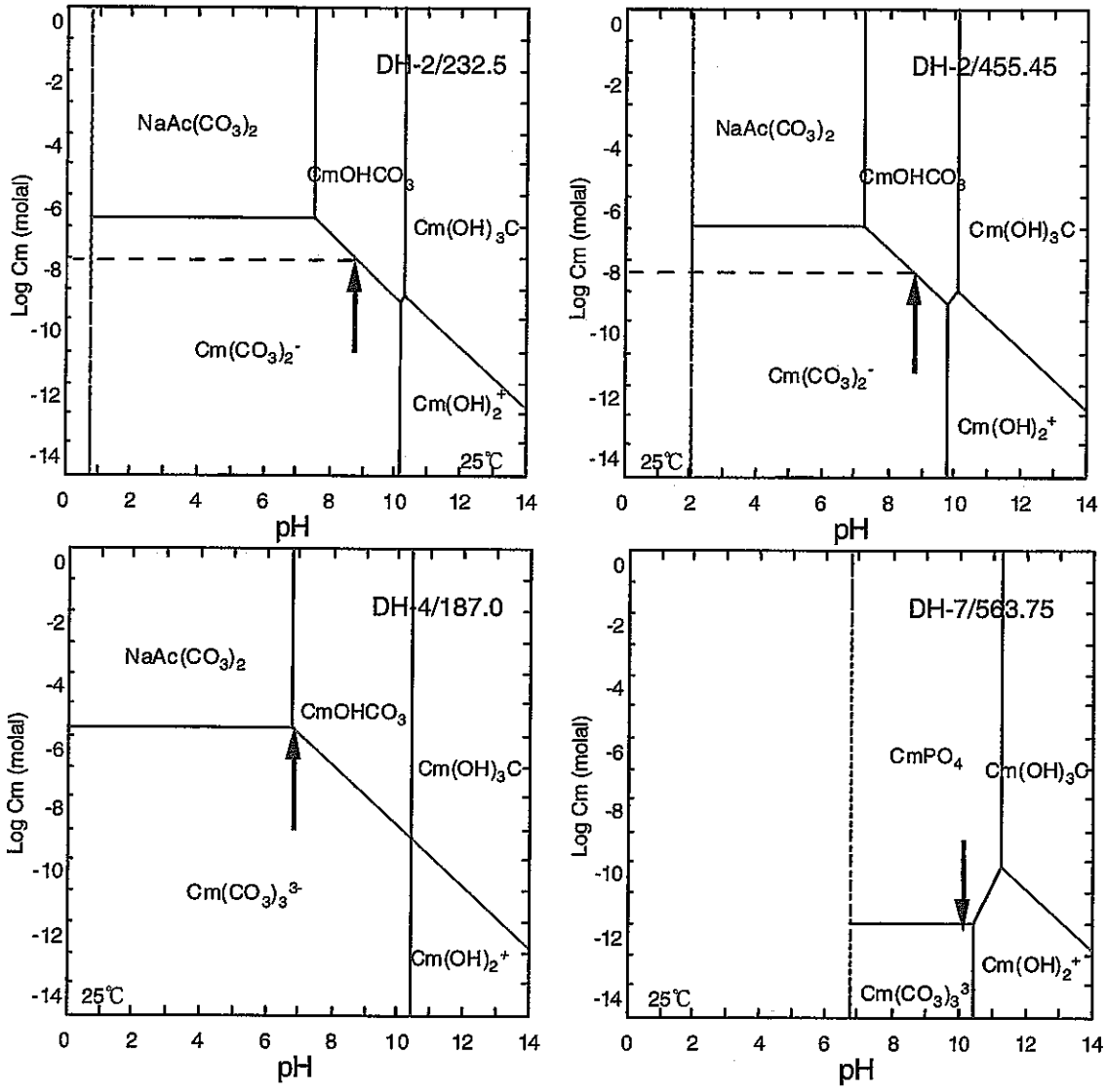

Figure 4.3-33 Variation of curium solubility with pH for a range of representative Tono groundwaters: DH-2/232.5 (intermediate pH, oxidising); DH-2/455.45 (intermediate pH, reducing); DH-4/187.0 (intermediate pH, oxidising); and DH-7/563.75 (high pH, reducing). The precise pH of each groundwater is arrowed and its accompanying Cm solubility indicated by a dashed line. Cm solubility ranges from approximately 10^{-7} to 10^{-6} M in shallow, oxidising groundwaters to 10^{-12} to 10^{-8} M in reducing groundwaters. Slight variations in pH (± 1 pH units) could shift Cm solubility by 1-2 orders of magnitude. Solubility control is by equilibration of with $CmOHCO_3$ in three cases and $CmPO_4$ in the other.

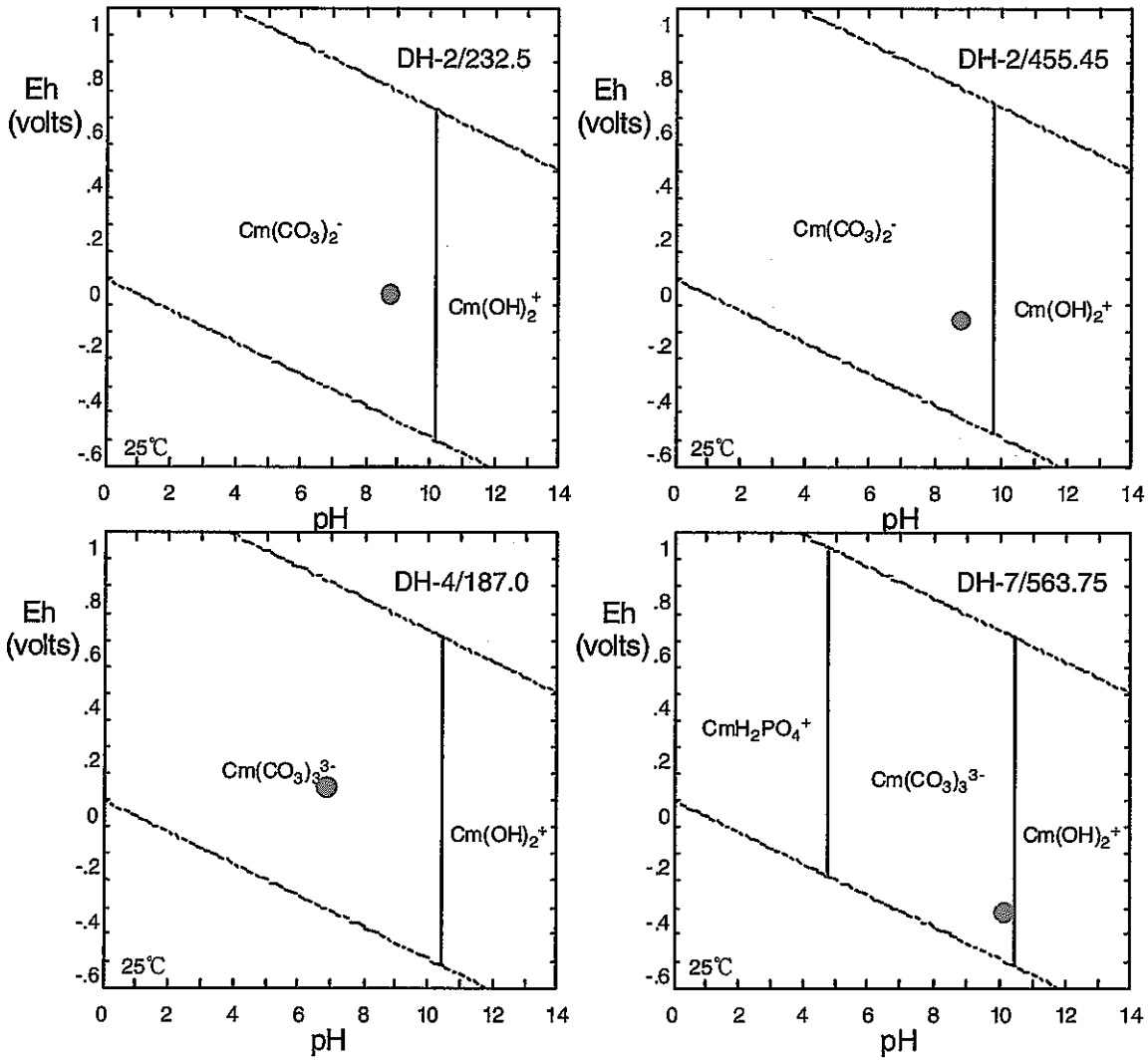

Figure 4.3-34 Eh-pH diagrams for curium in a range of representative Tono groundwaters: DH-2/232.5 (intermediate pH, oxidising); DH-2/455.45 (intermediate pH, reducing); DH-4/187.0 (intermediate pH, oxidising); and DH-7/563.75 (high pH, reducing). The precise Eh-pH values of each groundwater is indicated by a red dot. Cm speciation is dominated by $Cm(CO_3)_2^-$ or $Cm(CO_3)_3^{3-}$. Trace amounts of phosphate in groundwater DH-7/563.75 have a significant impact upon curium speciation at pH < 5. Cm speciation is independent of Eh.

The results of these calculations highlighted that Cs could not be solubility-controlled in these groundwaters. Therefore, in the remaining solubility calculations this element was not considered further.

These calculations revealed that the minerals in Table 4.3-1 would be the most important solubility controlling phases.

Table 4.3-1 Potential solubility-controlling mineral phases in the Tono groundwater system.

Element	Solubility-controlling phase[1]	Name	Comment
Se	Se		Appropriate for relatively oxidizing water
	$FeSe_2$		Appropriate for relatively reducing water
Zr	ZrO_2(am)		
Nb	Nb_2O_5		
Tc	Tc(cr)		
	TcO_2(C)		
Pd	Pd(cr)		
Sn	SnO_2	Cassiterite	
Sm	$SmOHCO_3$		
	$SmPO_4$		Appropriate for higher P-waters
Pb	$PbCO_3$		
	$Pb_5(PO_4)_3Cl$		Appropriate for higher P-waters
Ra	$RaSO_4$		
Ac	$AcOHCO_3$		
	$AcPO_4$		Appropriate for higher P-waters
Th	ThO_2(am)		
Pa	Pa_2O_5		
U	UO_2(am)		
Np	NpO_2(am)		
Pu	PuO_2(am)		
	$NaPu(CO_3)_2$		
	$PuOHCO_3$		
	$PuPO_4$(am)		Appropriate for higher P-waters
Am	$AmOHCO_3$		
	$Am(PO)_4$		Appropriate for higher P-waters
Cm	$CmOHCO_3$		
	$Cm(PO_4)$		Appropriate for higher P-waters

[1]This table uses conventional chemical notation and in some cases the formula is written differently to the way in which is appears in JNC's thermodynamic database 011213c0.tdb

4.3.2 Sensitivity calculations

Introduction to sensitivity calculations

Sensitivity calculations were carried out using PHREEQC v 2.8 and GWB. These calculations were of two types:

- Stochastic calculations were done in which a great many simulations were based on a particular real groundwater analysis. In these calculations, geochemical parameters were varied randomly between limits suggested by the analytical precision. The influences of these variations on the solubilities of the 17 elements was determined. For each of the 17 elements, 2000 simulations were carried out.

- Scoping calculations were performed to evaluate specific phenomena (drilling fluid contamination, charge balancing, groundwater mixing redox reactions etc) on element solubility.

Stochastic calculations

The first kind of calculations were based on the groundwater analysis 108 from borehole DH-7 between 560.5 and 567.0 m depth. This water is of particular interest since it contains relatively high concentrations of PO_4^{3-} and NH_4^+. Both of these could potentially influence the solublilities of certain elements. The calculations investigated the minimium uncertainty due to analytical errors. The error ranges used in the calculations are given in Table 4.3-2. Results are shown in Figure 4.3-35 to Figure

Figure **4.3-61**These figures plot the concentration of each element against the pH. The concentrations of some elements depend little upon pH and these plots do not give a true picture of all the controls on each element's solubility. However, they do indicate:

- the overall variation in concentration that is caused by the analytical uncertainty;

- a means by which to compare the different possible solubility controls exerted by different minerals on the same element;

- the relative importance of uncertainties in pH and other uncertainties (plots with a wide scattering of points indicate significant controls by other factors).

Table 4.3-2 Estimated analytical uncertainties used in sensitivity calculations

Analyte	Analytical Coef[t] of Variation (%)[1]	Analysis DH-7/ 563.75 (index 108)	Uncertainty used in sensitivity calculations	Comment
pH		10.1	0.025	Uncertainty not an analytical precision but is derived from the range of long-term monitoring results reported for Borehole KNA-6 in Ota and Hanamuro (1996)
Eh (V)		-0.4	20	
			2σ	
Na (ppm)	1	25.4	0.508	Uncertainty based on analytical uncertainty in Hama et al. (2000)
K (ppm)	1	2.30	0.046	Uncertainty based on analytical uncertainty in Hama et al. (2000)
Ca (ppm)	1	5.4	0.108	Uncertainty based on analytical uncertainty in Hama et al. (2000)
Mg (ppm)	1	0.31	0.0062	Uncertainty based on analytical uncertainty in Hama et al. (2000)
Sr (ppm)	1	0.08	0.00152	Uncertainty based on analytical uncertainty in Hama et al. (2000)
IC (ppm)	0.8	18.4	0.2944	Uncertainty based on analytical uncertainty in Hama et al. (2000)
SO_4 (ppm)	1	4.64	0.0928	Uncertainty based on analytical uncertainty in Hama et al. (2000)
F (ppm)	1	2.11	0.0422	Uncertainty based on analytical uncertainty in Hama et al. (2000)
Cl (ppm)	1	4.37	0.0874	Uncertainty based on analytical uncertainty in Hama et al. (2000)
NO_2 (ppm)	2	0.01	0.0002	Uncertainty based on analytical uncertainty in Hama et al. (2000)
NO_3 (ppm)	2	0.01	0.0004	Uncertainty based on analytical uncertainty in Hama et al. (2000)
NH_4^+ (ppm)	2	22.9	0.916	Uncertainty based on analytical uncertainty in Hama et al. (2000)
PO_4^{3-} (ppm)	2	0.086	0.00344	Uncertainty based on analytical uncertainty in Hama et al. (2000)
Si (ppm)	2	1.9	0.076	Uncertainty based on analytical uncertainty in Hama et al. (2000)
Al (ppm)	2	0.19	0.0076	Uncertainty based on analytical uncertainty in Hama et al. (2000)
Total Fe (ppm)	2	8.9	0.356	Uncertainty based on analytical uncertainty in Hama et al. (2000)
Fe^{2+} (ppm)	2	8.5	0.34	Uncertainty based on analytical uncertainty in Hama et al. (2000)
Total Mn (ppm)	2	0.16	0.0064	Uncertainty based on analytical uncertainty in Hama et al. (2000)

[1]Coef[t] of variation = Coefficient of variation(%) = 100 * standard deviation/Mean

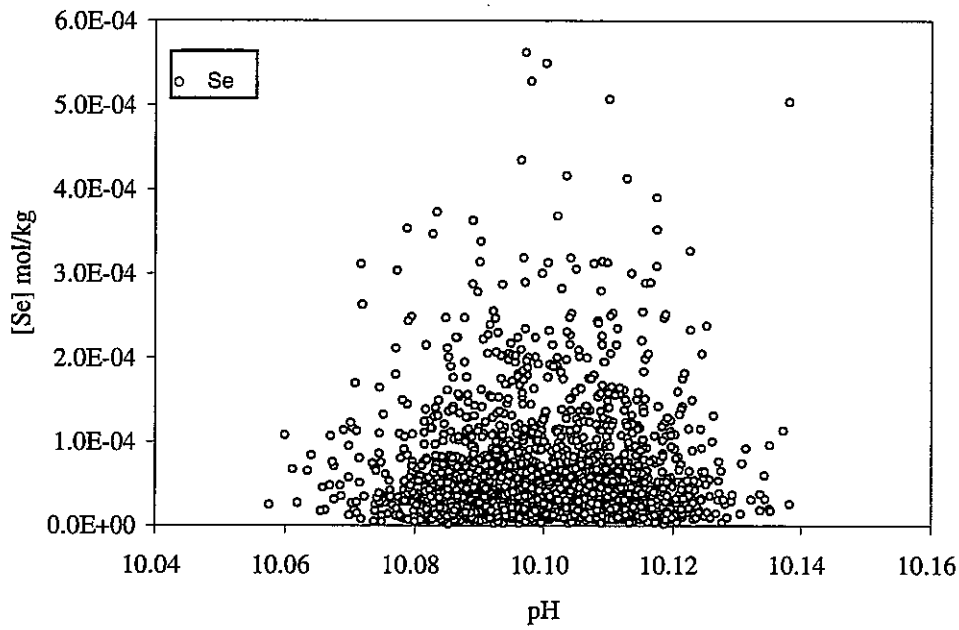

Figure 4.3-35 Total selenium concentration versus pH defined by the solubility of elemental Se in a Tono groundwater composition (DH-7/563.75) varied randomly according to analytical uncertainties. Note that variations in solubility depend more upon Eh than pH.

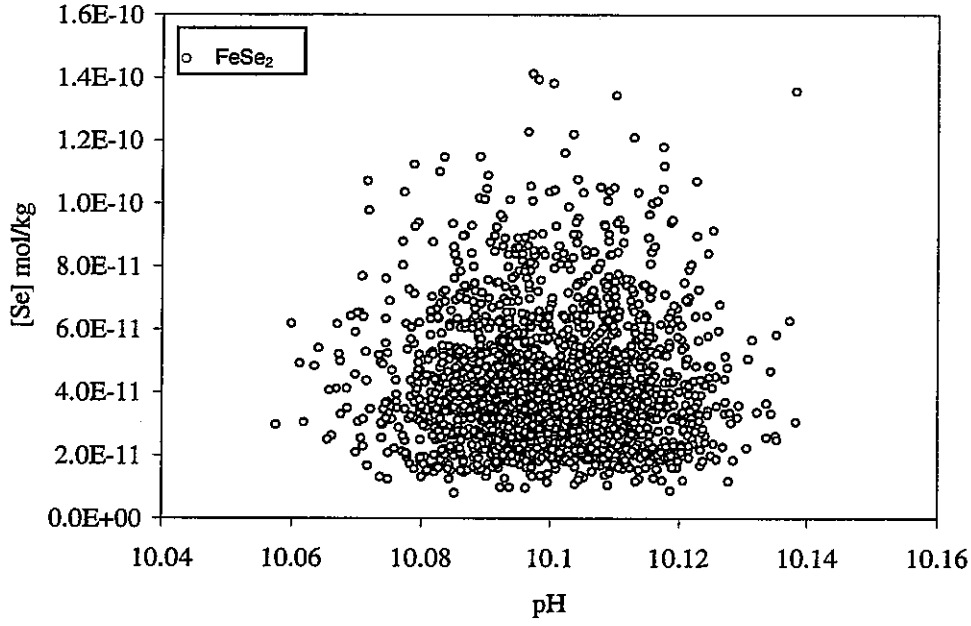

Figure 4.3-36 Total selenium concentration versus pH defined by the solubility of $FeSe_2$ in a Tono groundwater composition (DH-7/563.75) varied randomly according to analytical uncertainties. Note that solubility variations depend more upon Eh than pH. The solubility of $FeSe_2$ is lower than that of Se and $FeSe_2$ would be the solubility-controlling phase (assuming formation is kinetically favoured).

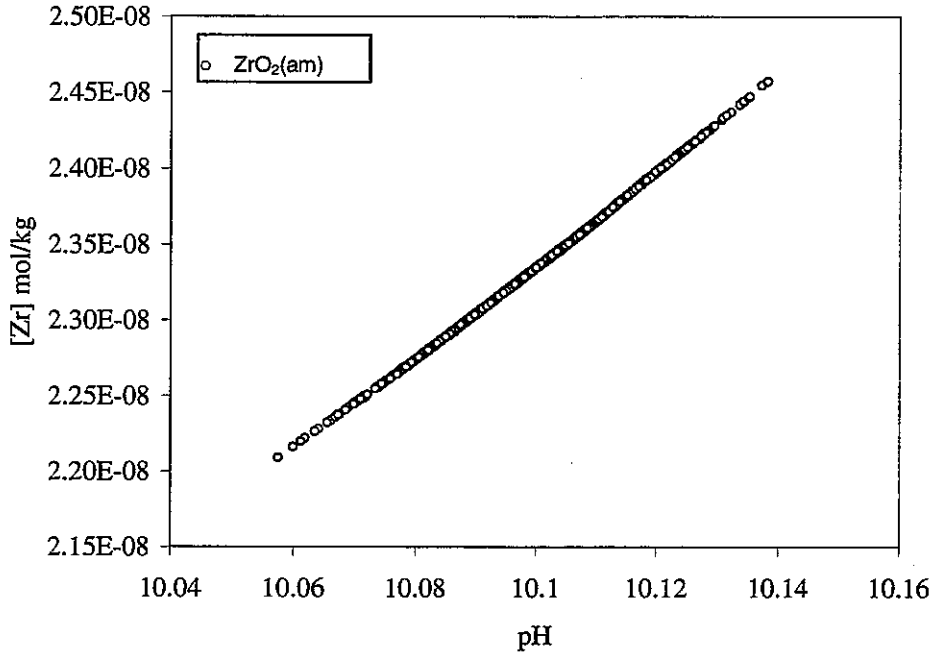

Figure 4.3-37 Total zirconium concentration versus pH defined by the solubility of amorphous zirconium dioxide in a Tono groundwater composition (DH-7/563.75) varied randomly according to analytical uncertainties. Note that variations in solubility are strongly dependent upon pH.

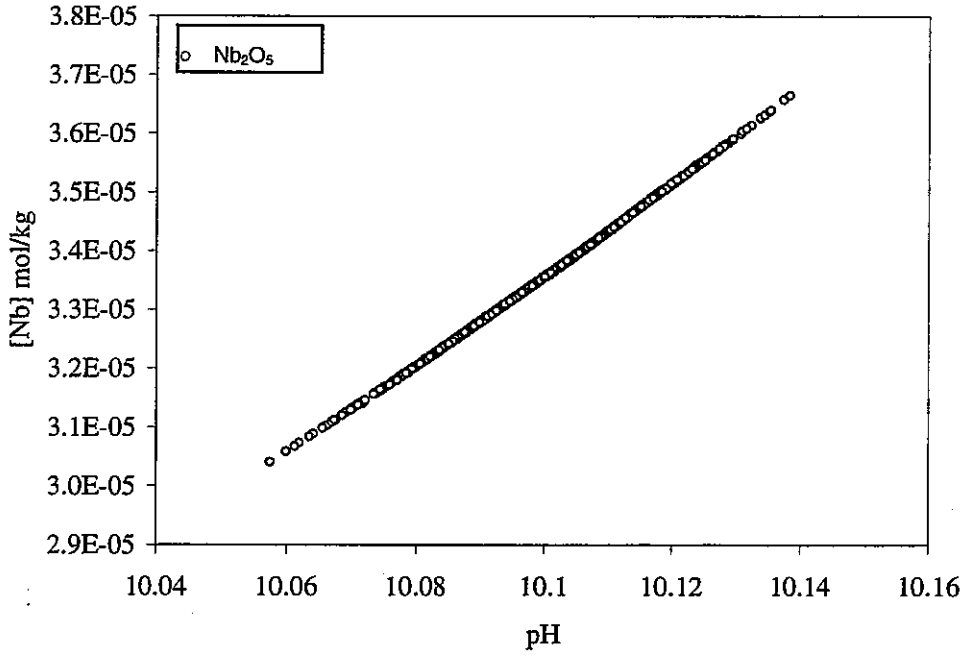

Figure 4.3-38 Total niobium concentration versus pH defined by the solubility of Nb_2O_5 in a Tono groundwater composition (DH-7/563.75) varied randomly according to analytical uncertainties. Note that variations in solubility depend strongly upon pH.

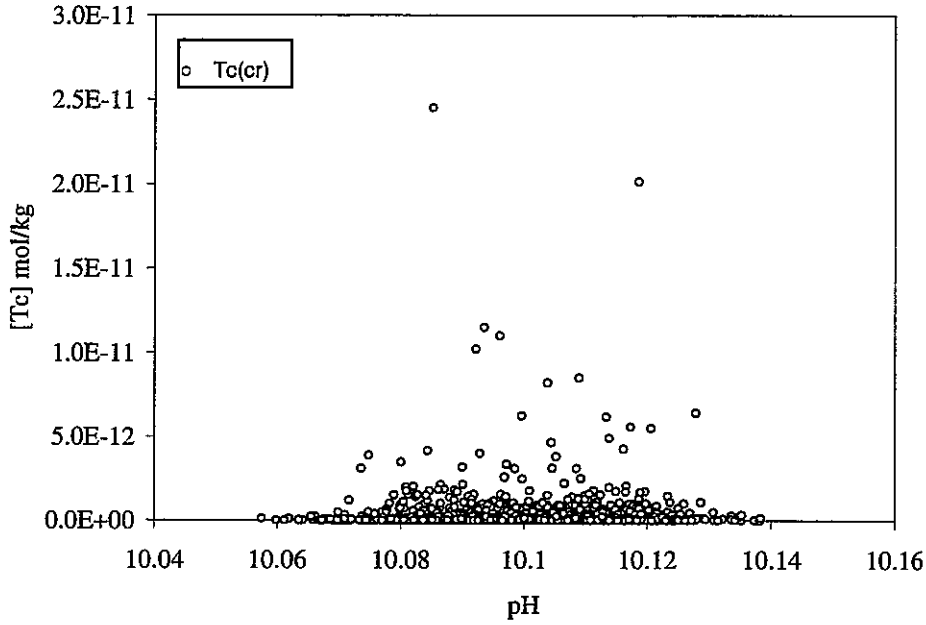

Figure 4.3-39 Total techentium concentration versus pH defined by the solubility of crystalline Tc in a Tono groundwater composition (DH-7/563.75) varied randomly according to analytical uncertainties. Note that variations in solubility depend more upon Eh than pH.

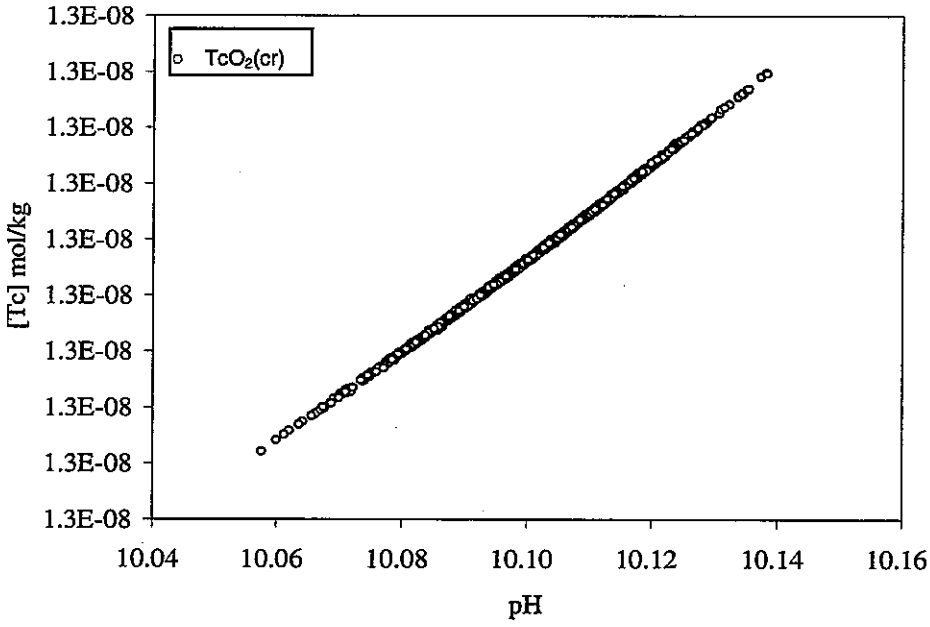

Figure 4.3-40 Total techentium concentration versus pH defined by the solubility of crystalline TcO_2(cr) in a Tono groundwater composition (DH-7/563.75) varied randomly according to analytical uncertainties. Note that variations in solubility depend more upon Eh than pH. The solubility of Tc(cr) is lower than that of TcO_2(cr) and hence Tc(cr) would be the solubility-controlling phase (assuming formation is kinetically favoured).

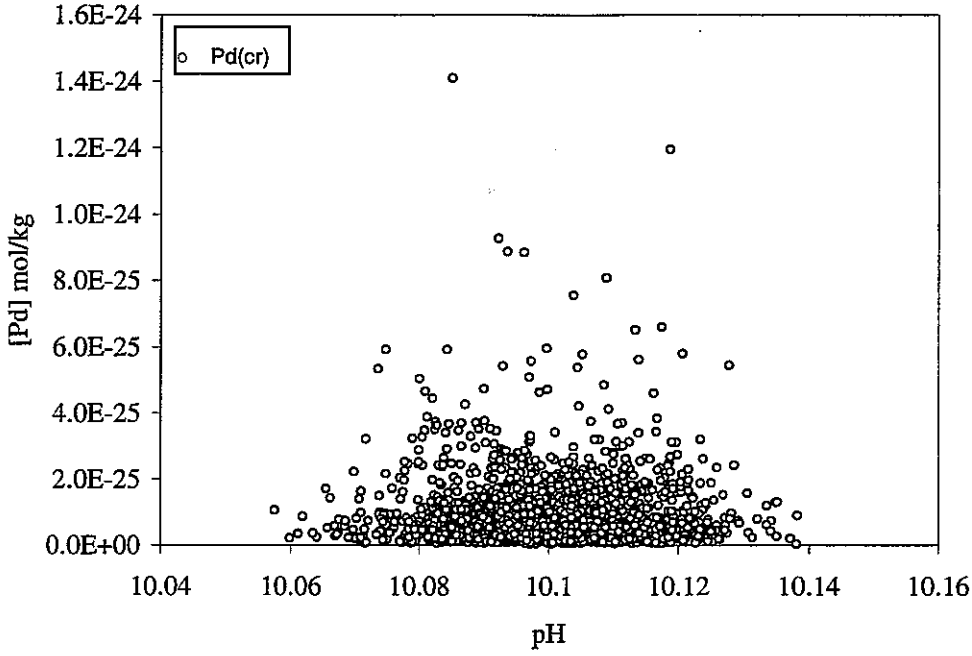

Figure 4.3-41 Total palladium concentration versus pH defined by the solubility of crystalline palladium in a Tono groundwater composition (DH-7/563.75) varied randomly according to analytical uncertainties.

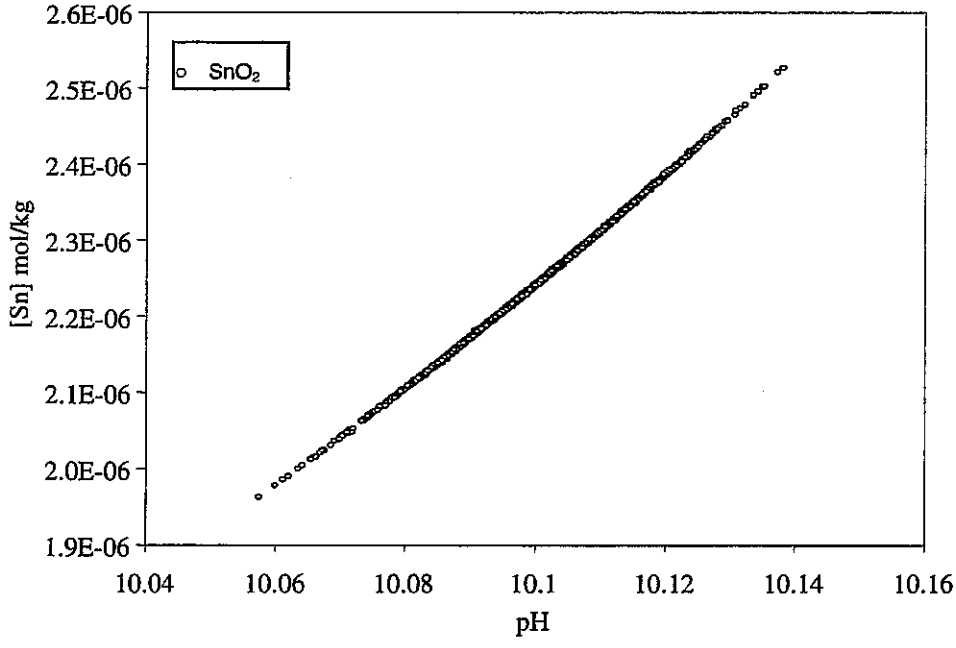

Figure 4.3-42 Total tin concentration versus pH defined by the solubility of tin dioxide (cassiterite) in a Tono groundwater composition (DH-7/563.75) varied randomly according to analytical uncertainties. Note that variations in solubility depend strongly upon pH.

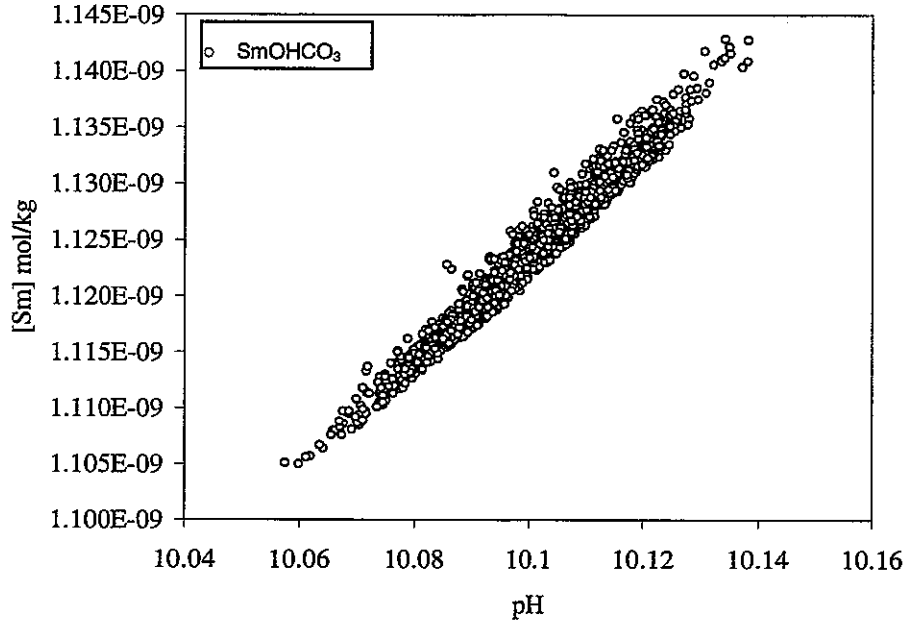

Figure 4.3-43 Total samarium concentration versus pH defined by the solubility of $SmOHCO_3$ in a Tono groundwater composition (DH-7/563.75) varied randomly according to analytical uncertainties. Note that variations in solubility depend strongly upon pH.

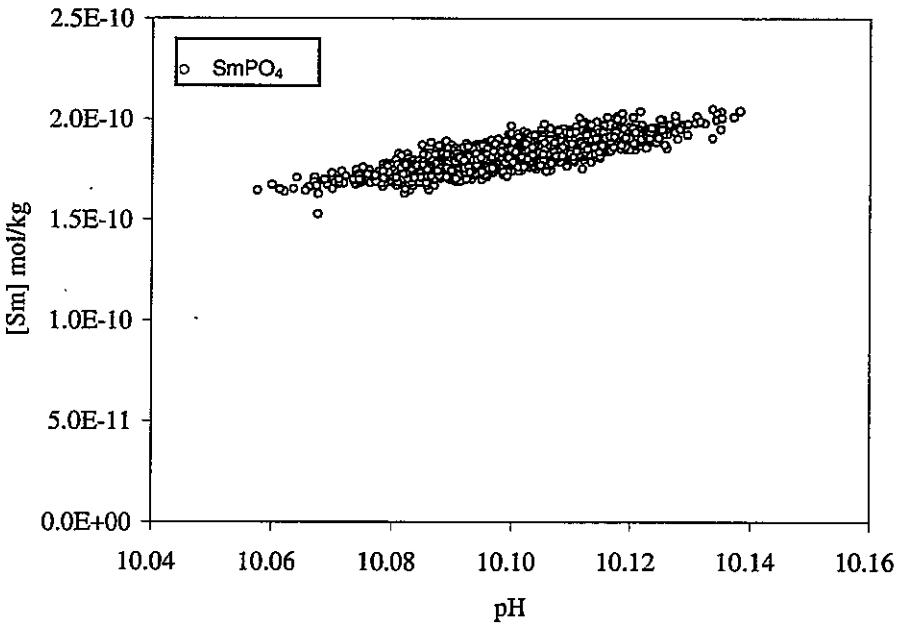

Figure 4.3-44 Total samarium concentration versus pH defined by the solubility of $SmPO_4$ in a Tono groundwater composition (DH-7/563.75) varied randomly according to analytical uncertainties. Variations in solubility depends only moderately upon pH. The solubility of $SmPO_4$ is lower than that of $SmOHCO_3$ and would be the solubility-controlling phase (assuming that its formation is kinetically favourable). PO_4 concentrations could exert an important control on the solubility of Sm.

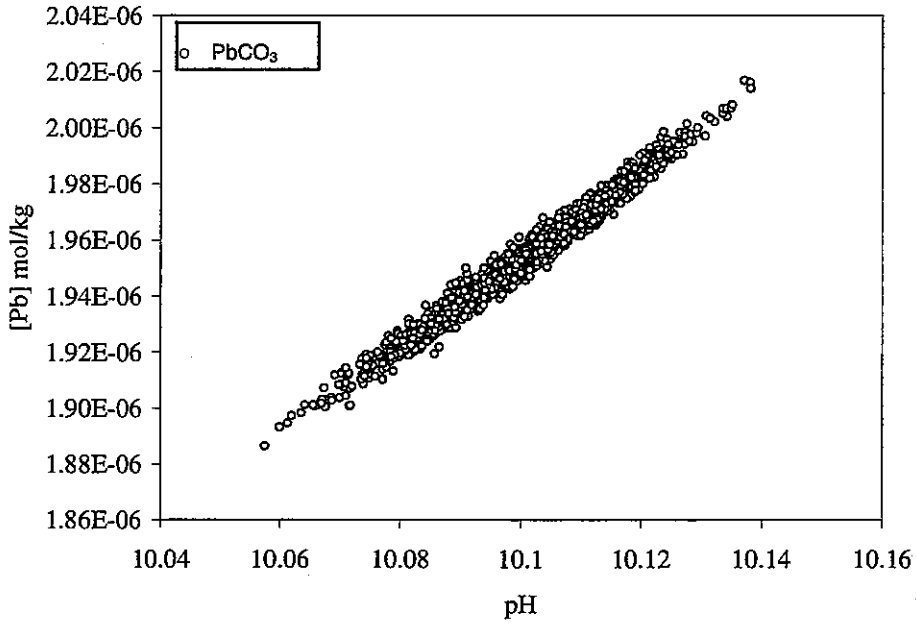

Figure 4.3-45 Total lead concentration versus pH defined by the solubility of $PbCO_3$ (cerussite) in a Tono groundwater composition (DH-7/563.75) varied randomly according to analytical uncertainties. Note that variations in solubility depend strongly upon pH.

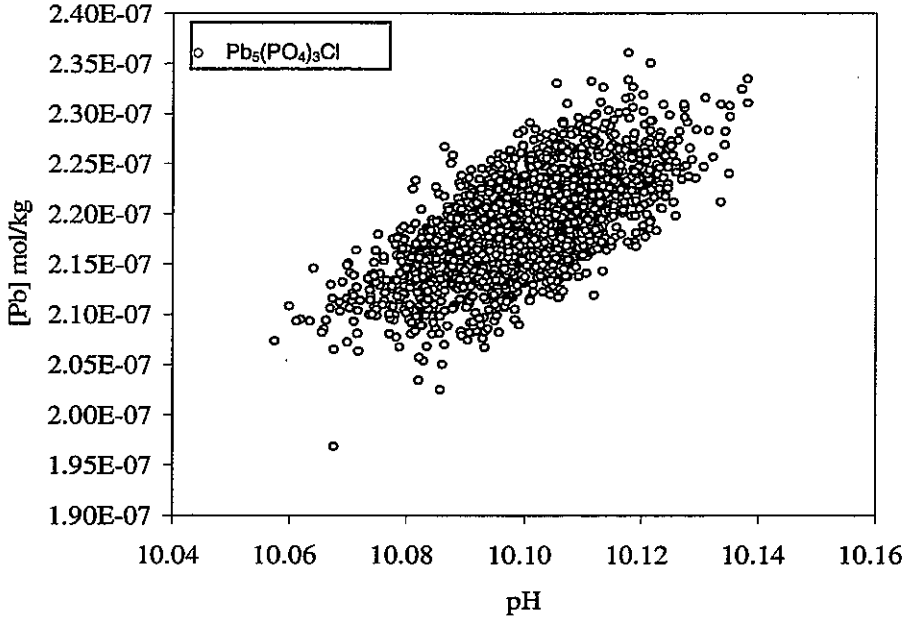

Figure 4.3-46 Total lead concentration versus pH defined by the solubility of $Pb_5(PO_4)_3Cl$ in a Tono groundwater composition (DH-7/563.75) varied randomly according to analytical uncertainties. Variations in solubility depend on pH, but other factors are more important (considerable scatter) than when $PbCO_3$ controls Pb concentration. The solubility of $Pb_5(PO_4)_3Cl$ is lower than that of $PbCO_3$ and would be the solubility-controlling phase (assuming that its formation is kinetically favourable). PO_4 concentrations could influence the solubility of Pb.

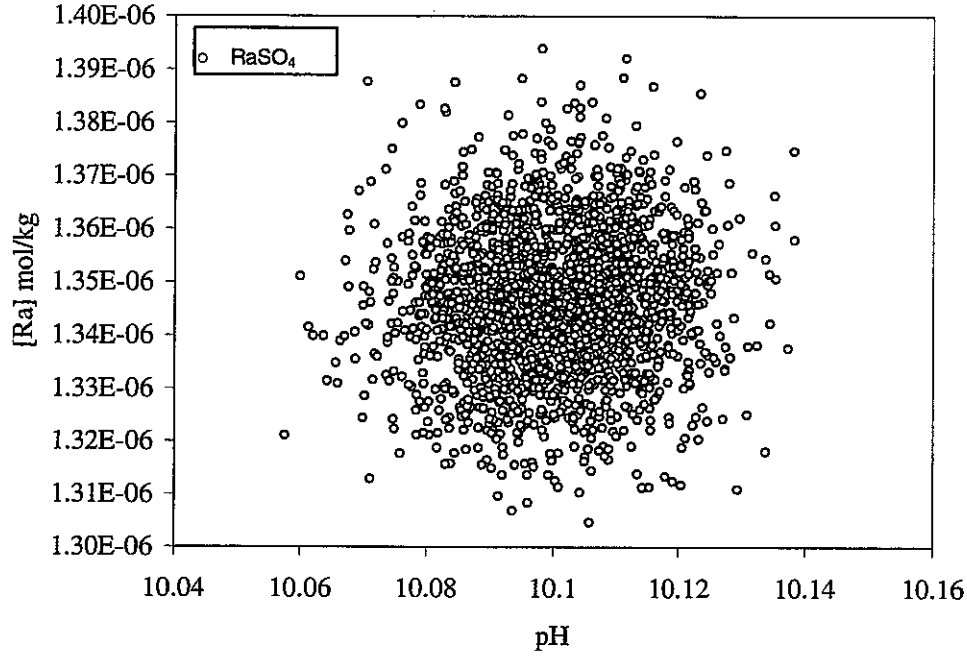

Figure 4.3-47 Total radium concentration versus pH defined by the solubility of radium in a Tono groundwater composition (DH-7/563.75) varied randomly according to analytical uncertainties. Note that variations in solubility are independent of pH and depend upon variations in the sulphate content of groundwaters.

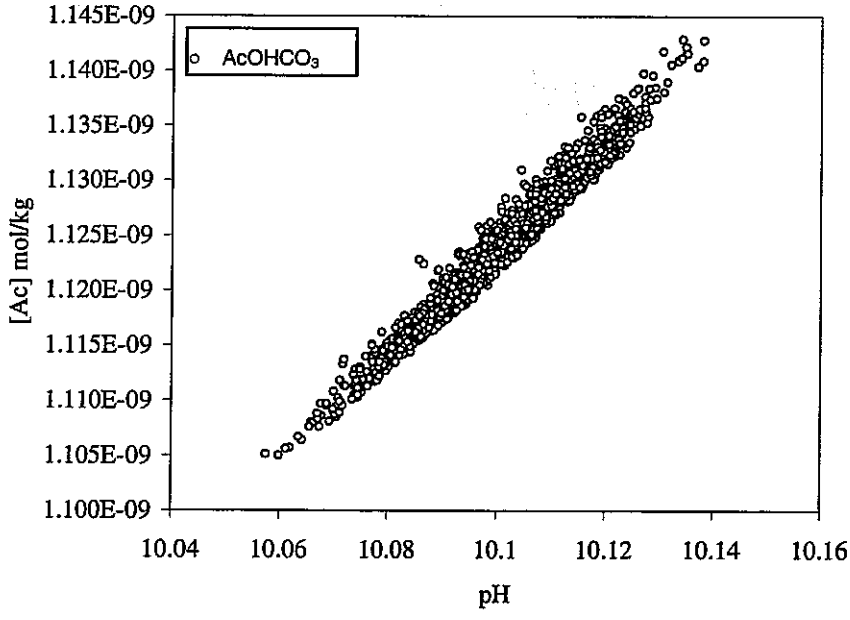

Figure 4.3-48 Total actinium concentration versus pH defined by the solubility of $AcOHCO_3$ in a Tono groundwater composition (DH-7/563.75) varied randomly according to analytical uncertainties. Note that variations in solubility depend strongly upon variations in pH.

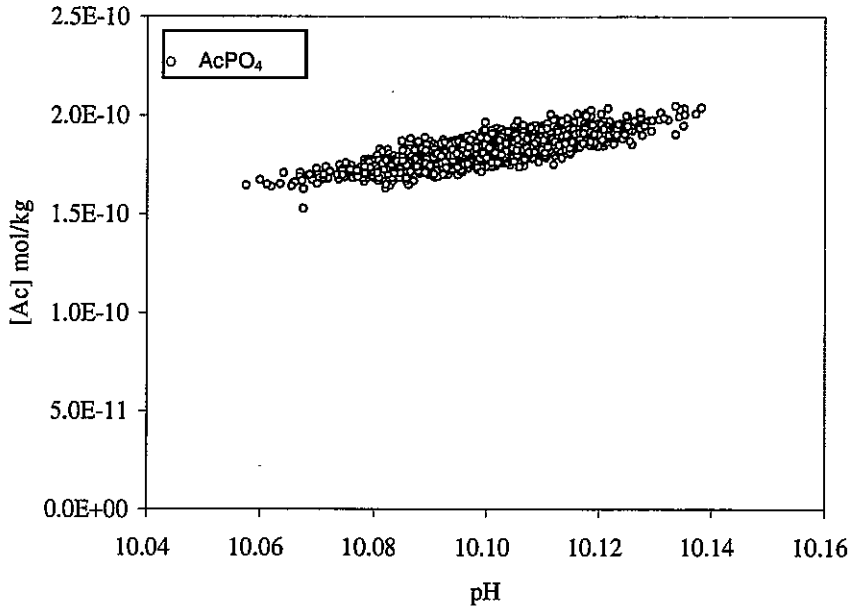

Figure 4.3-49 Total actinium concentration versus pH defined by the solubility of $AcPO_4$ in a Tono groundwater composition (DH-7/563.75) varied randomly according to analytical uncertainties. Variations in solubility depend only moderately upon pH variations. The solubility of $AcPO_4$ is lower than that of $AcOHCO_3$ and would be the solubility-controlling phase (assuming that its formation is kinetically favourable). PO_4 concentrations could exert an important control on the solubility of Ac.

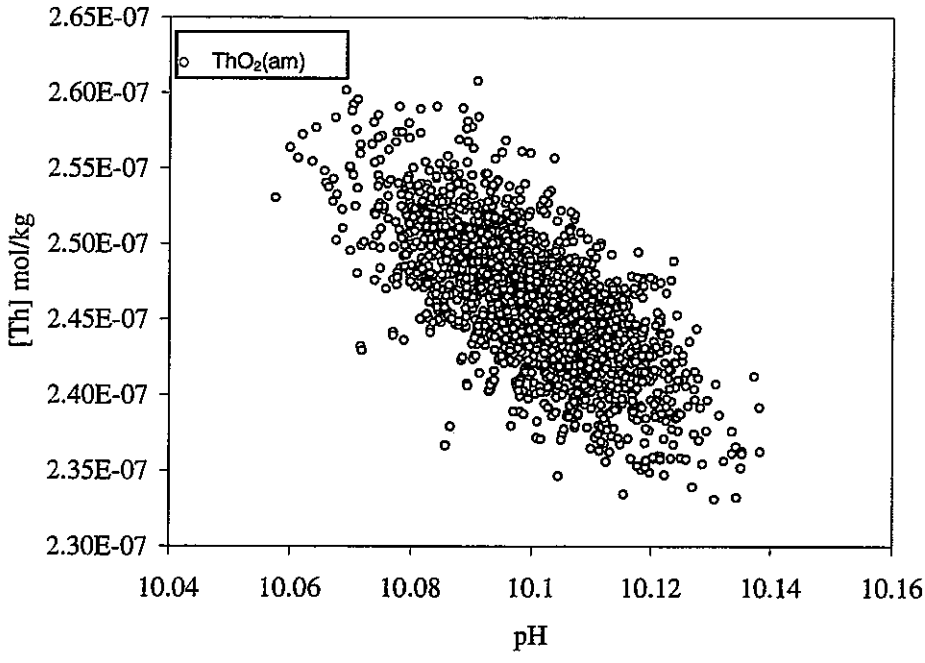

Figure 4.3-50 Total thorium concentration versus pH defined by the solubility of amorphous thorium dioxide in a Tono groundwater composition (DH-7/563.75) varied randomly according to analytical uncertainties. Note that variations in solubility depend strongly upon variations in pH.

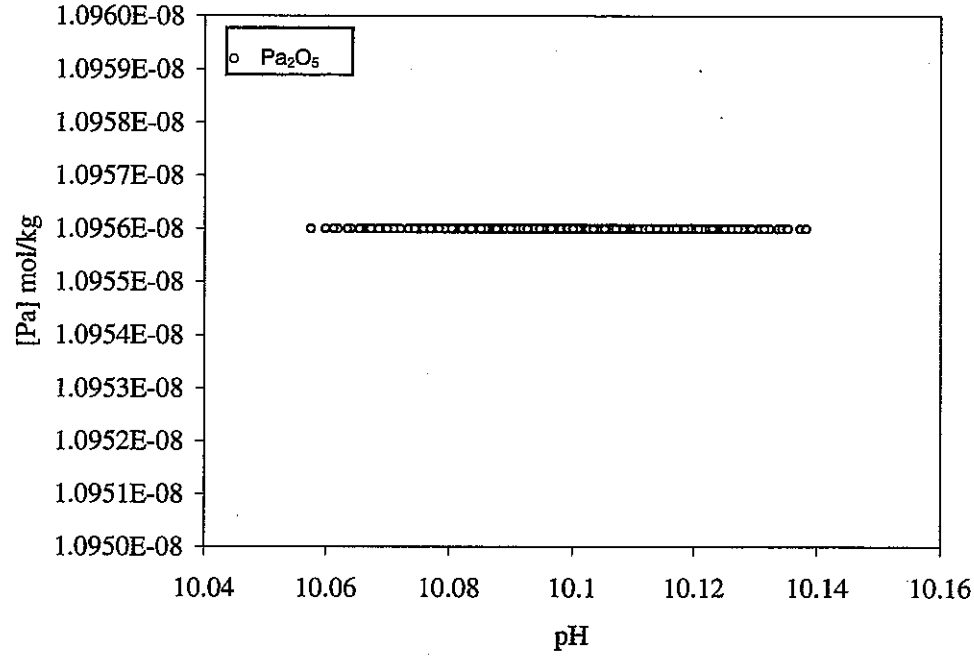

Figure 4.3-51 Total protoactinium concentration versus pH defined by the solubility of Pa_2O_5 in a Tono groundwater composition (DH-7/563.75) varied randomly according to analytical uncertainties. Note that solubility is invariant with respect to pH.

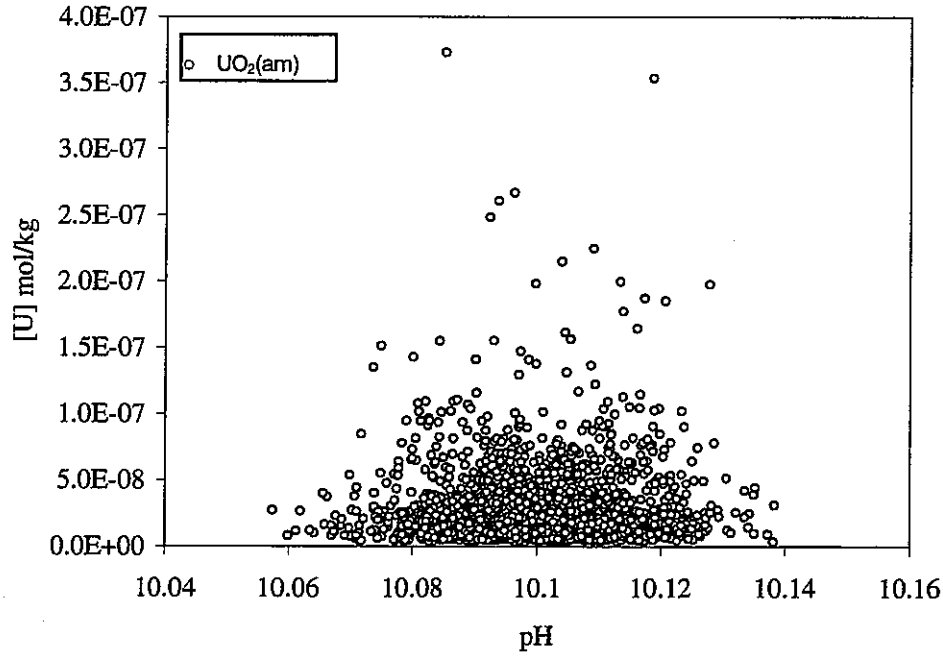

Figure 4.3-52 Total uranium concentration versus pH defined by the solubility of amorphous uranium dioxide in a Tono groundwater composition (DH-7/563.75) varied randomly according to analytical uncertainties. Note that variations in solubility depend more upon Eh than pH.

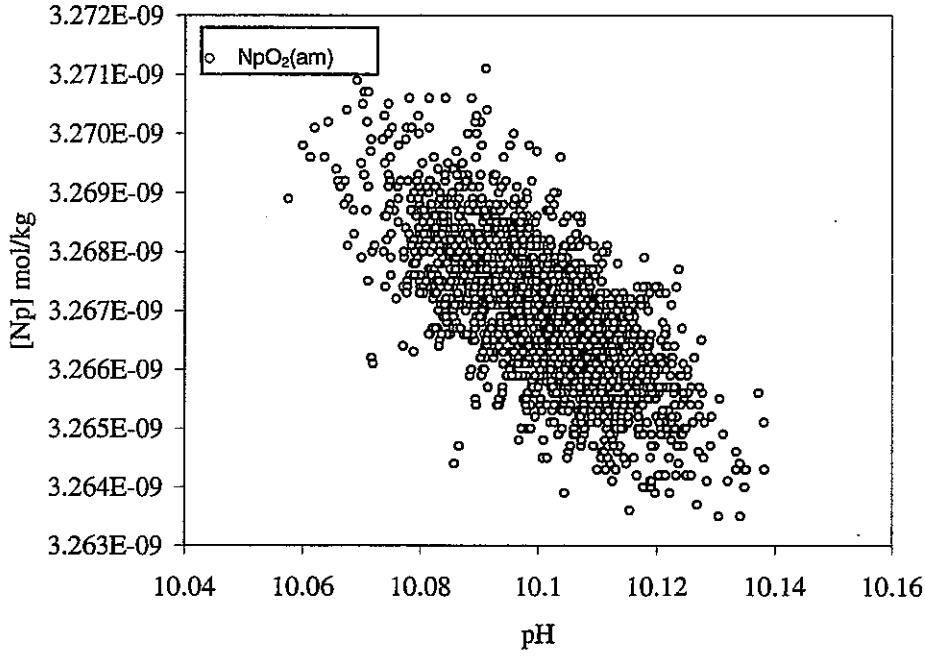

Figure 4.3-53 Total neptunium concentration versus pH defined by the solubility of amorphous neptunium dioxide in a Tono groundwater composition (DH-7/563.75) varied randomly according to analytical uncertainties. Note that variations in solubility depend strongly upon pH.

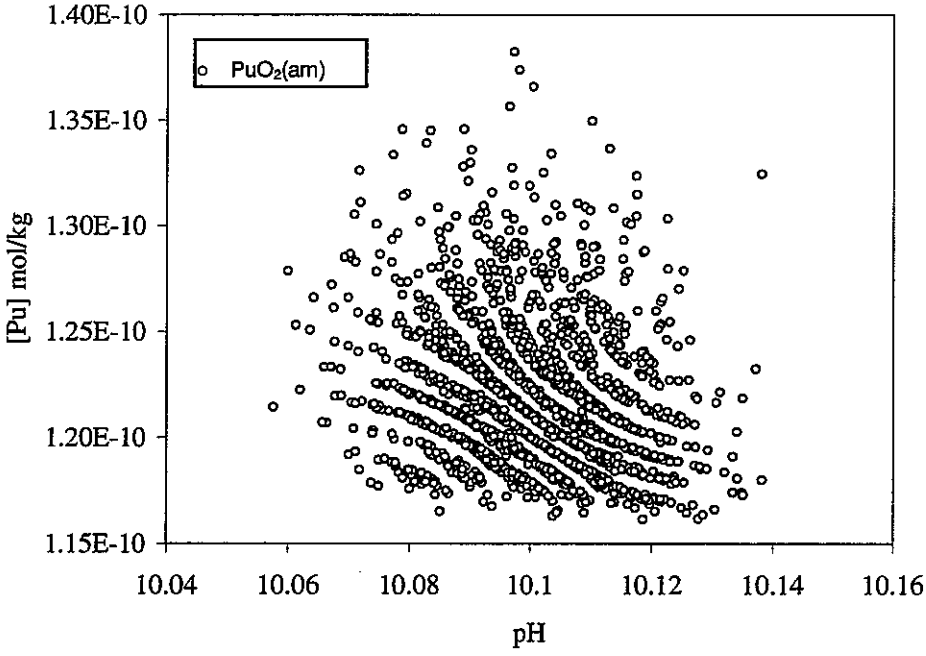

Figure 4.3-54 Total plutonium concentration versus pH defined by the solubility of plutonium dioxide in a Tono groundwater composition (DH-7/563.75) varied randomly according to analytical uncertainties. Note that variations in solubility depend more upon Eh than pH.

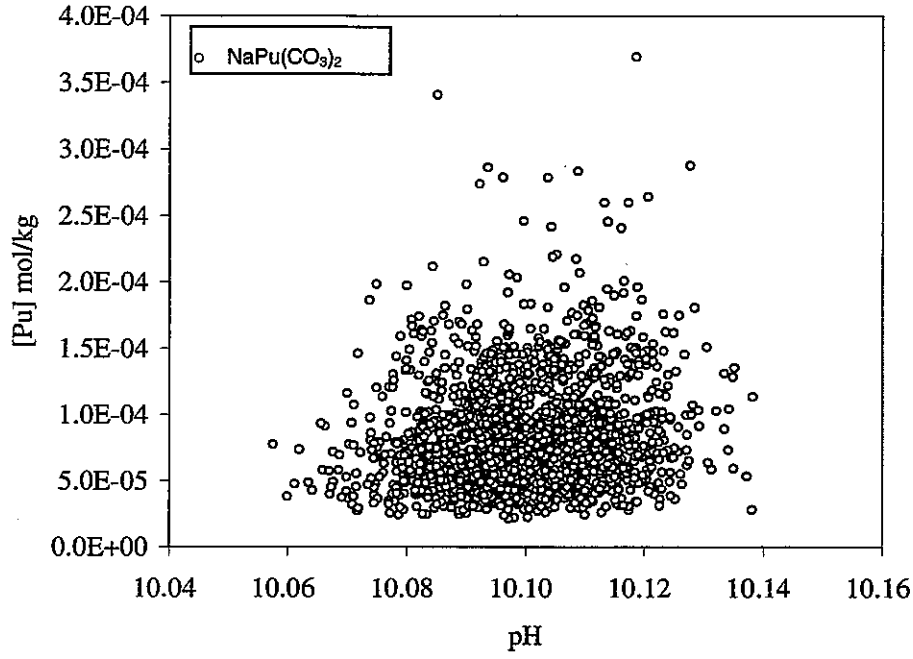

Figure 4.3-55 Total plutonium concentration versus pH defined by the solubility of $NaPu(CO_3)_2$ in a Tono groundwater composition (DH-7/563.75) varied randomly according to analytical uncertainties. Note that the solubility is much higher than PuO_2(am) and $NaPu(CO_3)_2$ would not be a solubility-controlling phase in this water.

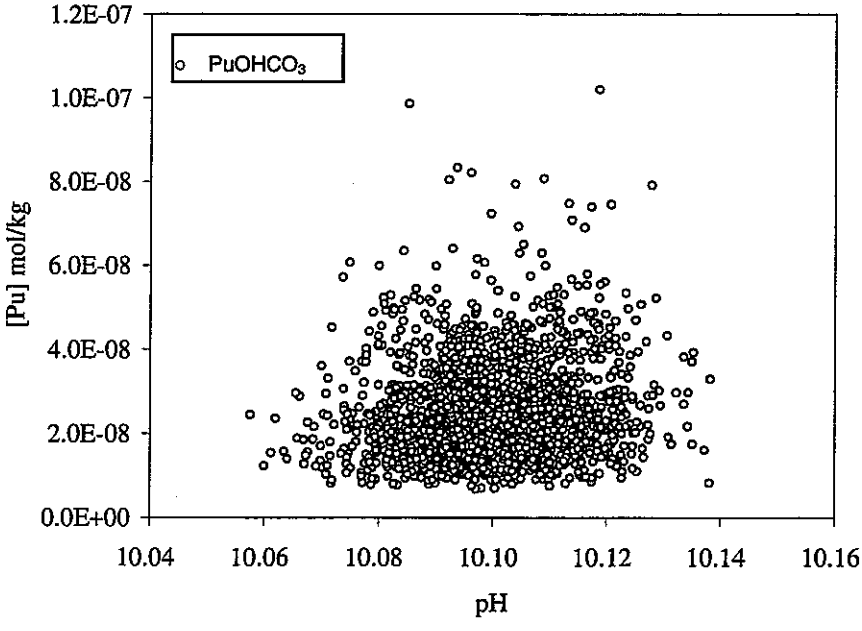

Figure 4.3-56 Total plutonium concentration versus pH defined by the solubility of $PuOHCO_3$ in a Tono groundwater composition varied randomly (DH-7/563.75) according to analytical uncertainties. Note that the solubility is higher than PuO_2(am) and $PuOHCO_3$ would not be a solubility-controlling phase in this water.

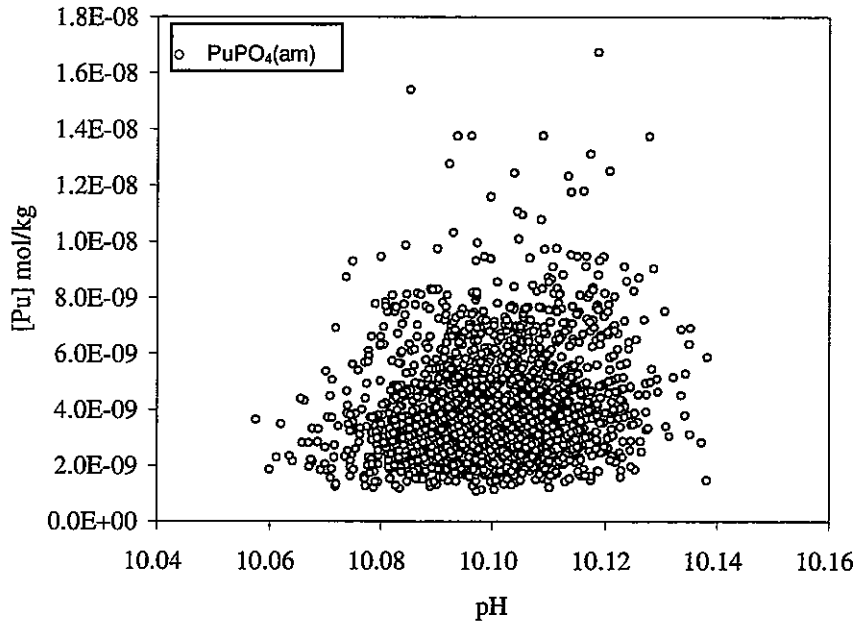

Figure 4.3-57 Total plutonium concentration versus pH defined by the solubility of $PuPO_4$ in a Tono groundwater composition varied randomly (DH-7/563.75) according to analytical uncertainties. Note that the solubility is higher than PuO_2(am) and $PuPO_4$ would not be a solubility-controlling phase in this water.

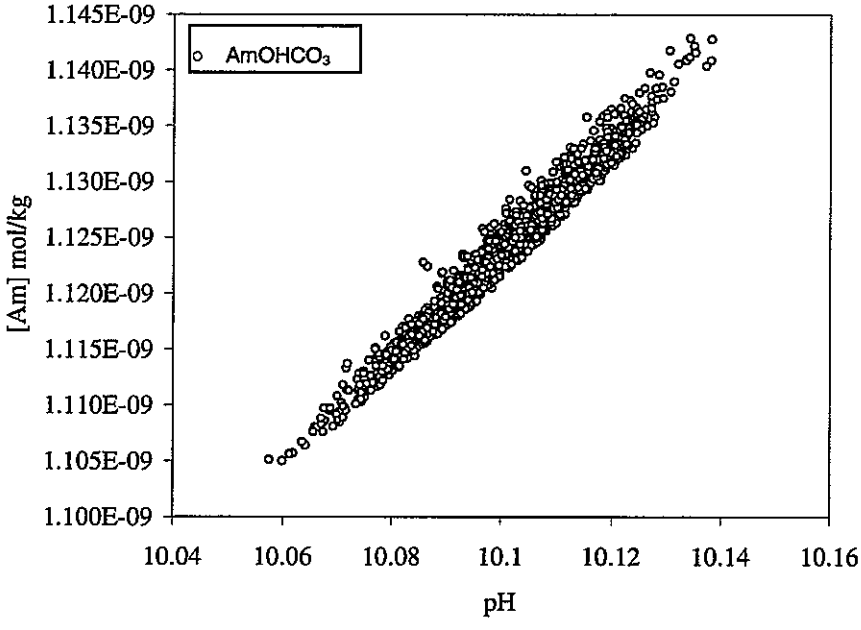

Figure 4.3-58 Total americium concentration versus pH defined by the solubility of $AmOHCO_3$ in a Tono groundwater composition varied randomly (DH-7/563.75) according to analytical uncertainties. Note that variations in solubility depend strongly upon pH.

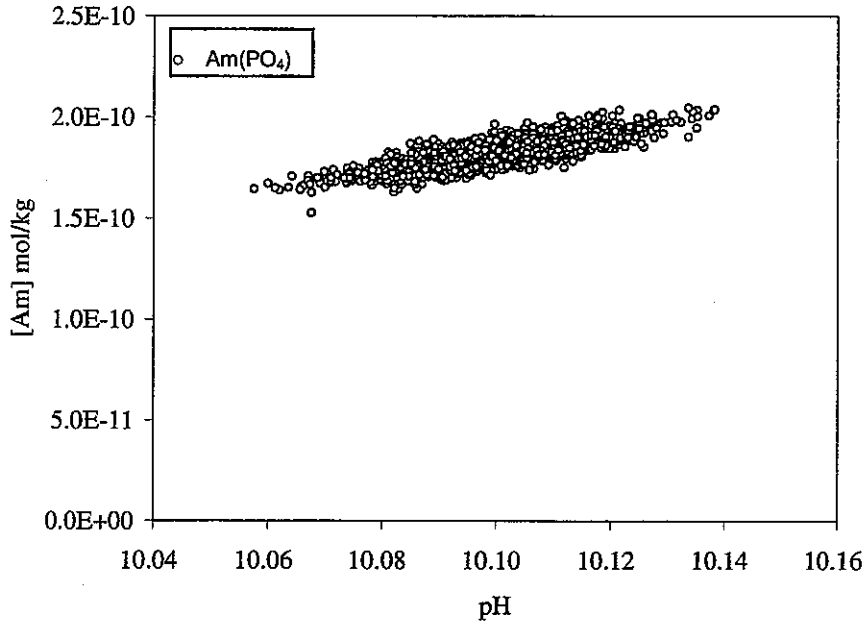

Figure 4.3-59 Total americium concentration versus pH defined by the solubility of $AmPO_4$ in a Tono groundwater composition (DH-7/563.75) varied randomly according to analytical uncertainties. Note that variations in solubility depend only moderately upon pH. The solubility of $AmPO_4$ is lower than that of $AmOHCO_3$ and would be the solubility-controlling phase (assuming that its formation is kinetically favourable). PO_4 concentrations could exert an important control on the solubility of Am.

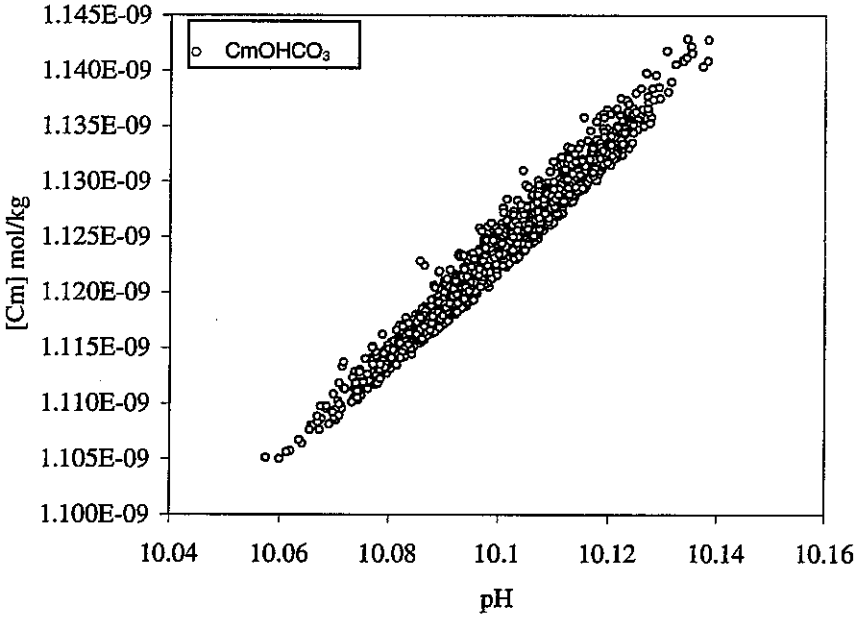

Figure 4.3-60 Total curium concentration versus pH defined by the solubility of $CmOHCO_3$ in a Tono groundwater composition (DH-7/563.75) varied randomly according to analytical uncertainties. Note that variations in solubility depend strongly upon pH.

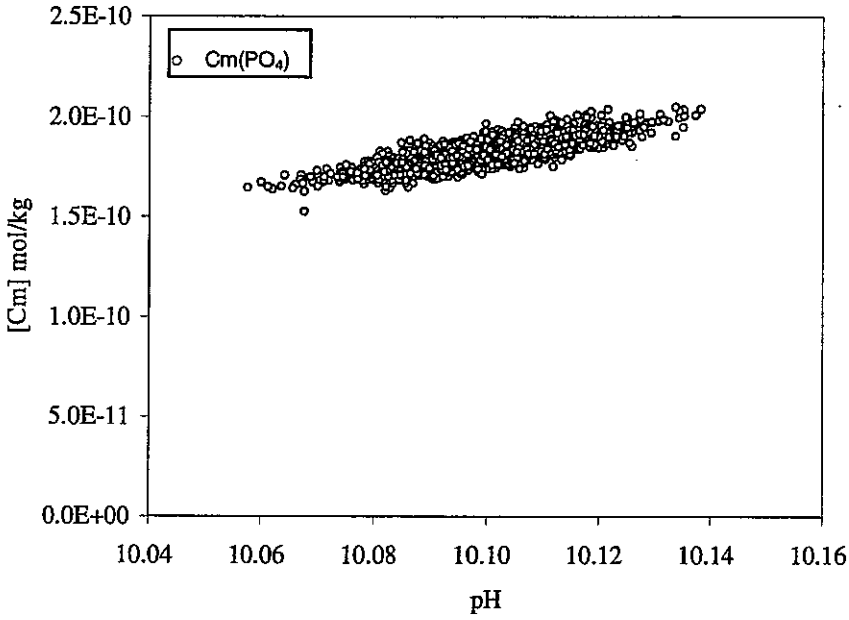

Figure 4.3-61 Total curium concentration versus pH defined by the solubility of $CmPO_4$ in a Tono groundwater composition (DH-7/563.75) varied randomly according to analytical uncertainties. Note that variations in solubility depend only moderately upon pH. The solubility of $CmPO_4$ is lower than that of $CmOHCO_3$ and would be the solubility-controlling phase (assuming that its formation is kinetically favourable). PO_4 concentrations could influence the solubility of Cm.

The importance of uncertainties in the chemical determinands can be understood more readily by calculating correlation coefficients between input parameter values and the output solubilities for each set of 2000 solubility calculations. In the present project this was done using an 'add-in' statistical analysis tool for Microsoft Excel™ called XlSTAT™ (produced by Addinsoft). The results are summarised in Table 4.3-3.

The magnitude of a correlation coefficient gives a general indication of the importance of a particular determinand as a control on solubility. For example, it can be seen that, when Pb solubility is controlled by $Pb_5(PO_4)_3Cl$, variations in pH and PO_4 (correlation coefficients 0.656 and -0.544 respectively) are more important than variations in C (correlation coefficient 0.353).

The correlations in Table 4.3-3 indicate the relative importance of determinands over relatively small variation ranges that are similar to analytical errors under reducing conditions that are typical of deep groundwaters. In order to judge the importance of larger variations it is necessary to consider:

- the differences in composition of alternative mineral phases that could control the solubility of a particular element (e.g.either solid Se or $FeSe_2$ controlling the solubility of Se, depending on the conditions);
- the mineral solubility diagrams and chemical speciation diagrams, Figure 4.3-2 to Figure 4.3-34.

Generally, variations in the chemical components that differ between two alternative phases will be important. In the example given above, large variations in Fe would be important as they could control whether Se or FeS_2 is the solubility-controlling phase.

Variations in a determinand may be important only near to the predominance boundary with another species and not within a field. Thus, although U may form carbonate complexes (Figure 4.3-26), under the reducing conditions of the deep Tono groundwaters the small ranges consistent with analytical uncertainties are unimportant (Table 4.3-3)

Table 4.3-3 Correlations between calculated solubilities and input parameter values. The coloured red indicate which parameters are important controls on the solubility of each element.

		Correlation coefficients representing the correlation of each determinand with the named element																		
	Phase	pH	Eh	Na	K	Ca	Mg	Sr	$C^{(+4)}$	$S^{(+6)}$	F	Cl	$N^{(+3)}$	$N^{(+5)}$	$N^{(-3)}$	P	Si	Al	$Fe^{(+2)}$	$Fe^{(+3)}$	Mn
Se	Se	0.004	**-0.840**	-0.009	0.014	-0.031	-0.004	-0.018	0.029	0.009	0.015	0.001	0.021	-0.031	-0.007	-0.015	-0.014	-0.001	-0.027	0.031	0.014
	$FeSe_2$	-0.004	**-0.950**	-0.016	0.020	-0.036	-0.002	-0.014	0.025	0.012	0.014	0.007	0.011	-0.038	-0.011	-0.014	-0.023	-0.002	**-0.053**	**0.045**	0.020
Zr	ZrO_2(am)	**1.000**	-0.026	-0.029	-0.002	-0.031	0.002	**-0.053**	-0.012	0.011	0.005	0.025	-0.023	0.007	-0.008	-0.016	-0.014	0.023	-0.028	-0.011	0.021
Nb	Nb_2O_5	**1.000**	-0.026	-0.029	-0.002	-0.031	0.002	**-0.053**	-0.012	0.011	0.005	0.025	-0.023	0.007	-0.008	-0.016	-0.014	0.023	-0.028	-0.011	0.021
Tc	Tc(cr)	0.015	**0.450**	0.007	-0.028	-0.017	-0.005	-0.007	-0.024	-0.008	-0.012	0.007	0.026	0.030	0.018	-0.010	0.029	-0.024	-0.032	**-0.079**	-0.019
	TcO_2(C)	**1.000**	-0.027	-0.030	-0.002	-0.032	0.002	**-0.053**	-0.006	0.011	0.005	0.025	-0.023	0.007	-0.009	-0.016	-0.014	0.023	-0.028	-0.010	0.021
Pd	Pd(cr)	-0.009	**0.798**	0.034	-0.028	0.010	-0.003	0.004	-0.017	-0.009	-0.010	-0.010	0.027	0.037	**0.082**	0.001	0.038	-0.002	0.009	**-0.074**	-0.025
Sn	SnO_2	**0.999**	-0.026	-0.028	-0.002	-0.031	0.001	**-0.053**	-0.009	0.011	0.005	0.025	-0.023	0.007	-0.008	-0.016	-0.014	0.024	-0.028	-0.011	0.021
Sm	$SmOHCO_3$	**0.983**	-0.010	-0.003	0.004	-0.019	-0.003	**-0.052**	**-0.125**	0.011	0.005	0.026	-0.021	0.007	-0.002	-0.017	-0.017	0.023	-0.022	-0.015	0.020
	$SmPO_4$	**0.823**	-0.034	**-0.050**	-0.015	**0.062**	0.031	-0.042	**0.145**	0.007	-0.001	0.000	-0.019	0.008	-0.010	**-0.537**	-0.016	0.033	0.010	0.005	0.021
Pb	$PbCO_3$	**0.989**	-0.036	-0.029	-0.003	-0.035	0.006	**-0.051**	**0.075**	0.013	0.007	0.025	-0.025	0.007	-0.006	-0.014	-0.011	0.025	-0.025	-0.007	0.020
	$Pb_5(PO_4)_3Cl$	**0.656**	**-0.054**	**-0.054**	-0.020	**0.062**	0.041	-0.029	**0.353**	0.009	0.004	**-0.096**	-0.024	0.004	-0.008	**-0.544**	-0.006	0.030	0.019	0.015	0.015

Table 4.3-3 Continued.

		Correlation coefficients representing the correlation of each determinand with the named element																		
		pH	Eh	Na	K	Ca	Mg	Sr	$C^{(+4)}$	$S^{(+6)}$	F	Cl	$N^{(+3)}$	$N^{(+5)}$	$N^{(-3)}$	P	Si	Al	$Fe^{(+2)}$	$Fe^{(+3)}$	Mn
Ra	$RaSO_4$	**0.059**	0.003	**0.045**	**-0.048**	0.020	-0.015	0.011	**0.084**	**-0.984**	-0.019	0.008	0.008	-0.019	**0.045**	-0.001	0.028	0.010	0.035	-0.013	0.004
Ac	$AcOHCO_3$	**0.983**	-0.010	-0.003	0.004	-0.019	-0.003	**-0.052**	**-0.125**	0.011	0.005	0.026	-0.021	0.007	-0.002	-0.017	-0.017	0.023	-0.022	-0.015	0.020
	$AcPO_4$	**0.823**	-0.034	**-0.050**	-0.015	**0.062**	0.031	-0.042	**0.145**	0.007	-0.001	0.000	-0.019	0.008	-0.010	**-0.537**	-0.016	0.033	0.010	0.005	0.021
Th	$ThO_2(am)$	**-0.691**	-0.037	0.004	-0.008	-0.001	0.022	0.042	**0.457**	-0.001	0.005	-0.015	0.004	-0.006	0.013	0.022	0.026	-0.009	0.028	0.025	-0.021
U	$UO_2(am)$	0.031	**0.800**	0.025	-0.033	0.006	-0.006	0.003	-0.004	-0.007	-0.012	-0.013	0.025	0.039	0.016	-0.001	0.037	-0.003	0.007	**-0.072**	-0.026
Np	$NpO_2(am)$	**-0.690**	-0.036	0.002	-0.007	-0.002	0.023	0.043	**0.453**	-0.002	0.005	-0.015	0.004	-0.006	0.013	0.022	0.026	-0.008	0.026	0.025	-0.022
Pu	$PuO_2(am)$	**-0.223**	**-0.921**	-0.008	0.021	-0.031	0.003	0.000	**0.120**	0.010	0.014	0.002	0.011	-0.038	-0.006	-0.009	-0.012	-0.005	-0.023	**0.049**	0.010
	$NaPu(CO_3)_2$	**0.145**	**0.925**	0.004	-0.030	0.015	-0.010	-0.003	**-0.054**	-0.010	-0.017	-0.015	0.014	**0.045**	0.010	0.002	0.036	0.005	0.020	**-0.070**	-0.027
	$PuOHCO_3$	**0.119**	**0.935**	0.027	-0.029	0.018	-0.008	-0.001	-0.037	-0.010	-0.016	-0.015	0.015	**0.044**	0.011	0.004	0.036	0.006	0.023	**-0.069**	-0.026
	$PuPO_4(am)$	**0.174**	**0.922**	0.021	-0.030	0.022	-0.005	-0.004	-0.023	-0.010	-0.017	-0.016	0.012	0.043	0.010	-0.040	0.033	0.007	0.024	**-0.067**	-0.025
Am	$AmOHCO_3$	**0.983**	-0.010	-0.003	0.004	-0.019	-0.003	**-0.052**	**-0.125**	0.011	0.005	0.026	-0.021	0.007	-0.002	-0.017	-0.017	0.023	-0.022	-0.015	0.020
	$AmPO_4$	**0.823**	-0.034	**-0.050**	-0.015	**0.062**	0.031	-0.042	**0.145**	0.007	-0.001	0.000	-0.019	0.008	-0.010	**-0.537**	-0.016	0.033	0.010	0.005	0.021
Cm	$CmOHCO_3$	**0.983**	-0.010	-0.003	0.004	-0.019	-0.003	**-0.052**	**-0.125**	0.011	0.005	0.026	-0.021	0.007	-0.002	-0.017	-0.017	0.023	-0.022	-0.015	0.020
	$CmPO_4$	**0.823**	-0.034	**-0.050**	-0.015	**0.062**	0.031	-0.042	**0.145**	0.007	-0.001	0.000	-0.019	0.008	-0.010	**-0.537**	-0.016	0.033	0.010	0.005	0.021

Bearing limitations in the thermodynamic data in mind, from these calculations, the following conclusions can be drawn:

- For Se, Tc and U, analytical uncertainties could potentially lead to uncertainties in concentrations that are > 1 order of magnitude.
- Analytical uncertainties do not lead to significant uncertainties in the estimated solubility of Pa.
- Analytical uncertainties could lead to large uncertainties in the estimated ratios of the considered elements at theoretical equilibrium with solubility-controlling phases.
- Nb is the most soluble of the considered elements in this water (in the order of 10^{-5} molal, equivalent to approximately 1 ppm), excluding Cs, which is not solubility-controlled.
- Pd is effectively insoluble in the water considered (all concentrations are $< 1.6 \times 10^{-24}$ molal, equivalent to 1 atom per kilogram).
- Uncertainties in PO_4 concentrations could lead to large uncertainties in the estimated solubilities of Sm, Pb, Ac, Am and Cm.
- Analytical uncertainties in C concentration could be important for all elements that can form carbonate minerals, namely Sm, Pb, Ac, Th, Np, Pu, Am and Cu.

Additional information can be gained about the importance of larger uncertainties in determinands than those due to analytical errors, by assessing the chemical variability of the actual groundwaters. A convenient way to do this is to apply Factor Analysis to the output from solubility calculations using the water chemical data in Table 4.2-1.

Factor analysis is a mathematical technique that identifies the principal components of variability in the data and then recombines them to make a smaller number of mutually independent factors. An additional procedure employed here was Varimax Rotation. This effectively 'rotates' the factors such that they are aligned as closely as possible with the data. A goal is to interpret these factors in terms of actual processes. Once again the Microsoft Excel™ addin XLSTAT™ was used for this purpose. The results are given in Figure 4.3-62, which shows how the input determinand values and calculated solubilities are correlated with each other and with the factors, which are represented by the axes.

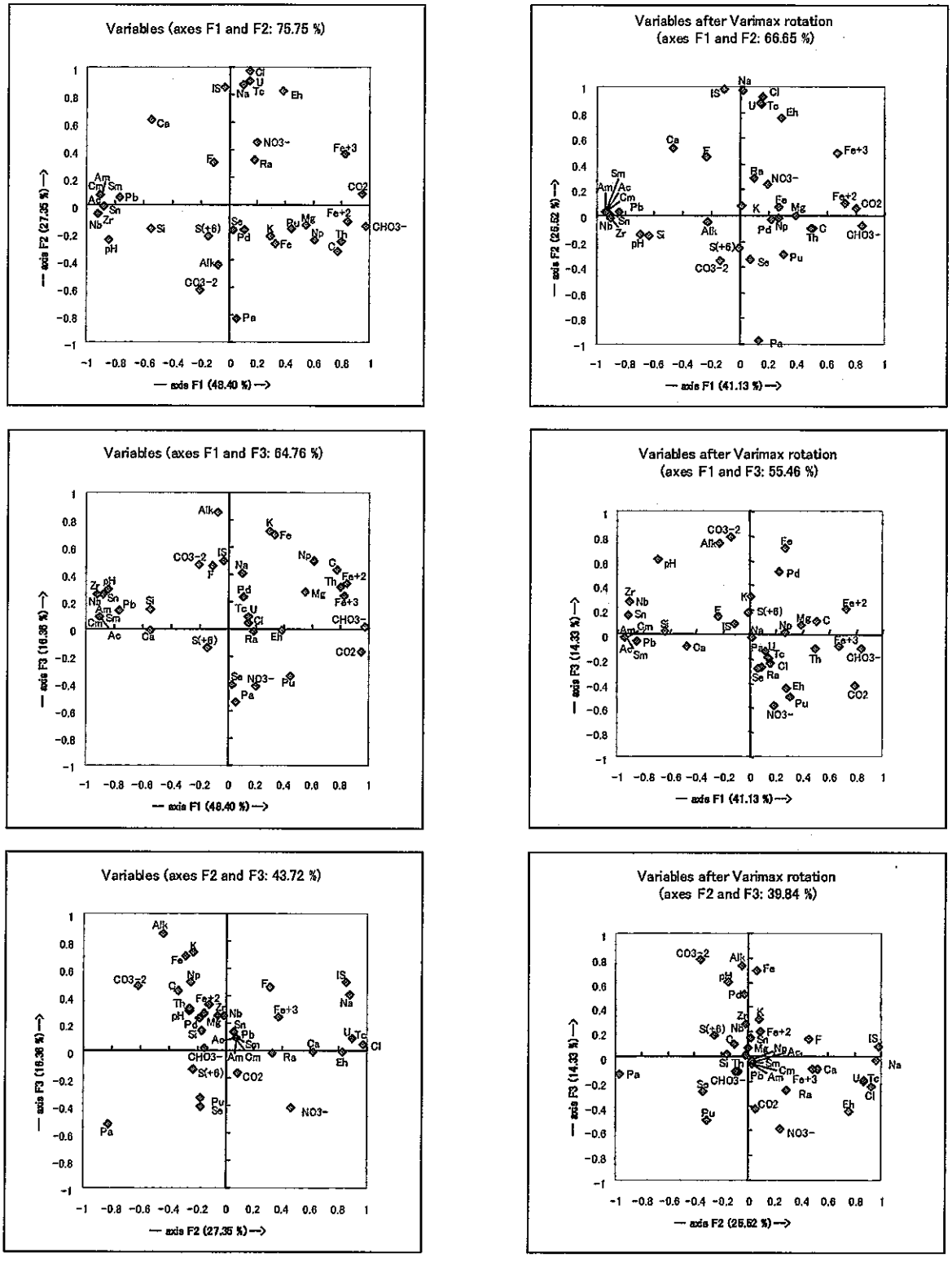

Figure 4.3-62 Results of factor analyses for the subset of samples in Table 4.2-1 for which solubility-controlled concentrations could be calculated for Sn Sm Pd Pa Th Pb Ac Tc U Pu Np Cm Am Ra Nb Zr Se. C = TIC, IS = Ionic Strength.

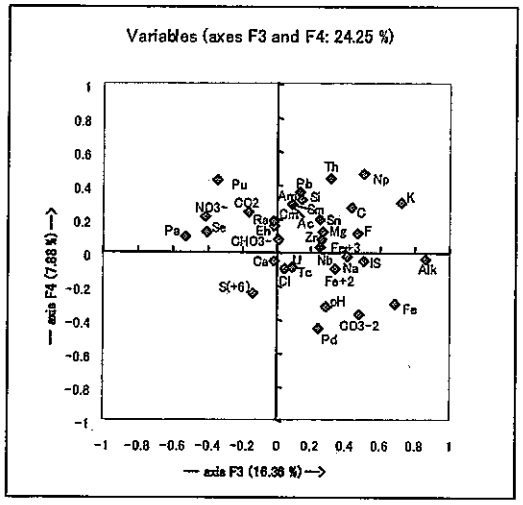

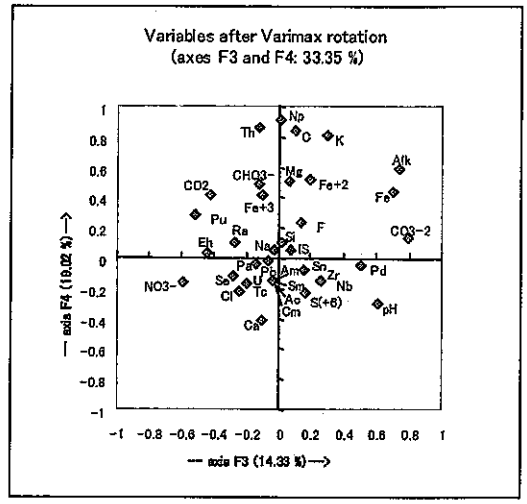

Figure 4.3-62 Continued.

Positively correlated input determinands and/or elements for which solubilities have been calculated plot close together. If they correlate with one of the processes represented by a factor, then they will also plot close to an end of the axis representing that factor. Two chemical components that plot at the opposite ends of an axis are negatively correlated. Completely un-correlated chemical components will plot at the ends of different axes.

A correlation identified from Figure 4.3-62, between an input determinand and an element of interest to this study, does not necessarily indicate that the determinand is important for determining the element's solubility. For example, in the uppermost part of the diagram Sn and Zr plot near the left end of the horizontal axis, while CO_2, and CHO_3^- plot at the right end. It might be interpreted that Sn and Zr solubilities are controlled by the dissolved carbon system. However, inspection of Figure 4.3-4 and Figure 4.3-12 indicate that these elements do not form carbonate complexes under the Tono groundwater conditions. Instead, pH is a major control on the solubilities of these elements and on the speciation of dissolved carbon, leading to the observed inverse correlation.

It is also clear from Figure 4.3-62 that the TIC (represented by C) plots in different locations to the carbon species CO_3^{2-}, CHO_3^- and CO_2. The reasons for this are possibly related to large uncertainties (and in some cases inconsistencies) between reported TIC, CHO_3^- and alkalinities which have been identified by Arthur (2003).

In contrast, Figure 4.3-62 indicates more directly where a particular determinand does not control the solubility of an element. For example, in the uppermost diagram, U plots near the top of the axis representing Factor 2. This indicates that there is no clear correlation with C. Therefore C does not appear to be important for controlling the solubility of U in the groundwaters at Tono. It is stressed, however, that in other groundwater systems, or even possibly elsewhere in the Tono area, variations in dissolved C could be important and should be investigated.

From this analysis, the following additional major conclusions can be drawn:

- Variations in salinity (ionic strength) over the range seen in the Tono groundwaters have no significant effect on solubility.
- Inspection of Figure 4.3-25 and Figure 4.3-26 reveals that the correlation between U and ionic strength, Na and Cl does not imply a direct control of salinity on U solubility. Instead, variations in redox (Eh) are the main control.
- Similarly from Figure 4.3-39 and Figure 4.3-40 it is apparent that the correlation between Tc and ionic strength, Na and Cl does not imply a direct control of salinity on Tc solubility. Instead, variations in redox (Eh) are the main control.
- Th and Np solubilities are influenced by the concentration of TIC.
- Ra shows little correlation with any of the four factors illustrated in Figure 4.3-62. This reflects the unique dependence (among the elements considered) of Ra solubility on SO_4 concentration. Variations in SO_4 concentration are not distinguished by the factors considered in this analysis.

Scoping calculations

As discussed in Section 4.2.2, an over-riding quality indicator is the degree of drilling fluid contamination. Therefore, calculations were undertaken to evaluate the possible significance of this contamination, using the code GWB. These calculations involved simulating mixing between 1 kg of a typical drilling fluid composition (based on the drilling fluid composition reported for boreholes DH-6, 7, 8 in Excel file 'Table_gwchem_ver up.xls', received from JNC on 28th February 2003) and groundwater. Each calculation considered mixing to occur in the presence of one of the solubility-controlling phases given previously.

In each calculation, equilibration between the reported drilling fluid and atmospheric O_2 was simulated initially. Mixing between the resulting water and 1 kg of water based on the groundwater from 563.75 m depth (midpoint of the sampling section) in borehole DH-7 was then simulated. The solution was charge balanced on CO_3^{2-}. Reduced sulphur species were suppressed to avoid sulphide precipitation.

The results of these simulations are given in Figure 4.3-63 to Figure 4.3-76.

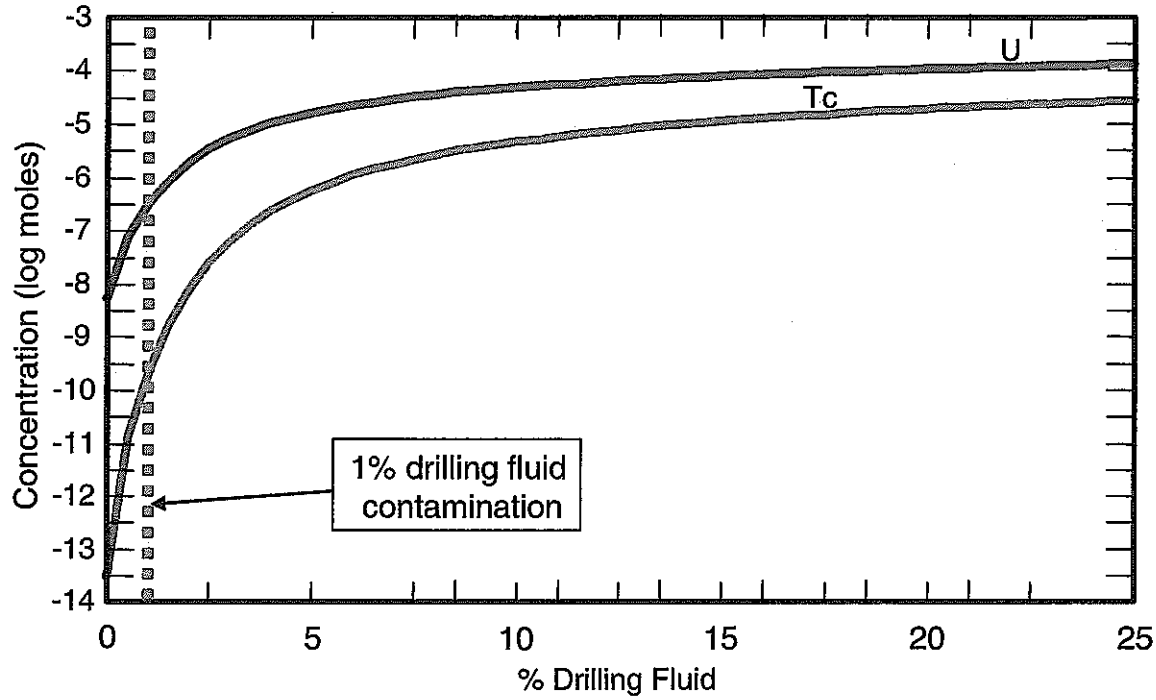

Figure 4.3-63 Simulation of the effects of drilling fluid contamination on the calculated solubilities of U and Tc.

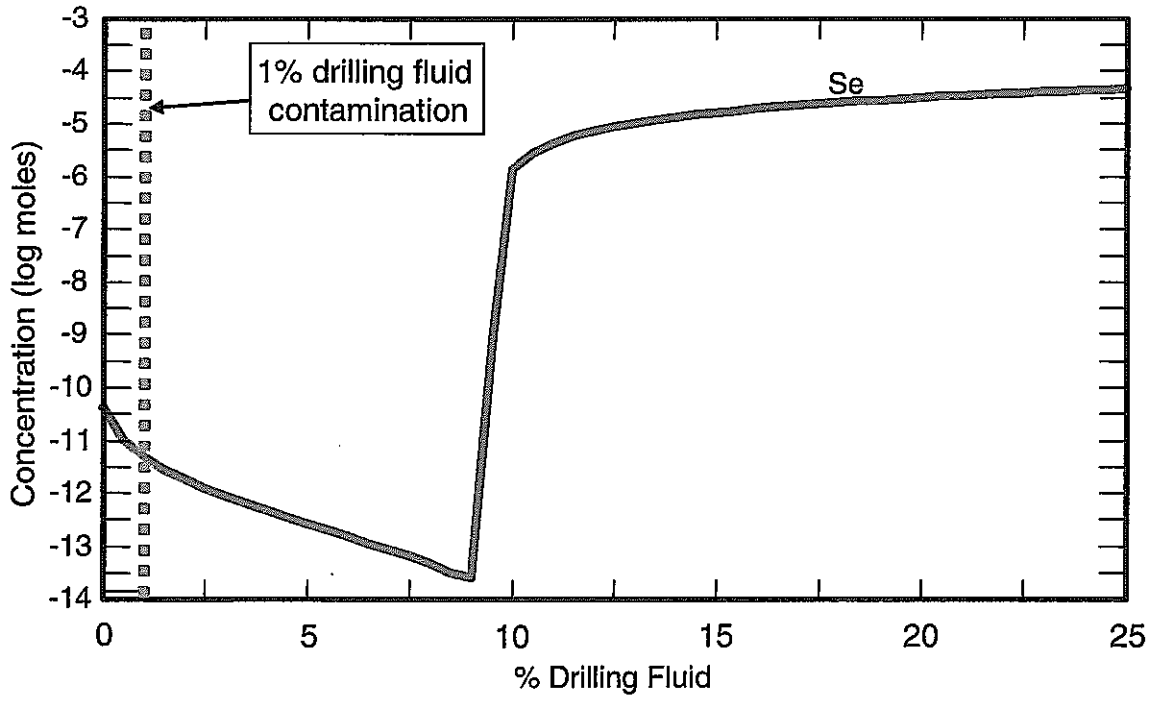

Figure 4.3-64 Simulation of the effects of drilling fluid contamination on the calculated solubility of Se ($FeSe_2$ was the solubility-controlling phase).

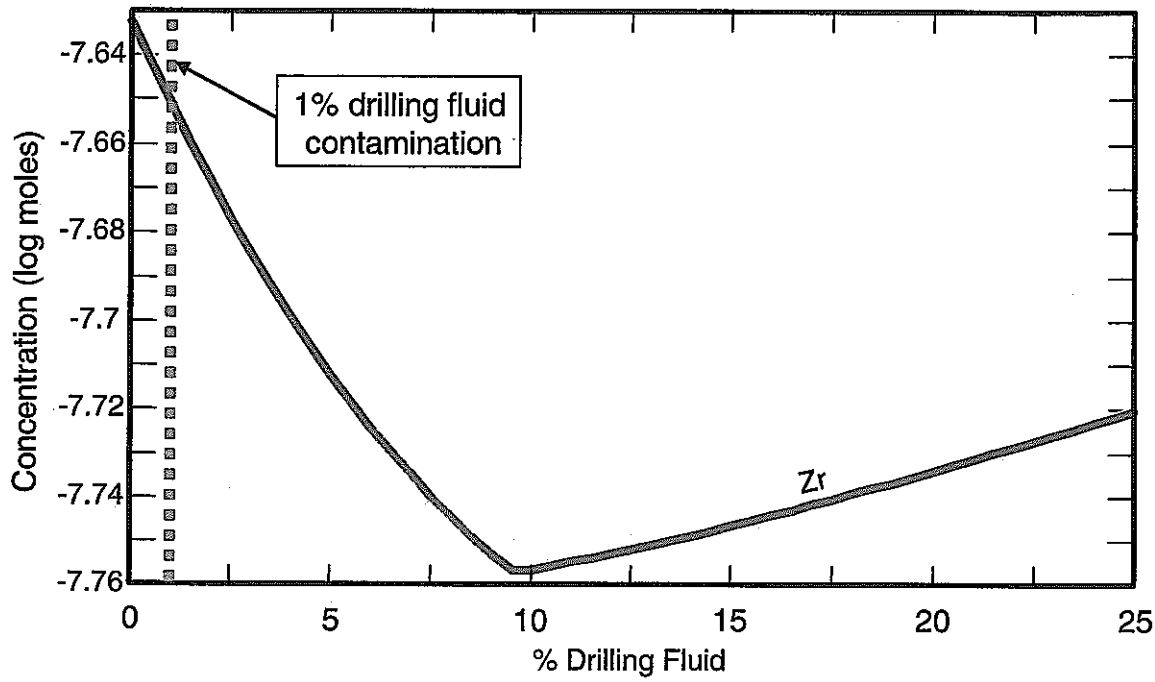

Figure 4.3-65 Simulation of the effects of drilling fluid contamination on the calculated solubility of Zr.

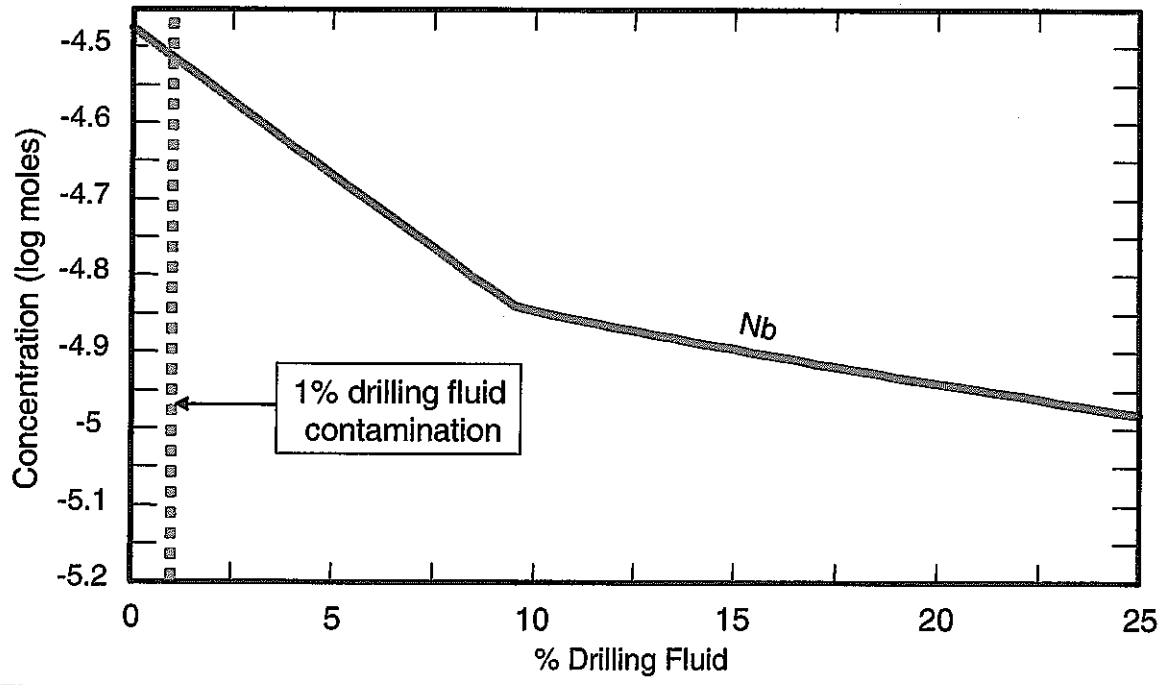

Figure 4.3-66 Simulation of the effects of drilling fluid contamination on the calculated solubility of Nb.

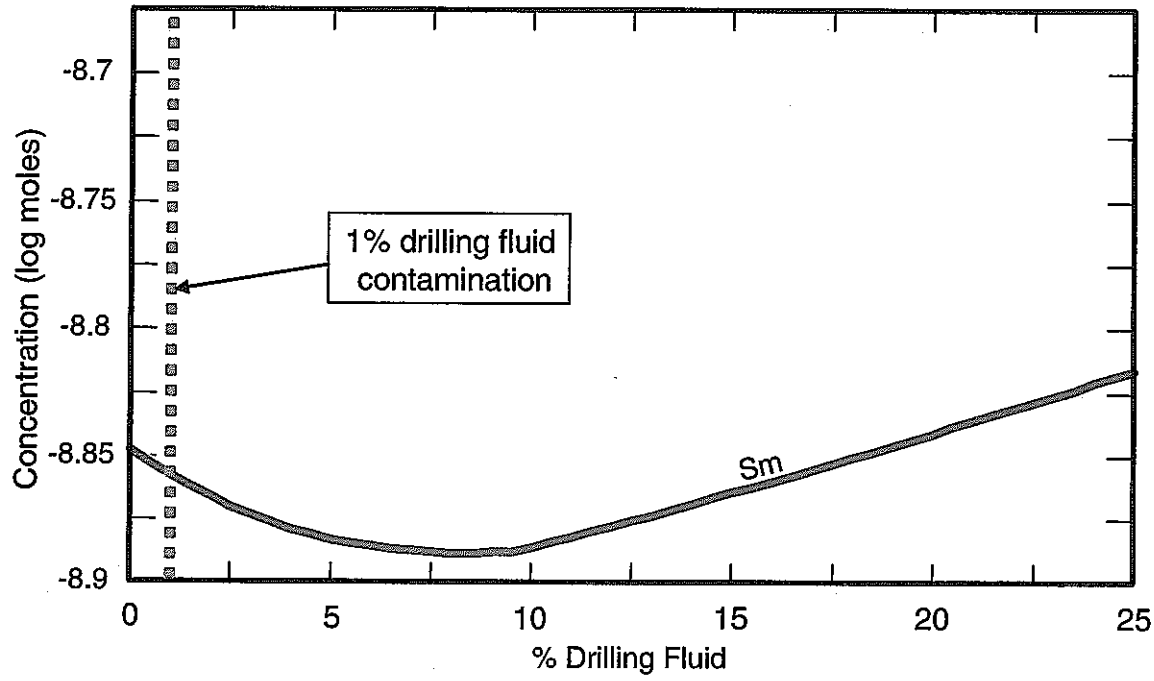

Figure 4.3-67 Simulation of the effects of drilling fluid contamination on the calculated solubility of Sm.

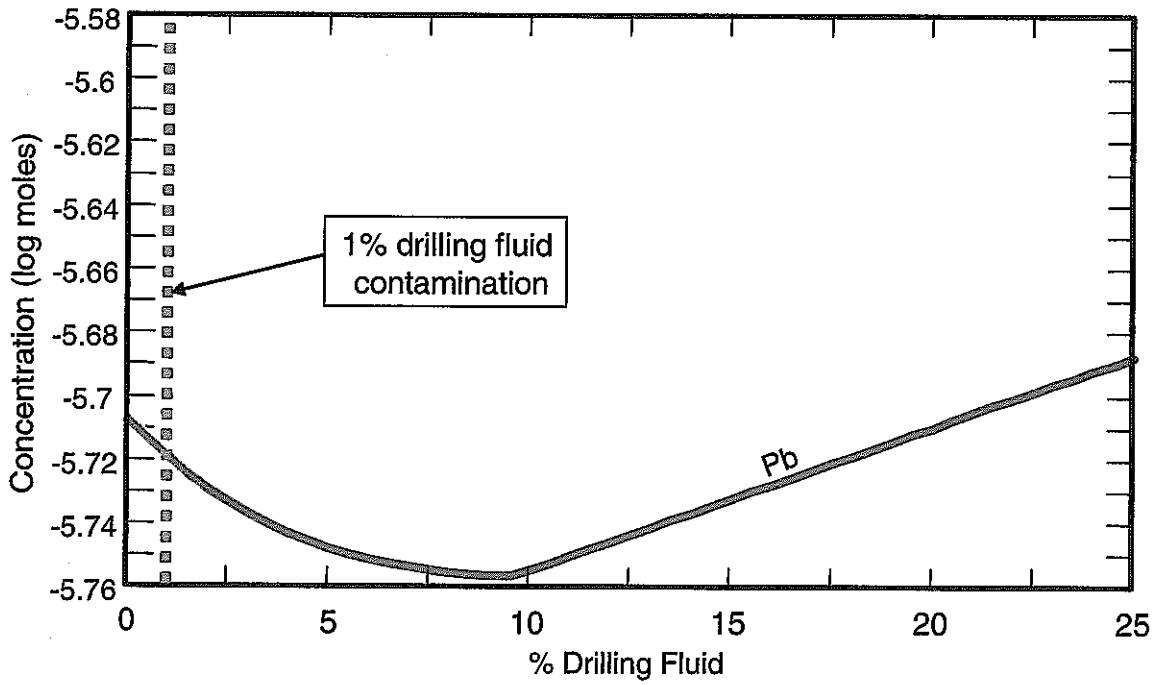

Figure 4.3-68 Simulation of the effects of drilling fluid contamination on the calculated solubility of Pb.

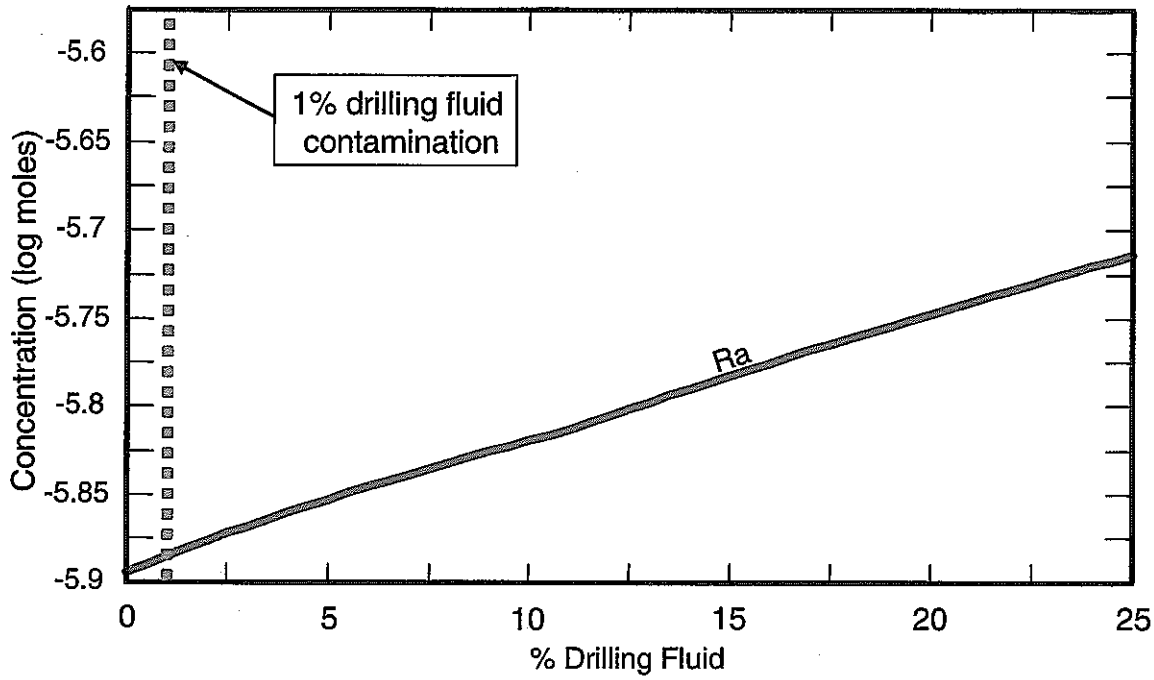

Figure 4.3-69 Simulation of the effects of drilling fluid contamination on the calculated solubility of Ra.

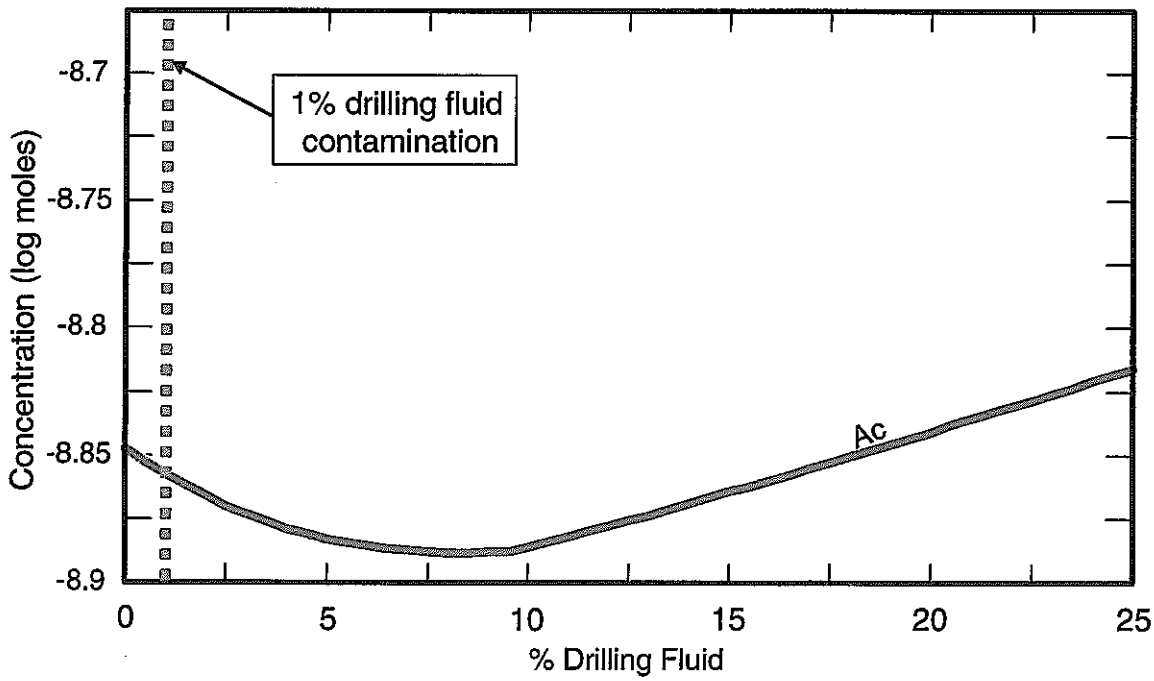

Figure 4.3-70 Simulation of the effects of drilling fluid contamination on the calculated solubility of Ac.

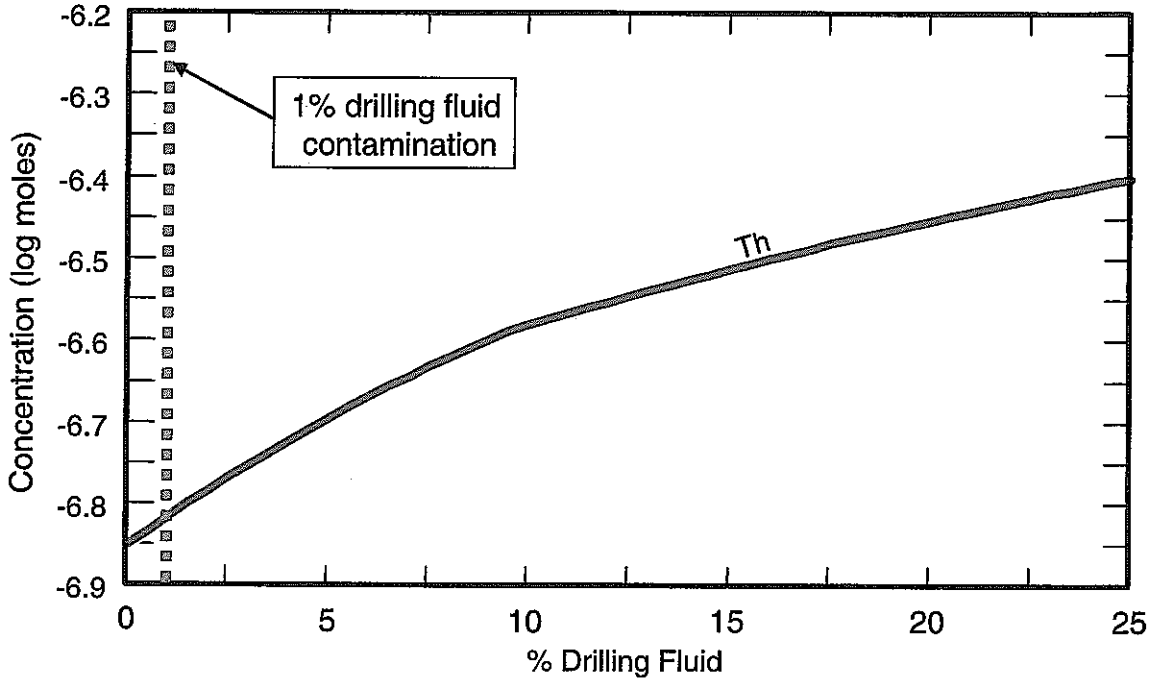

Figure 4.3-71 Simulation of the effects of drilling fluid contamination on the calculated solubility of Th.

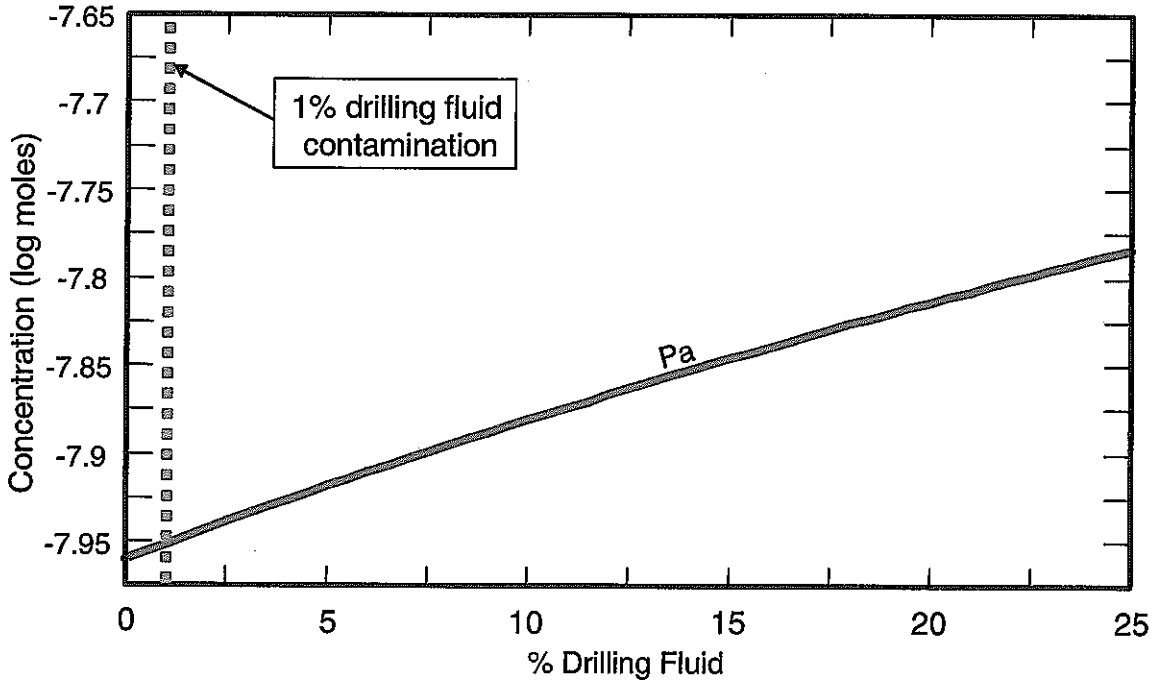

Figure 4.3-72 Simulation of the effects of drilling fluid contamination on the calculated solubility of Pa.

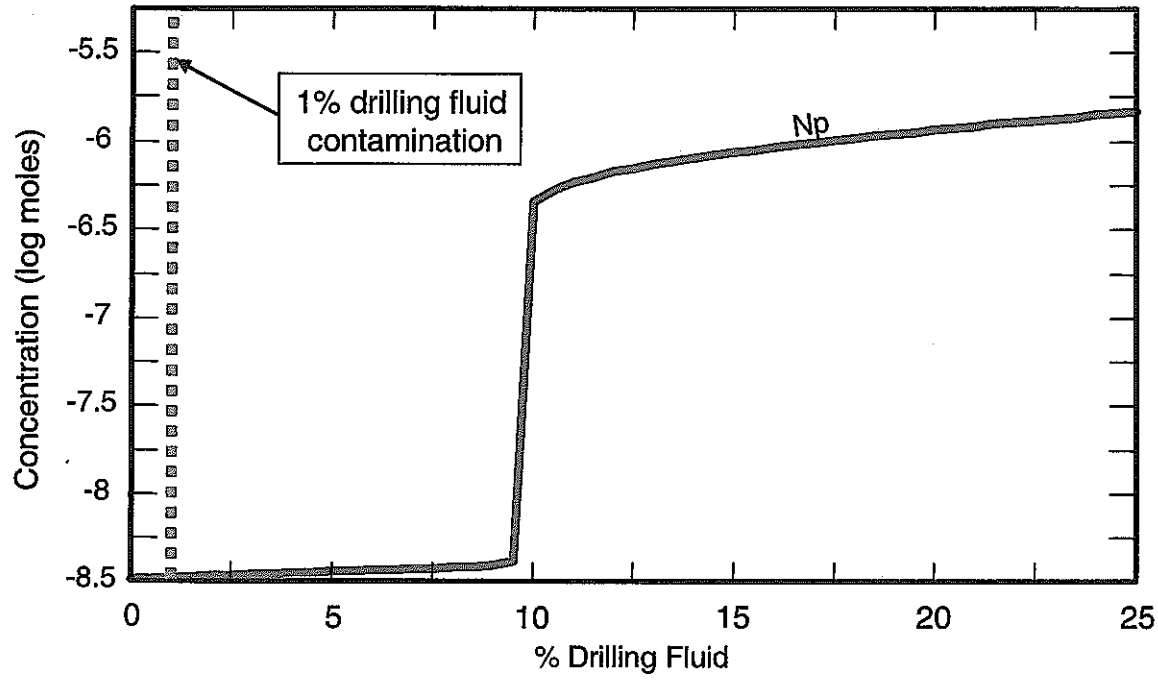

Figure 4.3-73 Simulation of the effects of drilling fluid contamination on the calculated solubility of Np.

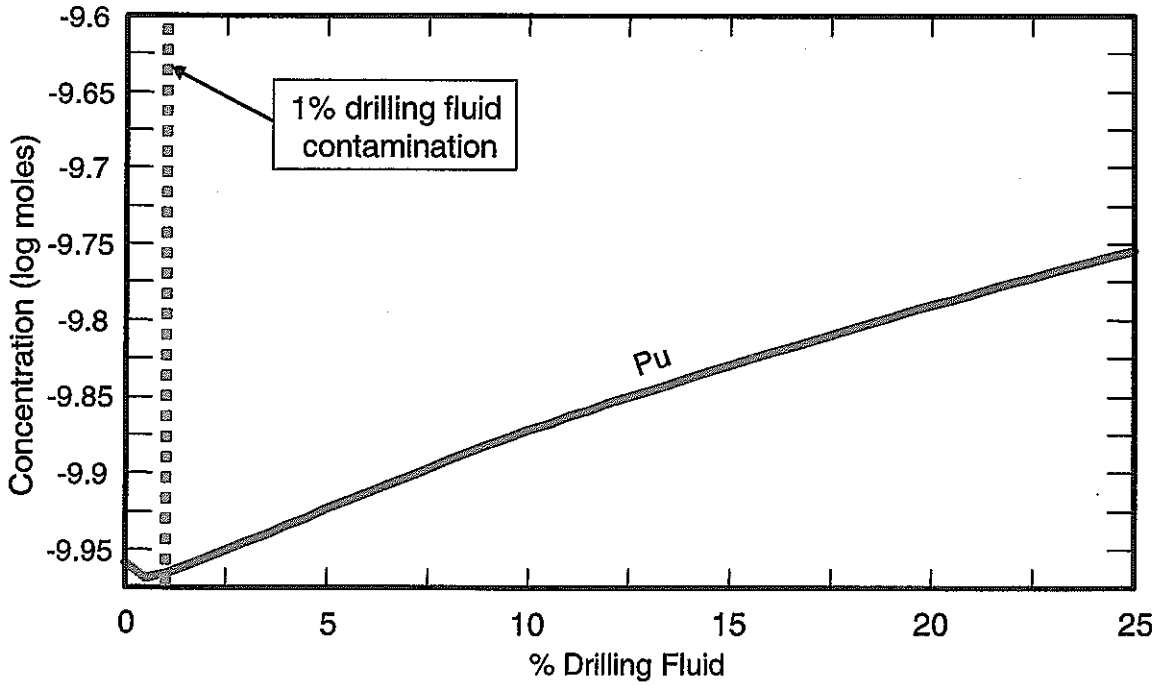

Figure 4.3-74 Simulation of the effects of drilling fluid contamination on the calculated solubility of Pu.

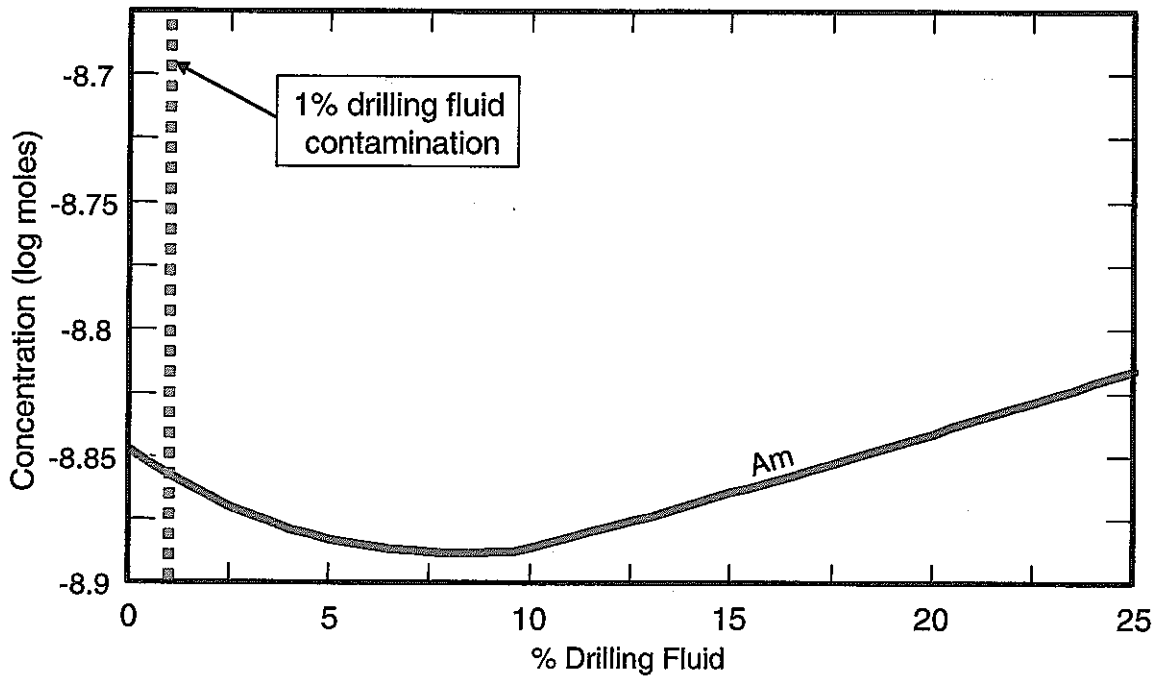

Figure 4.3-75 Simulation of the effects of drilling fluid contamination on the calculated solubility of Am.

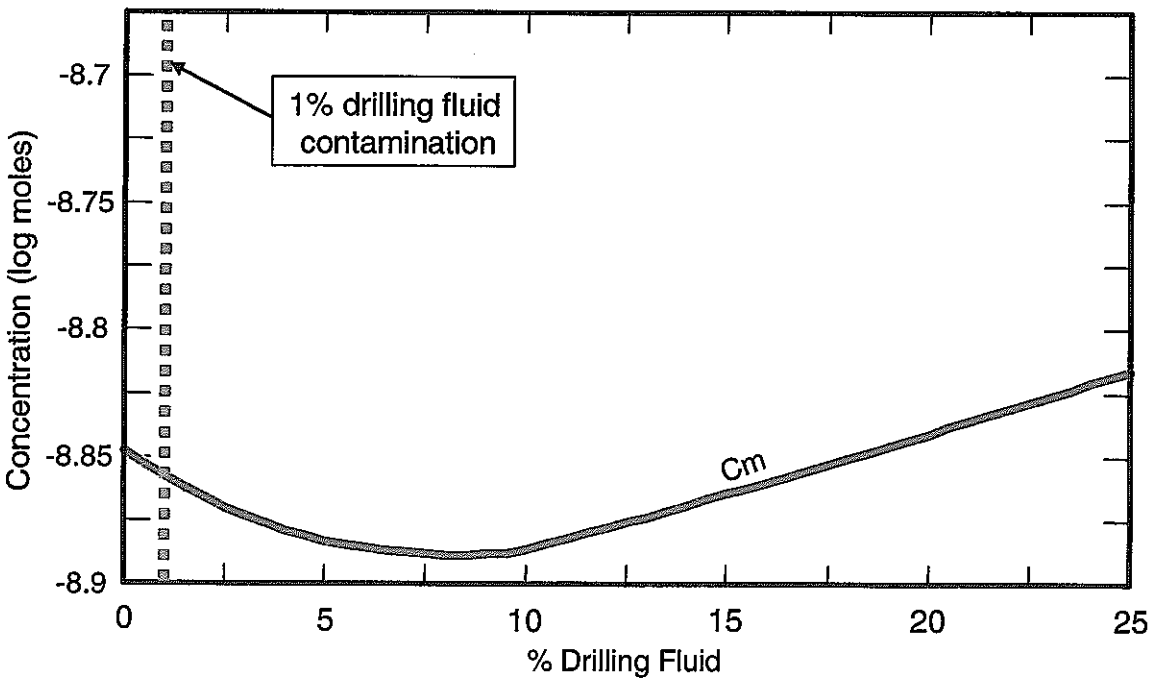

Figure 4.3-76 Simulation of the effects of drilling fluid contamination on the calculated solubility of Cm.

From these simulations it can be concluded that potentially, even small amounts of drilling fluid contamination (1%) could have a significant effect on the estimated solubilities of many of the elements considered. The greatest effect would potentially be on the estimated solubilities of U and Tc. In these cases, contamination of as little as 1% could potentially cause variations in the estimated solubilities in the orders of 1.5 and 4 respectively.

Additional scoping calculations were performed to evaluate the significance of:

- poor charge balances;
- variations in HCO_3^- content;
- uncertainties in redox conditions.

The approach was to carry out calculations using PHREEQC in which different chemical constraints were imposed on the composition reported for the groundwater composition from a depth of 563.75 m in borehole DH-7. The results are shown in Figure 4.3-77 and Figure 4.3-78.

From these figures it is apparent that:

- The poor charge balance (among the largest for the Tono groundwater samples) does not cause significant uncertainties in the calculated solubilities.
- Inconsistencies between measured alkalinities and TIC could lead to relatively large uncertainties in the calculated concentration of any element controlled by the solubility of a carbonate mineral (Sm, Ac, Pu, Am, Cm and to a lesser extent Th).
- Differences between measured Eh (-400 mV) and Eh consistent with pyrite equilibration (-413 mV) are negligible.

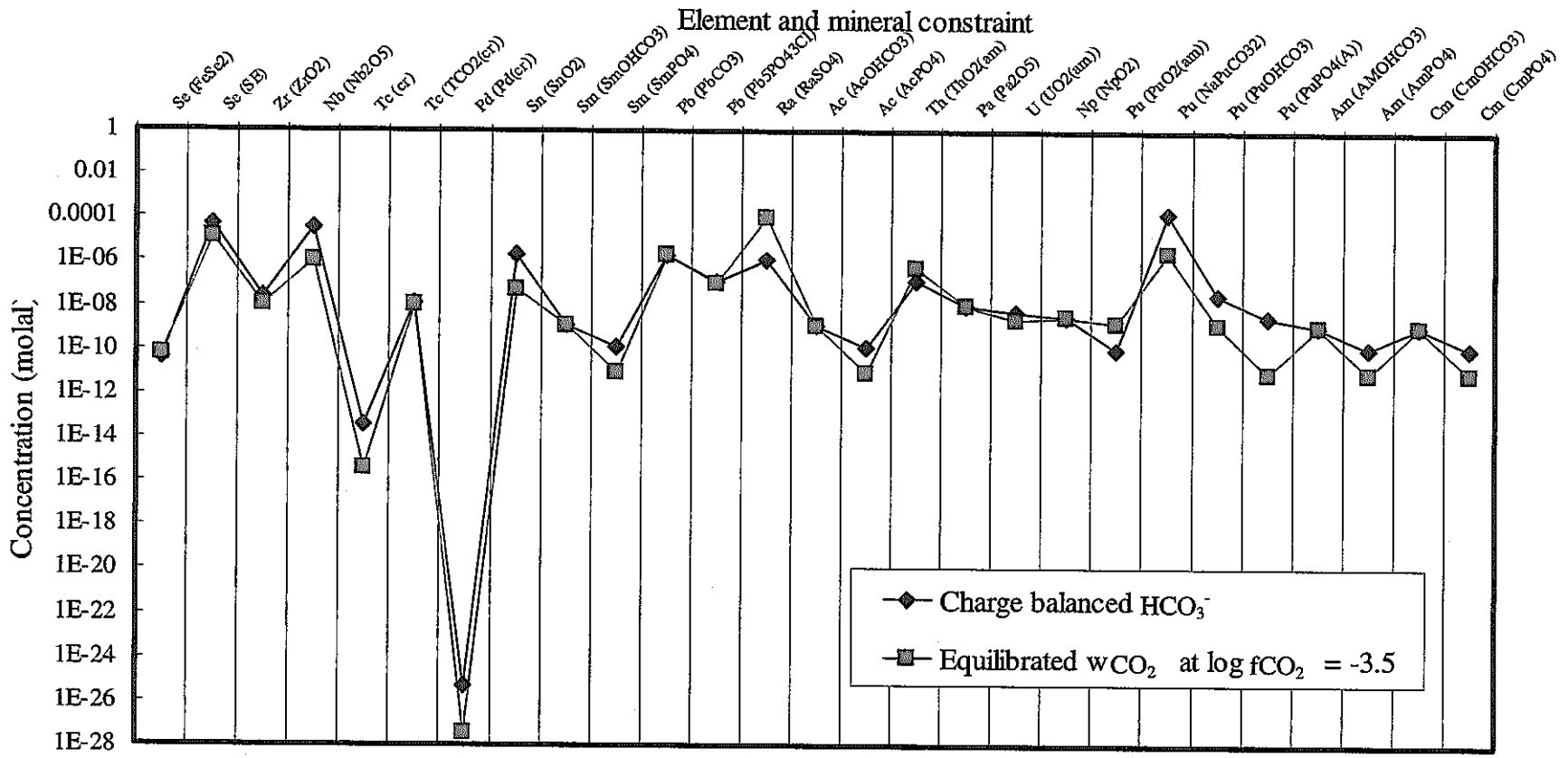

Figure 4.3-77 Comparison between element concentrations calculated when the water from DH-7, 563.75 m depth is charge-balanced with HCO_3^-, and concentrations calculated when the same water is equilibrated with atmospheric CO_2.

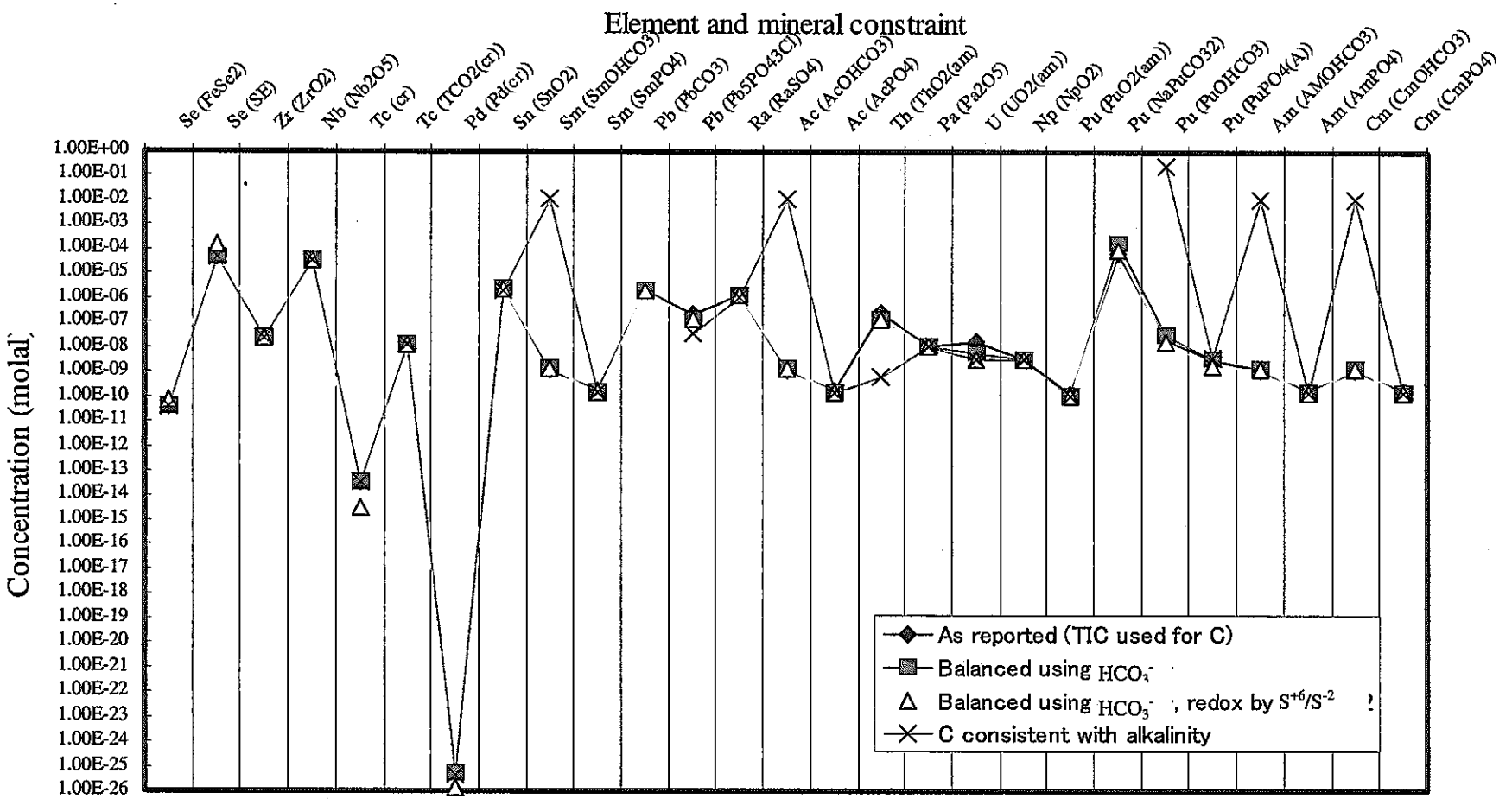

Figure 4.3-78 Comparison between element concentrations calculated when various constraints are imposed on redox and the concentration of dissolved carbon in the water from 563.75 m depth in DH-7.

5 Initial analysis of 3D heterogeneity in geochemical characteristics

5.1 3D heterogeneity in chemical conditions

In the Tono area, the Cretaceous Toki Granite is unconformably overlain by sedimentary rocks. These include, lignite-bearing rocks of the Miocene (c. 18-20 Ma) Toki Lignite-bearing Formation, up to a few tens of metres above the unconformity.

The sedimentary sequence contains several unconformities and mostly is cut by the Tsukiyoshi Fault (c. 30 m apparent reversed displacement).

The granite is fractured, with fractures probably having a range of origins. Some of these are associated with faulting, the most major of which is the Tsukiyoshi Fault which cuts the area.

In some areas, the granite crops out at the surface and recharge occurs directly to the granite (or via a relatively thin layer of soil). However, over most of the area, the granite is overlain by the sedimentary sequence.

The upper part of the granite is believed to be generally more permeable than the deeper granite, reflecting a higher density of fracturing towards the unconformity and also a higher degree of palaeo-weathering (associated at least in part with the unconformity itself).

The main variations in groundwater types and redox conditions are summarized in Figure 5.1-1, Figure 5.1-2, and Figure 5.1-4.

Generally, more than 1 km or so to the north of the Toki River shallower groundwaters are Ca-HCO_3 dominated. However, with increasing depth groundwaters are interpreted to become progressively Na-Ca-HCO_3 and then Na-HCO_3 dominated. In contrast, in the southern part of the area, in and around the Toki River valley, the deep groundwaters are Na-Cl dominated. The groundwater salinities are also somewhat higher than those of the carbonate-dominated waters further north.

There is also evidence of variations in redox conditions. Of particular relevance is the observation that some fracture zones apparently contain Na-Ca-Fe-HCO_3 dominated waters (e.g. Iwatsuki and Yoshida, 1999). The Fe^{2+} in these waters is considered to originate in the dissolution of biotite, by reactions such as:

$$\text{Biotite} + 7H^{+} + 0.5H_2O = \text{Kaolinite} + K^{+} + 3Fe^{2+} + Si(OH)_4$$

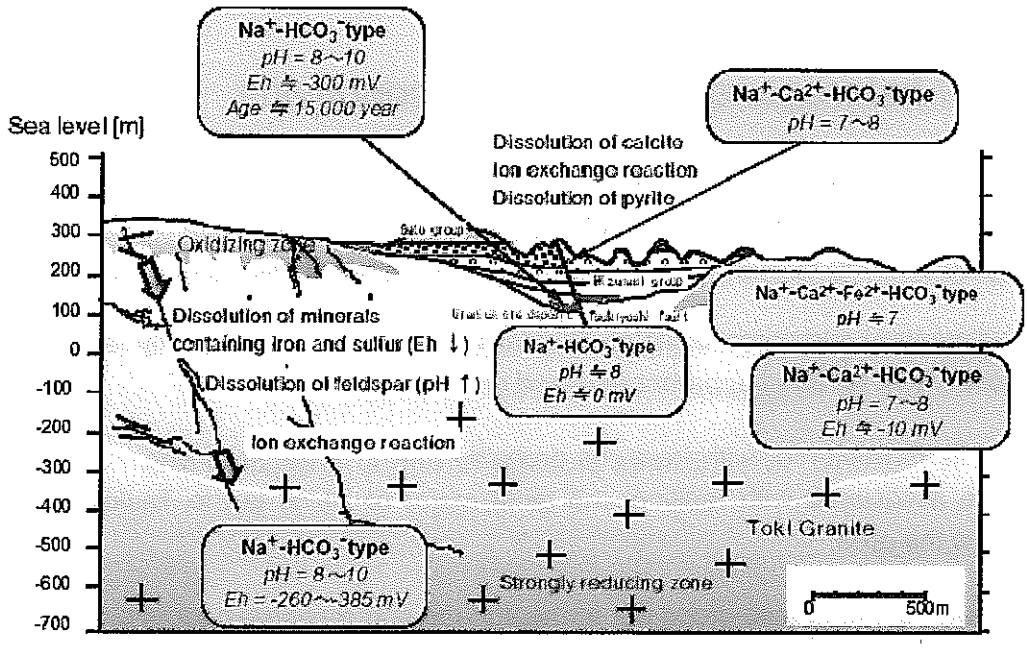

Geochemical reactions in sedimentary rocks

Dissolution and precipitaion of calcite	$CaCO_3 + H_2O \sim Ca^{2+} + OH^- + HCO_3^-$
Ion exchange reaction	$Ca^{2+} + 2(\text{Na-Montmorillonite}) \sim \text{Ca-Montmorillonite} + 2Na^+$
Redox reaction of sulfur minerals	$FeS_2 + 8H_2O \sim 2SO_4^{2-} + Fe^{2+} + 16H^+ + 14e^-$
	$SO_4^{2-} + 8e^- + 9H^+ \sim HS^- + 4H_2O$
Microbial activity	$SO_4^{2-} + 2C(\text{organic}) + 2H_2O \sim H_2S + 2HCO_3^-$
	$3H_2S + SO_4^{2-} \sim 2H_2O + 2CO_2 + 4S$

Geochemical reactions in granite

Dissolution and precipitation of calcite	$CaCO_3 + H_2O \sim Ca^{2+} + OH^- + HCO_3^-$
Redox reaction of iron minerals	$Fe^{2+} + 3H_2O \sim Fe(OH)_3 + 3H^+ + e^-$
Dissolution of feldspar	$\text{Albite} + 2H^+ + 9H_2O \sim 2Na^+ + 4Si(OH)_4 + \text{Kaolinite}$
	$\text{Anorthite} + 2H^+ + H_2O \sim Ca^{2+} + \text{Kaolinite}$
	$\text{Albite} + 6H^+ + 20H_2O \sim 6Na^+ + 10Si(OH)_4 + \text{Montmorillonite}$
	$\text{Anorthite} + 12H^+ + 8Si(OH)_4 \sim 6Ca^{2+} + 16H_2O + \text{Montmorillonite}$
Ion exchange reaction	$Ca^{2+} + 2(\text{Na-Montmorillonite}) \sim \text{Ca-Montmorillonite} + 2Na^+$
Redox reaction of sulfur minerals	$FeS_2 + 8H_2O \sim 2SO_4^{2-} + Fe^{2+} + 16H^+ + 14e^-$
	$SO_4^{2-} + 8e^- + 9H^+ \sim HS^- + 4H_2O$

Figure 5.1-1 Variations in groundwater chemistry in the Tono area (after JNC, 2000).

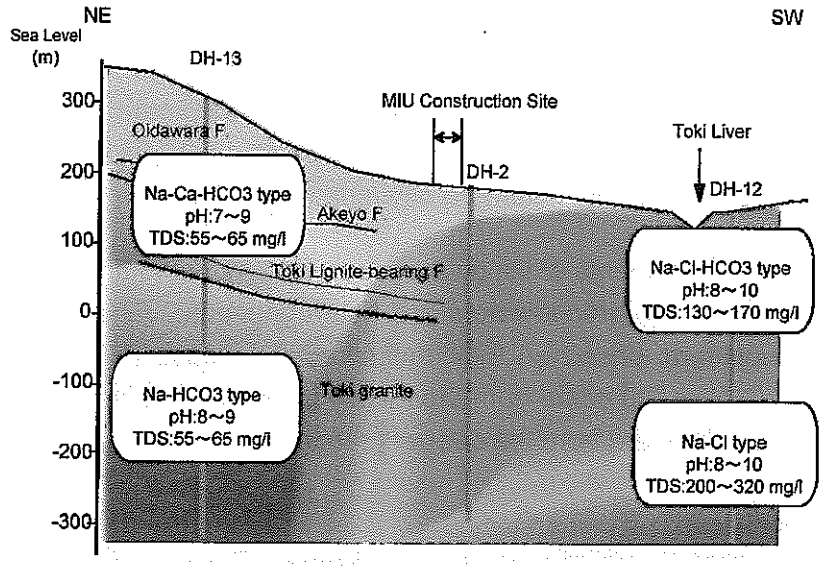

Figure 5.1-2 Variations in groundwater chemistry in the area around the Mizunami Underground Research Laboratory site (from JNC, 2003).

The liberated Fe can then be oxidized to give Fe-oxihydroxides ($Fe(OH)_3$). This process is thought to occur in the upper granite where Eh potentials are considered to be controlled by the $Fe(OH)_3$ (ferrihydrite)/Fe^{2+} couple. These conditions are more oxidizing (+100 mV to -100 mV) than those in the deeper granite (redox generally <-250 mV). In the deeper granite reactions involving dissolution of pyrite potentially become more important. The water is thought to become more alkaline with increasing water/rock interaction (inferred but not proved to correspond to distance traveled along a flow path).

Key issues for understanding the migration of redox conditions in the Toki Granite are:

- There could be 'fingering' of recharge to the granite, caused by the heterogeneous distribution of the sedimentary cover sequence in the recharge areas. Where the cover sequence is absent, there is a potential for relatively oxidizing recharging water to enter the granite directly. However, where the granite is overlain by the sedimentary rocks, a proportion of the recharge could be through the sedimentary sequence.

- The redox buffering capability of the superficial deposits or rocks overlying the granite, notably:
  - water recharging through any soil cover could potentially be reduced by processes such as the microbially-mediated decay of organic matter
  - water recharging through the sedimentary cover rocks could react with diagenetic pyrite present in these rocks and/or with abundant organic matter.

- The spatial distribution and characteristics (whether or not transmissive) of fracture zones could control the penetration of any oxygenated groundwater into the Toki granite.

- The palaeo-weathering (at least partially related to the erosion that preceded the deposition of the sedimentary rocks at around 18Ma before the present) could control the distribution of redox-buffering minerals. Potentially, palaeo-fingering of oxygenated water could locally have depleted the redox buffering capacity of the rocks. This would then exert an effect on the penetration depths of more recently recharged oxygenated groundwater.

There are direct measurements of Eh on the groundwaters in the area that suggest the actual redox states of the groundwaters are heterogeneous. There are two distinct groups of groundwaters, based on their measured Eh values (Figure 5.1-3). More oxidizing waters (higher Eh) come from the mostly from the uppermost Toki Granite. In contrast, reducing values are from the deeper granite.

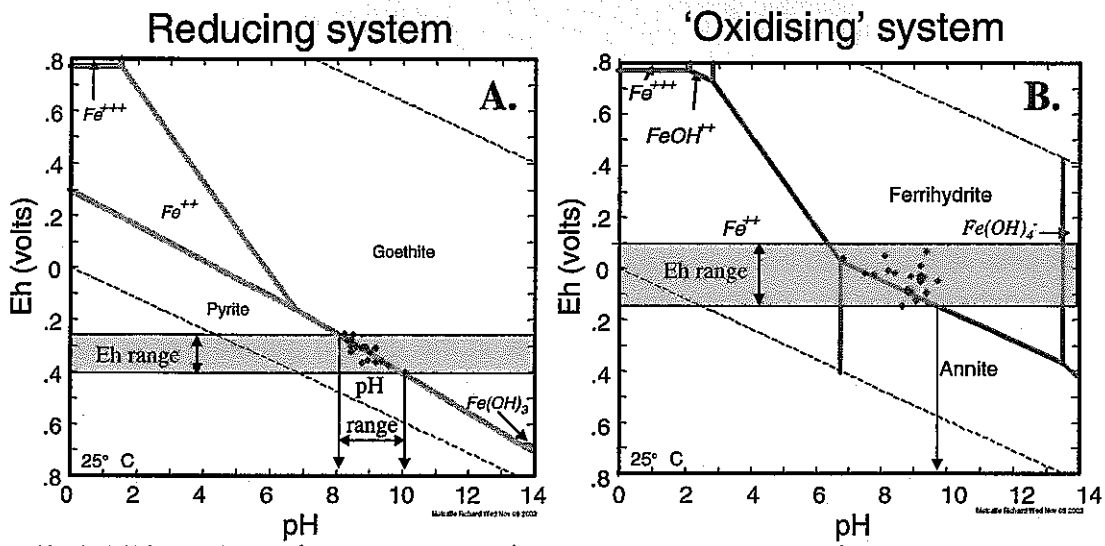

Figure 5.1-4 Illustration of the variations in redox conditions observed in groundwaters from the Tono area (water analyses represented by blue circles). Relatively reducing waters (A) plot near the equilibrium line between pyrite and goethite. More oxidising waters (B) plot near the ferrihydrite-annite (the Fe-end-member of biotite) equilibrium line.

There is considerable evidence for heterogeneous distribution of reduced minerals in the Toki Granite. Iwatsuki and Yoshida (1999) classified the rock into: intact zones; moderately fractured zones; and intensely fractured zones, based on the frequencies and widths of fracturing. Pyrite associated with some of the intensely fractured zones was reported to have etched (have undergone dissolution) at relatively great depths in some boreholes (e.g. 527 m in borehole DH-3), whereas in other boreholes pyrite is fresh and keeps its original form at shallower depths (e.g. 80 m in DH-4).

There is thus substantial circumstantial evidence for the dual porosity characteristics of the granite controlling the penetration of oxidizing water.

Since the Toki granite contains effectively zero organic matter, only the effects of inorganic mineral reactions on redox conditions are considered. The potential influence of organic matter (or other mineral reactions) in the overlying sedimentary rocks and soil zone is considered to control the oxygen content of recharging groundwater.

To understand further the coupling between flow and redox conditions, a simple coupled 1D model was developed using Quintessa's code Ozone (O3). The model is described in detail in Metcalfe et al. (2003) and is illustrated in Figure 5.1-.

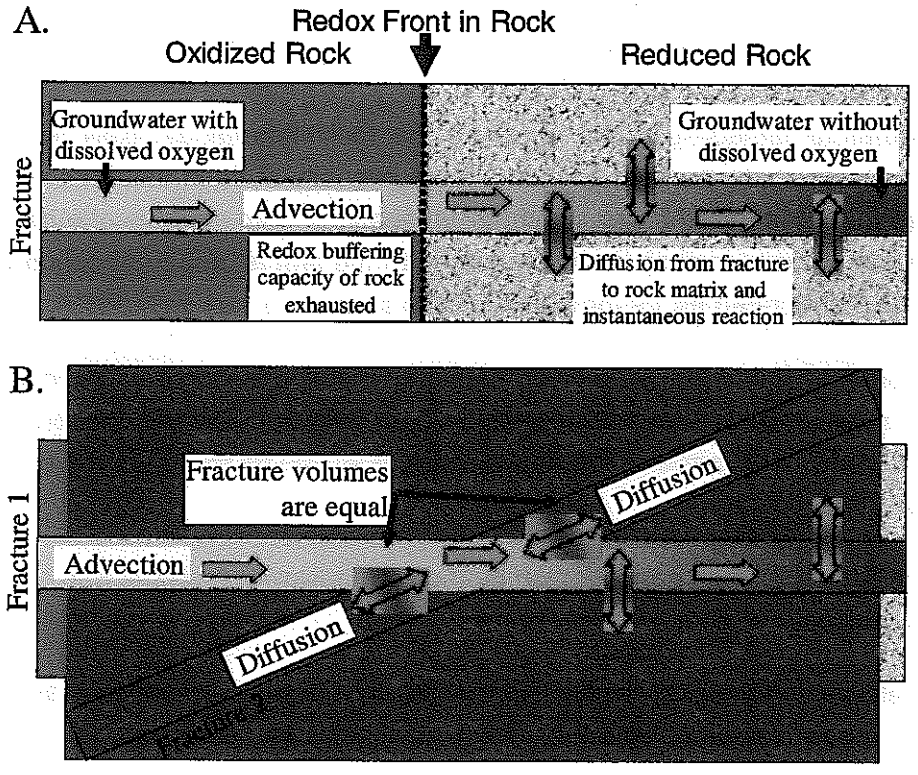

Figure 5.1-4 Schematic illustration of Ozone(O3) simulations of redox front migration. The results for two cases are given in .

The simulations of redox variations were based on several assumptions.

- ▲ The rate of oxygen consumption by water/rock reactions was assumed to be fast compared to the rate of oxygen supply by advective groundwater flow.
- ▲ The water/rock reactions were assumed to be controlled by the accessibility of reactive minerals to the dissolved oxygen-bearing water.
- ▲ All the minerals in the rock were assumed to be available for reaction, once they come into contact with oxygenated water.
- ▲ Diffusion from fractures, where the water moves by advection, was assumed to transport oxygenated water into the rock matrix, where redox reactions may take place.

It was therefore unnecessary to represent the rock mineralogy explicitly within the calculations. Instead, the total oxygen uptake capacity of each unit rock volume was calculated from a reported bulk-rock chemical analysis. An analysis of a sample from 645 m in DH-10 was used since this sample had the largest apparent concentration of reduced elements reported for the granite in the Tono area.

The assumptions mean that for a given permitted matrix diffusion depth, the redox front propagation distance in a given time for a given inflowing oxygen concentration is a minimum value. The propagation of the redox front will be more rapid if one or more of the following occurs:

- ▲ the rate of oxygen consumption by the rock is slower than the rate of supply by advection;
- ▲ the effective capacity of the rock to uptake oxygen is lower, than assumed by the model, which will occur if:
  - the actual reduced minerals in the rock are less abundant;
  - the actual reduced minerals in the rock are less accessible to oxygenated water;
  - the depths over which matrix diffusion may occur is less.

A complete description of all the model cases and their results is presented in Metcalfe et al. (2003). Example results are given in Figure 5.1-5. The penetration rate of the redox front could be substantial, depending upon the model parameter values. For example, in Case 1, the redox front propagated around 250 m from the recharge zone in c. 20,000 years.

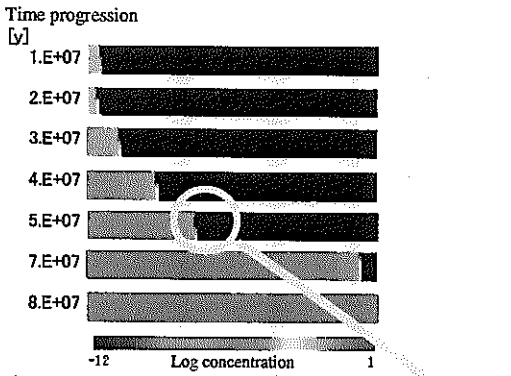

Dissolved oxygen concentration (mol/m³) distribution in the fractured medium Reference Case
Horizontal: Flow direction Length 1000 m 100 cells
Perpendicular: Matrix diffusion Depth 1 m 10cells
Vertical and horizontal scales different.
Figure showing output after 6.E+07 years omitted.

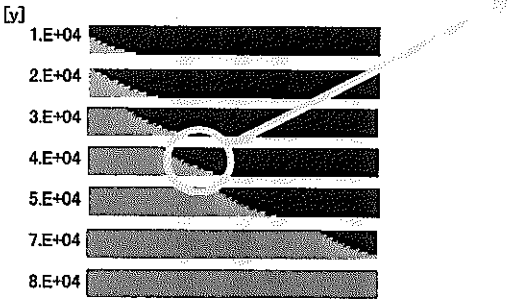

Dissolved oxygen concentration (mol/m³) distribution in the fractured medium Case 1
Horizontal: Flow direction Length 1000 m 100 cells
Perpendicular: Matrix diffusion Depth 1 m 10cells
Vertical and horizontal scales different.
Figure showing output after 6.E+04 years omitted.

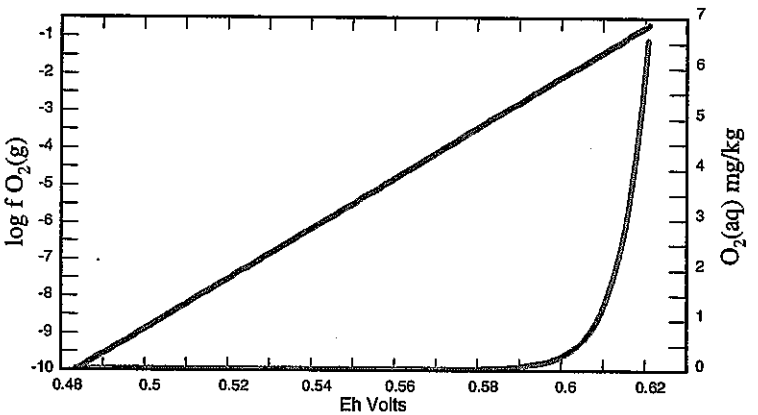

Figure 5.1-5 Calculated propagation of a redox front at which oxygen is completely depleted through the Toki Granite. Immediately to the right of the front (on the reducing side), no oxygen is detectable, but Eh valies are still positive. Variation in redox conditions observed in the Tono groundwaters (Figure 5.1-43) would be expected to the right of the front.

Based on this result, it is possible that there could be considerable redox variability related to the spatial heterogeneity of hydraulic conductive in the rock mass. More conductive features such as fractures might potentially contain more oxidizing water than less conductive rock volumes.

Based on geological and hydrogeological considerations, the distributions of Inferred Major Faults (IMFs) is possibly an important hydrogeological control on redox heterogeneity. The distributions of these fractures is uncertain, but alternative distributions which are consistent with observed fracture frequencies have been constructed (Figure 5.2-1 and Figure 5.2-2). It can be seen from these figures that, if these fracture zones indeed conduct relatively oxidizing water, they could results in a highly heterogeneous pattern of solubilities.

It is important to note that, Figure 5.1-5 shows the spatial distribution of dissolved oxygen. The complete loss of oxygen from the water at the redox front still corresponds to Eh values that are far higher (more positive) than those measured (c.f. Figure 5.1-4). Redox conditions corresponding to these measured Eh values would occur some distance to the right of the redox front at which dissolved oxygen disappears.

5.2 3D variations in element solubilities

By comparing this evidence for chemical heterogeneity in the Tono groundwater system, with the results of speciation calculations in Section 4.3 it is apparent that:

- ▲ Variations in redox conditions and pH related to water/rock interactions accompanying the recharge and subsequent flow of meteoric water could potentially cause variations in solubilities of some elements at:
  - the site scale (more oxidizing waters expected to occur at shallowe depths and nearer to recharge) ;
  - the local scale (e.g. the scale of heterogeneity of hydraulic conductivity and possibly as small as the scale of individual fractures).
- ▲ Solubilities of none-redox or pH sensitive elements are likely to show relatively little variation.
- ▲ While variations in TIC could cause variations in solubilities of some elements, systematic spatial variations in the concentration of TIC are not clear.
- ▲ Variations in salinity across the Tono area are likely to cause little variation in element solubilities.

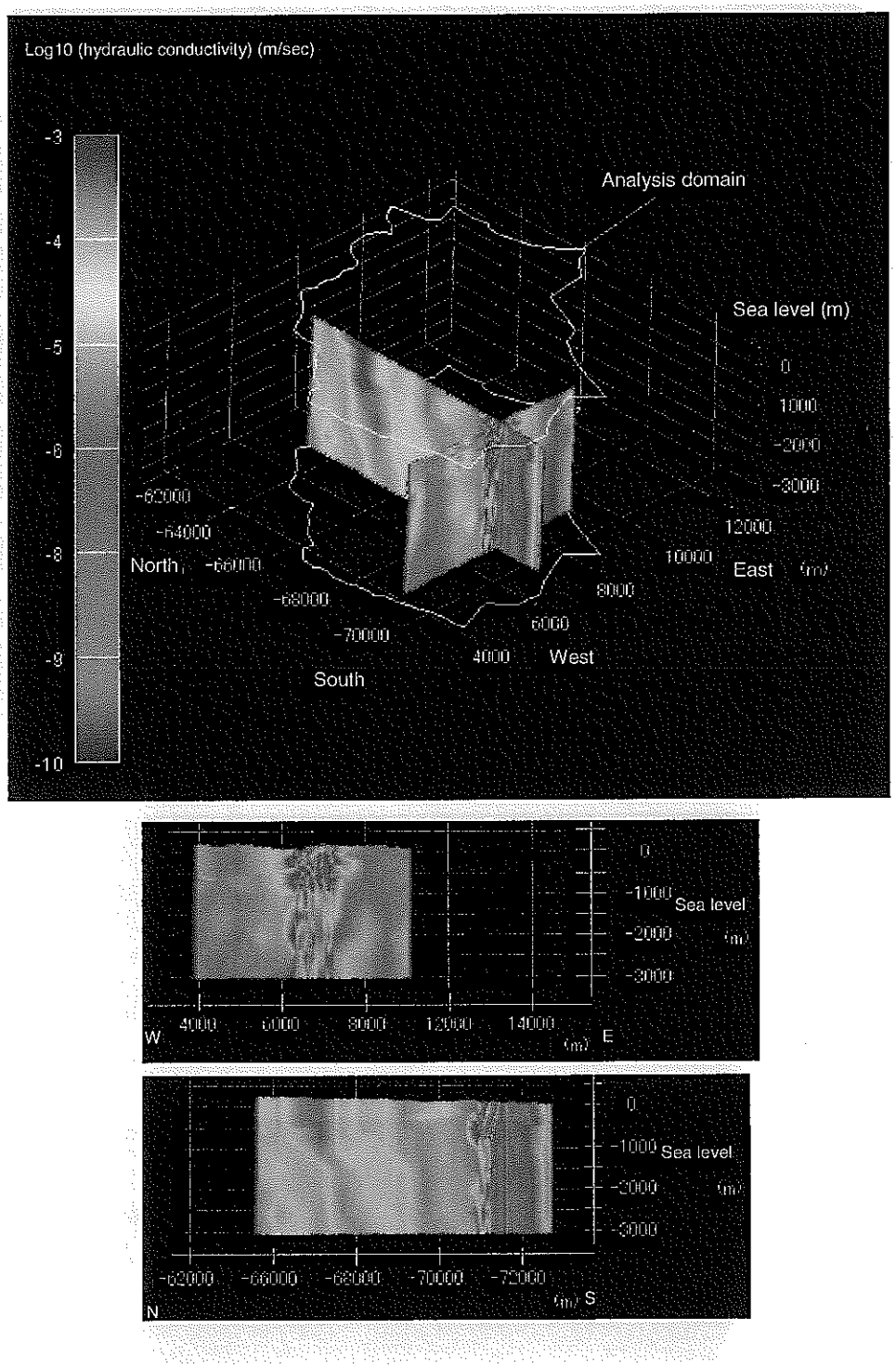

Figure 5.2-1 Permeability field around the Mizunami Underground Research Laboratory site consistent with the maximum interpreted frequency of IMFs.

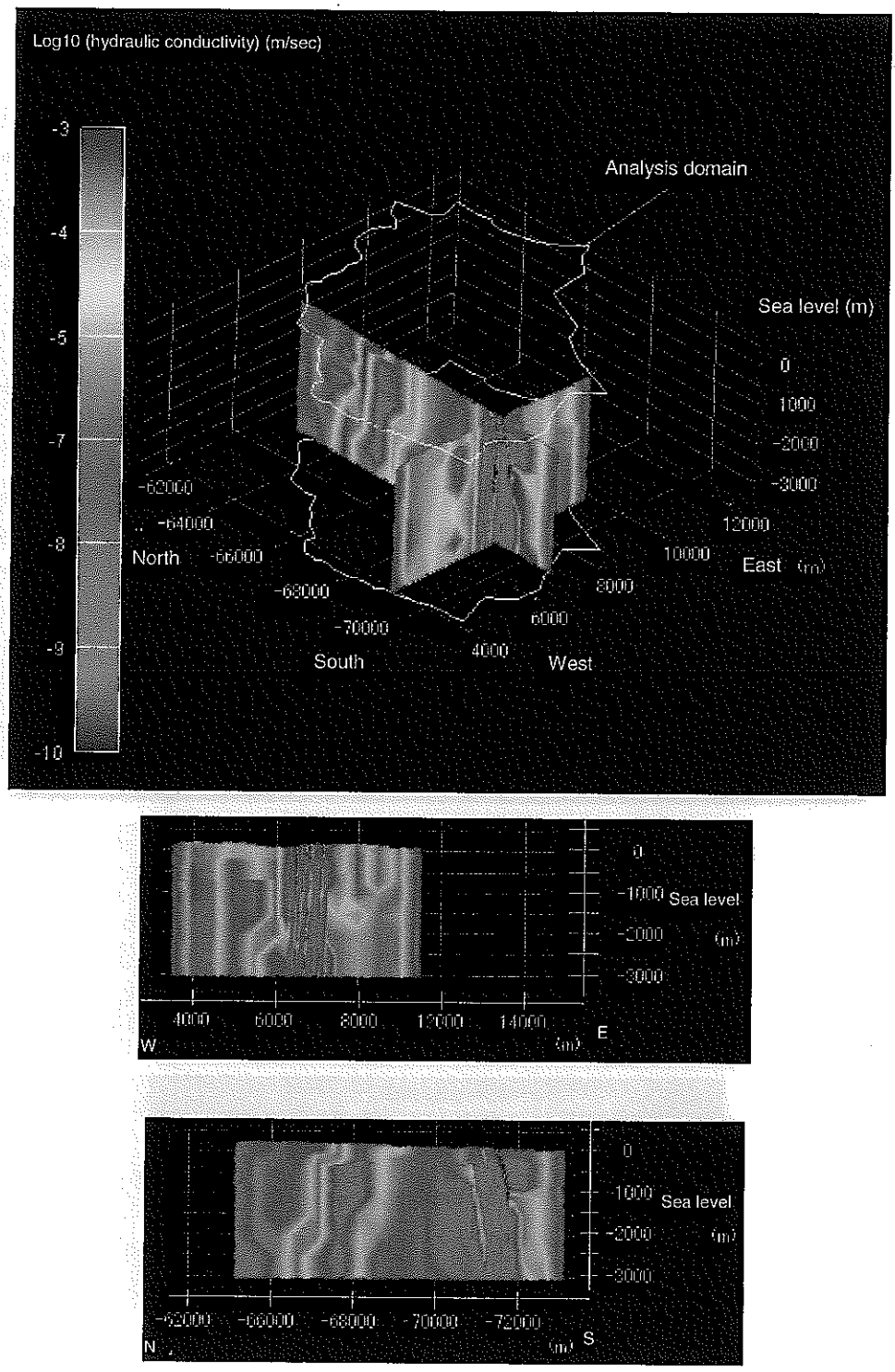

Figure 5.2-2 Permeability field around the Mizunami Underground Research Laboratory site consistent with the minimum interpreted frequency of IMFs.

- ▲ The north to south change in groundwater chemistry from Ca-Na-HCO_3^- dominated to Na-Cl dominated would have little effect if any on the solubilities of the elements.

Two approaches were used to evaluate further the significance of this chemical heterogeneity:

- ▲ Solubilities were calculated for elements in the groundwater samples listed in Table 4.2-1.

- ▲ Scoping calculations were carried out to investigate the likely significance of the observed variations in redox conditions.

A sub-set of the water compositions reported in Table 4.2-1 were used to calculate solubilities of the elements of interest. Only those compositions for which Total Inorganic Carbon (TIC) analyses are reported were used. These TIC values were used to specify the carbon content of the water, rather than reported values of HCO_3^- and CO_3^{2-}, which in fact were calculated from alkalinities. In other respects, the analyses were 'as reported'.

Many of the analyses show significant charge imbalances. Generally, these are not likely to exert a significant influence on the calculated element solubilities (Figure 4.3-77 and Figure 4.3-78). However, if there is a large charge imbalance and balancing is carried out using HCO_3^-, then there could potentially be en effect on the concentrations of those elements controlled by carbonate mineral solubility.

The results of these solubility calculations are reported in Figure 5.2-3, Figure 5.2-4, Figure 5.2-5, and Figure 5.2-6. These figures plot results from samples in and near the MIU site towards the left. Samples from the west of the Tono area are given towards the right. From these figures it can be seen that there is little evidence for a systematic variation in the solubilities of the elements across the Tono area. The high solubilities of U in the samples MSB-4/42 and MSB-2/41 are related principally to the fact that the combination of pH and Eh in these samples lie very close to the limit of UO_2(am) stability. For example, in the case of MSB-4/42, when the reported Eh is used, but pH varies, the U solubility changes from 3.86×10^{-3} molal at pH 8 to 45 molal at pH 8.8.

It is noteworthy that there is no discernible difference between solubilities calculated for groundwaters of Na-Cl type and groundwaters of Na-Ca-HCO_3 type.

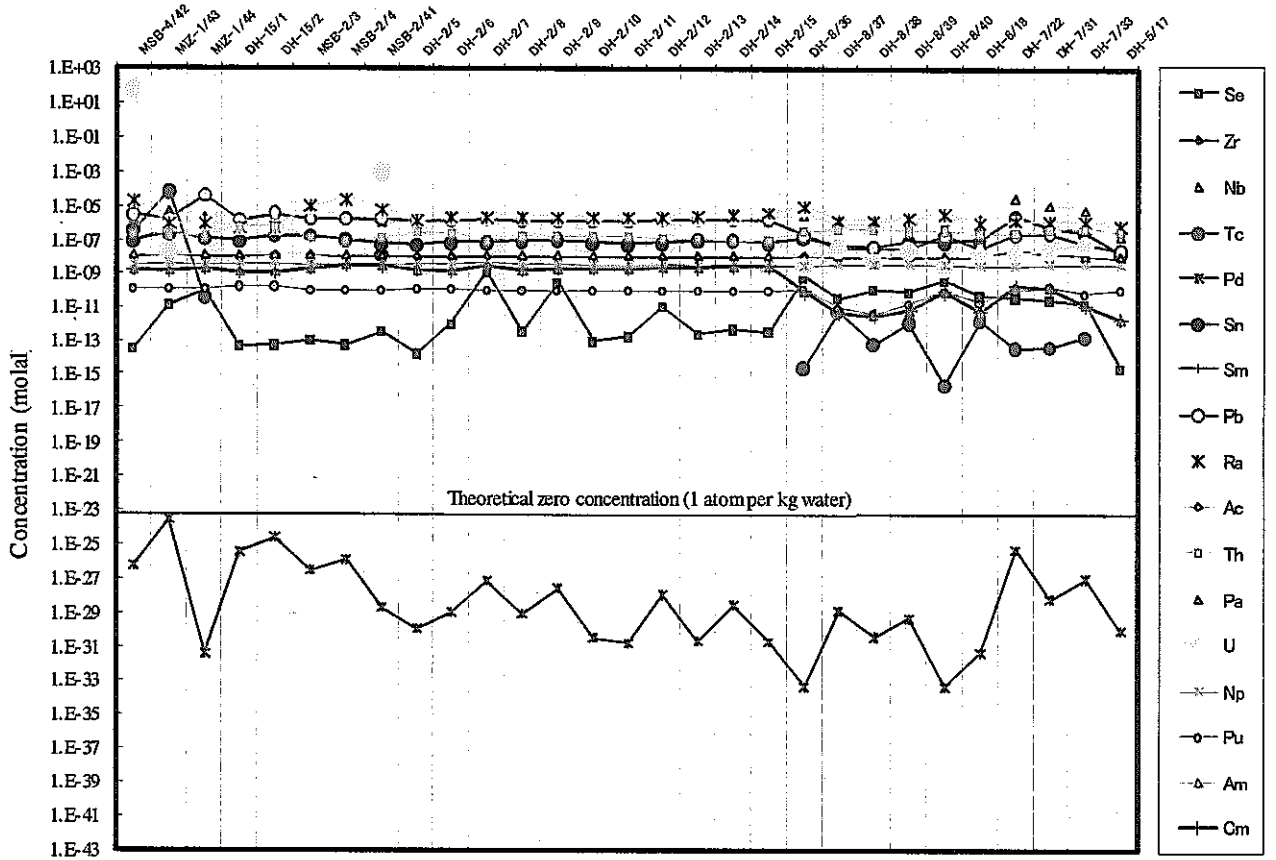

Figure 5.2-3 Summary of calculated element solubilities in the groundwaters from Table 4.2-1. Analyses used as reported and dissolved C was constrained by TIC. The numbers refer to reference numbers used in the project and given in the column at the left of Table 4.2-1.

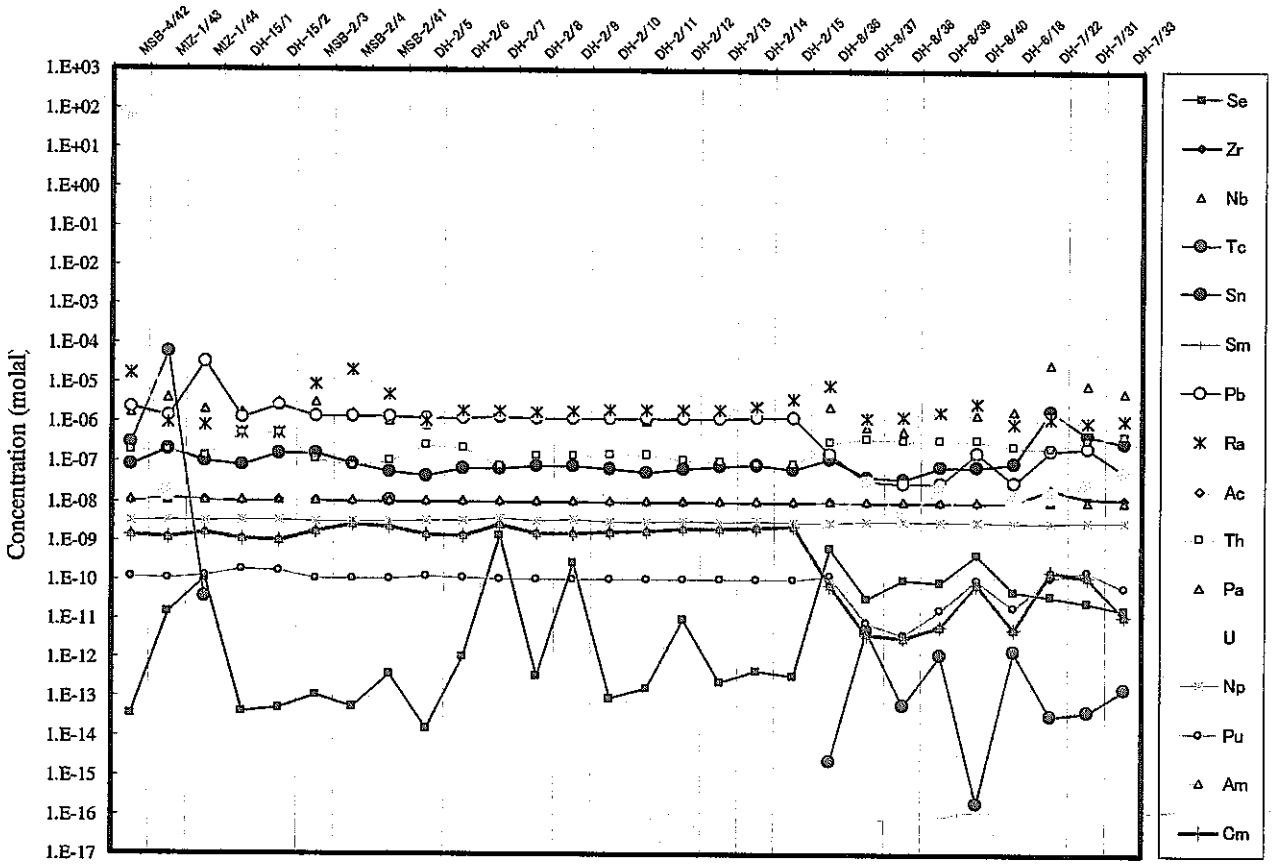

Figure 5.2-4 Summary of calculated solubilities shown in Figure 5.2-3 with an expanded concentration scale and with Pd removed.

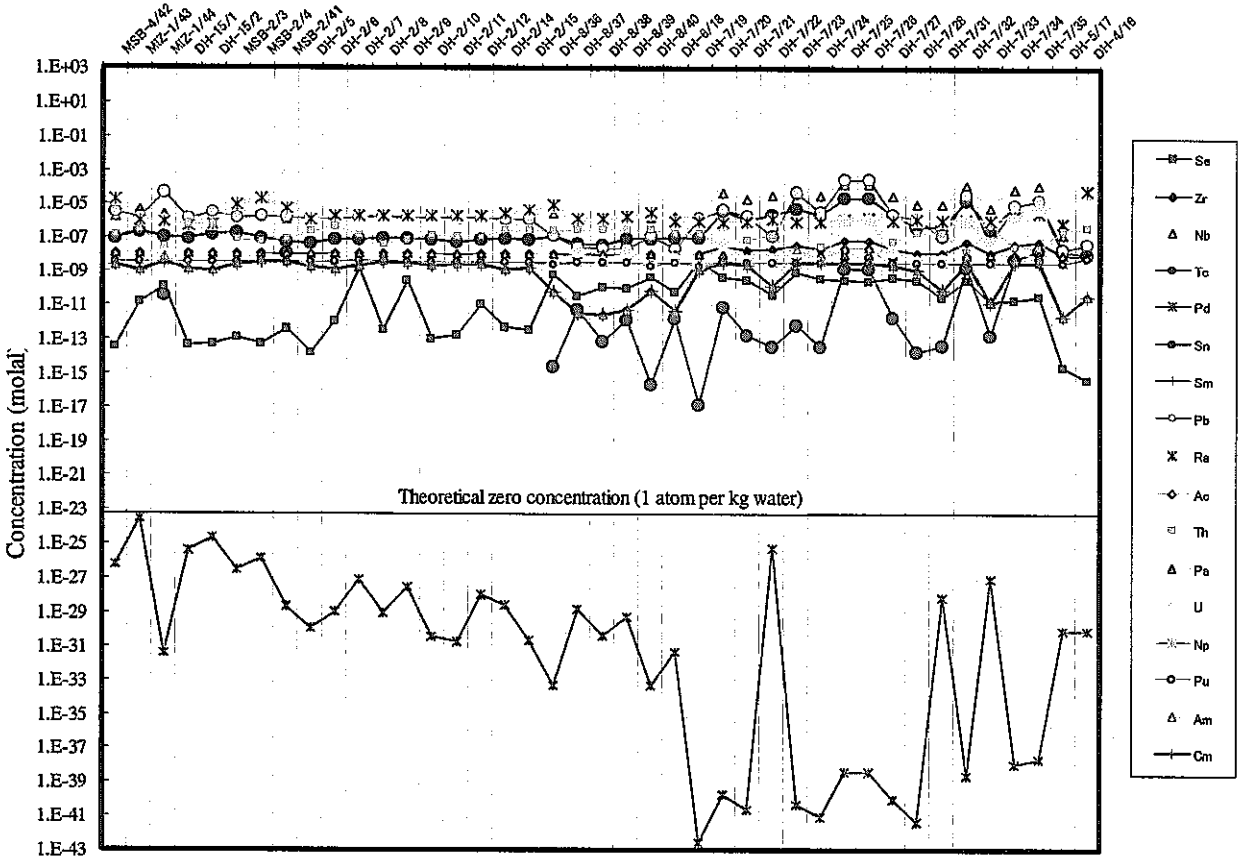

Figure 5.2-5 Summary of calculated element solubilities in the groundwaters from Table 4.2-1. Compositions charge balanced using HCO_3^-. The numbers refer to reference numbers used in the project and given in the column at the left of Table 4.2-1.

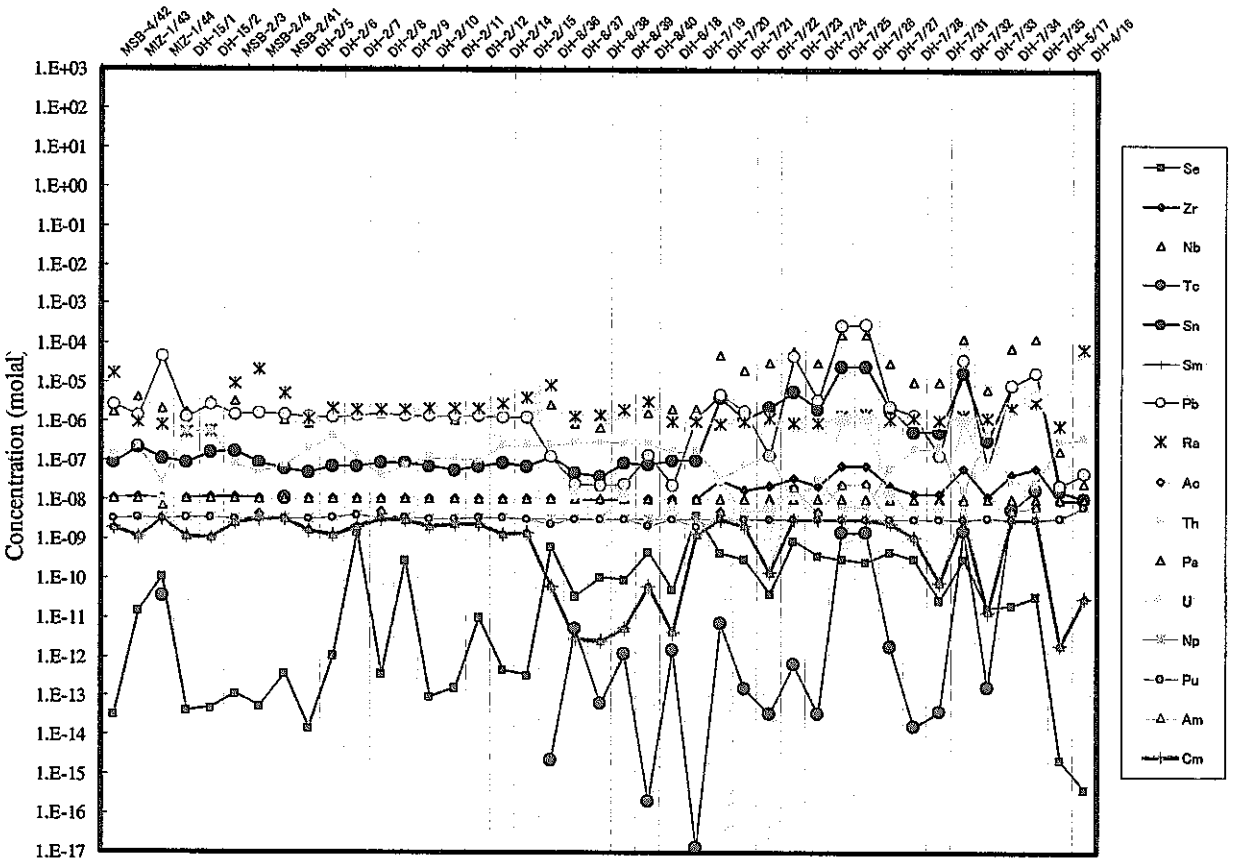

Figure 5.2-6 Summary of calculated solubilities shown in Figure 5.2-5 with an expanded concentration scale and with Pd removed.

Variations in the solubilities of elements in the groundwater samples are plotted with respect to Eh in Figure 5.2-7. Only a sub-set of the groundwaters in Table 4.2-1 are shown, because not all elements were calculated to be solubility-limited in all the waters. However, the ranges of Eh covered by the waters considered span the ranges observed in the overall Tono groundwater dataset (Figure 5.1-4).

Important observations from the plot are:

- Se, Tc and, to a lesser extend possibly Zr show a systematic trends with respect to redox variations.
- Se is generally the least soluble element in the more oxidized group of waters (to the right of the diagram).
- Tc is generally the least soluble element in the more reduced group of waters.
- The U concentrations in two samples, which are from MSB-2/41 and MSB-2/42 are high compared to the typical concentrations in other samples.
- Pa shows no change with respect to Eh; actually a very small variation was calculated, but this is negligible.
- Ac, Am and Cm vary in exactly the same way, reflecting the fact that the thermodynamic data for these elements are identical.
- Apart from Se and U there is little variation in the relative solubilities of the elements in the more oxidized groundwaters.
- Apart from Tc there is little variation in the relative solubilities of the elements in the more reduced groundwaters.

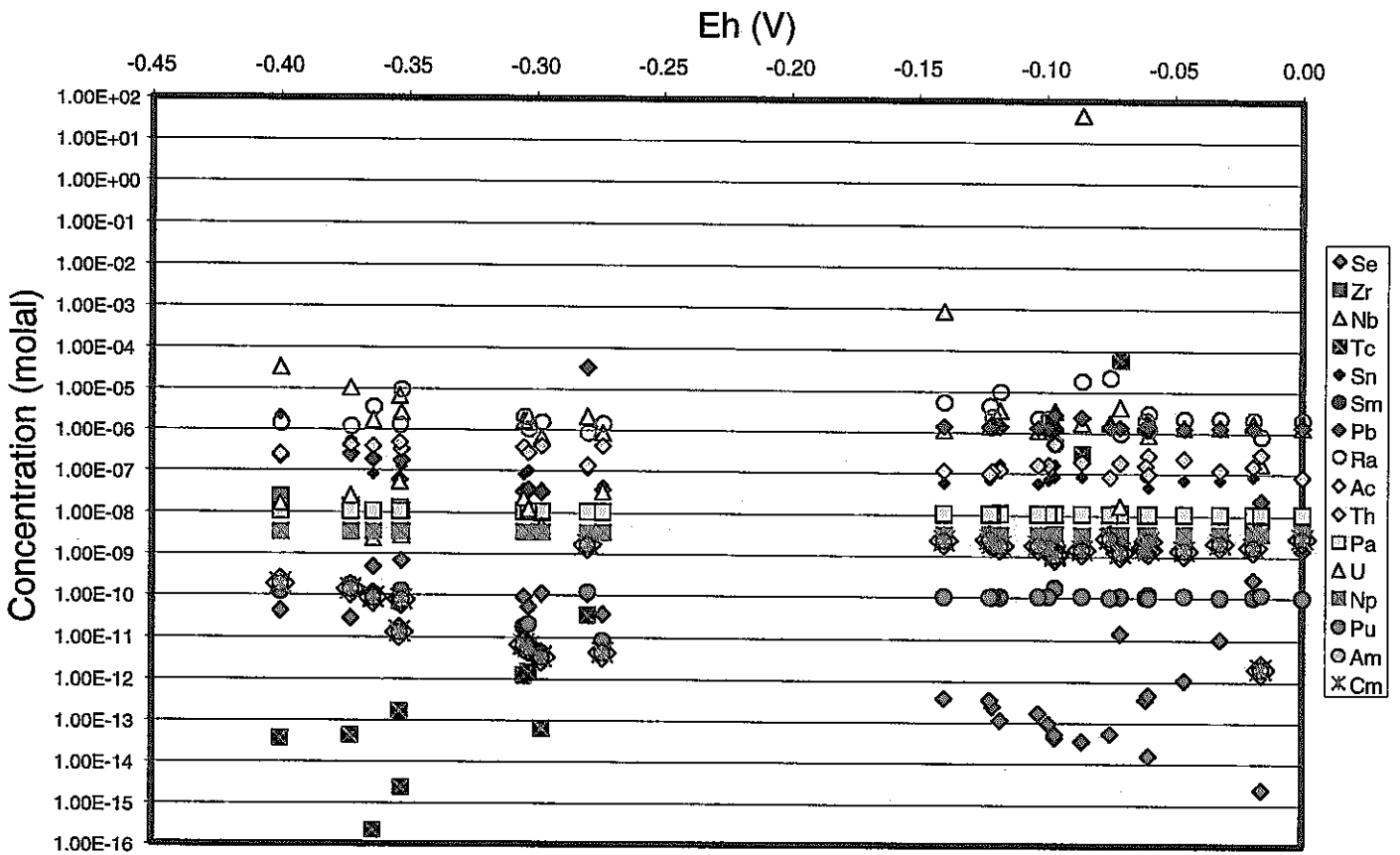

Figure 5.2-7 Solubilities of elements as a function of Eh for all the reported groundwaters in Table 4.2-1 for which solubilities of the listed elements could be calculated.

A water composition was also calculated, based on that reported for 563.75 m depth in borehole DH-7. The reported TIC was used for the dissolved C content, while the water was charge-balanced using Na^+. A series of solubility calculations were then carried out.

- Firstly, pH was initially at the reported value and Eh was varied across the range observed in Tono groundwaters.
- Secondly, Eh was initially at the reported value and pH was varied across the range observed in Tono groundwaters.

In each simulation, the water was specified to be in equilibrium with a single mineral phase as a control on the element of interest.

It is important to note that during each simulation, the pH (first case) or Eh (second case) could also vary; that is ***both pH and Eh varied in both simulations***. In essence, the first simulation is similar to adding oxygen to the water and observing what happens to the solubility; in the second case H^+ is added to the water. The Eh and pH are related through aqueous equilibria and the solution reaction of the mineral of interest.

The results are shown in Figure 5.2-8 and Figure 5.2-9.

From Figure 5.2-8 it can be seen that :

- Se (controlled by $FeSe_2$), Nb, Tc, Pd, Sn, Sm, Pb, Ac, U, Nb, Pu, Am and Cm all show concentration variations greater than 0.5 order of magnitude in response to changes pH and/or Eh.
- Zr, Th and Pa show variations that are smaller than 0.5 order of magnitude and are relatively insensitive to changes in pH and Eh.
- Nb, Sn, Sm, Pb, Ac (if controlled by $AcOHCO_3$ solubility), Pu (if controlled by PuO_2(am)) Am, and Cm concentrations are all more sensitive to pH variations than to Eh variations.
- Se (if controlled by $FeSe_2$), Tc, Pd, U, Np, and Pu (if controlled by $PuPO_4$) are all more sensitive to Eh variations than to pH variations.
- Pa solubility shows almost no variation when Eh or pH varies.
- The largest variations caused by Eh fluctuations are concentrations of Pd (16 orders of magnitude), Se, Tc (10 orders of magnitude), and U (6 orders of magnitude).

- ▲ In contrast, the largest variation caused by pH fluctuations is in the order of 3, in the case of Nb; Sn shows a fluctuation in the order of 2.5; Sm, Ac, Pu, Am, and Cm show variations in the order of 1.5.

Figure 5.2-8 does not show Ra because concentrations of this element are directly sensitive only to concentrations of SO_4, since the solubility-controlling mineral is $RaSO_4$. However, it is noted that variations in pH and/or redox could potentially cause the concentration of SO4 to vary, which could in turn affect the solubility of Ra.

The overall conclusions that can be drawn by evaluating the solubility diagrams in Section4.3.2 together with the solubilities calculated in this section:

- Chemical variations in the deep groundwater system (where dissolved oxygen is absent) would not cause systematic variations in element solubilities at the scale of the Tono area.

- Potentially, near to recharge, any variations in redox conditions could cause significant differences in solubilities compared to the solubilities calculated for the sampled groundwaters considered here.

- Significant variations in solubilities of redox and pH-sensitive elements could potentially occur at the local scale (scale of permeability variations), related to the heterogeneous distribution of hydraulically-conductive fractures and the invasion of oxidizing groundwater.

- The size of these variations will depend upon the coupling between reactions controlling redox and pH and will reflect partly the relative rates of these reactions. However, generally:
  - Redox variations will cause greater perturbations than pH variations.
  - Concentrations of Pd, Se, Tc and U are most likely to be affected by local chemical heterogeneity in the rock mass related to the invasion of oxygenated water.

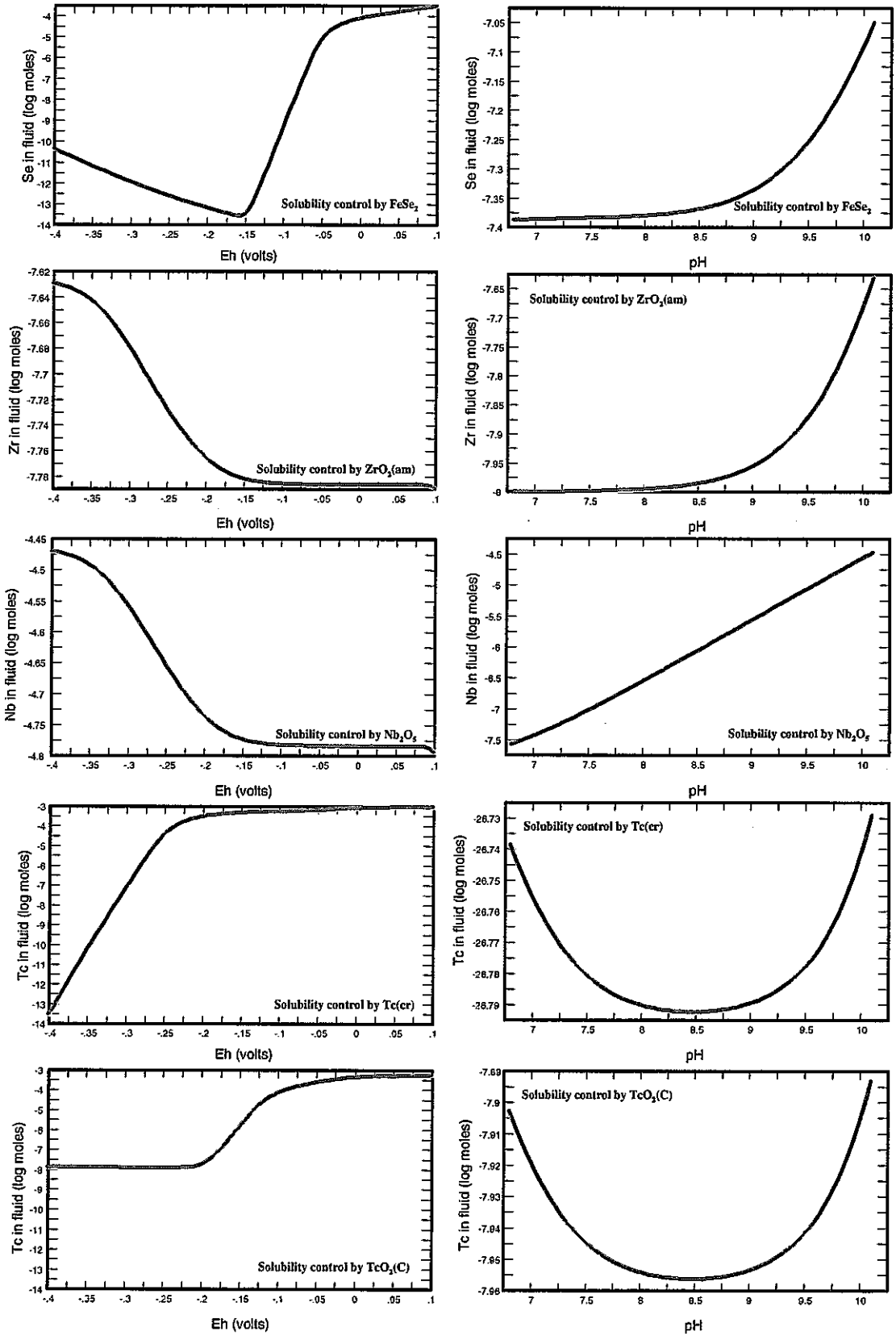

Figure 5.2-8 Relationships between element concentrations, Eh and pH for a water composition based on that from DH-7, depth of 563.75 m. The composition is mostly as reported with dissolved carbon specified by TIC. However, Na^+ is

47.14 mg/l to ensure charge balance. The observed ranges of Eh and pH are presented.

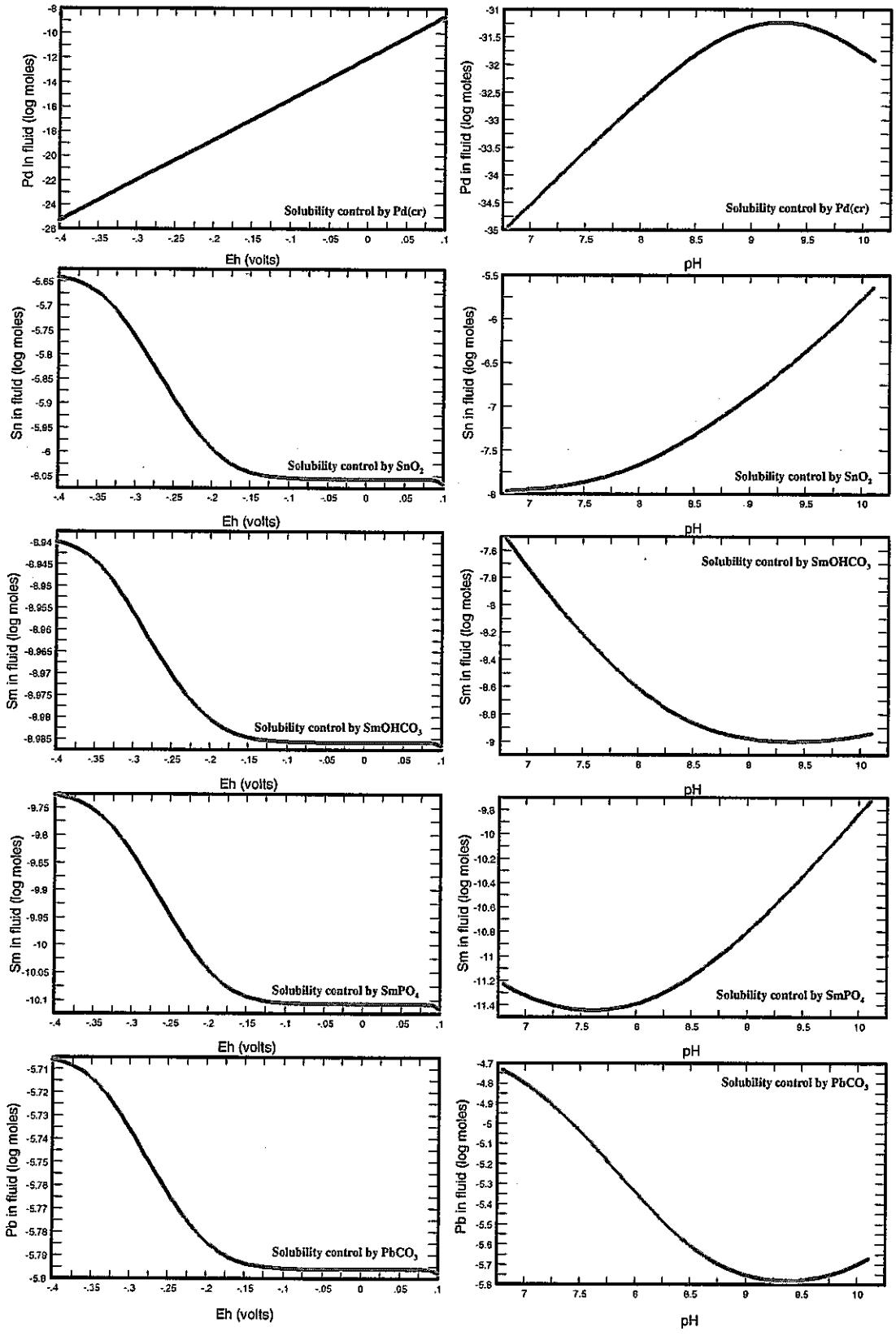

Figure 5.2.8 Continued.

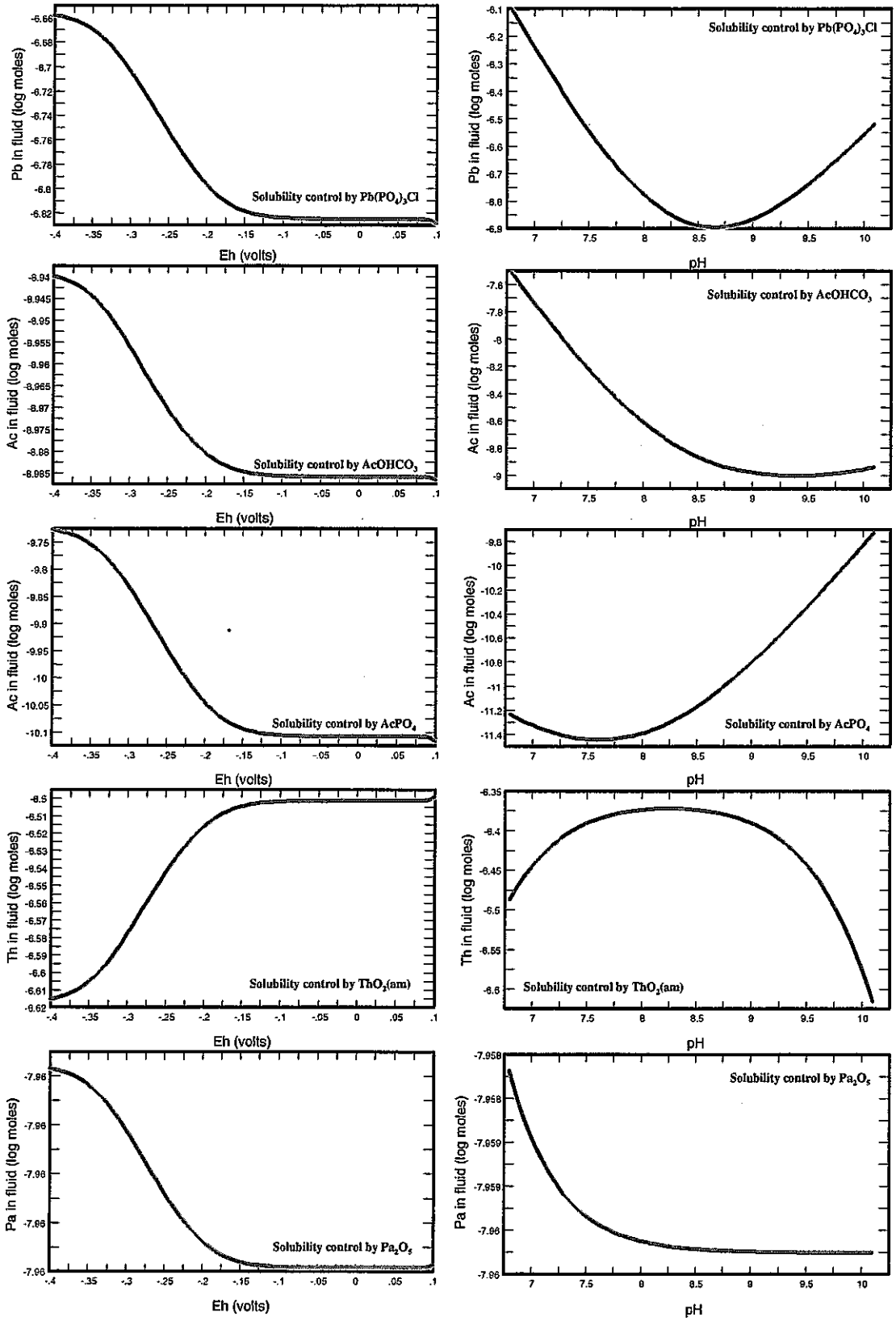

Figure 5.2.8 Continued.

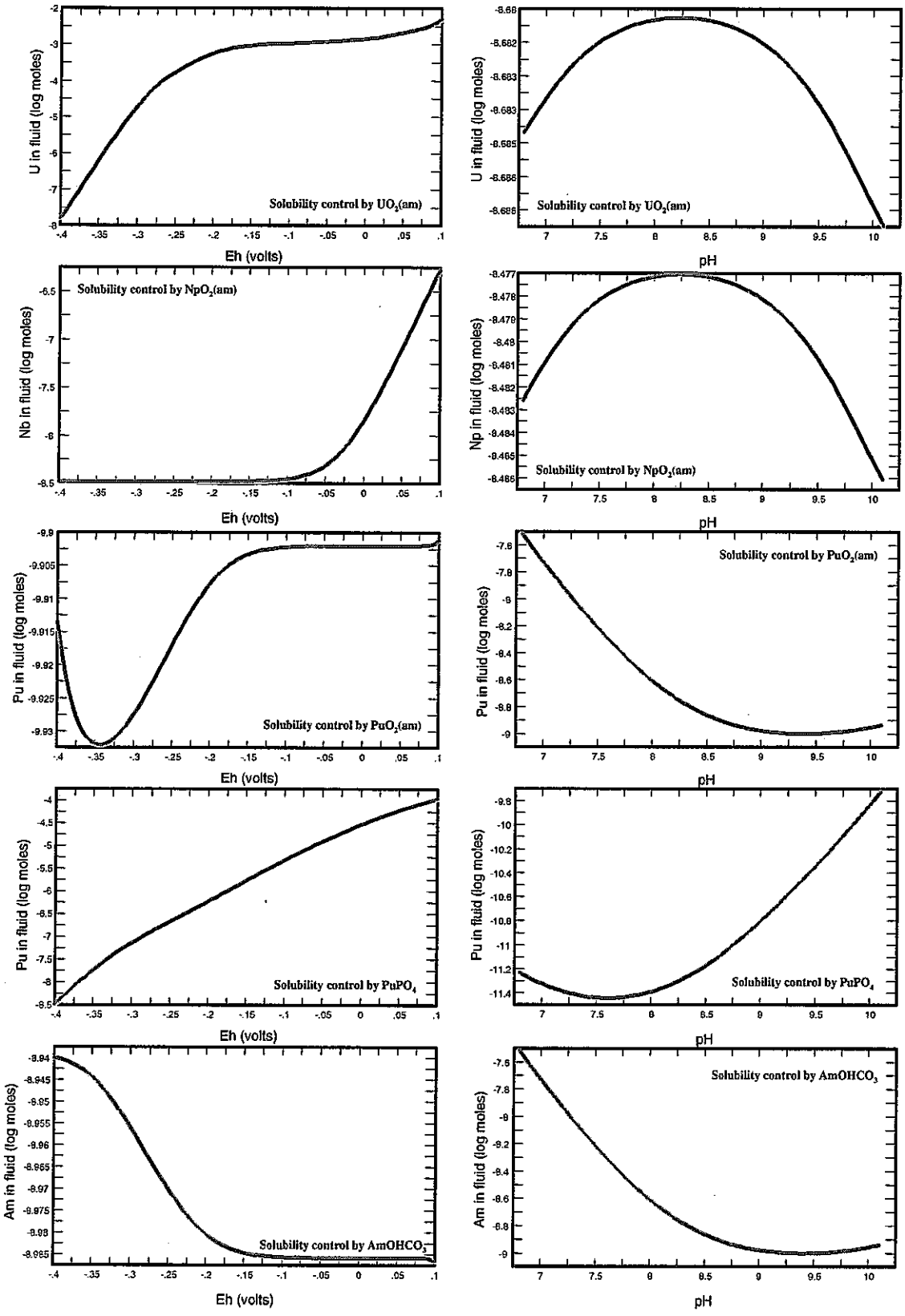

Figure 5.2.8 Continued.

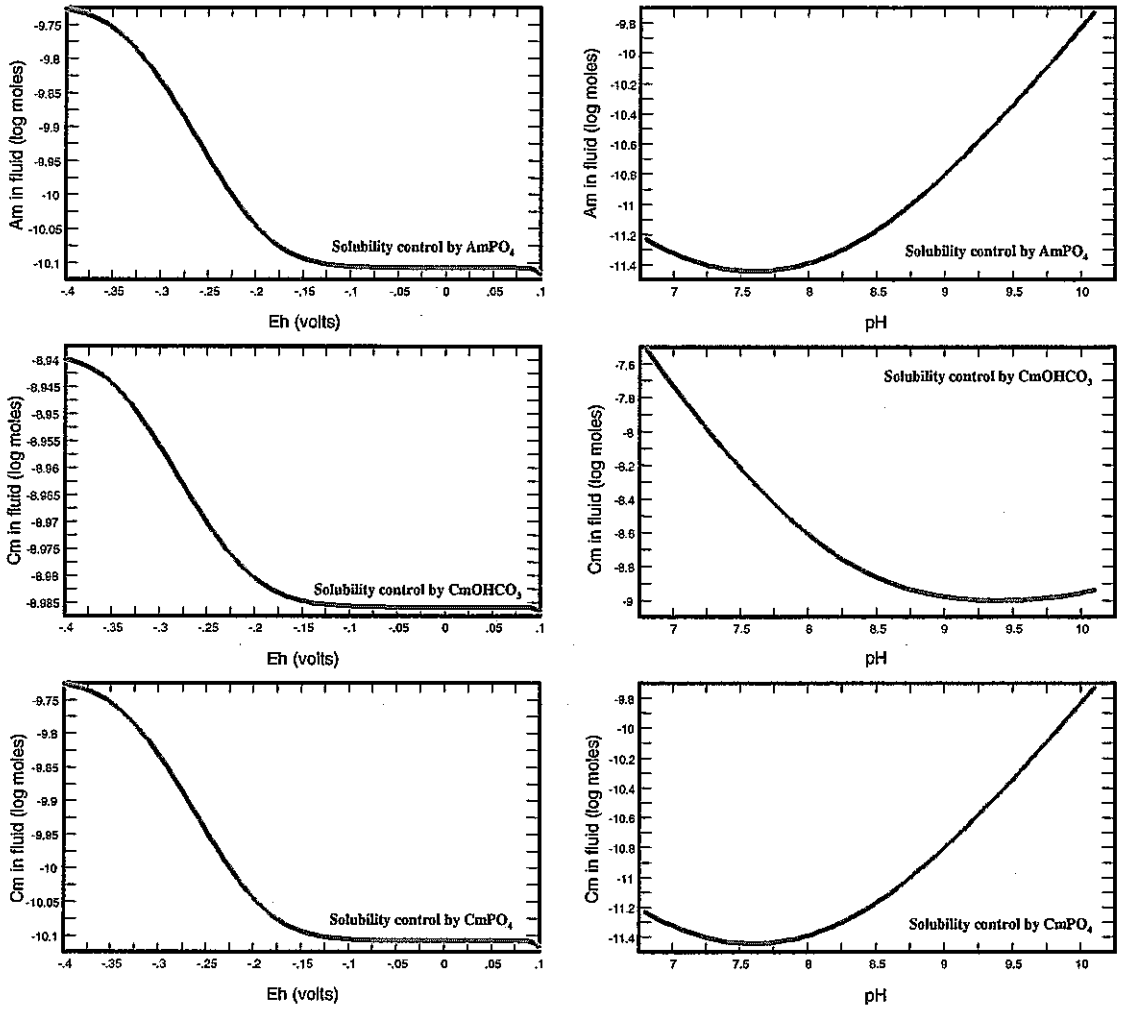

Figure 5.2.8 Continued.

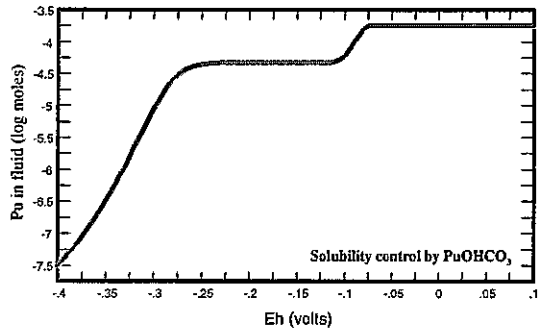

Figure 5.2-9 Relationship between Pu concentration and Eh for a water composition based on that from DH-7, depth of 563.75 m. The composition is the same as reported except that pH is 6.8, the lowest value reported for the samples in Table 4.2-1. Dissolved carbon is specified by TIC Na^+ is set to 47.14 mg/l to ensure charge balance. The observed range of Eh is represented.

6 Geochemical uncertainty over PA time scales

PA typically considers timescales of several hundreds of thousands of years to around 1 Ma. During such long time intervals groundwater conditions can change considerably. Climate change is a major factor controlling these changes. Variations in climate may cause:

- Changes in precipitation
- Changes in temperature
- Changes in vegetation
- Changes in sea level

These factors may all influence, directly or indirectly, the rate of invasion of oxygenated groundwater. Any redox variations that are caused in the deep sub-surface as a result could potentially influence the solubilities of redox-sensitive minerals, as discussed in Section 5.

Uplift or subsidence, which in Japan are likely to be driven principally by tectonic processes (c.f. northern Europe or northern North America where glaciation and deglaciation are usually the main causes of subsidence and uplift) may also exert an influence. Dilation or sealing of fractures as a consequence of such tectonic variations could conceivably influence the distribution of oxygenated water.

7 Evaluation of calculation results

The calculations have several important implications for site investigations:

- redox and pH are the two parameters that will have a major control on the solubilities of certain elements of interest.
- Trace quantities of PO_4^{3-} could control the solubilities of some elements.
- Alkalinities, carbonate contents and pH are inconsistent in many of the samples. This leads to considerable uncertainties in the solubilities of some elements.
- The constituent NH_4^+ may have an indirect effect on calculated solubilities owing to its influence on alkalinities. It is important to measure this determinand in the Tono groundwaters.

Consequently, future investigations should make sure that these parameters are determined to an adequate standard.

Future evaluations of data quality should not consider specific chemical parameters independently and should recognise that quality indicators are not strictly additive. That is, a high quality analysis does not, for example, compensate for a highly contaminated sample.

References

Alaux-Negrel G, Beaucaire C, Michard G, Toulhoat P, Ouzounian G, 1993. Trace metal behaviour in natural granitic waters. Journal of Contaminant Hydrology 13, 309-325.

Arthur, R.C. 2003. Empirical constraints on theoretical models of the chemical evolution of groundwaters in the Tono area. JNC TJ7400 2003-007.

Baes C.F. and Mesmer R.E, 1976. The Hydrolysis of Cations. New York. John Wiley and Sons.

Barrett, T.J. and Anderson, G.M. 1988. The solubility of sphalerite and galena in 1-5 m NaCl solutions to 300 °C. Geochimica et Cosmochimica Acta 52: 813-820.

Berner U, 1994. Estimates of solubility limits for safety relevant radionuclides. NTB 94-08.

Bethke, C.M. 1996. Geochemical reaction path modeling. Oxford University Press. Oxford. 397pp.

Bockris J.O.M, Ed., 1977. Environmental Chemistry. New York, Plenum Press.

Brookins D.G, 1988. Eh-pH Diagrams for geochemists. New York. Springer-Verlag Pubs.

Brookins D.G, 1989. Aqueous Geochemistry of Rare Earth Elements in Geochemistry and Mineralogy of Rare Earth Elements (B.R. Lipin and G.A. McKay, Eds.). Blacksburg. Mineralogical Society of America. Reviews in Mineralogy, Vol. 21.

Bruno J, Cross J.E, Eikenberg J, McKinley I.G, Read D, Sandino A, Sellin P, 1992. Testing models of trace element geochemistry at Poços de Caldas. Journal of Geochemical Exploration 45, 451-470.

Bruno J., Casas I, 1994. Spent fuel dissolution modelling. in Final Report of SKB/AECL Cigar Lake Analogue Study (J.J. Cramer and I.A.T. Smellie, Eds.). SKB-AECL Technical Report TR 94-04 (10851).

Bruno J., Sellin P, 1992. Radionuclide solubilities to be used in SKB 91. SKB 92-13.

Byrd J.T, Andreae M.O, 1986. Geochemistry of tin in rivers and estuaries. Geochimica et Cosmochimica Acta 50: 835-845.

Caballero E, Reyes E, Huertas F, Yanez J, Linares J, 1986. Elementos traza en las bentonitas de Almeria. Boletin Sociedad Espanola de Mineralogia 9, 63-70.

Calvert S.E. and Piper D.Z, 1984. Geochemistry of ferromanganese nodules from DOMES Site A, northern equatorial Pacific; multiple diagenetic metal sources in the deep sea. Geochimica et Cosmochimica Acta 48, 1913-1928.

Carpenter, A.B., Trout, M.L. and Pickett, E.E. 1974. Preliminary report on the origin and chemical evolution of lead- and zinc-rich oil field brines in central Mississippi. Economic Geology, 69, 1191-1206.

Choppin G.R, Stout B.E, 1989. Actinide behaviour in natural waters. The Science of the Total Environment 83, 203-216.

Copenhaver S.A, Krishnaswami S.L, Turekian K.K, Epler N, Cochran J.K, 1993. Retardation of ^{238}U and ^{232}Th decay chain radionuclides in Long Island and Connecticut aquifers. Geochimica et Cosmochimica Acta 57, 597-603.

Cramer J, Vilks P, Miller H, Bachinski D, l994. Hydrogeochemistry: Water sampling and analysis. In Final Report of SKB/AECL Cigar Lake Analogue Study (J.J. Cramer and J.A.T. Smellie, Eds.). SKB-AECL. Technical Report TR 94-04 (10851).

Cutter, G.A. 1989. Selenium in fresh water systems. In: Occurrence andDistribution of Selenium (M. Ihnat, ed.). CRC Press, Florida, Chap. 10.

Dickson B.L, 1985. Radium isotopes in saline seepages, southwestern Yilgarn, Western Australia. Geochimica et Cosmochimica Acta 49, 349-360.

Doerner H.A, Hoskins W.M, 1925. Co-precipitation of radium and barium sulphates. Journal of the American Chemical Society 47, 662-675.

Doyle G.A, Lyons W.B, Miller G.C, Donaldson S.G, 1995. Oxyanion Concentrations in Eastern Sierra Nevada Rivers. I. Selenium. Applied Geochemistry 10:5, 553-564.

Edmunds W.M, Cook J.M, Kinniburgh D.G, Miles D.G, Trafford J.M, 1989. Trace-element occurrence in British groundwaters. British Geological Survey Research Report SD189/3. Nottingham.

Edmunds W.M, Cook J.M., Miles D.L, Cook J.M, 1987. The origin of saline groundwaters in the Carnmenellis granite (U.K.): further evidence from minor and trace elements. In Saline Water and Gases in Crystalline Rocks (P. Fritz and S.K. Frape, Eds.). Geological Association of Canada Special Paper 33, pp 127-143.

Elderfield H, Upstill-Goddard R, Sholkovitz E.R, 1990. The rare earth elements in rivers, estuaries, and coastal seas and their significance to the composition of ocean waters. Geochimica et Cosmochimica Acta 54, 971-991.

Elderfield H., Greaves M., 1989. The rare earth elements in seawater. Nature 296: 5854, 214-219.

Elkin E.M, 1982. Selenium and selenium compounds. In Encyclopaedia of Chemical Technology Volume 20, John Wiley & Sons, New York.

Erel, Y. and Morgan, J.J. 1992. The relationships between rock-derived lead and iron in natural waters. Geochimica et Cosmochimica Acta, 56, 4157-4167.

Erel, Y., Morgan, J.J. and Patterson, C.C. 1991. Natural levels of lead and cadmium in a remote mountain stream. Geochimica et Cosmochimica Acta 55: 707-719.

Fabryka-Martin J, Curtis D.B, Dixon P, Rokop D, Roensch F, Aguilar R., Attrep M, 1994. Nuclear reaction product geochemistry: Natural nuclear products in the Cigar Lake deposit. In Final Report of SKB/AECL Cigar Lake Analogue Study (J.J. Cramer and J.A.T. Smellie, Eds.). SKB-AECL. Technical Report TR 94-04 (10851).

Fukai R, Yokoyama Y, 1982. Natural Radionuclides in the Environment. In The Handbook of Environmental Chemistry. The Natural Environment and the Biogeochemical Cycles (O. Hutzinger, Ed.). Springer-Verlag Berlin Heidelberg. Vol. I.

Gauthier-Lafaye F, 1995. Oklo, Analogues naturels. Rapport final: Volume 2: Les Reacteurs de Fission et les Systemes Geochimiques. 2eme partie: Geologie des reacteurs, etudes des epontes et des transferts anciens. Institut de Protection et de Surete Nucleaire. Oklo-Rapport final 2-2. Strasbourg.

Gosselin D.C, Smith M.R, Lepel E.A, Laul J.C, 1992. Rare earth elements in chloride-rich groundwater, Palo Duro Basin, Texas, USA. Geochimica et Cosmochimica Acta 56, 1495-1505.

Grauch R.I, 1989. Rare Earth Elements in Metamorphic Rocks. In Geochemistry and Mineralogy of Rare Earth Elements (B.R. Lipin and G.A. McKay, Eds.). Blacksburg. Mineralogical Society of America. Reviews in Mineralogy. Vol. 21.

Hama, K., Kunimaru, T. and Amano, K. 2000. Compilation of data from field and laboratory activities (DH-7), May 1997 – July 1998. JNC Report JNC TN7450 2000-001.

Howard J.H, 1977. Geochemistry of selenium: formation of ferroselite and selenium behaviour in the vicinity of oxidising sulphide and uranium deposits. Geochimica et Cosmochimica Acta 41, 1665-1678.

Ikeda N, 1955. Determination of minute quantities of tin in hot spring waters. Nippon Kagaku Zassi 76, 1011.

Iwatsuki, T. and Yoshida, H. 1999. Characterising the chemical containment properties of the deep geosphere: water-rock interactions in relation to fracture systems within deep crystalline rock in the Tono area, Japan. In: Metcalfe, R. and Rochelle (eds) Chemical containment of wastes in the geosphere. Geological Society of London Special Publications, 157, pp 71 - 84.

JNC 2000. H12:Project to Establish the Scientific and Technical Basis for HLW Disposal in Japan. TN1410 2000-001～2000-004

JNC 2003. 高レベル放射性廃棄物の地層処分技術に関する研究開発。平成14年度報告書。JNC TN1400 2003-004.

Kharaka, Y.K., Lico, M.S., Wright, V.A. and Carothers, W.W. 1980. Geochemistry of formation waters from Pleasant Bayou No 2 well and adjacent areas in coastal Texas. Proceedings of Geopressured-Geothermal Energy Conference Austin, Texas, 1980, pp 168-193.

Kraemer T.F, Kharaka Y.K, 1986. Uranium geochemistry in geopressured-geothermal aquifers of the U.S. Gulf Coast. Geochimica et Cosmochimica Acta 50, l233-1238.

Kraemer T.F, Reid D.F, 1984. The occurrence and behaviour of radium in saline formation water of the U.S. Gulf Coast region. Isotope Geoscience 2, 153-174.

Krauskopf K.B, 1967. Introduction to Geochemistry. McGraw-Hill, New York.

Krishnaswami S, Graustein W.C, Turekian K.K, 1982. Radium, thorium and radioactive lead isotopes in groundwaters: applications to the in situ determination of absorption-desorption rate constants and retardation factors. Water Resources Research 18, 1633-1675.

Langmuir D, Herman J.S, 1980. The mobility of thorium in natural waters at low temperatures. Geochimica et Cosmochimica Acta 44, 1753-1766.

Langmuir D, Melchior D, 1985. The goechemistry of Ca, Sr, Ba and Ra sulfates in some deep brines from the Palo Duro Basin, Texas. Geochimica et Cosmochimica Acta 49, 2423-2432.

Langmuir D, Riese A.C, 1985. The thermodynamic properties of radium. Geochimica et Cosmochimica Acta 49, 673-680.

Laul J.C, Smith M.R, Hubbard N, 1985a. $^{234}U/^{230}Th$ ratio as an indicator of redox state and U, Th and Ra behaviour in briney aquifers. Mater. Res. Soc. Symp. Proceedings MRS Vol. 44, 475-482.

Laul J.C, Smith M.R, Hubbard N, 1985b. Behaviour of natural uranium, thorium and radium isotopes in the Wolfcamp brine aquifers, Palo Duro Basin, Texas. Materials Research Society Proceedings 44, 475-482.

Liang, J-J. and Sherriff, B.L. 1993. Lead exchange into zeolite and clay minerals: a ^{29}Si, ^{27}Al, ^{23}Na solid-state NMR study. Geochimica et Cosmochimica Acta 57: 3885-3894.

Lloyd J.W, Heathcote J.A, 1985. Natural inorganic hydrochemestry in relation to groundwater An Introduction. Oxford. Oxford University Press.

MacKenzie A.B, Scott R.D, Linsalata P, Miekeley N, Osmond J.K, Curtis D.B, 1991. Natural radionuclide and stable element studies of rock samples from the Osamu Utsumi mine and Morro do Ferro analogue study sizes, Poços de Caldas, Brazil. SKB. Poços de Caldas Report 7.

Mazor E, 1962. Radon and radium content of some Israeli water sources and a hypothesis on underground reservoirs of brines, oils and gases in the Rift valley. Geochimica et Cosmochimica Acta 26, 706-786.

McKelvey B.A, Orians K.J, 1993. Dissolved zirconium in the North Pacific Ocean. Geochimica et Cosmochimica Acta 57, 3801-3805.

McLennan S.M, 1989. Rare Earth Elements in Sedimentary Rocks: Influence of Provenance and Sedimentary Processes. In Geochemistry and Mineralogy of Rare Earth Elements (B.R. Lipin and G.A. McKay, Eds.). Blacksburg. Mineralogical Society of America. Reviews in Mineralogy. Vol. 21.

Metcalfe, R., Savage, D., Benbow, S.J., Takase, H., Noguchi, T., Guimerà, J., Ruiz, E., Luna, M., Arcos, D., and Jordana, S. 2003. A coupled geochemical/hydrogeological model of the Tono area. Quintessa Report to JNC.

Michard A, Beaucaire C, Michard G, 1987. Uranium and rare-earth elements in CO_2 rich waters from Vals-les-Bains (France). Geochimica et Cosmochimica Acta 51, 901-909.

Michel J, Moore W.S, 1980. ^{228}Ra and ^{226}Ra content of groundwater in Fall Line aquifers. Health Physics 38, 663-671.

Miller W.M, Smith G.M, Towler P.A, Savage D, 1994. Natural elemental mass movement in the vicinity of the Aspo Hard Rock Laboratory. Intera Information Technologies IG3427-2. Melton.

Möller P, Dulski P, Szacki W, Malow G, Riedel E, 1988. Substitution of tin in cassiterite by tantalum, niobium, tungsten, iron and manganese. Geochimica et Cosmochimica Acta 52, 1497-1503.

Nordstrom D.K, Smellie J.A.T, Wolf M, 1991. Chemical and isotopic composition of groundwaters and their seasonal variability at the Osamu Utsumi and Morro do Ferro analogue study sizes, Poços de Caldas, Brazil. SKB. Poços de Caldas Report 6.

Ota, K. and Hanamuro, T. 1996. Tono Natural Analogue Project (TAP). Data compilation of field and lab activities, June 1995 – May 1996. Technical Note 96-01.

Oudin E. and Cocherie A, 1988. Fish debris record the hydrothermal activity in the Atlantis II deep sediments (Red Sea). Geochimica et Cosmochimica Acta 52, 177-184.

Paige, C.R., Kornicker, W.A., Hileman, O.E. and Snodgrass, W.J. 1992. Modelling solution equilibria for uranium ore processing: The $PbSO_4$-H_2SO_4-H_2O and $PbSO_4$-Na_2SO_4-H_2O systems. Geochimica et CosmochimicaActa 56: 1165-1173.

Paige, C.R., Kornicker, W.A., Hileman, O.E. and Snodgrass, W.J. 1993. Study of the dynamic equilbrium in the $BaSO_4$ and $PbSO_4$/aqueous solution systems using $^{133}Ba^{2+}$ and $^{210}Pb^{2+}$ as radiotracers. Geochimica et Cosmochimica Acta 57, 4435-4444.

Parkhurst, D.L. and Appelo, C.A.J. 1999. User's guide to PHREEQC (Version 2) – A computer program for speciation, batch-reaction, one-dimensional transport and inverse geochemical calculations. United States Geological Survey, Water-Resources Investigations Report 99-4259. 312pp.

Pentcheva, G. 1965. The distribution of rare and dispersed elements in Bulgarian saline underground waters. Comptes Rendus de l'Academie Bulgare des Sciences 18: 149-152.

Rittenhouse G, Fulton R.B, Grabowski R.J, Bernard J.L, 1969. Minor elements in oilfield waters. Chemical Geology 4, 189.

Salvi S, Williams-Jones A.E, 1990. The role of hydrothermal processes in the granite-hosted Zr, Y, REE deposit at Strange Lake, Quebec/Labrador: evidence from fluid inclusions. Geochimica et Cosmochimica Acta 54, 2403-2418.

Santschi P.H, Bajo C, Mantovani M, Orciuolo D, Cranston R.E. Bruno J, 1988. Uranium in pore waters from North Atlantic (GME and Southern Nares Abyssal Plain) sediments. Nature Vol. 331, (6152) 155-157.

Sebesta F, Sedlacek J, John J, Sandrik R, 1981. Behaviour of radium and barium in a system including uranium mine waste waters and adjacent surface waters. Environmental Science and Technology 15, 71-75.

Seward, T.M. 1984. The formation of lead (II) chloride complexes to 300 °C: a spectrophotometric study. Geochimica et Cosmochimica Acta, 48, 121-134.

Shanbhag P.M, Morse J.W, 1982. Americium Interaction with Calcite and Aragonite Surfaces in Seawater. Geochimica et Cosmochimica Acta 46, 241-246.

Short S.A, Lowson R.T, 1988. $^{234}U/^{238}U$ and $^{230}Th/^{234}U$ activity ratios in the colloidal phases of aquifers in lateritic weathered zones. Geochimica et Cosmochimica Acta 52, 2555-2563.

Siu K.W.M, Berman S.S, 1989. The marine environment. In Occurrence and Distribution of Selenium (M. Ihnat, Ed.). CRC Press, Boca Raton, pp 263-293.

Smedley P.L, 1991. The geochemistry of rare earth elements in groundwater from the Carnmenellis area, southwest England. Geochimica et Cosmochimica Acta 55, 2767-2779.

Smellie J, Cramer J, Mac.Kenzie A, 1994. Mineralogy and Lithogeochemistry: Geochemical and isotopic features of the host sandstones and clay halo. In Final Report of SKB/AECL Cigar Lake Analogue Study (J.J. Cramer and J.A.T. Smellie, Eds.). SKB-AECL. TR 94-04 (10851).

Spalding R.F, Druliner A.D, Whitside L.S, Struempler A.W, 1984. Uranium geochemistry in groundwater from Tertiary sediments. Geochimica et Cosmochimica Acta 48, 2679-2692.

Sturchio N.C., Bohlke J.K, Markun F.J, 1993. Radium isotope geochemistry of thermal waters, Yellowstone National Park, USA. Geochimica et Cosmochimica Acta 57, 1203-1214.

Turner D.R, Whitfield M, Dickson A.G, 1981. The equilibrium speciation of dissolved components in freshwater and seawater at 25°C and 1 atm pressure. Geochimica et Cosmochimica Acta 45, 855-~81.

Weast R.C, Ed, 1975. Handbook of Geochemistry and Physics. Cleveland, CRC-Press Inc.

Wedepohl K.H, 1978. Handbook of Geochemistry II-3. Springer-Verlag, Berlin.

Whitfield M, Turner D.R, 1987. The role of particles in regulating the composition of seawater. In Aquatic Surface Chemistry: Chemical Processes at the Particle-Water Interface (W. Stumm, Ed.). New York. J. Wiley and sons. Environmental Science and Technology.

Wollenberg H.A, 1975. Radioactivity of geothermal systems. In Second U.N. Symposium on the Development and Use of Geothermal Resources, San Francisco, Lawrence Berkeley Laboratory, University of California, 1283-1292.

Yang, M.M., Crerar, D.A. and Irish, D.E. 1989. A Raman spectroscopic study of lead and zinc acetate complexes in hydrothermal solutions. *Geochimica et Cosmochimica Acta* 53: 319-326.

Yoshida, Y. and Yui, M. 2003. JNC Thermodynamic Calculation Code. JNC Technical Report, JNC TN8400 2003-005 (2003) (in Japanese).

Zukin, J.G., Hammond, D.E., Ku, T-L. and Elders, W.A. (1987) Uranium-thorium series radionuclides in brines and reservoir rocks from two deep geothermal boreholes in the Salton Sea geothermal field, southeastern California. Geochimica et Cosmochimica Acta 51: 27192731.